

Regeneration of ocular tissue using gene transfer

Daniel Kampik

A thesis submitted for the degree of
Doctor of Philosophy (PhD)

2017

Department of Genetics
Institute of Ophthalmology
University College London

Declaration

I, Daniel Kampik confirm that the work presented in this thesis is my own. Where information has been derived from other sources, I confirm that this has been indicated in the thesis.

Daniel Kampik

4 September 2016

Mr Daniel Kampik, MD

Abstract

Gene therapy of the eye has made huge advances in recent years, which led to first clinical trials. While these were aimed at replacing a defective gene in inherited disease, research is now expanding to using augmentation gene therapy where a gene is used to modulate the course of disease. We investigated the possibilities of gene transfer of cell cycle modulating genes to induce proliferation in two amitotic tissues essential for vision, the corneal endothelium and retinal pigment epithelium.

Corneal endothelial cells (CEC) maintain the water content of the cornea and thereby its clarity. Low CEC density in corneal diseases causes blindness and requires corneal transplantation. Transfer of *E2F2*, a transcription factor regulating G1 to S phase progression, increases CEC density in human *ex vivo* cultivated corneas, but only when transferred by adenoviral vector, not lentiviral vector. Instead, lentiviral overexpression of ZONAB, a transcription factor normally inactivated by tight junction protein ZO-1, increased CEC density. Lentiviral downregulation of ZO-1, mimicking loss of cell-cell contacts and loss of contact inhibition, led to CEC proliferation. However, CEC density increase was only achieved in young corneas up to ~60 years-of-age, indicating loss of proliferative capacity with age.

RPE loss, as seen in age related macular degeneration (AMD), causes photoreceptor loss and blindness. RPE proliferation could be induced using non-integrating lentiviral vectors delivering *E2F2*. We showed this *in vitro* and *in vivo* after subretinal injection of vector in normal RPE of wildtype mice. To a certain extent, the proliferative effect could also be seen in a transgenic mouse model with degenerated RPE.

This concept of *in situ* regeneration by induction of proliferation could lead to new strategies for CEC loss, especially in donor corneas stored in eye banks. For the RPE, it could be used for treatment of early stages of AMD.

Publications arising from this work

Experimental gene transfer to the corneal endothelium. D. Kampik, R.R. Ali, D.F.P. Larkin. *Experimental Eye Research*, Volume 95, Issue 1, February 2012, p. 54–59.

Lentiviral gene transfer of *E2F2* induces regeneration of retinal pigment epithelium *in situ*. Daniel Kampik, Ulrich F.O. Luhmann, Koji M. Nishiguchi, Mark Basche, Alexander J. Smith, Hong Han, Jennifer A.E. Williams, John Greenwood, Steve E. Moss, Daniel F.P. Larkin, Robin R. Ali. Poster presentation at the annual meeting of the Association for Research in Vision and Ophthalmology, Seattle, 2016. Awarded the ARVO Alcon Early Career Research Award 2016.

Acknowledgements

Firstly, I would like to thank my supervisors: from the clinical perspective, Mr Frank Larkin, for his ever-positive outlook, his continuous support and inspirational mentorship; and from the biological perspective, Professor Robin Ali for his gifted scientific oversight and guidance.

I thank Professor Nancy Joyce and Deshea Harris, Schepens Eye Research Institute, Harvard Medical School, Boston, USA, for providing the E2F2 plasmid and adenoviral vectors, and for their valuable input on corneal endothelial transduction and imaging. I also thank Professor Steve Moss, Professor John Greenwood and Dr Jennifer Williams, Department of Cell Biology, UCL Institute of Ophthalmology, for providing the RPE^{CreER}/DTA mice; Professor Adrian Thrasher and Dr Steve Howe, Molecular and Cellular Immunology, UCL Institute of Child Health, for their technical input on lentiviral vector production; and Luis Apolonia, Ph.D. from Adrian Thrasher's group for his input on lentivirus mediated protein transduction. Thank you also to the staff of Moorfields Eye Bank, Moorfields Eye Hospital, and the Department of Eye Pathology, UCL Institute of Ophthalmology, for making human corneal samples available for research. Furthermore, I would like to acknowledge the generous funding from the National Institute for Health Research that made this research possible. I am indebted to Professor Gerd Geerling, who encouraged me to apply for this program in the first place, and Professor Franz Grehn for his excellent clinical mentorship at the University of Würzburg.

After starting as the only cornea researcher in a predominantly retina-oriented lab, I was very happy that Marc Basche joined me – thank you for such a fruitful cooperation. Satoshi Kawasaki, Department of Ophthalmology, Osaka University School of Medicine, Japan, joined later with an interesting project on gene transfer to corneal epithelial stem cells.

I am grateful for the opportunity to work with a team whose every member was helpful in any technical problem, was open for productive discussions, and organised many spare time

events which made life in London so special – a big thank you to everybody, especially Selina Azam (thank you for your help with vector production!), Amanda Barber, Cédric Boucherie, Livia Carvalho, Tassos Georgiadis, Anai Gonzalez, Philipp Herrmann, Claire Hippert, Sophia KleineHolthaus, Heather Kneale, Clemens Lange, Koji Nishiguchi, Scott Robbie, Matteo Rizzi, Tiina Sepp, Kate Warre-Cornish, Emma West. Subretinal vector injections were done with great skill by Yanai Duran, Scott Robbie and Jim Bainbridge.

A special mention deserve Sander Smith, for his invaluable and kind help with any scientific problem, and Ulrich Luhmann, for his assistance in the planning of experiments and for virtually any aspect of scientific analysis, and his lasting friendship.

Most importantly, I am very grateful to have the support of my family. My deepest gratitude to my wife Katharina, who has supported me throughout this project and on top of it gifted me with three wonderful daughters, Josefine, Mathilda and Charlotte, who, each in their very own way, has contributed to this thesis (Josefine, thank you for counting cells on the iPad!). Finally, I would like to dedicate this thesis to my parents, Ursula and Anselm – without their encouragement and unlimited support this thesis would not have been possible.

Table of Contents

Abstract	3
Publications arising from this work	4
Acknowledgements	5
Table of Contents.....	7
List of Figures.....	13
1. Introduction.....	16
1.1. Overview and aim of study	16
1.2. The cell cycle.....	17
1.3. Gene therapy.....	21
1.4. Corneal endothelium.....	23
1.4.1. Anatomy and physiology.....	23
1.4.2. Pathological conditions.....	24
1.4.3. Clinical relevance of endothelial cell density.....	26
1.4.4. Proliferative capacity of corneal endothelial cells.....	28
1.5. Gene transfer to corneal endothelium	31
1.5.1. Choice of gene delivery methods	32
1.5.2. Non-viral methods of gene transfer	33
1.5.3. Viral vectors.....	34
1.5.3.1. Adenoviral vectors	34
1.5.3.2. Adeno-associated viral vectors	35
1.5.3.3. Herpes simplex virus vectors.....	37
1.5.3.4. Lentiviral vectors.....	37
1.5.4. Applications of gene delivery to corneal endothelium	42
1.5.4.1. Immune modulation to prevent graft rejection	42
1.5.4.2. Increasing corneal endothelial cell density	43
1.5.5. Methods to increase corneal endothelial cell density.....	46

1.6.	Retinal pigment epithelium.....	48
1.6.1.	Anatomy and physiology.....	48
1.6.2.	Pathological conditions.....	50
1.6.3.	Current methods for treating RPE defects.....	52
1.6.4.	Proliferative capacity of the RPE	55
1.7.	Gene transfer to the retinal pigment epithelium.....	56
1.8.	Central hypothesis and aims of this study.....	60
2.	Materials and Methods.....	61
2.1.	General molecular biology	61
2.1.1.	Cloning strategies.....	61
2.1.2.	Polymerase chain reaction (PCR).....	62
2.1.3.	Restriction enzyme digests	62
2.1.4.	DNA electrophoresis	63
2.1.5.	DNA extraction from agarose gels.....	63
2.1.6.	DNA ligations	63
2.1.7.	Amplification of plasmid DNA.....	64
2.1.8.	Sequencing of plasmid DNA.....	65
2.1.9.	mRNA extraction and cDNA synthesis	65
2.1.10.	Real-time PCR.....	66
2.1.11.	Western blot.....	68
2.2.	Lentiviral vectors.....	70
2.2.1.	Production.....	70
2.2.2.	Concentration and purification	73
2.2.3.	Titration	73
2.2.3.1.	Infectious titre: expression of GFP in 293T cells	73
2.2.3.2.	Quantification of reverse transcriptase.....	74
2.3.	Histological analysis	75
2.3.1.	Cryosections.....	75
2.3.2.	Immunocytochemistry and immunohistochemistry.....	75
2.4.	<i>In vitro</i> experiments.....	79
2.4.1.	Cell lines	79
2.4.2.	Passaging of cell cultures	80
2.4.3.	Cell line long-term storage	80

2.4.4.	Test for <i>Mycoplasma</i> contamination	80
2.5.	<i>Ex vivo</i> experiments: Human corneal samples	82
2.5.1.	Ethical requirements	82
2.5.2.	Types of available samples.....	82
2.5.3.	Culture of donor corneas	83
2.5.4.	Transduction of corneal endothelium <i>ex vivo</i>	84
2.5.5.	mRNA extraction from corneal endothelium	85
2.5.6.	Corneal flatmounts	86
2.5.7.	Corneal endothelial cell density assessment.....	87
2.6.	<i>In vivo</i> experiments.....	88
2.6.1.	Animals.....	88
2.6.2.	Anaesthesia.....	88
2.6.3.	Subretinal injection of vector.....	88
2.6.4.	Labelling of S phase nuclei	89
2.6.5.	RPE flatmounts.....	90
2.6.6.	RPE cell density counts.....	91
2.7.	Statistical calculations	91
3.	Assessment of viral vectors for human corneal endothelium <i>ex vivo</i>	93
3.1.	Introduction.....	93
3.1.1.	Aims	94
3.2.	Adenovirus	94
3.3.	Adeno-associated virus	97
3.4.	Lentivirus.....	99
3.5.	Discussion.....	101
3.5.1.	Choice of human corneal samples for this study.....	101
3.5.2.	Variability of human corneal samples under culture conditions.....	102
3.5.3.	Sample types and their characteristics	105
3.5.4.	Choice of vector for <i>ex vivo</i> corneal endothelium transduction.....	106
3.5.5.	Conclusions.....	108
4.	Cell cycle modulation via the Rb/E2F pathway.....	109
4.1.	Introduction.....	109

4.1.1.	The Rb/E2F pathway.....	109
4.1.2.	Alterations in the Rb/E2F pathway.....	111
4.1.3.	Aims	112
4.2.	Proliferation analysis in <i>ex vivo</i> human corneal endothelium	113
4.2.1.	Bromodeoxyuridine labelling	113
4.2.2.	Antigen Ki67 immunostaining.....	115
4.3.	Adenovirus mediated E2F2 overexpression	120
4.3.1.	Characterization of adenoviral vectors.....	120
4.3.2.	Effect of vector dose on cell viability.....	123
4.3.3.	Ad-E2F2 increases corneal endothelial cell density in young corneas	125
4.4.	Lentivirus mediated E2F2 overexpression.....	127
4.4.1.	Construction and characterization of lentiviral plasmids.....	127
4.4.1.1.	LNT-E2F2	127
4.4.1.2.	LNT-E2F2-IRES-GFP	132
4.4.2.	<i>E2F2</i> overexpression in human corneal endothelium	138
4.4.3.	Effect of E2F2 overexpression	139
4.4.3.1.	Effect on proliferation marker Ki67.....	139
4.4.3.2.	Effect on endothelial cell density	141
4.4.3.3.	Effect on cell density over time	144
4.5.	Discussion.....	146
4.5.1.	Proliferation assays and endothelial cell density in cultured donor corneas.....	146
4.5.2.	Adenovirus mediated E2F2 overexpression in relation to other studies	151
4.5.3.	Adenoviral versus lentiviral vectors for E2F2 overexpression.....	153
4.5.4.	Conclusions.....	157
5.	Cell cycle modulation via the ZO-1/ZONAB pathway	158
5.1.	Introduction.....	158
5.1.1.	Intercellular junctions in the corneal endothelium	158
5.1.2.	Contact inhibition in the corneal endothelium	159
5.1.3.	The ZO-1/ZONAB pathway	160
5.1.4.	Aims	162
5.2.	Correlation of contact inhibition and proliferation in corneal endothelium	162
5.3.	Lentivirus vector mediated down-regulation of ZO-1.....	165
5.3.1.	Effect of LNT-shZO-1 on ZO-1 mRNA in corneal endothelial cells.....	165

5.3.2.	Effect on cell cycle status determined by gene expression analysis	167
5.3.3.	Effect on corneal endothelial cell density	168
5.3.4.	Proliferative effect of LNT-shZO-1 is age-dependent.....	171
5.4.	Lentiviral vector-mediated ZONAB overexpression	173
5.4.1.	LNT-ZONAB vector characterization <i>in vitro</i>	173
5.4.2.	Effect on cell cycle status determined by gene expression.....	175
5.4.3.	Effect on corneal endothelial cell density	176
5.5.	Discussion	178
5.5.1.	Breakdown of contact inhibition enables regeneration.....	178
5.5.2.	Marker gene upregulation.....	180
5.5.3.	Influence of age and cell density on proliferative capacity.....	180
5.5.4.	Role of proposed stem cells and transient amplifying cells	182
5.5.5.	Limitations of the studies	183
5.5.6.	Conclusions.....	184
6.	Retinal pigment epithelium regeneration	186
6.1.	Introduction	186
6.1.1.	The concept of <i>in situ</i> RPE proliferation	186
6.1.2.	The RPE ^{CreER} /DTA mouse.....	187
6.1.3.	Aims	188
6.2.	Results	189
6.2.1.	Effect of E2F2 overexpression <i>in vitro</i>	189
6.2.2.	Effect of E2F2 overexpression on the cell cycle <i>in vivo</i>	193
6.2.2.1.	LNT-E2F2 induces S phase progression in wildtype mice RPE.....	193
6.2.2.2.	LNT-E2F2 mediated S phase progression in relation to vector dose.....	200
6.2.3.	Effect of E2F2 on RPE cell density in wildtype mice	202
6.2.4.	Duration of E2F2 mediated proliferation.....	205
6.2.5.	Effect of LNT-E2F2 on RPE in a transgenic RPE-ablated mouse line.....	208
6.2.5.1.	Reduced RPE cell density in the RPE ^{CreER} /DTA mouse.....	209
6.2.5.2.	LNT-E2F2 increases BrdU uptake and central RPE cell density	210
6.3.	Discussion	213
6.3.1.	E2F2 gene transfer to RPE cells induces mitosis <i>in situ</i>	213
6.3.2.	Limitations of the studies	213
6.3.3.	Risk of induction of epithelial-mesenchymal transition	215

6.3.4. Inherent capacity of regeneration in the RPE	215
6.3.5. Conclusions.....	216
7. Final discussion	217
7.1. Summary of findings and implications for therapeutic applications.....	217
7.1.1. Corneal endothelium	218
7.1.2. Retinal pigment epithelium	222
7.2. Safety measure for gene transfer to induce cell replication	225
7.2.1. Modulation of cDNA integration	225
7.2.2. Modulation of transgene expression.....	227
7.2.3. Reverse transcription defective lentiviral vectors	228
7.2.4. Lentivirus particle mediated protein transfer	229
7.2.5. Non-viral vectors.....	231
7.3. Which cells regenerate?	232
7.4. Outlook.....	233
8. References	236
9. Appendix.....	273
9.1. Abbreviations.....	273
9.2. Ethical approval for use of human tissue.....	278
9.2.1. Study Protocol (12 December 2008)	279
9.2.2. Participant Information Sheet (02 February 2009)	283
9.2.3. Participant Consent Form (02 February 2009).....	286
9.2.4. Letter of Approval (9 February 2009).....	287

List of Figures

Figure 1. Overview of the cell cycle of mammalian cells.....	18
Figure 2. Preparation of lentiviral vectors.....	72
Figure 3. Test for <i>Mycoplasma</i> contamination of cell lines by PCR.	81
Figure 4. Adenovirus mediated transduction of corneal endothelium <i>ex vivo</i>	96
Figure 5. AAV2/8 mediated transduction.	98
Figure 6. Lentivirus mediated transduction.....	100
Figure 7. The Rb/E2F pathway.....	110
Figure 8. BrdU uptake in endothelium of corneal specimen cultured for 3 days.	114
Figure 9. Test of Ki67 antibody <i>in vitro</i>	115
Figure 10. BrdU and Ki67 labelling of proliferating HEK293T cells <i>in vitro</i>	116
Figure 11. Ki67 staining in <i>ex vivo</i> -cultured corneal endothelium.	117
Figure 12. Ki67 distribution in a corneal specimen in culture.	119
Figure 13. Characterization of adenoviral vector delivering <i>E2F2</i>	121
Figure 14. Transgene overexpression at different concentrations of adenoviral vector.	122
Figure 15. Effect of vector dose on corneal endothelial cell density.....	124
Figure 16. Ad-E2F2 increases endothelial cell density in young corneal samples.....	126
Figure 17. Outline of the cloning strategy for LNT-E2F2.....	129
Figure 18. Characterization of lentiviral vector LNT-E2F2.....	131
Figure 19. Design of the entry clone TOPO-E2F2.....	133
Figure 20. Construction of LNT-E2F2-IRES-eGFP.....	135

Figure 21. Characterization of lentiviral vector LNT-E2F2-IRES-eGFP on mRNA level.....	136
Figure 22. Characterization of lentiviral vector LNT-E2F2-IRES-eGFP on protein level.....	137
Figure 23. Expression of transgene E2F2 protein after transduction with lentiviral vectors.	139
Figure 24. Effect of LNT-E2F2 on Ki67 expression.....	140
Figure 25. Effect of E2F2 overexpression on cell density.....	143
Figure 26. Effect of E2F2 overexpression on cell density over time in corneal endothelium <i>ex vivo</i>	145
Figure 27. The ZO-1/ZONAB pathway.....	161
Figure 28. Correlation between tight junctions and proliferation in human corneal endothelium.	164
Figure 29. Downregulation of ZO-1 mRNA by LNT-shZO-1.....	166
Figure 30. Relative expression of cell cycle related genes after transduction with LNT-shZO-1 in corneal endothelium.....	168
Figure 31. Effect of downregulation of ZO-1 in human corneal endothelium <i>ex vivo</i>	170
Figure 32. Effect of LNT-shZO-1 on corneal endothelium from older donors.	172
Figure 33. Characterization of lentiviral vector LNT-ZONAB <i>in vitro</i>	174
Figure 34. Relative expression of cell cycle related genes after transduction with LNT-ZONAB in corneal endothelium.	175
Figure 35. Effect of overexpression of ZONAB in human corneal endothelium <i>ex vivo</i>	177
Figure 36. Effect of donor age and initial cell density on responsiveness to LNT-shZO-1 treatment.....	182
Figure 37. Growth arrest in ARPE19 cells.....	190

Figure 38. <i>E2F2</i> overexpression induces proliferation in a growth arrested, confluent monolayer of ARPE19 cells <i>in vitro</i>	192
Figure 39. Confocal laser scanning images of whole RPE flatmounts 10 days after subretinal vector injection.	195
Figure 40. LNT-E2F2 induces BrdU uptake in RPE <i>in vivo</i>	196
Figure 41. LNT-E2F2 induces BrdU uptake in RPE in both young and old mice.....	198
Figure 42. LNT-E2F2 induces BrdU uptake in RPE <i>in vivo</i>	199
Figure 43. LNT-E2F2 mediated S phase progression in relation to vector dose.....	201
Figure 44. <i>E2F2</i> overexpression increases RPE cell density <i>in vivo</i>	204
Figure 45. Differential pulse labelling of S phase nuclei to assess duration of proliferative effect.	207
Figure 46. The RPE ^{CreER} /DTA mouse line shows reduced RPE cell density most prominently in the centre.....	210
Figure 47. LNT-E2F2 induces increased BrdU uptake in RPE ^{CreER} /DTA mice and increases RPE cell density.	212
Figure 48. Lentivirus particle mediated protein transfer.....	230

1. Introduction

1.1. Overview and aim of study

Perception of light in the eye requires the interplay of a variety of highly specialized cells: for example, photoreceptor cells in the retina to relay impulses generated by light; mucosal immune cells of the conjunctiva to guard the eye against external pathogens; stromal cells of the cornea and lens to assure the clarity of the eye's optic system. The high grade of differentiation of many cell types of the eye goes along with a loss of regenerative capacity. Photoreceptors, bipolar cells, and ganglion cells in the retina are terminally differentiated and have no ability to undergo cell division. Few cell types, especially those lining the outer surface of the eye, the conjunctival and corneal epithelium, constantly regenerate from their respective stem cells, which undergo cell divisions throughout lifetime. Some cell types, however, do not regenerate under normal conditions, but have retained their capacity to regenerate in special circumstances (e.g. *in vitro* after cell separation). In the human eye, two cell types of high metabolic activity share this feature: the corneal endothelium and the retinal pigment epithelium. For both tissue types, the loss of cells can cause blinding disease and is not compensated by cell division. Yet both can be externally stimulated to undergo mitosis, which gives rise to the idea of *induced in situ regeneration*. Transferring genes controlling the cell cycle might induce mitosis in these normally amitotic cells, resulting in tissue regeneration.

Aim of this study is to develop methods of regeneration through gene therapy in two tissues of the eye affected by degeneration through age or disease: corneal endothelium and retinal pigment epithelium.

1.2. The cell cycle

Regeneration of tissue requires cells in the active stages of the cell cycle. The cell cycle is a series of tightly regulated molecular events controlling cell growth, replication of the DNA, division of the nucleus, and partitioning of the cytoplasm, all eventually leading to the formation of two daughter cells. The following outline of key events of the cell cycle refers to the eukaryotic cell. Every step of the cell cycle has been highly conserved throughout evolution. It can be divided into four specific phases, G1, S, G2, and M, as shown in Figure 1 (adapted from Vermeulen et al., 2003, Joyce, 2003, and Hochegger et al., 2008). The preparatory steps taking place before mitosis, G1, S, and G2, are termed interphase.

Progression through the cell cycle is regulated by different cyclins and their partners, the cyclin dependent kinases (CDKs). Cyclins are regulatory proteins whose concentrations vary in a cyclical fashion during the cell cycle, dependent on mitogens and other positive growth regulatory signals (Evans et al., 1983). Cyclins bind to and thereby activate their specific CDKs, serine-threonine protein kinases that phosphorylate other regulators to induce specific events in the cell cycle. This cyclic production (regulated by gene expression) and degradation (through the ubiquitin mediated proteasome pathway) of cyclins induce oscillations in CDK activity to orchestrate the cell cycle.

In vivo, many cells such as hepatocytes and neurons can enter a non-proliferating, quiescent stage (G0) for very long periods (Pardee, 1989). These cells express low levels of cell-cycle dependent proteins and their DNA is present in unduplicated (2N) form, and account for the major part of the non-growing, non-proliferating cells in the human body (Vermeulen et al., 2003). *In vitro*, suboptimal conditions such as medium with little serum can force cells to move out of cycle and into G0 (Larsson et al., 1985).

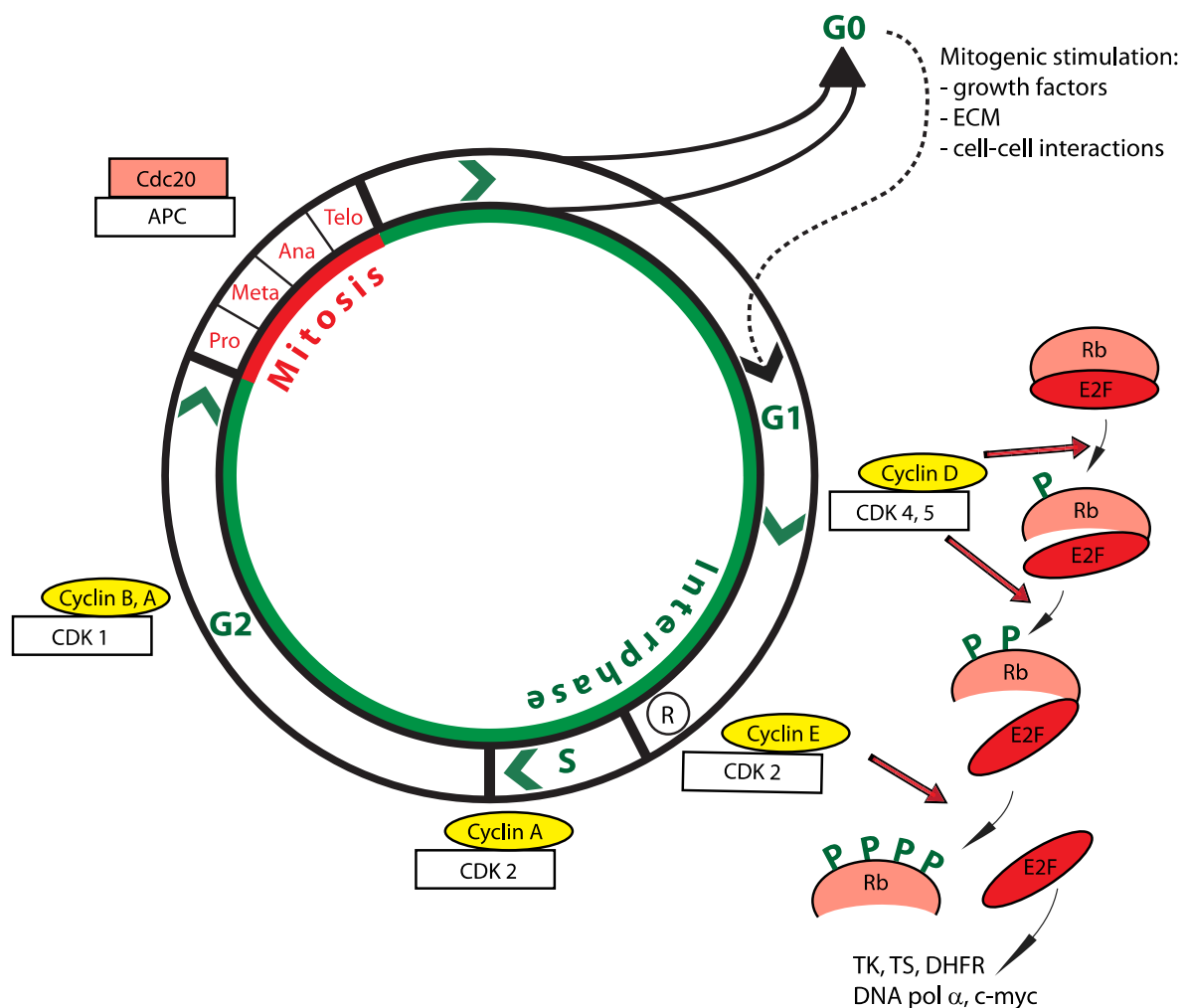


Figure 1. Overview of the cell cycle of mammalian cells.

The cell cycle consists of four phases: first gap phase (G1), DNA synthesis (S), second gap phase (G2), and mitosis (M), which can be further divided into prophase, metaphase, anaphase, and telophase. G1–S–G2 are summarized as interphase. Transition between phases is regulated by different cyclins and their partners, cyclin dependent kinases. In the absence of growth factors and other mitogenic stimuli, cells will enter a quiescent state (G0).

CDK: cyclin dependent kinase; ECM: extracellular matrix; APC: anaphase-promoting complex; R: restriction point; Rb: retinoblastoma gene product (P indicates phosphorylation state); TK: thymidin kinase; TS: thymidylate synthase; DHFR: dihydrofolate reductase; DNA pol α : DNA polymerase α .

Figure adapted from (Vermeulen et al., 2003) and (Joyce, 2003)

External mitogenic stimulation drives cells resting in G0 phase to enter G1 (gap 1), the longest phase of the cell cycle (6 hours in exponentially growing 3T3 fibroblasts, (Campisi et al., 1984)). G1 is a growth phase that prepares the cell for DNA duplication (Massague, 2004;

Trimarchi and Lees, 2002). Progression through G1 to S is dependent on growth factors, the extracellular matrix, cell-cell contacts as well as stress conditions (Boonstra, 2003).

Accumulation of sufficient growth stimuli enables the cell to overcome the restriction point (R), a critical point in late G1 after which the cell is bound to undergo DNA replication and is no longer sensitive to growth factor signalling. The restriction point incorporates a checkpoint mechanism that monitors multiple biochemical and architectural parameters of cell cycle progression, such as DNA integrity and cell size. If the restriction point is not overcome and correcting mechanisms fail, the cell will either go back into a quiescent stage (G0) or undergo apoptosis.

The following S phase, in which DNA synthesis occurs, commits a cell-to-cell division, or if aborted, leads to apoptosis (La Thangue, 2003). S phase entry requires activation of transcription factor E2F, a central regulator of cell cycle progression (DeGregori et al., 1997). In quiescent cells, E2F is tightly bound to the retinoblastoma gene product, pRb (Leone et al., 1999). Already during mid to late G1 phase, the Cyclin D/CDK4 and Cyclin E/CDK2 complexes sequentially phosphorylate Rb on several residues (DeGregori et al., 1995). This phosphorylation causes the release and activation of E2F, allowing transcription of genes crucial for DNA synthesis and progression through S phase, such as thymidin kinase, thymidylate synthase, dihydrofolate reductase, DNA polymerase α , and *c-myc* (Blake and Azizkhan, 1989; DeGregori et al., 1995; Pearson et al., 1991; Slansky et al., 1993; Thalmeier et al., 1989). The S phase is characterized by Cyclin A binding with CDK2 (Walker and Maller, 1991).

A second gap phase, G2, is necessary to prepare the M (mitosis) phase. Similar to the first gap phase, G2 is devoted to biosynthesis for cell growth and especially production of microtubules. Again a checkpoint mechanism controls chromatin fidelity and integrity of the now duplicated DNA. DNA damage leads to rapid induction of p53, which in turn stimulates the transcription of *p21* (Agarwal et al., 1998). p21, a cyclin kinase inhibitor (CKI), results in CDK inhibition and cell cycle arrest, preventing the replication of damaged DNA (Vermeulen et al., 2003). Bind-

ing of Cyclin A to CDK1 promotes progression towards the M phase (Arellano and Moreno, 1997). The end of G2 is marked by a threshold level of active Cyclin B1/CDK1, also known as maturation promoting factor (MPF) (Sha et al., 2003).

The M phase, during which chromosome segregation and cell division occur to finally generate two daughter cells, is comparatively brief and accounts for only 10% of the cell cycle. It is highly regulated and can be divided into four stages: prophase (chromatin condensation, disintegration of the nuclear membrane, microtubules arrangement), metaphase (alignment of chromosomes), anaphase (splitting of chromosomes and shortening of kinetochore microtubules), and telophase (decondensation of chromosomes, formation of two nuclear membranes). A metaphase (spindle) checkpoint ensures that separation of sister chromatids only takes place when all chromosomes are attached to the mitotic spindle at their kinetochores, the points of attachment of chromatids to the spindle fibres.

Transition from metaphase to anaphase is marked by the formation of anaphase-promoting complex (APC), a ligase that marks cell cycle proteins for degradation by proteasomes (Passmore et al., 2003). Especially S and M cyclins and CDKs are inactivated through APC activity, permitting progression through anaphase and telophase. Cytokinesis, the formation of two daughter cells from the dividing cytoplasm, starts after anaphase in parallel to karyogenesis and happens only after APC binds with Cdc20, a central activator of APC. This allows for the separation of chromosomes and contraction of myosin filaments at the cell's equator to work simultaneously. Cdc20 activity is blocked by unattached kinetochores via Mad2, a spindle checkpoint protein (Li and Benezra, 1996).

The tight control through cell cycle checkpoints ensures that processes at each phase of the cycle have been accurately completed. At any stage the cell cycle can be blocked to enable repair mechanisms or, if repairs are unsuccessful, the cell is forced to undergo apoptotic death (Hartwell and Weinert, 1989; Nojima, 2004). Defects in these checkpoints are the molecular basis of many forms of cancer.

1.3. Gene therapy

Transfer of genes to a cell enables modulation of the cell's protein expression. The introduced transgene DNA is transcribed, the resulting mRNA then translated into a protein with therapeutic effect. In classical gene therapy, the transgene replaces a missing or defective gene in recessive monogenic disorders. In the early 1990s this concept has been taken into clinics in the first gene therapy trial for severe combined immunodeficiency (SCID) (Blaese et al., 1995), but major success was achieved ten years later: Children with X-linked SCID, who, due to the lack of a suitable donor, could not be treated by traditional bone marrow transplantation, received gene therapy. Delivering the gene encoding the γ c subunit, a component of certain cytokine receptors, via a retroviral vector resulted in normal lymphocyte cell counts and restored cellular immune function (Cavazzana-Calvo et al., 2000).

Meanwhile, improved vector design led to several other clinical trials proving safety and efficacy of gene therapy. Retroviral-mediated gene replacement achieved immune reconstitution in adenosine deaminase deficient SCID patients (Aiuti et al., 2009; Gaspar et al., 2006), lentiviral *ABCD1* gene transfer for adrenoleukodystrophy stopped progressive cerebral demyelination (Cartier et al., 2009), and lentiviral β -globin gene transfer in β -thalassaemia resulted in independence from monthly transfusions (Cavazzana-Calvo et al., 2010). Recently, adeno-associated virus (AAV) mediated gene transfer achieved long-term correction of haemophilia B and allowed patients to discontinue their regular prophylactic treatment (Nathwani et al., 2011).

A major success was achieved in the eye by improving visual function in patients with Leber's Congenital Amaurosis (LCA), a group of recessively inherited severe infantile-onset rod-cone dystrophies (Bainbridge and Ali, 2008). In three independent clinical trials that started in 2007, subretinal injection of recombinant AAV delivering the *RPE65* gene was safe and led to a significant improvement in visual function tested by microperimetry, dark-adapted perimetry,

or pupillometry compared to the untreated eye (Bainbridge et al., 2008; Hauswirth et al., 2008; Maguire et al., 2008).

As at June 2015, according to latest available data of the Journal of Gene Medicine, a total of 2210 patients participated in clinical trials applying gene therapy (The Journal of Gene Medicine, 2015), the majority of them in phase I trials (1283 patients, 58.1%), followed by phase I-II trials (446 patients, 20.2%) and phase II trials (374 patients, 16.9%). The most common indications for gene therapy were cancer diseases (1415 patients, 64%), cardiovascular diseases (175 patients, 7.9%) and infectious diseases (174 patients, 7.9%). Gene therapy for ocular diseases sits in 6th place with 31 patients treated so far (1.4%). To date, no gene therapy clinical trial has addressed regeneration of tissue as a primary aim. While many trials in cancer therapy involve gene transfer of a tumour suppressor gene (171 patients, 7.7%), a suicide gene (163 patients, 7.4%) or a replication inhibitor gene (92 patients, 4.2%), no trials use transfer of genes promoting the cell cycle. This reflects the understandable fear of uncontrolled regeneration, i.e. cancer. In classical gene replacement therapy, uncontrolled clonal proliferation can be inadvertently induced by insertional mutagenesis: the vector integrates near a protooncogene in the host genome, causing overexpression of a normally silenced gene. This has occurred in two independent clinical trials for gene therapy for SCID-X1, causing leukaemia between 2 and 6 years after initially successful treatment (Hacein-Bey-Abina et al., 2003; Howe et al., 2008).

Gene therapy interfering with the cell cycle of normally amitotic cells imposes new, additional mechanisms of inducing of clonal proliferation. Only slightly higher transgene expression levels could potentiate the proliferative effect. Low vector specificity could lead to transduction of neighbouring naturally proliferating cells causing uncontrolled proliferation. Therefore, additional and new safety mechanisms need to be introduced (see also Final Discussion, Safety measure for gene transfer to induce cell replication, p. 225).

1.4. Corneal endothelium

1.4.1. Anatomy and physiology

The back surface of the cornea of the eye is covered by a monolayer of endothelial cells, separated from the corneal stroma by Descemet's membrane. It is formed during the sixth week of gestation by the migration and proliferation of neural crest-derived mesenchymal cells located at the periphery of the presumptive cornea (Johnston et al., 1979). Connected by apical tight junctions and gap junctions, endothelial cells form a leaky barrier towards the aqueous humour controlling corneal hydration and nutrition (Waring et al., 1982). A constant stromal water content of 78% is necessary to maintain corneal transparency, otherwise corneal oedema leads to swelling, increase of corneal thickness and opacity. To regulate stromal hydration, endothelial cells employ an ATPase-dependent metabolic pump that is located in the lateral plasma membranes (Waring et al., 1982). By an osmotically active HCO_3^- transport system they constantly dehydrate the stroma, thereby maintaining the physiologic collagen arrangement and preserving corneal transparency (Dikstein and Maurice, 1972; Waring et al., 1982). Abundant mitochondria reflect their high metabolic activity, and extensive rough and smooth endoplasmic reticulum as well as a distinct Golgi apparatus provide evidence of significant protein synthesis (Marshall and Grindle, 1978; Tuft and Coster, 1990; Waring et al., 1982).

It is noteworthy that corneal endothelial cells differ from vascular endothelial cells, which line the inner layer of blood vessels, in function and in their tissue of origin. Vascular endothelium is mesodermally derived while corneal endothelium is derived from the neural ectoderm. They have little in common regarding surface markers.

Unlike the corneal epithelium, the human corneal endothelium rarely undergoes mitotic division in a normal eye after foetal development (Joyce, 2003). A high endothelial cell density of

3500–4000 cells/mm² is measured after birth. Density then decreases at a relatively rapid rate mainly due to normal eye growth and increase in corneal size, resulting in an average of 2000 to 3500 cells/mm² in adults (Murphy et al., 1984; Nucci et al., 1990). Throughout adult life, a gradual decrease in endothelial cell density can be observed with an average cell loss of 0.3 to 0.6% per year (Bourne et al., 1997; Hollingsworth et al., 2001). This loss is compensated only by migration, focal spreading (enlargement) and thinning of the neighbouring cells, resulting in irregularities in the appearance of the previously uniform mosaic of cells. Normally, the endothelium has a large enough reserve of cells to maintain its important barrier and pump functions for a lifetime (Edelhauser, 2000; Joyce, 2005).

1.4.2. Pathological conditions

All pathological conditions of the endothelium can eventually lead to loss or absence of endothelial cells, causing corneal oedema. But even in healthy corneas, endothelial cell loss can be observed throughout lifetime. Physiological endothelial cell loss is attributed to apoptosis and/or necrosis caused by light-induced oxidative damage (Cho et al., 1999), which in turn is a cause for their incapacity to proliferate (Joyce et al., 2009).

Abnormal conditions can cause a significant loss of endothelial cells and compromise the ability of the endothelium to maintain corneal clarity. Insufficient pump function of the osmotically active HCO₃⁻ transport system causes water accumulation in the corneal stroma, disrupting the physiologic collagen arrangement. Corneal decompensation occurs invariably when the cell density drops below 300 to 500 cells/mm², leading to stromal swelling, loss of vision and eventually, blindness (Bourne, 1998, 2001). To date, the only treatment for permanent endothelial decompensation is corneal transplantation.

Endothelial cell loss can result from primary endothelial disease. Most common Fuchs' endothelial corneal dystrophy (FECD) is a bilateral condition starting with blurred vision and glare

in the fourth decade of life, gradually leading to painful blindness within 25 years (Fuchs, 1910; Vogt, 1921; Waring et al., 1978). Most common are cases without known inheritance; some autosomal-dominant cases are reported (Weiss et al., 2008). A gene defect is known only for the early onset variant. Here, a defect in *COL8A2* gene encoding collagen type VIII $\alpha 2$ causes symptoms in the first decade of life (Gottsch et al., 2005).

More rare dystrophies include posterior polymorphous corneal dystrophy (PPCD), an autosomal-dominant disease featuring deep blister-like corneal lesions, which can be caused by either a defect in the *OVOL2* promoter, controlling gene expression of a zinc-finger transcription factor that regulates mesenchymal-to-epithelial transition (PPCD type 1, (Davidson et al., 2016)), or *COL8A2* (collagen type VIII $\alpha 2$, PPCD type 2, (Krafchak et al., 2005)) or in *ZEB1* (two-handed zinc-finger homeodomain transcription factor 8, PPCD type 3, (Shimizu et al., 2004; Yellore et al., 2012)). Congenital hereditary endothelial dystrophy (CHED) is characterized by corneal clouding at birth with sparse and atrophic endothelial cells (Kenyon and Antine, 1971). CHED type 1 is autosomal-dominant and has recently been identified as the extreme form of PPCD1 as it is caused by a defect in the same *OVOL2* promoter (Davidson et al., 2016). CHED type 2 is autosomal-recessive and caused by a defect in *SLC4A11*, encoding a sodium borate transporter (Jiao et al., 2007). X-linked endothelial corneal dystrophy (XECD) affects males and features progressive corneal clouding leading to a milky appearance of the cornea (Schmid et al., 2006). The gene has not yet been identified.

Iridocorneal endothelial syndrome (ICE syndrome) is characterized by an abnormal endothelial cell layer, which can proliferate but shows reduced pump function. Pathological endothelial cells adopt an epithelium-like phenotype and cover areas beyond the normal borders of endothelium, especially the trabecular meshwork and iris, causing severe glaucoma (Hirst et al., 1995).

More common is mechanical trauma to the endothelium, especially during cataract surgery. After cataract extraction, Bourne et al. found an increase in endothelial cell loss to 2.5% per year

from 1 to 10 years even after uneventful surgery (Bourne et al., 1994b), which can lead to pseudophakic bullous keratopathy, still the leading indication for penetrating keratoplasty in the United States (Ghosheh et al., 2008a; Ghosheh et al., 2008b). Further reasons for endothelial cell loss are intraocular foreign body, or direct corneal trauma. Non-mechanical damage to the endothelium can result from inflammation, increased intraocular pressure, contact lenses, or topical medication.

Previous corneal transplantation itself is invariably accompanied by increased endothelial cell loss (Bourne, 2001). Even in the absence of any immune reaction (also in corneal autografts), a gradual decrease of endothelial cells finally leads to graft decompensation (Bell et al., 2000; Matsuda and Manabe, 1988). The time for a graft to reach a critically low endothelial cell density of 500 cells/mm² can be predicted by a biexponential decay model proposed by Armitage et al. (Armitage et al., 2003). Corneal grafts with initial cell densities of 2000 cells/mm² could reach the critical density in less than 20 years, whereas grafts with an initial cell density of 2500 cells/mm² is likely to remain functioning for at least 30 years. Late endothelial failure (LEF) is the primary cause of graft failure after the first 5 postoperative years and accounts for over 90% of the failures between 5 and 10 years after keratoplasty (Bourne et al., 1994a; Ing et al., 1998). LEF may be considered as the ultimate fate of all grafts if the recipients live for a sufficient time. A repeat keratoplasty is the only treatment at present.

1.4.3. Clinical relevance of endothelial cell density

Corneal transplantation is the most common form of transplantation with approximately 3700 grafts in the United Kingdom (NHS Blood and Transplant, 2016), over 76.000 grafts undertaken in the United States annually (Eye Bank Association of America, 2014), and 184,576 corneal transplants performed in 2012 globally (Gain et al., 2016). In a UK cohort, the primary indication for corneal transplantation can be attributed to endothelial failure, accounting for

41% of grafts (Rahman et al., 2008). Even if a transplant survives for more than 5 years, a low endothelial cell density is the primary overall reason for graft failure (90%). Re-grafts, which have a considerably reduced survival rate compared to primary grafts, account for 20% of all transplants.

On the other hand, there is a shortage of donor corneas available for transplantation, which is often due to insufficient endothelial cell density. Falling endothelial cell density due to high donor age and post-mortem cell death is the reason for discard of 33% of donor corneas in eye banks in the UK (Armitage and Easty, 1997). The increasing average age of cornea donors (currently 62 years) contributes further to low endothelial cell density. During corneal storage and during transplantation surgery, 10% and up to 23% of the donor endothelial cells are lost, respectively (Bourne and O'Fallon, 1978; Builles et al., 2006). Newly established endothelial transplantation alone (Descemet stripping with endothelial keratoplasty, DSEK, and Descemet membrane endothelial keratoplasty, DMEK) reduces surgical trauma and rejection rate, but seems to go along with a higher endothelial cell loss (Price and Price, 2008).

Transplants that eventually fail from low endothelial cell density do not appear to have lost endothelial cells faster than grafts that do not fail, but instead have fewer endothelial cells in the beginning (immediately after transplantation) and diminish to a critically low endothelial cell density earlier (Bourne, 2001).

It should therefore be possible to prevent or delay graft failure by increasing the number of endothelial cells before transplantation. Augmenting the number of endothelial cells in the donor cornea *ex vivo* would not only prolong long-term graft survival but also help to increase the number of suitable donor corneas. In addition, these *ex vivo* techniques may elicit ways for use *in vivo* for any cornea with endothelial deficiency and, thus, may eliminate the need for corneal transplantation in some cases.

1.4.4. Proliferative capacity of corneal endothelial cells

In humans and non-human primates, corneal endothelial cells do not divide at a sufficient rate to replace dead or injured cells. After complete formation of the endothelial monolayer at birth, a constant cell loss can be observed throughout lifetime. Histologic and *in vivo* confocal microscopy studies indicate that average cell loss is 0.3–0.6% per year (Bourne et al., 1997; Hollingsworth et al., 2001; Murphy et al., 1984).

Cell cycle arrest in human corneal endothelial cells

Several mechanisms of active repression of corneal endothelial cells re-entry to the cell cycle have been identified: (1) lack of response to positive growth factors; (2) the anti-proliferative effect of TGF- β 2 in the aqueous humour; (3) contact inhibition through mature cell-cell junctions (reviewed in Joyce, 2003, 2005, 2012).

(1) Although a plethora of growth factors is present in the aqueous humour and some of them are produced by endothelial cells themselves, they seem resistant to these stimuli. Positive growth factors detected in aqueous humour include acidic-FGF, basic-FGF (Schulz et al., 1993), insulin-like growth factor-I and -II, insulin-like growth factor binding protein (Arnold et al., 1993), and hepatocyte growth factor (HGF) (Araki-Sasaki et al., 1997). Endothelial cells express EGF and its receptor, acidic and basic FGF, FGF-1 and FGF-2 receptors, TGF- β 1, TGF- α , HGF and its receptor, and keratinocyte growth factor (KGF) and its receptor (Wilson and Lloyd, 1991; Wilson et al., 1991; Wilson et al., 1993b). All these factors are known to promote proliferation in various cell types. Descemet's membrane, the underlying extracellular matrix secreted by corneal endothelial cells, acts as a carrier for these growth factors (Blake et al., 1997; Kay et al., 1994; Vlodavsky et al., 1987). Many of the growth factors present in the aqueous humour or Descemet's membrane *in vivo* were shown to promote proliferation of human corneal endothelial cells at physiologic levels *in vitro*, especially HGF and KGF (Wilson et al., 1993b) and FGF (Kay et al., 1998). *In vivo*, cell division does not appear to occur in human corneal endothelium,

even in response to injury and disruption of cell-cell contacts (Joyce, 2012). It is not known whether growth factors surrounding endothelial cells are not sufficient in concentration, are present in inactive forms, are antagonized by other cytokines, or do not bind effectively enough to induce proliferation in low density or injured endothelium.

(2) TGF- β 2 is present in relatively high concentration in aqueous humour (Granstein et al., 1990; Kokawa et al., 1996). Picht et al. measured a concentration of 127.4 ± 40.0 pg/ml (mean \pm SD) of active TGF- β 2, and 762.1 ± 345.5 pg/ml of total TGF- β 2 (Picht et al., 2001). Although present mostly in latent form, it can be converted into active TGF- β 2 by thrombospondin-1 expressed by corneal endothelial cells (Hiscott et al., 1997; Schultz-Cherry et al., 1994). CEC express all three receptors necessary for optimal TGF- β signal transduction (Joyce and Zieske, 1997). Physiologic levels of TGF- β 2 potently inhibit S-phase entry and DNA synthesis in cultured corneal endothelial cells of rabbits (Harris and Joyce, 1999) and rats (Chen et al., 1999), and this effect is dose-dependent. The anti-proliferative activity of TGF- β 2 is mediated by constant high nuclear levels of p27Kip1, a cyclin kinase inhibitor that prevents activation of cyclin-D/CDK4 and cyclin-E/CDK2 and thereby keeps cells arrested in G1 (Chen et al., 1999; Kim et al., 2001a; Kim et al., 2001b). Lu et al. investigated the crosstalk of anti-proliferative TGF and proliferative FGF (Lu et al., 2006). In human corneal endothelium, TGF- β 2 can override the stimulating effects of FGF-2 by increasing COX-2 expression.

(3) The presence of mature cell-cell junctions in the endothelial monolayer was shown to be an important anti-proliferative factor and is responsible, in large part, for total cessation of corneal endothelial cell proliferation *in vivo*. Release of cells from their confluent monolayer to create a single cell suspension is the principle for culturing primary corneal endothelial cells *in vitro*. Mitotic contact inhibition *in vivo* was investigated in rats, where corneal endothelial cells continue to mature after birth (Joyce et al., 1998). Proliferation of endothelial cells did not cease until stable cell-cell contacts, represented by connexin-43 and ZO-1 expression, and cell-substrate contacts, represented by an organized pattern of fibronectin and collagen IV, were

established. This was completed by postnatal day 13, when uptake of S phase marker BrdU in endothelial cells did not occur any more.

Senoo and Joyce established a model to disrupt the endothelial monolayer of human corneal samples *in situ, ex vivo* by EDTA, and assessed proliferation by Ki67 immunostaining. EDTA disruption alone was not sufficient to induce proliferation, nor was incubation in mitogen-containing medium (medium containing 10% FCS, supplemented with EGF and FGF). Combination of EDTA mediated contact disruption and mitogen-containing medium conferred sensitivity to growth factors and promoted proliferation (Senoo et al., 2000).

Proliferation of corneal endothelial cells

Although human corneal endothelium *in vivo* does not divide sufficiently to replace lost cells, there is evidence that corneal endothelial cells retain proliferative capacity (Joyce, 2003, 2005, 2012). Human corneal endothelial cells can be cultured and proliferate *in vitro* after isolating them from their monolayer and exposing them to appropriate mitogens (Engelmann et al., 1988; Hitani et al., 2008; Senoo and Joyce, 2000). By analysing the relative expression and subcellular localization of several cell cycle proteins in the endothelium, Joyce et al. showed that endothelial cells retained their proliferative capacity, but are actively repressed in a non-replicative state (Joyce et al., 2002; Joyce et al., 1996a). Expression and subcellular localization of proteins known to regulate the G1/S-phase transition, including pRb, E2F, p53, and the cyclin-dependent kinase inhibitors (CKI), p21CIP1 and p16INK4a, indicated that endothelial cells are arrested before the mid-G1 phase of the cell cycle (Joyce et al., 1996b).

Age-related differences in proliferative capacity

Replicative senescence due to short telomere length is not the cause of cell cycle arrest in mature human corneal endothelium (Egan et al., 1998). Nevertheless, age-related differences were observed. Senoo and Joyce used an *ex vivo* endothelial wound healing model and found that only half as many cells were proliferating in the old age group (>50 years of age) than in the young age group (<30 years of age), determined by (Senoo and Joyce, 2000).

Differences between species in corneal endothelium proliferation

The proliferative capacity of corneal endothelial cells differs among species (Joyce, 2003). Bovine (Savion et al., 1982), rabbit (Raymond et al., 1986), rat (Chen et al., 1999), and murine (Joo et al., 1994; Scheef et al., 2007) endothelial cells grow easily in culture. In contrast, human and monkey CEC do not culture as readily (Baum et al., 1979; Matsubara and Tanishima, 1983). Wound healing studies *in vivo* in monkey led to the conclusion that mitosis did not contribute significantly to wound closure and that cell migration and enlargement was the major means of healing (Matsubara and Tanishima, 1983). The age-related increase in endothelial cell size can be observed clinically by specular microscopy in humans (Laing et al., 1983), and after surgical trauma, the human endothelium shows practically no proliferative activity and the damaged area is covered by means of cell migration (Mishima, 1982). Yet in mice, rats (Schwartzkopff et al., 2010; Tuft et al., 1986), and rabbits (Hirsch et al., 1975; Minkowski et al., 1984), even large endothelial wounds heal comparatively quickly by mitosis. Cats are capable of mostly restoring endothelial function after the entire endothelium is damaged; this takes a long time (several months) and occurs by a process of predominantly migration and heterotrophy (Honda et al., 1982; Huang et al., 1989; Petroll et al., 1999b; Van Horn et al., 1977).

1.5. Gene transfer to corneal endothelium

A number of characteristics of the corneal endothelium confer significant potential for gene-based treatment of corneal endothelial diseases. These include the relatively simple monolayer arrangement, the theoretical accessibility of every cell for gene transfer, the ability of the cornea with its exposed endothelial surface to be maintained in *ex vivo* culture for several weeks

as in donor human cornea banking, and the relative immune privilege of the anterior chamber of the eye (Jun and Larkin, 2003). Although a number of monogenic disorders of the endothelium have been characterised at a molecular level (Biswas et al., 2001; Toma et al., 1995; Vithana et al., 2006), gene correction strategies have not been investigated, in part due to the lack of animal models to verify treatment concepts and the availability of corneal transplantation as current therapy. Benefits of gene therapy in inherited corneal endothelial disease would have to match those of transplantation and outweigh any risks associated with gene transfer. A more likely application of gene transfer as a treatment modality lies in *ex vivo* modification of donor cornea and its endothelium in the period of eye bank storage prior to transplantation. This provides a window for gene transfer, reducing the risks of *in vivo* application of viral or non-viral vectors. Several *ex vivo* gene therapy approaches to endothelium have shown promise in experimental studies. In the following sections, we review current techniques of gene transfer to the corneal endothelium with respect to their prospects for clinical application.¹

1.5.1. Choice of gene delivery methods

A crucial decision in the planning of gene transfer is the choice of methodology to enable the genetic sequence of interest to be incorporated into the cell. Factors to be considered include the estimated proportion of endothelial cells in which transgene expression is required, the duration of expression, the size of the gene of interest and associated regulatory sequences. Although cells take up naked DNA to a certain extent, this does not provide sufficient levels of transgene expression for a biological effect in most studies. Non-viral gene transfer using chemical or electrical methods has been reported to enable transgene expression in up to 50% of

¹ Major parts of this chapter were published in a review during the course of this thesis. Reprinted in part from *Experimental Eye Research*, Volume 95, Issue 1, February 2012; D. Kampik, R.R. Ali, D.F.P. Larkin: Experimental gene transfer to the corneal endothelium, pages 54–59. Copyright 2012, with permission from Elsevier.

corneal endothelial cells, but this is transient. In contrast, some recombinant viral vectors can transfer large transgenes and achieve high and persistent expression levels in all endothelial cells, but bear additional risks compared to non-viral methods.

1.5.2. Non-viral methods of gene transfer

Non-viral methods of gene transfer are comparatively straightforward to use and quality control is not difficult (Uchida et al., 2002). They evoke almost no immune response and in principle do not carry the risks inherent in viral vectors resulting from cell surface expression of viral proteins or insertional mutagenesis. Non-viral vector methods reported for gene transfer to corneal endothelium *ex vivo* include polyamidoamine dendrimers (Hudde et al., 1999), liposomes coupled to antibodies to allow selective targeting of gene delivery (Tan et al., 2003), and a polylysine-based vector (Collins and Fabre, 2004).

Electroporation and ballistic gene transfer are physical methods of DNA transfer in which a vector is not used. Electroporation has been used to transduce cultured human corneal endothelial cells (Engler et al., 2009; Joyce and Harris, 2010) and rat corneal endothelium *in vivo* following marker plasmid DNA injection into the anterior chamber (Oshima et al., 1998). Electroporation can cause significant endothelial cell injury (Joyce and Harris, 2010), and transgene expression is both short-term and very inefficient, only a small percentage of cells expressing the gene.

In conclusion, non-viral gene transfer methods are useful in experimental applications in which transgene expression limited to a small proportion of cells and for a short term is sufficient, possibly with repeat applications, and in which the absence of immunogenicity is important (Pleyer et al., 2001). Potential applications in human corneal disease are currently limited.

1.5.3. Viral vectors

Since earliest reports in the mid-1990s there have been developments in construction, production and safety of engineered viral vectors. Their main advantage over non-viral techniques is the potential for high transduction efficacy and, if desired, long-term transgene expression. Since human corneal endothelial cells normally do not undergo mitosis, only those viruses capable of transducing non-dividing cells can be considered in this species (Parker et al., 2009a). It is noteworthy that AAV, although used in current clinical gene therapy trials for retinal pigment epithelium (Bainbridge et al., 2008; Maguire et al., 2008) and for possibly many future applications in the retina (Buch et al., 2008), shows little or no transduction efficacy in mice, rabbit, or human corneal endothelium (Hudde et al., 2000) (Lai et al., 2002). Even with novel pseudotyping strategies combining the vector genome of one AAV serotype with the capsid of another serotype (Auricchio, 2003), transduction levels remain low (as shown for AAV2/1, 2/2, 2/5, 2/7, and 2/8 in human corneas *ex vivo*, (Liu et al., 2008)) or undetectable (as shown for AAV2/1, 2/2, 2/5, 2/7, 2/8, and 2/9 in mice (Lebherz et al., 2008)).

1.5.3.1. Adenoviral vectors

Adenovirus was the first viral vector used for gene transfer to corneal endothelium (Larkin et al., 1996). 75-100% of rabbit corneal endothelial cells showed transgene expression after *ex vivo* infection with recombinant adenovirus. In addition to high transduction efficacy, main advantages of adenoviral vectors are their large transgene capacity of 5–8 kb, which can be increased up to 36 kb by depletion of all coding viral regions (gutless, high-capacity or helper-dependent adenovirus) (Alba et al., 2005; Parks and Graham, 1997; Weber and Fussenegger, 2006). Further advantages of adenoviral vectors are their ability to transduce both dividing and non-dividing cells, easy large-scale production and safe handling. For these reasons adenoviruses are the most widely used vectors in gene therapy clinical trials. Adenoviral vectors have been

shown to transduce corneal endothelium of mouse (Budenz et al., 1995; Qian et al., 2004), rat (Fehervari et al., 1997; Jessup et al., 2005b; Lai et al., 2001; Pleyer et al., 2000), rabbit (Hudde et al., 2002; Larkin et al., 1996), sheep (Klebe et al., 2001b; Klebe et al., 2001c), pig (Thiel et al., 2005), as well as human endothelium *ex vivo* (Bertelmann et al., 2003; Jessup et al., 2005a; McAlister et al., 2005). It is noteworthy that immunogenicity limits the use of adenoviral vectors. Adenovirus activates broad innate immune responses (Hartman et al., 2008) in addition to, in the anterior segment of the eye, a cell-mediated immune response which accounts for the transient nature of transgene expression and makes it inappropriate for some applications (Bennett, 2003; Hoffman et al., 1997). New generation helper-dependent or 'gutless' adenovirus devoid of all viral coding regions result in a highly reduced immune response and might therefore be applied even in a cornea transplantation setting (Alba et al., 2005).

1.5.3.2. Adeno-associated viral vectors

Adeno-associated virus (AAV), non-pathogenic in humans, is gaining importance as a gene therapy vector thanks to its low immunogenicity, stability and the potential to integrate into the host genome without known side-effect (Büning et al., 2008). The first clinical gene therapy trial for the eye used AAV serotype 2 to deliver human *RPE65* cDNA to correct the gene defect causing Leber's Congenital Amaurosis and demonstrated safety and efficacy of subretinal virus application (Bainbridge et al., 2008; Maguire et al., 2008). AAV remains the most widely used vector for ocular gene delivery, with prospects not only for gene replacement therapy, but also for applications like vector-mediated neuroprotection, modulation of angiogenesis and inflammation to treat a wide range of acquired retinal disorders (Buch et al., 2008). By 'pseudotyping' the vector, i.e. combining the vector genome of one AAV serotype with the capsid of another serotype, the characteristics of the vector can be modulated with respect to target cell type and expression time (Auricchio, 2003). Among the vectors discussed here, AAV's 4.8 kb transgene capacity is the smallest (Dong et al., 1996). This can be doubled by splitting the transgene and

packaging it into two AAV vectors. After co-transduction, the genome is rejoined and requires the use of eukaryotic RNA splicing signals to yield the coding mRNA (Sun et al., 2000).

The naturally high prevalence of neutralizing antibodies against AAV2 in the adult population does not hamper AAV vector efficiency when administered in the subretinal space (Barker et al., 2009; Simonelli et al., 2010). Readministration of AAV-2 into subretinal space 2–3 years after the first treatment for LCA was found safe without immune responses or toxicities, and effective in terms of improving visual functions (Bennett et al., 2012).

However, the use for corneal endothelium proved far less promising. *Ex vivo* in whole-thickness rabbit and human corneas, only 2% of endothelial cells showed transgene expression after infection with AAV2, with a peak at 3 or 4 weeks (Hudde et al., 2000). Also in mice low endothelial transduction was observed (Lai et al., 2002). Consistent with findings in non-ocular tissues, AAV delivered transgene expression was inducible by inflammation in rabbits: after injection of lipopolysaccharide into the anterior chamber and thereby inducing a cellular inflammatory response, over 90% of endothelial cells expressed AAV mediated transgene. But without inflammation, only 3% of cells expressed the transgene (Tsai et al., 2002). With novel serotypes using pseudotyping strategies, some new vectors effectively transduced corneal stromal cells in mice (AAV2/7, 2/8, and 2/9), but not endothelial cells. Neither AAV2/1 nor 2/2 nor 2/5 transduced any corneal cells (Lebherz et al., 2008). Liu et al. were able to detect low levels of GFP in all corneal layers after infection with AAV2/1, 2/2, 2/5, 2/7, and 2/8 in a human corneal culture (Liu et al., 2008). AAV might therefore not be suitable for applications requiring high protein expression levels in the endothelium, but has advantages in targeting the stromal keratocytes. High transduction rate and long-term expression (up to 17 months *in vivo* in mice) are reported after transduction with AAV2/8 (Hippert et al., 2012).

1.5.3.3. Herpes simplex virus vectors

Herpes simplex virus infects a variety of host cells, both dividing and nondividing. Due to comparatively low transduction efficacy (5% in human corneas *ex vivo*) and unacceptable toxicity it has not been investigated further as a vector for the cornea (Hudde et al., 2000; Klebe et al., 2001b).

1.5.3.4. Lentiviral vectors

Lentiviruses are a subgroup of retroviruses and deliver single stranded RNA to the host cell, which is reverse transcribed into cDNA. This transcript then integrates into the host genome and yields stable, long-term transgene expression. In contrast to other retroviruses, lentivirus can transduce non-dividing cells, making this a candidate vector for gene transfer to post-mitotic neurons and other non-dividing cells in target organs including liver, eye, heart and pancreas (reviewed in Cockrell and Kafri, 2003; Wiznerowicz and Trono, 2005). The transgene capacity for common lentiviral vector platforms is 8 kb. When transgene size exceeds 10 kb, viral titres decreased significantly (Kumar et al., 2001), and the larger the transgene, the lower is transduction efficacy (Cante-Barrett et al., 2016). However recently, standard lentiviral vectors with a large transgene of approximately 11,000 kb have been produced and successfully used *in vitro* to deliver full-length dystrophin gene with GFP (Counsell et al., 2017).

The most prominent lentivirus is human immunodeficiency virus (HIV). Other species are simian immunodeficiency virus (SIV), equine infectious anaemia virus (EIAV), caprine arthritis-encephalitis virus (CAEV), and the feline and bovine immunodeficiency viruses (FIV and BIV). All have been engineered into vectors to mediate gene delivery.

Research has focused on the safety of lentiviral vectors (LV), deleting as many viral accessory genes as possible while maintaining its transduction capability (Somia and Verma, 2000; Zufferey et al., 1997). Four generations of LV have evolved so far (reviewed in Cockrell and Kafri, 2007, Delenda, 2004). All packaging generations harbour *gag* and *pol*, the indispensable

genes encoding structural proteins (MA, matrix protein; CA, capsid protein; SP1, spacer peptide 1; NC, nucleocapsid protein; SP2, spacer peptide 2; and p6 in *gag*) and viral enzymes (reverse transcriptase, integrase, and HIV protease in *pol*).

First generation LV were devoid of *env* encoding the wildtype viral envelope, but still contained viral accessory genes, *vif*, *vpr*, *vpu*, and *nef*, which are required for infection or reproduction, or act as virulence factors (Naldini et al., 1996a; Naldini et al., 1996b). LV were rendered replication incompetent by deleting the ψ packaging element from the helper plasmid, thereby preventing the retroviral RNA genome to be packaged into the vector capsid. Only the expression cassette with the transgene is incorporated.

Second generation LV provide increased biosafety through deletion of all accessory genes, while regulatory genes *tat* and *rev* are conserved (Naldini et al., 1996a; Zufferey et al., 1997). Second generation LV contain less than 5% of the wild type viral genome. In current third generation LV platforms, *tat* is deleted and *gag/pol* separated from *rev*, which is provided on a separated plasmid. This further reduced the risk of recombination and hence the chance of producing replication competent virus (Dull et al., 1998). Additional modifications in the transfer vector genomes (harbouring the gene of interest) include a deletion of viral promoter sequences in the U3 region of the 3' LTR. Upon transduction of the host cell, the mutated U3 is copied to the 5' LTR, which inactivates the LTR promoter, thereby rendering the LV 'self-inactivating' (SIN) (Iwakuma et al., 1999; Zufferey et al., 1998).

HIV based vectors usually do not use the wildtype viral envelope, which would restrict tropism to CD4+ T cells, macrophages, and microglial cells. Instead, the VSV G envelope glycoprotein from the vesicular stomatitis virus is used to coat (pseudotype) the LV, giving it a broad tropism to infect almost any cell type (Akkina et al., 1996). With these modifications, HIV-based LV are now used in phase I clinical trials to treat systemic disorders like X-linked adrenoleukodystrophy (Cartier et al., 2009), β -thalassaemia (Cavazzana-Calvo et al., 2010), and adenosine

deaminase-severe combined immunodeficiency (ADA-SCID, ClinicalTrials.gov identifier NCT01279720, estimated study completion date 2018).

A major concern in LV application is the risk of malignant transformation of transduced cells through insertional mutagenesis. Integration of proviral DNA into the host genome may damage the natural genetic arrangement of the target cell (Romano et al., 2009). Such vector-induced insertional events may stimulate oncogene transactivation or tumour-suppressor gene inactivation. Oncogene transactivation has been observed in two patients in the French SCID-X1 trial in which a Moloney-derived retroviral vector retrovirus was used (Hacein-Bey et al., 1996; Hacein-Bey-Abina et al., 2003; Li et al., 2002). For lentiviral vectors no instances of oncogene activation have been described so far (Cockrell and Kafri, 2007). The introduction of SIN vectors has reduced the likelihood of insertional mutagenesis by deleting the viral promoter/enhancer sequences. In applications where host genome integration is not required, non-integrating LV have been developed by mutating the viral *integrase* gene, almost eliminating the risk of insertional mutagenesis (Philpott and Thrasher, 2007; Yanez-Munoz et al., 2006).

In vivo transduction of corneal endothelium has been shown in mice, rats and rabbits, with different outcomes regarding transduction efficacy. Bainbridge et al. injected VSV-G pseudotyped self-inactivating lentiviral vectors delivering GFP (2 μ l, 4×10^8 transducing units/ml) into the anterior chamber of mice (Bainbridge et al., 2001). Transgene expression was detected in the endothelium by 7 days and was stable for at least 4 weeks. Balaggan et al. investigated equine infectious anaemia virus (EIAV) pseudotyped with VSV-G in mice. $2-3 \times 10^7$ virus particles injected into the anterior chamber produced long-term transduction of the corneal endothelium for up to 10 months (Balaggan et al., 2006). In contrast, a rabies-G-pseudotyped vector mediated no detectable eGFP fluorescence in the majority of endothelial cells.

In rats, a single lentiviral injection of 10^7 or more viral particles into the anterior chamber resulted in a high expression of the reporter gene (Challa et al., 2005), but no detailed information was given about transduction efficacy or duration. In rabbits, 4×10^6 viral particles of

feline immunodeficiency virus (FIV)-based injected into the anterior chamber resulted in more than 95% of the corneal endothelial surface expressing GFP fluorescence above background within 7 days (Liu et al., 2010). GFP fluorescence disappeared within 40 days after injection, probably due to an inflammatory reaction against GFP.

Ex vivo settings enable investigation of vector behaviour and transgene effects without the interference of the immune system. Beutelspacher et al. compared two lentiviral vectors, self-inactivating HIV-1 and equine infectious anaemia virus (EIAV)-based vectors (Beutelspacher et al., 2005). They demonstrated a transduction rate of ~20% for HIV, ~40% for EIAV-based vectors (5×10^5 vector particles) in rabbit corneas cultivated *ex vivo*. Expression remained constant over 8 weeks.

For *ex vivo* transduction of rat and sheep corneas, Parker et al. used 2.5×10^7 transducing units (TU) / cornea of HIV based lentiviral vectors expressing eYFP under the control of the Simian virus type 40 intermediate early promoter (Parker et al., 2007). At a multiplicity of infection (MOI) of 400 (rat) and 20 (sheep), 88% of rat and 84% of ovine corneal endothelial cells expressed the transgene. Interestingly, rat endothelium reached its peak expression level after 2 days post transduction, ovine endothelium showed a delay of one to two weeks. For long-term transgene expression, transduced corneas were transplanted and observed *in vivo*. eYFP could be detected after 2 months in rat corneal isografts, and 1 month in sheep corneal allografts.

To investigate human corneal endothelial transduction, Suh et al. transduced primary endothelial cells using 5×10^8 to 1×10^9 TU/mL of EIAV-based lentivirus, pseudotyped with either vesicular stomatitis virus (VSVG) or rabies virus. At a corresponding to a MOI of 100, they achieved transgene expression in ~30% of cells after 3 days (Suh et al., 2007). FACS sorting after 7 days showed a higher transduction efficacy of the EIAV-rabies vector (16.12%) over the EIAV-VSVG vector (4.92%), in contrast to the findings of Balaggan et al. in mice described earlier (Balaggan et al., 2006). However, this study was done using primary cultures of human corneal

endothelial cells obtained from a 3-year-old donor. Cells from young donors are easier to cultivate but are usually not available for routine experiments.

Ex vivo transduction of human corneal endothelium in situ has been first done using a VSV-G pseudotyped HIV-based lentiviral vector (Wang et al., 2000). Corneo-scleral rims from the eye bank and corneal specimens obtained at corneal transplant surgery were cut in pieces and exposed to 10^6 – 10^7 lentiviral particles for 24h. GFP transgene was visualized at all layers exposed to the virus, in the epithelium, endothelium and stromal cut edge after 3 days in culture, but not quantified. A long transgene expression for 60 days was shown, but only for primary keratocytes in culture, not for the endothelium.

Beutelspacher et al. assayed different lentiviral vectors for transduction efficiency in human corneal endothelium (Beutelspacher et al., 2005). EIAV-based lentivirus achieved higher transduction rates than HIV-based lentivirus (~20% versus ~5%, respectively, using 5×10^5 infectious particles per cornea for 3h). For both vectors, expression in the endothelium was stable over 8 weeks in *ex vivo* culture. Extended quantifications were performed by Parker et al., who used 2.5×10^7 TU/cornea (MOI 120) of HIV-based LV in 200 μ l HEPES-RPMI medium containing 2% FCS (Parker et al., 2007; Wang et al., 2000). 14 days after transduction, 83.0% of endothelial cells were transduced (range 77–89%, n=2 corneas). When comparing two doses of virus, MOI of 30 versus MOI of 120, they observed a higher transduction in the higher MOI group: 25–35% for the lower MOI and 15–95% for the higher MOI (n=7 human corneas). However, the high variability between samples suggests other (unidentified) factors to determine transduction efficacy. No correlation was seen between transduction efficacy and days in culture (maximum 14 days) or number of days the cornea had been stored in the eye bank (0–25 days).

Although lentiviral vectors elicit innate and adaptive immune responses (Follenzi et al., 2007), no significant immune response is described after ocular administration. However compared to non-integrating adenoviral vectors, non-integrating and even integrating LV are less

efficient in corneal endothelium (Parker et al., 2010), a disadvantage that in a corneal transplant setting might be outweighed by their lower immunogenicity.

1.5.4. Applications of gene delivery to corneal endothelium

1.5.4.1. Immune modulation to prevent graft rejection

Transduction of immunomodulatory genes to donor corneal endothelium prior to transplantation has been a widely used strategy to prevent or delay allogeneic rejection and the most frequent application of gene transfer methodology. As a number of mechanisms of corneal immune privilege and of rejection are mediated by cell surface proteins or soluble factors in the aqueous humour, it may be possible to supplement immune privilege or attenuate the impact of rejection by modulating their expression. Because expression of an immunomodulatory molecule on the endothelial cell surface or secretion of a soluble protein into the anterior chamber might be required for several months' duration in order to delay transplant rejection to a clinically meaningful extent, virus vector-mediated gene transfer has been investigated in most studies to enable sustained high efficiency expression using replication-deficient adenoviral or lentiviral vectors. Following transfer to donor cornea prior to transplantation, therapeutic transgenes encoding the following proteins have been shown to prolong corneal graft survival: soluble TNF receptor (Rayner et al., 2001), soluble CTLA4.Ig (Comer et al., 2002), interleukin-10 (Klebe et al., 2001c), the p40 subunit of interleukin-12 (Klebe et al., 2005; Ritter et al., 2007), indoleamine 2,3-dioxygenase (Beutelspacher et al., 2006) and nerve growth factor (Gong et al., 2007). Transplant models in which these candidate genes have been investigated are mouse, rat, rabbit and sheep. The factor common to these studies was the transfer of the immunomodulatory gene of interest to the highest possible number of donor endothelial cells in order to either enable the most widespread cell protection or maximise the secreted soluble protein into the anterior chamber post-transplant.

Two of the above studies are especially worth comment. The cytokine interleukin (IL)-10 down-regulates MHC class II and co-stimulatory molecule expression on monocytes, macrophages, and dendritic cells and inhibits the synthesis of pro-inflammatory cytokines. Using a sheep corneal transplant model, *ex vivo* transfection of donor corneal endothelium with an adenoviral construct encoding IL-10 demonstrated significant prolonged survival of transduced donor corneas (median survival time (MST) 55 days) compared with vector control corneas (MST 21 days). IL-10 expression was detected at 21 days, and no evidence of immunologic or inflammatory responses was present after transplantation (Klebe et al., 2001c). The more beneficial effect on transplant survival in this report indicates the importance of cDNA selection in such studies. In a second study Beutelspacher et al. investigated the effect of indoleamine 2,3-dioxygenase (IDO) overexpression by a lentivirus in donor murine cornea on allograft survival. Excised donor C3H strain corneas were transduced *ex vivo* with the lentivirus equine infectious anaemia virus (EIAV) expressing IDO prior to transplantation into fully mismatched BALB/c recipients. Significantly prolonged survival of IDO-transduced allografts (MST 21 days) resulted, compared with GFP-transduced or mock-transduced corneas (MST 11 days). Immunohistochemistry indicated IDO expression in the endothelial layer (Beutelspacher et al., 2006). There is clear potential for improvement in effects of such gene modification strategies in transplantation. The main challenges are to reduce immunogenicity of viral vectors, or increase efficacy of non-viral vectors.

1.5.4.2. Increasing corneal endothelial cell density

Corneal endothelial cell density is the main parameter used to assess graft quality before transplantation. New posterior lamellar surgical techniques enable selective transplantation of Descemet's membrane and endothelium, but require even higher cell densities to compensate for cell loss due to intraoperative manipulation. A method to increase corneal endothelial cell density during storage might help not only to reduce the proportion of donor corneas deemed

unsatisfactory for transplantation on account of low cell density, but also to extend graft longevity after transplantation. Two concepts have emerged so far, inhibition of apoptosis and induction of cell cycle progression.

Apoptosis (in contrast to necrosis) has been proposed as the predominant cause of endothelial cell death in donor corneas maintained in 34°C culture (Albon et al., 2000; Komuro et al., 1999), but this finding is disputed. While Albon et al. have determined apoptosis by TUNEL staining, Crewe et Armitage used a more sensitive method by caspase 3 staining and conclude that apoptosis is not a significant mechanism of endothelial cell loss in organ culture (Crewe and Armitage, 2001). Nevertheless, anti-apoptotic strategies have been used during organ culture to increase corneal endothelial cell density. Over-expression of mammalian *Bcl-xL*, a gene of the anti-apoptotic *Bcl-2* family, in mouse corneal endothelial cells *in vitro* using a lentivirus vector has been reported to significantly reduce experimentally induced apoptosis. Furthermore, *Bcl-xL* transduction into corneal endothelium in a mouse allotransplant model extended graft survival (Barcia et al., 2007). p35 is a protein discovered in baculovirus, a virus incapable of infecting mammals, and inhibits apoptosis by a wide range of stimuli. Overexpression of p35 in human corneal endothelial cells prevents apoptosis, with a greater protective effect against apoptosis mediated via the intrinsic pathway than *Bcl-xL* (Fuchsluger et al., 2011b). This was also tested on endothelium of human corneas under eye bank conditions modified to induce cell death. Lentivirus mediated p35 prevented experimentally induced apoptosis more effectively than *Bcl-xL* during both 37°C and hypothermic (4°C) storage conditions (Fuchsluger et al., 2011a).

A different approach to increase corneal endothelial cell density uses gene transfer to directly control genes and transcription factors regulating the cell cycle. Proliferation is a process tightly regulated by the cell-division cycle, a series of molecular events that has been highly conserved throughout evolution. After completing G1 phase, which prepares the cell for DNA duplication, it advances into the S phase in which DNA synthesis occurs, which leads to a cell

division, or, if aborted, to apoptosis. The subsequent G2 and M phases generate two daughter cells. Unlike corneal epithelium, endothelial cells have not exited the cell cycle but remain arrested in the G1 phase and retain their proliferative capacity (Joyce, 2003, 2005; Joyce et al., 1996b). E2F is a transcription factor family regulating the transition from G1 to S phase (DeGregori et al., 1997; DeGregori et al., 1995). Overexpression of *E2F2* in non-proliferating rabbit corneal endothelial cells induced cell cycle progression, as shown by upregulation of cell cycle specific marker genes such as Ki67 or cyclin B1 (Joyce et al., 2004). Gene transfer of *E2F2* using an adenovirus vector resulted in replication of human corneal endothelial cells in corneal culture, leading to an increase in cell density without inducing significant apoptosis (McAlister et al., 2005). These encouraging results do not alone justify application of these methods in human corneal transplantation, as adenovirus-induced changes in immunogenicity would be likely to increase the rates of immune rejection of such gene-modified donor corneas. Alternative vectors are currently under investigation in our laboratory.

Another strategy for modulating the cell cycle is to down-regulate inhibitory signals preventing cells from entering the cell cycle. This was shown for cyclin-dependent kinase inhibitors p21 and p16, both negative regulators of the cell cycle (G1-phase inhibitors). Small interfering RNA (siRNA) transfected into corneal endothelial cells *in vitro* decreased protein levels of p21 and p16, thereby increasing the number of cells expressing Ki67, a marker of cell cycle progression, and total number of cells (Joyce and Harris, 2010). This gene knock-down approach is another with potential for translation in eye banking.

Both the above strategies, inhibition of apoptosis and induction of cell cycle progression, use transgenes with oncogenic potential. Reliable safety mechanisms for use in clinical settings have yet to be established. These will probably include a combination of features. Non-integrating vectors cannot integrate the transgene into the host genome and therefore minimize the risk of insertional mutagenesis. Inducible promoters are already available, and it may be possible to develop endothelium-specific promoters, which would be active only in corneal

endothelium. Endothelial cells being easily accessible in *ex vivo* culture, repeat applications would allow titration of the desired biological effect.

1.5.5. Methods to increase corneal endothelial cell density

To date, the only method used therapeutically in humans to increase corneal endothelial cell density is corneal transplantation, either as a full thickness graft or as a posterior lamellar graft. Posterior lamellar grafts techniques evolved from thick lamellar grafts used in Descemet's Stripping Automated Endothelial Keratoplasty (DSAEK, between 150 and 50 μm in thickness) to Descemet Membrane Endothelial Keratoplasty (DMEK, 12–14 μm thickness), the current method of choice (Anshu et al., 2012b; Kruse et al., 2014; Melles et al., 2006). Here, Descemet's membrane with the attached endothelial cell layer is peeled off the donor cornea. Descemet's membrane spontaneously forms a roll, which can be injected into the anterior chamber through a 2.2 mm incision. Once in the anterior chamber, the roll is unfolded with the help of an air bubble, which then presses donor Descemet's membrane into place at the posterior corneal surface. Advantages of thin grafts are better anatomical outcome and an almost negligible risk of immunologic graft rejection (Anshu et al., 2012a; Price and Price, 2013). Compared to full thickness transplants, however, any lamellar procedure requires more manipulation both for preparing the graft and for intraoperative positioning, exposing the fragile endothelial layer to more stress and causing higher surgery-induced endothelial cell loss (Nanavaty et al., 2014). Long term outcomes of endothelial keratoplasty procedures in large patient cohorts are not yet available, but it would not be unexpected if faster rates of donor endothelial cell density decline were found in these eyes compared to penetrating transplants. To make use of the advantages of the new procedure, we need donor corneas with high endothelial cell count.

A variety of methods have been proposed to increase corneal endothelial cell density in *ex vivo* or *in vitro* models. Corneal storage methods have been improved constantly by using nor-

mothermic culture at 31°C to 37°C, limiting the endothelial cell loss in donor corneas to 8% at two months postoperatively (Redmond et al., 1992). Adding growth factors to culture medium slowed down endothelial cell loss, but no method so far proved useful to increase endothelial cell density (Bourne, 2001). Tissue engineered endothelial sheets are a promising new concept allowing also autologous grafts (Audet C, Proulx S, Uwamaliya J et al., Determination of the Minimal Size of a Biopsy for the Reconstruction of an Autologous Corneal Endothelium by Tissue Engineering. ARVO abstract 1798/A466, 2009), but are still far from clinical application (Proulx et al., 2009; Yamagami et al., 2006). Okumura et al. describe a new cell culture protocol that enables transplantation of CECs in the form of a cell suspension without the use of a carrier (Okumura et al., 2014a). In an ongoing clinical trial, cultured CECs together with a ROCK inhibitor are injected into the anterior chamber of the eye, as an alternative to penetrating or lamellar corneal transplantation for bullous keratopathy (clinical trial registration: UMIN000012534). Further research is optimising the culture conditions for this procedure (Hamuro et al., 2016; Toda et al., 2017).

Studies using the first direct molecular approach to induction of corneal endothelial cell replication have been undertaken by this laboratory in collaboration with Dr Nancy Joyce (Schepens Eye Research Institute, Boston). A recombinant adenoviral vector was used to transfer cDNA encoding the transcription factor *E2F2* *ex vivo* to whole thickness rabbit (Joyce et al., 2004) and human corneas (McAlister et al., 2005), resulting in cell cycle progression and increase in endothelial cell density. Another molecular strategy is using siRNA to down-regulate expression of p21WAF1/cip1, a G1-phase inhibitor normally expressed at high levels in endothelial cells from older donors (Joyce and Harris, 2010).

1.6. Retinal pigment epithelium

1.6.1. Anatomy and physiology

The retinal pigment epithelium (RPE) is a monolayer of pigmented cells covering the outer retina (extensively reviewed by (Strauss, 2005)). On its apical side, long microvilli closely interact with the photoreceptor outer segments and the interphotoreceptor matrix. Its basolateral side faces Bruch's membrane, a multilayered, elastin- and collagen-rich extracellular matrix that separates the RPE from the fenestrated choriocapillaris (Booij et al., 2010). Its thickness increases from 2 μm at birth to 4–6 μm at the tenth decade of life (Ramrattan et al., 1994). The RPE consists of melanin containing, hexagonally packed epithelial cells connected by tight junctions, gap junctions and adherens junctions. It is a highly polarized structure, with the surface of the apical membrane being three times greater than the one of the basolateral membrane (Strauss, 2005). Due to different functions depending on location, RPE cells in the central retina are smaller than in the periphery. Macular RPE cells are 14 μm in diameter and 12 μm in height; peripheral RPE cells can have a diameter of 60 μm with variable height (Strauss, 2005; Streeten, 1969).

“Located between the photoreceptors of the retina and their principal blood supply, the choriocapillaris, the retinal pigment epithelium is critical for the survival and function of retinal photoreceptors.” (Marmorstein, 2001). For this purpose, the RPE acts as three types of cell – epithelium, macrophage, and glia (Steinberg, 1985).

Epithelial functions

Already during embryologic development, the functional differentiation of photoreceptors depends on growth and differentiation factors of the RPE and vice versa (Hollyfield and Witkovsky, 1974). In the developed eye, the RPE transports ions, water and metabolic end products from the subretinal space to the blood and delivers nutrients from the blood to the

photoreceptors. The vitamin A derivative retinal, a key molecule necessary to initiate a visual response, is transported as all-*trans*-retinal from photoreceptors to the RPE. Only RPE cells are capable of isomerising all-*trans*-retinal into 11-*cis*-retinal, which is transported back into the photoreceptors to maintain their excitability. Furthermore, the RPE is responsible for stabilising ion composition in the subretinal space, an additional prerequisite for phototransduction (Steinberg, 1985). By secreting immunosuppressive factors, the RPE plays an important role in establishing the immune privilege of the eye (Ishida et al., 2003; Streilein et al., 2002). With its apical tight junctions the RPE constitutes the outer blood-retina barrier by separating the choroidal space with fenestrated capillaries from the subretinal space.

Macrophage functions

These epithelial qualities aside, RPE cells also act as macrophages. The constant shedding of photoreceptor outer segment discs into the subretinal space accounts for the bulk of material metabolised in the RPE. Discs are phagocytised by the RPE, digested and essential substances are recycled and returned to the photoreceptors, while some of the breakdown products are voided into the choroidal blood supply via Bruch's membrane (Finnemann, 2003; Marshall, 1987). Each retinal rod produces 80–90 discs per day, and the entire complement of outer segment discs is replaced every 9–13 days. Each RPE cell engulfs and destroys about 2000–4000 outer segment discs daily (Young, 1971). Phagocytosis and lysis of discs cause a high load of toxins and reactive oxygen species (Miceli et al., 1994).

Glial functions

RPE cells also function as glia by maintaining the structural integrity of the photoreceptor outer segments (Steinberg, 1985). With its microvilli, the RPE forms sheaths for photoreceptor outer segments. Together with the interphotoreceptor matrix, RPE cells help maintain photoreceptor alignment (Bonilha, 2013; Hollyfield, 1999; Spitznas and Hogan, 1970).

Light absorption and protection

Another crucial function of the RPE is the absorption of light. By forming a dark cover of the inner wall of the eye, the melanin granules of the RPE increase optical quality through the absorption of scattered light. The focus of light onto the highly pigmented fovea in the human eye results in a strong concentration of photo-oxidative energy and a high load of free radicals at the RPE (Strauss, 1995). To avoid photooxidative damage, the RPE has three lines of defence (Boulton and Dayhaw-Barker, 2001). Firstly, the RPE's complex composition of pigments containing melanin, lutein and zeaxanthin ensures light absorption and filtering especially of dangerous blue light. Secondly, high levels of antioxidants, both enzymatic (superoxide dismutase and catalase) and non-enzymatic (ascorbate, α -tocopherol, β -carotene, glutathione) help to reduce oxidative stress (Miceli et al., 1994; Newsome et al., 1990; Organisciak and Vaughan, 2010). The third line of defence is the cell's physiological ability to repair damaged DNA, lipids, and proteins (Strauss, 2005).

1.6.2. Pathological conditions

Under physiologic conditions, the human retinal pigment epithelium is a non-dividing cell system (Kaldarar-Pedotti, 1979; Marshall, 1987). However, the continuous load of photoreceptor discs to be phagocytised by the RPE can lead to long-term damage. In contrast to a normal macrophage which has a transient existence and dies after ingesting its target material, a single RPE cell ingests 2000–4000 outer segment discs daily over a whole life span (Marshall, 1987; Young, 1971).

With increasing age, the RPE suffers a net loss of cells, which is compensated by increase in size of the cells remaining. From apoptosis marker studies in young and old human donor eyes, Del Priore et al. calculated that nearly 20% of the macular RPE would be lost per decade in older human eyes (Del Priore et al., 2002). However, metabolic capabilities of the remaining cells

seems to decline with age and result in the accumulation of incompletely degraded particles called lipofuscin granules (Feeney, 1973; Marshall, 1987). In humans, at about the age of 40 years waste products begin to accumulate in the RPE and cells attempt to rid themselves by pushing them out through Bruch's membrane, leading to toxic waste deposits (Kinnunen et al., 2012; Marshall, 1987; Sparrow et al., 2010). When reaching a certain size, these become visible on clinical fundus examination as drusen, the most important symptom of age-related macular degeneration (AMD) (Delori et al., 2000; Delori et al., 2001; Hageman et al., 2001; Sarks, 1976). Accumulation of toxic substances induces apoptosis of RPE cells, while the epithelial layer initially remains intact (Dorey et al., 1989). The remaining cells enter a vicious circle: their higher metabolic burden causes further accumulation of reactive oxygen species, further deposits of lipofuscin and toxic end products, which weaken the cell's metabolic efficiency, leading to a further loss of RPE cells with a secondary loss of photoreceptors (atrophic, non-neovascular, "dry AMD") (Zarbin, 2004). Inflammatory processes including complement activation play an additional role in RPE apoptosis and can lead to abnormal vessel formation through Bruch's membrane. These choroidal neovascularisations (CNV) cause blood and protein leakage into the subretinal space (neovascular, exudative, "wet" AMD) (Jager et al., 2008).

AMD is the leading cause of blindness in the elderly worldwide, affecting 30–50 million individuals, 14 million of which are blind or severely visually impaired (Gehrs et al., 2006). Up to one-third of the people older than 75 have some form of AMD (Klein et al., 1997; Klein et al., 1992). Due to the rapidly aging population, the number of persons suffering from advanced forms of AMD will increase by 50% to 2.95 million in 2020 (Friedman et al., 2004).

Currently, there is neither a preventive nor curative treatment for AMD. No established treatment options can be offered to the majority of patients (~90%) affected with non-neovascular AMD. For neovascular AMD, the most widely used treatment involves administration of antibodies against vascular endothelial growth factor (VEGF) to prevent the formation of

new blood vessels (Brown et al., 2009; Catt Research Group et al., 2011; Ivan Study Investigators et al., 2012; Rosenfeld et al., 2006).

While age-related conditions account for the majority of cases causing vision loss, primary gene defects in the RPE can cause hereditary retinal dystrophies. Owing to the close interaction of RPE and photoreceptor cells, mutations in genes of the RPE first manifest in changes in the photoreceptors (Preising and Lorenz, 2009). Endpoint of all these diseases is a loss of both photoreceptors and RPE. Examples are autosomal recessive Leber's Congenital Amaurosis (LCA) caused by a defect in the *RPE65* gene (den Hollander et al., 2008), Best disease (defect in *BEST1*, Petrukhin et al., 1998), chorioideremia (defect in *REP1*, van den Hurk et al., 1997), oculocutaneous albinism (defect in *TYR*), early-onset severe retinal dystrophy (defect in lecithin retinol acyltransferase gene, *LRAT*, Thompson et al., 2001) and certain forms of autosomal recessive retinitis pigmentosa (defects in *MERTK* or *RLBP1*, Wang et al., 2001).

Besides these relatively few primary RPE disorders, there are many photoreceptor dystrophies that lead to secondary RPE loss (da Cruz et al., 2007; Michaelides et al., 2006). Stargardt disease, an AR disorder and the commonest form of childhood macular dystrophy, is caused by a defect in *ABCA4*. The encoded protein plays as key role in recycling of the visual pigment, resulting in RPE cell death (Sundaram et al., 2012; Walia and Fishman, 2009). Defects in *RP2* or *RPGR* cause X-linked retinitis pigmentosa (Michaelides et al., 2006). Achromatopsia is due to defects in *CNGA3*, *CNGB3*, *GNAT2* and *PDE6C*, genes involved in the cone phototransduction cascade, and can be accompanied with RPE degeneration (Johnson et al., 2004; Kohl et al., 2002; Thiadens et al., 2009).

1.6.3. Current methods for treating RPE defects

Replacement of RPE is a treatment concept for age-related macular degeneration and other diseases caused by RPE loss or dysfunction. It has been pursued over decades in various tech-

niques in animal models and clinical trials. However, no method so far was both efficient and technically feasible to be translated into standard treatment.

Macular translocation surgery aims to relocate the neuroretina to an area where pigment epithelium is less diseased. It involves complete retinal detachment followed by a peripheral circumferential retinotomy. The whole retina is then rotated so that the fovea comes to lie on a more peripherally located, healthy part of the RPE and choroid. First described by Machemer in 1993 (Machemer and Steinhorst, 1993), there is now an extensive literature showing recovery of some useful visual function and reversal of loss of acuity (da Cruz et al., 2007). At one to five years after surgery, distance and near visual acuity improved in more than half of the patients (Aisenbrey et al., 2002; Mruthyunjaya et al., 2004; Pertile and Claes, 2002; Takeuchi et al., 2012; Toth et al., 2004). Overall, the success of macular translocation is held as a proof of principle that RPE repopulation under the macula restores vision (da Cruz et al., 2007). However, the complex surgery involving two or more procedures (oculomotor globe counterrotation) can have serious complications and long-term effect is often limited (Chen et al., 2010; MacLaren et al., 2005; Yamada et al., 2010). It is therefore not recommended as a standard treatment (Eandi et al., 2008).

Great hope lies in RPE transplantation, either as autologous RPE or allogeneic RPE derived from stem cells (extensively reviewed by Binder et al., 2007 and da Cruz et al., 2007). First RPE transplantation experiments in animals were described 30 years ago (Gouras et al., 1985; Gouras et al., 1984; Gouras et al., 1989). Human transplants used initially were allogeneic (from a freshly enucleated eye or a fetal eye), but did not have beneficial effects due to immune reaction, which occurs despite the immune-privilege of subretinal space (Algvere et al., 1994; Algvere et al., 1999; Peyman et al., 1991). Therefore, autologous transplantation was put forward.

An interesting concept is to use the iris pigment epithelium (IPE) as autologous source for RPE replacement, which showed better results regarding stabilisation of visual acuity

(Aisenbrey et al., 2006; Thumann et al., 2000; Thumann et al., 1997). Owing to their common embryogenesis from neuroepithelium, both cell types share their ability to phagocytose photoreceptor outer segments, though for IPE cells at a lower capacity (Dintelmann et al., 1999), and IPE does not express certain crucial enzymes of the visual cycle (Cai et al., 2006).

Promising results were achieved using autologous full-thickness grafts harvested from the midperiphery, comprising RPE, Bruch's membrane, choriocapillaris and choroid (Heussen et al., 2008; Jousseaume et al., 2007; MacLaren et al., 2007; van Meurs and Van Den Biesen, 2003). The difficulty of this technique and its possible complications and limitations, have so far prevented this becoming a standard procedure. In order to facilitate the surgical procedure, Binder et al. transplanted RPE cell suspensions harvested through a retinotomy in the nasal area of the optic disc (Binder et al., 2004). van Meurs et al. undertook a similar approach (van Meurs et al., 2004).

Stem cells could provide a readily available source of standardised donor RPE cells and would solve the problem of harvesting cells from the affected patient eye. Possible sources include embryonic stem (ES) cells, retinal progenitor cells, and bone marrow-derived stem cells (Haruta et al., 2004; Heller and Martin, 2014; Lund et al., 2006). In an ongoing clinical trial, human embryonic derived RPE cells are transplanted as a cell solution into one patient with Stargardt's disease and one patient with dry AMD, slightly improving visual acuity (Schwartz et al., 2012; Schwartz et al., 2015). Human induced pluripotent stem cells (iPS cells, Takahashi and Yamanaka, 2006) have also been used to derive RPE cells and have now been granted permission to be used in a clinical trial to treat AMD (Cyranoski, 2013; Song et al., 2013).

Despite decades of research, to date there is no consensus over the best method to treat RPE defects. The complex anatomy of subretinal space, the various functions of RPE cells and their intricate interaction with photoreceptors and Bruch's membrane impose difficulties greater than expected. For autologous RPE transplantation, harvesting of sufficient cells and maintenance of their metabolic functions are the biggest problems. For allogeneic RPE, it is not yet clear if the immune privilege of the subretinal space is sufficient to avoid immune reactions.

1.6.4. Proliferative capacity of the RPE

RPE cells can proliferate *in vivo* as a natural reaction to disruption of the subretinal space during retinal detachment (Anderson et al., 1981; Machemer and Laqua, 1975; Machemer et al., 1978). However, when they leave their natural environment of the subretinal space these cells transdifferentiate into macrophages and fibroblast-like cells and may achieve myofibroblast-like characteristics (Kampik et al., 1981).

Al-Hussaini et al. investigated the capacity of RPE cells to enter the cell cycle *in vivo* while the retina is in place (i.e. not detached) (Al Hussaini et al., 2008). In rats as well as in humans, they demonstrated the presence of a few RPE cells in the periphery expressing proliferation markers (Ki67, PCNA, BrdU uptake in rats; Ki67 in humans), and reported evidence that these cells undergo a full cell cycle. The majority of cells, however, are being retained abnormally in the cell cycle and are not able to progress through to full cell division (Adams et al., 2010). In humans, the proliferation rate is insufficient to compensate loss due to age or disease (Del Priore et al., 2002).

In vitro, mammalian RPE cells can be released from cell cycle arrest and can be cultured for up to six months, undergoing several population doublings (Albert et al., 1972). They retain their morphologic characteristics, show polarity, and are capable of photoreceptor outer segment phagocytosis and metabolism. Only a fraction of the harvested cells divide. The rate of cell division depends on the age of the donor: the younger, the faster the growth curves (Flood et al., 1980). RPE cells from the periphery grow better *in vitro* than those harvested from the macular region, and this differential increases with age (Flood et al., 1984; Marshall, 1987).

If it was possible to either abrogate cell cycle arrest or induce proliferation in the RPE in a controlled manner, this may have therapeutic effects on diseases with loss of RPE such as age-related macular degeneration.

1.7. Gene transfer to the retinal pigment epithelium

Thanks to (i) its natural phagocytic activity, (ii) its accessibility via the subretinal space between photoreceptors and RPE, (iii) its pump function directed from the subretinal space toward its basolateral side, (iv) its immune privilege, and (v) its amitotic state, the RPE is more amenable to gene delivery than many other cells, as for instance corneal endothelium without phagocytic activity and a pump function directed away from the cell layer. For several diseases of the RPE causing severe visual impairment, the causative gene defect is well defined. Most forms of retinal degeneration show a recessive inheritance pattern with a loss-of-function mutation that can be addressed by gene replacement. For these reasons, gene therapy for RPE-based diseases is a well-developed field of research not only in animal models but also in clinical trials (Smith et al., 2009). Furthermore, retinal degenerations originating in the RPE show a slower disease progression than those originating in the photoreceptors.

Surgical procedures to deliver vector to the subretinal space have been developed for almost any animal model. In mice, trans-scleral / trans-choroidal injections posterior to the eye's equator can deliver vector suspension as a subretinal bleb covering up to 80% of the RPE; the bleb (i.e. retinal detachment) is absorbed within hours. In larger animals, a trans-vitreous / trans-retinal approach through the limbus or pars-plana is easier. In humans, subretinal vector injections are performed with a pars-plana vitrectomy followed by a small retinectomy to access the subretinal space. After vector injection, the retinal wound is closed by laser photocoagulation. All these surgical steps are well-standardized interventions for other common retinal diseases, especially retinal detachment.

Both non-viral as well as viral vectors have been used for RPE transduction. Physical methods including electroporation and iontophoreses have been used in small animal models (Charbel Issa and MacLaren, 2012; Trapani et al., 2014). Chemical methods allow transduction of the RPE, mainly liposomes, cationic polymers such as polypeptides and polysaccharides, and

compacted nanoparticles. The advantages here are safety (no immune reaction, no gene insertion) and large size of gene that can be delivered, allowing delivery of the gene of interest with gene regulatory elements and intronic sequences to enhance expression. All non-viral methods, however, are associated with a significant degree of physical damage or toxic side effects to both the photoreceptors and the RPE, and furthermore, non-virally administered DNA is prone to gene silencing by methylation (Chen et al., 2004). Strategies to confer DNA integration into the host genome applying Sleeping Beauty transposon or viral integrase could overcome this disadvantage (Trapani et al., 2014). Overall, studies using non-viral gene transfer report variable results regarding transduction efficacy, and no direct comparisons to viral gene delivery have been made so far.

Until today, viral vectors have been the method of choice for effective transduction of the RPE. Most widely used vectors are lentivirus, adenovirus and adeno-associated virus. Only LV integrate their transgene into the host genome, for the other two the transgene remains episomal. They differ in cloning capacity from 4.8 kb for AAV, 8 kb for LV, up to 36 kb for Ad (cf. Chapter 1.5.3 Viral vectors, page 34, for references).

Ad vectors, with a particle size of 100 nm the largest of the vectors, efficiently transduce the RPE and photoreceptors with a fast onset of expression, and were among the first vectors to be used in ocular gene therapy clinical trials: to treat retinoblastoma with suicide gene therapy using an Ad vector to deliver the *thymidine kinase* gene intravitreally (Chevez-Barrios et al., 2005); and to treat neovascular AMD using intravitreal delivery of adenoviral vector expressing human pigment epithelium-derived factor (Campochiaro et al., 2006). However, due to their immunogenicity even at an immune privileged site as the subretinal space, so far no clinical trials using Ad for RPE or photoreceptor delivery have been performed.

Lentiviral vectors are slightly smaller than Ad vectors, and show similar transduction efficacy in the RPE. They achieve transgene integration in the host cell genome, which offers potential advantages in longevity of expression even in the amitotic RPE of the adult human. The high

capacity offers transfer of large genes or even two or more genes in a bicistronic or dual-promoter construct. They elicit almost no immunological response in the subretinal space. Currently, clinical trials (phase I/IIA) delivering EIAV vectors pseudotyped with VSV-G via subretinal delivery are being carried out for patients with Usher syndrome type 1B (or associated with retinitis pigmentosa, ClinicalTrials.gov Identifier NCT02065011, NCT01505062) and Stargardt's macular degeneration (NCT01367444, NCT01736592).

AAV vectors are the smallest (25 nm) vectors available, facilitating efficient transduction of not only the RPE but also various retinal layers. Various available serotypes can be combined with different capsids which themselves can be mutated in myriad ways, offering the possibility to systematically modulate tropism. All variants used to date transduce the RPE to some extent after subretinal delivery. Highest transduction efficacy for the RPE is achieved by AAV2/1, 2/4, 2/6, 2/Tyr mutant (reviewed in Trapani et al., 2014). For AAV2/7m8, RPE transduction is reported even after intravitreal injection (Dalkara et al., 2013). AAV's low immunogenicity allows for long-term transgene expression and even re-administration of the vector to the subretinal space (Bennett et al., 2012).

Proof-of-concept studies of AAV-mediated correction of RPE-originating retinal degenerations date back to 2003: Smith et al. demonstrated rescue of the RCS rat model of retinitis pigmentosa by subretinal application of using AAV2/2 delivering *MERTK* (Smith et al., 2003). This has now led to a phase I clinical trial using a rAAV2/2-VMD2-hMERTK vector (ClinicalTrials.gov Identifier NCT01482195).

The very first clinical trials for an inherited retinal degeneration using gene therapy were directed to treat Leber congenital amaurosis (LCA), and used AAV2/2 delivering *RPE65* gene (Bainbridge et al., 2008; Hauswirth et al., 2008; Maguire et al., 2008). Conclusions from these trials were that AAV administration is safe and well tolerated and can improve retinal function. A new phase III trial is ongoing, with vision improvement as primary outcome measure (assessed in mobility testing), treating both eyes via surgical procedures on separate days, and

including patients as young as 3 years (NCT00999609). To restrict gene expression to the RPE, the same transgene, but with the specific RPE65 promoter in the more RPE-specific AAV2/4, is used in a different phase I/II trial (NCT01496040).

With safety and tolerability now addressed in several clinical trials, other gene replacement therapies are likely to follow soon. For instance, defects in *lecithin retinol acyltransferase* (LRAT), an enzyme expressed in the RPE, also cause LCA. An animal's vision has been rescued using AAV1 (Batten et al., 2005). The far larger group of patients, however, could be addressed by augmentation gene therapy for multifactorial, chronic diseases, foremost AMD. Neovascular AMD is currently treated with monthly intravitreal injections of anti-antibodies against vascular endothelial growth factor (VEGF). A first clinical trial for neovascular AMD has recently been published (NCT01494805, Rakoczy et al., 2015). Rakoczy et al. used AAV2 encoding sFLT-1, a highly potent naturally occurring VEGF inhibitor, delivered by a single subretinal injection. One-year results from 6 treated patients showed no adverse events and no evidence of chorioretinal atrophy. Four out of 6 patients required no more anti-VEGF injections, indicating a treatment effect.

1.8. Central hypothesis and aims of this study

While all tissues of the eye are affected by degeneration to some extent, degeneration of certain tissues is sight threatening. Both the corneal endothelium and the retinal pigment epithelium are associated with blinding disease. Despite their capacity to undergo replication, their natural replication rates are insufficient to compensate for natural loss, especially when age and disease coincide.

The central hypothesis of this study was:

Gene transfer of cell cycle modulating genes can induce proliferation in naturally amitotic tissues of the eye, specifically the corneal endothelium and retinal pigment epithelium.

Overall aim was to develop methods to induce cell regeneration *in situ*, i.e. without displacing these cells from their basal lamina – in contrast to regeneration by cell transplantation. For the corneal endothelium, *in situ* regeneration could be applicable in the eye bank to improve corneal graft quality. We aimed

- (1) to evaluate available vectors to transduce human corneal samples *ex vivo*
- (2) to assess the effect of overexpression of cell cycle regulating factor E2F2, using adenoviral or lentiviral vectors
- (3) to harness the regulatory potential of the ZO-1/ZONAB pathway to induce endothelium proliferation, either through lentiviral vector-mediated knockdown of *ZO-1* or overexpression of *ZONAB*.

The concept of *in situ* regeneration was then extended to the retinal pigment epithelium *in vivo*. We aimed to assess the effect of lentivirus mediated E2F2 overexpression on cell cycle status, RPE cell density and integrity, *in vivo* in wildtype and RPE deficient transgenic mice.

2. Materials and Methods

2.1. General molecular biology

2.1.1. Cloning strategies

In general, cloning of the gene of interest into a vector backbone was achieved by opening up the vector plasmid with a double restriction digest to ideally create sticky DNA ends. The insert DNA was amplified by PCR with proofreading polymerase (*Pfu* polymerase), or used directly from amplified plasmid DNA. Insert fragments were subjected to the same restriction digest as the backbone. After purification, ligation reactions were performed and the new plasmid transformed into *E. coli*.

If appropriate restriction enzymes could not be found, a transfer vector was used. The PCR-amplified gene of interest, flanked by recognition sequences for topoisomerase I, was first ligated with a linear vector carrying the topoisomerase enzyme at either end. This transfer vector also contained a set of two flanking recombination sequences, enabling site-specific recombination. The gene was then shuttled into a suitable destination vector (Gateway cloning technology, Invitrogen, UK). Cloning strategies were developed using Lasergene software, version 7.0.1 (DNASar, USA).

2.1.2. Polymerase chain reaction (PCR)

Primers for PCR reactions were designed by PrimerSelect software, version 7.0.1 (DNASar, USA) or online using the Universal ProbeLibrary Assay Design Center provided by Roche Diagnostics Ltd. (<https://www.roche-applied-science.com/sis/rtpcr/upl/index.jsp?id=UP030000>).

A standard PCR reaction mix (25 μ L total volume) consisted of the following components: 2.5 μ L 10 \times buffer, 2.5 μ L MgCl₂ (25 mM), 1 μ L dNTP mix (10 mM), 1 μ L of each forward and reverse primer (10 μ M), 0.5 – 1 μ L polymerase enzyme (GoTaq DNA polymerase, 5 U/ μ L, Promega, UK), 10 – 20 ng template DNA from plasmid (50 – 100 ng for genomic DNA), ultra-pure H₂O (free of DNase and RNase) to make up 25 μ L. All reactions were carried out in duplicate or triplicate. A positive control containing a DNA sequence of interest, and a negative control with H₂O instead of the template, were run alongside. Typical PCR cycling conditions were:

Initial denaturation	3 min at 95°C	
Denaturation	30 sec at 95°C	} 35 cycles
Annealing	30 sec at 50-54°C	
Extension	1 min at 72°C	
Final extension	10 min at 72°C	

Products of PCR were analysed by electrophoresis (see 2.1.4).

2.1.3. Restriction enzyme digests

To characterize DNA plasmids or fragments, or to isolate fragments of interest, DNA was selectively cut using restriction enzymes (Promega, UK, or New England Biolabs, UK). Typically, 0.5 – 1 μ g of DNA, were added to 1 μ L of appropriate 10 \times buffer, 0.5 μ L restriction enzyme (10 U/ μ L), filled up with sterile, deionized water to a total volume of 10 μ L. The mix was incubated for one to four hours at the recommended temperature.

2.1.4. DNA electrophoresis

To separate DNA fragments of PCR reactions or restriction enzyme digests, samples were loaded on a 1-2% (w/v) agarose gel prepared with 1x TBE buffer containing ethidium bromide (1 μ L of 10 mg/mL concentration per 50 mL of gel). Samples were prepared with gel-loading buffer (Blue/Orange Loading Dye, 6 \times ; Promega, UK). A 1 kb or 100 bp DNA ladder (Promega) was run alongside to estimate the size of the fragments. For a 200 mg gel, a voltage between 120 and 180 V was applied for 30 to 60 min, according to the expected size of the DNA bands. Gels were photographed digitally on an ultraviolet transilluminator.

Ethidium bromide concentration was reduced to a 1:100 dilution when attempting difficult cloning procedures in order to reduce DNA chelation that hinders ligation.

2.1.5. DNA extraction from agarose gels

DNA fragments used for cloning were cut out of the agarose gel and extracted using a silica-gel-based purification kit (QIAquick Gel Extraction Kit, QIAGEN, UK) according to the manufacturer's instructions. Concentration of eluted DNA was measured by photospectroscopy at 260 nm (NanoDrop ND-1000 Spectrophotometer, LabTech Int., UK).

2.1.6. DNA ligations

Ligation of the gel purified DNA fragment with the appropriate vector backbone was performed using 1:3 molar ratio of insert to vector. DNA was first heated to 45°C for 5 min to melt any annealed cohesive ends, and then cooled on ice. 20 – 100 ng of DNA was added to a mixture of 1 μ L T4 DNA ligase (New England Biolabs, UK), 2 μ L of the provided 10x ligation buffer containing ATP and MgCl₂, filled up to 20 μ L with H₂O. For blunt end ligations, a higher concentra-

tion of DNA and ligase was used. After incubation overnight at 4°C or for 3 – 4 h at 16°C, the ligase was heat inactivated for 10 min at 65°C. 5 – 10 µL of the ligation mixture was used to transform competent bacterial cells.

2.1.7. Amplification of plasmid DNA in bacteria

Plasmids were amplified in *E. coli*. Each plasmid used contained an ampicillin or kanamycin resistance gene as a selection marker for successfully transformed bacteria.

For transformation, chemically competent DH5α cells (α-Select, Bioline, UK) from -80°C were thawed on wet ice. 50 µL of cells were incubated with 5 – 10 µL of ligation mixture for 30 min on ice. After heat shock for 40 sec at 42°C in a water bath, cells were re-placed on ice for 5 min. 1 mL SOC medium (Invitrogen, UK) was added and cells were incubated for 1 h at 37°C to allow sufficient expression of the resistance gene. Bacteria were then plated on agar plates containing the appropriate antibiotic and incubated at 37°C overnight.

Agar plates were prepared using Luria Bertani (LB) medium (25 g powder, Merck, UK, for 1 L of H₂O) supplemented with 15 g/L of bacteriological agar (Oxoid, UK). After autoclaving and cooling to ~37°C, 100 µg/mL ampicillin or 100 µg/mL kanamycin (both Sigma-Aldrich, UK) was added and the agar poured into 10 cm Petri dishes to harden.

Bacterial colonies grown on selective agar plates were inoculated into 5 mL of LB medium with antibiotic and incubated over night at 37°C with agitation to further amplify the bacterial clone. An alkaline-SDS lysis, spin column based kit (GenElute Plasmid Miniprep Kit, Sigma-Aldrich, UK) was used to recover up to 20 µg of plasmid DNA. For large-scale preparation of up to 2.5 mg transfection grade plasmid DNA, bacteria were grown in 0.5 L of LB medium with antibiotic for 16 h and an anion-exchange column based kit was used (Plasmid Mega Kit, Qiagen, UK).

For long-term storage, 800 μ L of LB overnight culture of the desired clone was mixed with 200 μ L of sterile glycerol (Sigma-Aldrich, UK) in a cryo tube and kept at -80°C .

2.1.8. Sequencing of plasmid DNA

Clones were first screened for correct insertion of the gene of interest using appropriate single or double restriction digests. Plasmid DNA of up to five positive clones was then sent for sequencing (MWG Biotech, UK). Appropriate primers (synthesized by Sigma-Aldrich, UK) were ordered to obtain sequence readings of the whole insert with neighbouring parts of the backbone, especially the promoter region. Sequence readings were compared using Seqman Pro software, version 7.0.1 (DNASTar, USA).

2.1.9. mRNA extraction and cDNA synthesis

For gene expression analysis of transgenes or cell cycle related genes, total RNA was extracted using a silica membrane / salt buffer system (RNeasy Mini Kit, Qiagen, UK) according to the manufacturer's instructions. RNA concentration was determined by measuring the absorbance at 260 nm in a spectrophotometer (NanoDrop ND-1000, Labtech International, UK). Yields were typically ~ 5 μ g from cells grown to confluency in a 24-well plate. Total RNA was stored at -80°C .

Keeping all samples on ice, RNA was immediately reverse transcribed into cDNA using the QuantiTect Reverse Transcription Kit (Qiagen, UK), which contains oligo-dT and random primers to ensure cDNA synthesis from all regions of RNA transcripts. To ensure equal efficacy of later PCRs, in each experiment an equal amount of total RNA was used per sample (1 μ g for cell culture samples, 80-150 ng for corneal endothelial samples). The kit includes a genomic DNA

elimination step and provides a nearly 1:1 conversion ratio of RNA:cDNA. Total cDNA was stored at -20°C.

2.1.10. Real-time PCR

Gene expression was quantified by real-time PCR assays containing hydrolysis probes labelled at the 5' end with fluorescein and at the 3' end with a dark quencher dye (Roche Applied Science, UK). Assays were designed using the online Universal Probe Library Assay Design Center (Roche Applied Science). Primers used in this study (ordered from Sigma-Aldrich, UK) are listed in Table 1.

Table 1. Primers used for qPCR gene expression analysis.

*) Universal Probe Library number.

Gene	Forward primer, 5' → 3'	Reverse primer, 5' → 3'	*
<i>hβ-actin</i>	CCAACCGCGAGAAGATGA	CCAGAGGCGTACAGGGATAG	64
<i>h18S rRNA</i>	ATCCATTGGAGGGCAAGTC	GCTCCCAAGATCCAACACTACG	66
<i>hCDC20</i>	GACATCCTGCAGCTTTTGC	CTGCTGCACATCCCATAGC	64
<i>hCDK4</i>	AGCCAGAGAACATTCTGGTGA	GAACTTCGGGAGCTCGGTA	31
<i>hCyclin D1</i>	GAAGATCGTCGCCACCTG	GACCTCCTCCTCGCACTTCT	67
<i>hDHFR</i>	GCAAATAAAGTAGACATGGTCTGG	GATGGCCTGGGTGATTCAT	87
<i>hE2F2</i>	GCATCTATGACATCACCAACG	TCAAACATCCCCTGCCTAC	42
<i>hKi67</i>	TCACTGAAGGAAAAGTTTCAGGA	TTCTTATGTTTTTGTGGAGAATTTTG	73
<i>hPCNA</i>	GCGCTAGTATTTGAAGCACCA	TCTGGAATCCGAGTTGTTCA	2
<i>hZO-1</i>	TGATCATTCCAGGCACTCG	CTCTTCATCTCTACTCCGGAGACT	66
<i>hZONAB-B</i>	CCCAAGGTACCGGAGAGG	GGCTGCTTGTTGGTTCTCTT	41

Per qPCR reaction, 10 ng (corneal endothelial samples) to 100 ng (cell culture samples) of cDNA in 5 μ L volume was added to a master mix containing the following:

Component	Volume	Final concentration
FastStart TaqMan® Probe Master 2x (Roche, UK)	15 μ L	1x
Hydrolysis Probe (25 μ M)	0.3 μ L	250 nM
Forward primer (20 μ M)	0.3 μ L	200 nM
Reverse primer (20 μ M)	0.3 μ L	200 nM
H ₂ O	9.1 μ L	
Total volume	30 μ L	

The PCR was run on an ABI Prism 7900HT Fast Real-time Sequence Detection System (Applied Biosystems, UK) and the manufacturer's software (SDS, Version 2.4) was used to obtain threshold cycle values (C_T) for the reactions. Three identical replicates were run for each sample, and the averaged C_T value was used for relative quantification using the comparative C_T method ($\Delta\Delta C_T$ method, AppliedBiosystems, 2008). Target gene expression is calculated as the fold-difference of treated samples in relation to untreated controls (set as 1). First, ΔC_T was calculated from the target gene and a reference gene (β -actin or 18S rRNA):

$$\Delta C_T = C_{T \text{ target}} - C_{T \text{ reference}}$$

$\Delta\Delta C_T$ was then calculated by subtracting ΔC_T values of test sample (e.g. virus treated sample) and calibrator sample (e.g. untreated control):

$$\Delta\Delta C_T = \Delta C_{T \text{ test sample}} - \Delta C_{T \text{ calibrator sample}}$$

To calculate fold-differences between treated and untreated sample, the exponential amplification of PCR has to be taken into account (assuming 100% efficiency for both genes tested):

$$\text{fold difference} = 2^{\Delta\Delta C_T}$$

The standard deviation (*SD*) of triplicates was used to calculate the standard deviation of ΔC_T (which is the same as the *SD* of $\Delta\Delta C_T$), which was incorporated into the fold-difference to be expressed as a range, using s_1 (lower range) and s_2 (upper range):

$$s_1 = 2^{-\left(\Delta\Delta C_T - \sqrt{(SD_{C_T \text{ target}})^2 + (SD_{C_T \text{ reference}})^2}\right)}$$

$$s_2 = 2^{-\left(\Delta\Delta C_T + \sqrt{(SD_{C_T \text{ target}})^2 + (SD_{C_T \text{ reference}})^2}\right)}$$

The $\Delta\Delta C_T$ method relies on the choice of a suitable reference gene whose expression is not affected by the experimental conditions. β -actin was suitable for most applications using 293T cells or APRE19 cells. Under certain experimental conditions, β -actin has been found unreliable as a reference gene (Goidin et al., 2001; Selvey et al., 2001) – an experience we shared in the case of human corneal endothelium. Here, 18S rRNA proved to be more stable than β -actin.

For statistical analysis of relative expression results, REST software was used (Relative Expression Software Tool, REST 2009, Version 2.0.13, downloaded from Qiagen, UK, <http://www.qiagen.com/Products/REST2009Software.aspx>). The software employs randomization methods to calculate confidence intervals and *P* values, and can use multiple reference genes for normalization (Pfaffl, 2001; Pfaffl et al., 2002).

2.1.11. Western blot

For protein detection, cells were collected in ice-cold Radioimmunoprecipitation assay (RIPA) buffer (Sigma, UK; 40 μ L for corneal endothelium, 100 μ L per well for confluent cells in a 24 well plate) containing protease inhibitor (1:100, Protease Inhibitor Cocktail for use with

mammalian cell extracts, Sigma) and lysed by vortexing. Samples were spun at maximum speed for 10 min to pellet cell fragments. For cultured cells, 5 μ L of sample supernatant in triplicates was used for protein quantification in a Lowry assay (SC Protein Assay, Biorad, Hemel Hempstead, UK). The remaining supernatant was diluted in 2 \times sample buffer (12.5 mL Tris-Cl/SDS pH 6.8, 10mL glycerol, 2 g SDS, 1.5 g DTT, 0.5 g bromophenol blue) and boiled at 95 $^{\circ}$ C for 5 min.

Polyacryamide gels were composed of a 12% separating (Tris-Cl/SDS pH 8.8; 91 g Tris base, 2 g SDS in 500 mL H₂O) and a 4% stacking gel (Tris Cl/SDS pH 6.8; 12.1 g Tris base, 0.8 g SDS in 200 mL H₂O).

Equal protein amounts (typically 5 to 10 μ g) were loaded. A pre-stained molecular weight marker (Biorad, UK) was run alongside. Protein separation was performed in running buffer (for 5 \times running buffer: 1.51 g Tris base, 7.2 g glycine, 0.5 g SDS in 100 mL H₂O) at 150 V, 90 min or until bromophenol blue was visible at the bottom of the gel. A PVDF membrane (Immobilon P, Amersham, UK) was submerged first in methanol (30 sec), then in H₂O (2 min), and equilibrated for 5 min in transfer buffer (7.2 g glycine, 1.515 g Tris base, 100 mL methanol, 0.5 g SDS in 500 mL H₂O). Glass plates were separated and the gel placed on the PVDF membrane. Gel and membrane were separated from the electrodes by 3 mm filter paper. Electroransfer was performed at 20 V for 30 min, with the gel facing the cathode, the membrane facing the anode.

Blocking of non-specific binding sites was achieved by incubating the membrane in blocking buffer for one hour with agitation (5% non-fat dry milk, 1% BSA, 0.05% Tween-20 in PBS). The primary antibody was diluted in blocking buffer and incubated with the membrane overnight at 4 $^{\circ}$ C. After washing three times in PBS/Tween 0.05%, the membrane was exposed to horse-radish peroxidase (HRP)-conjugated secondary antibody in blocking solution for one hour at room temperature. After final washing five times in PBS/Tween 0.05%, HRP was visualized using ECL reagents (Amersham, UK) and X ray film or a chemiluminescence camera (UVItec Cambridge, UK).

2.2. Lentiviral vectors

2.2.1. Production

HIV based lentiviral vectors were produced using a second generation, three-plasmid system, to minimize the risk of generating replication competent viral particles.

(a) As packaging (helper) plasmid, pCMV Δ R8.74 (11.921 bp) was used delivering *gag*, *pol*, *tat*, and *rev* (the original HIV accessory genes *vpr*, *vif*, *vpu*, and *nef* were deleted or inactivated (Zufferey et al., 1997)). pCMV Δ R8.74 is a derivative of pCMV Δ R8.91 (as used previously in Bainbridge et al., 2001), in which a splice donor site has been deleted from the CMV-derived region upstream of the HIV sequences to optimize expression (Dull et al., 1998). For non-integrating lentiviral vectors, pCMV Δ R8.74intD64V was used (Yanez-Munoz et al., 2006). A mutated integrase reduced the integration of viral genome to 1/10.000 of wild type HIV (Leavitt et al., 1996).

(b) The envelope plasmid pMD2.G (5824 bp) was used to pseudotype the virus with the vesicular stomatitis virus G envelope (VSV-G) (Dull et al., 1998).

(c) The transfer vector was based on the self-inactivating lentiviral vector, pHR'SIN-cPPT. It contains the 5' and 3' LTR sequences and the central polypurine track (cPPT) fragment from wild type HIV-1 virus. To mediate self-inactivation (SIN), the U3 region of the 3' LTR has been deleted, which alleviates the risk of vector mobilization and recombination in the infected host cell (Zufferey et al., 1998). Two versions of the vector were used; pHR'SIN-cPPT-CEW, delivering the transgene under a cytomegalovirus (CMV) promoter, and pHR'SIN-cPPT-SEW, containing the U3 part of the spleen focus forming virus (SFFV) strain P long terminal repeat sequence as a promoter (Bainbridge et al., 2001; Demaison et al., 2002). The transgene was flanked by a

downstream enhancer, the woodchuck hepatitis virus posttranscriptional regulatory element (WPRE) (Zufferey et al., 1999).

A schematic overview of the virus preparation process is depicted in Figure 2. HEK-293T cells were maintained in DMEM supplemented with 10% FCS, 100 U/mL penicillin G, 100 µg/mL streptomycin, and 0.25 µg/mL amphotericin B (all Invitrogen) and used at passage 10 to 24. To keep their transfection efficacy high, cells were split frequently three times a week at a ratio of 1:3 to 1:6, and were not grown above 80% confluence. For a standard virus preparation, 10 plates were used (Nunclon Surface, Nunc, Denmark; culture area 150 cm²).

Three days before transfection (normally Friday afternoon), cells were seeded at 2.5×10^6 cells per plate in 25 mL medium. This is roughly equivalent to a 1:7 split of a near-confluent 15 cm dish, so typically 2 plates were sufficient for a 10 plate production. Medium was changed one hour before transfection. Cells were transfected using polyethylenimine (PEI) at a PEI to DNA ratio of 2.25 : 1 (w/w). Linear PEI (MW 40,000, Polysciences, Germany) was prepared at 2 mg/mL in H₂O, adjusted to pH 7.4 with HCl, and stored at -80 °C. Per 15 cm plate, 112.5 µg PEI was added to 1300 µL OptiMEM (Invitrogen) and mixed. The three plasmids, packaging, envelope, and transfer vector, were prepared at a molar ratio of 50 : 17.5 : 32.5. Per 15 cm plate, 80 µg of total plasmid DNA was added to 1300 µL OptiMEM. PEI and DNA solutions were mixed by vortexing and incubated at room temperature for 20 min to allow DNA-PEI complex formation. This was added drop wise to the 15 cm plate containing 24 mL of DMEM/10% FCS. After 4-6 h of transfection, medium was replaced with 22 mL complete DMEM/10% FCS. Culture medium was harvested 48 h post transfection and immediately replaced with fresh medium for a second harvest at 72 h. Supernatant was centrifuged at 3500 *g* for 10 min to pellet cell debris, and passed through a vacuum driven 0.45 µm filter (Stericup-HV PVSF 500ml, Millipore, UK). Supernatant was kept on ice for immediate concentration and purification.

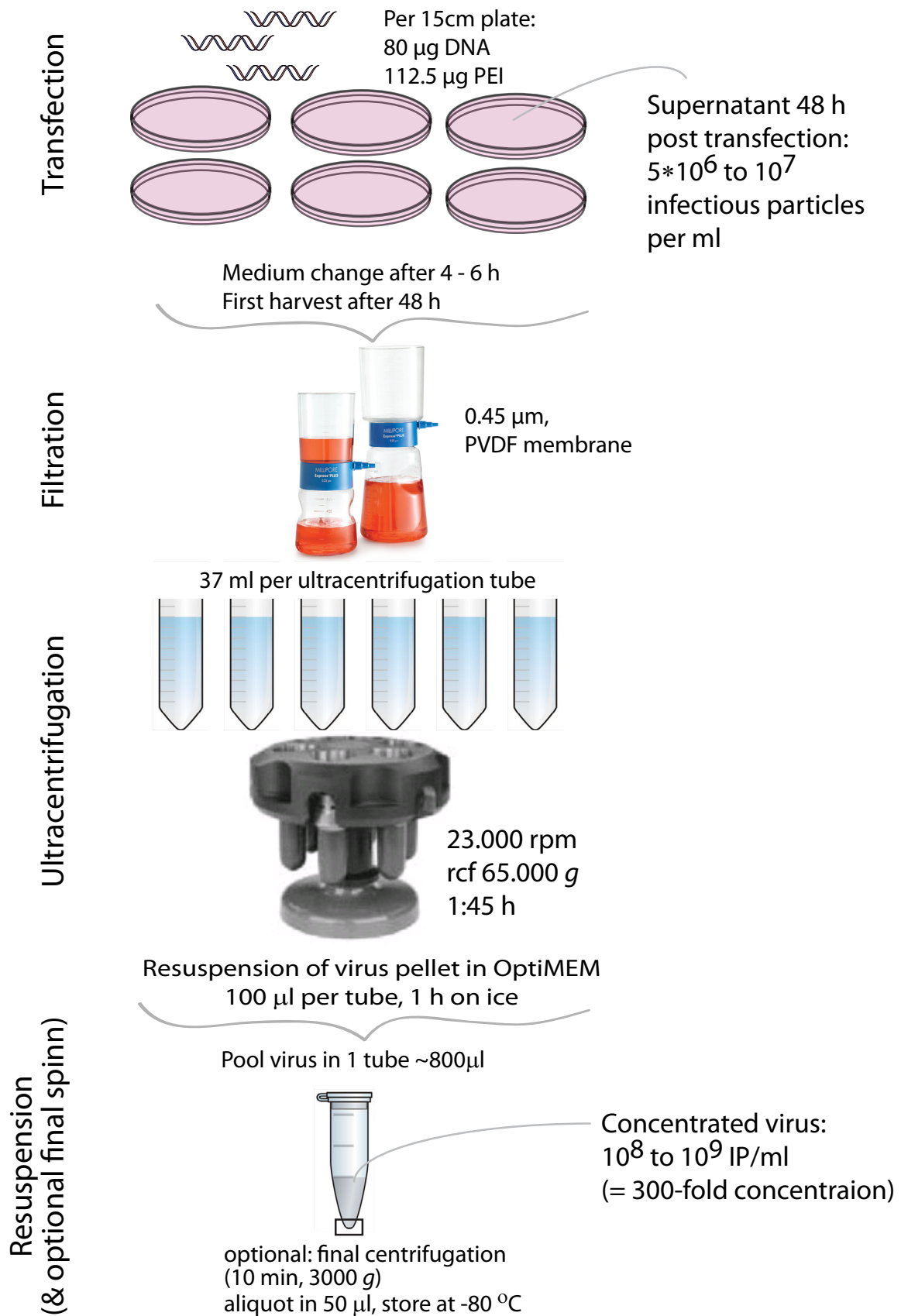


Figure 2. Preparation of lentiviral vectors.

2.2.2. Concentration and purification

Supernatant of cells 48 h after transfection contained approximately 10^5 to 10^6 virus particles per ml. For further concentration of virus, the supernatant was transferred into polyallomer ultra-centrifuge tubes (UltraClear, 38.5 ml, Beckman Coulter, UK) and ultra-centrifuged at 23.000 rpm for 1 h 45 min (rotor SW 32 Ti, Beckman Coulter), corresponding to an average relative centrifugation force of 6500 *g*. In the safety cabinet, the supernatant was decanted off and the tubes maintained upside down on tissue paper to drain the remaining supernatant. The last drops around the rim were dried with paper. 100 μ L of OptiMEM (or 50 μ L if the virus was used for subretinal injections) were added to each tube, pipetted up and down carefully ten times to dislodge the pellet. Tubes were sealed with parafilm and left on ice for 45 min to allow virus resuspension. After pipetting another ten times, all tubes were pooled and mixed. A final centrifugation step (10 min at 4000 rpm) was only done when a higher purity of virus was required, accepting a lower yield. Aliquots of concentrated virus were stored at -80 °C.

The average yield of a 10 plate virus preparation was approximately 600 μ L of concentrated virus of 10^8 to 10^9 infectious particles per ml. For the non-integrating lentivirus with a mutation in the *integrase* gene, yield was 10- to 100-fold lower.

2.2.3. Titration

2.2.3.1. Infectious titre: expression of GFP in 293T cells

For vectors containing a reporter gene (green fluorescent protein, GFP), the infectious titre (infectious viral particles per mL of virus preparation) was determined by counting GFP positive cells. 293T cells were seeded at 50.000 cells per well in a 24 well plate one day before infection. For duplicate samples, the following dilution series of concentrated virus was prepared in complete DMEM/10%FCS:

Final 1 : 10 ³	1 : 10 ⁴	1 : 10 ⁵	1 : 10 ⁶	1 : 10 ⁷	1 : 10 ⁸
2.4 µL of virus	111 µL of 2 : 10 ³ dilution	111 µL of 2 : 10 ⁴ dilution	111 µL of 2 : 10 ⁵ dilution	111 µL of 2 : 10 ⁶ dilution	111 µL of 2 : 10 ⁷ dilution
1.2 mL medium	1.0 mL medium	1.0 mL medium	1.0 mL medium	1.0 mL medium	1.0 mL medium

500 µL of each dilution was added to a well containing cells in 500 µL medium and incubated for 3 days. Medium was then replaced with PBS or 2% PFA to count the number of GFP positive cells per well under an inverted microscope (Observer.Z1, Zeiss, 10× objective). Wells of two suitable dilution steps in duplicates were averaged.

2.2.3.2. Quantification of reverse transcriptase

For vectors without reporter gene, the activity of retroviral reverse transcriptase (RT) was measured using a Reverse Transcriptase Assay colorimetric kit (Roche), according to the manufacturer's instructions. In principle, virus is lysed to free RT, which then reverse transcribes a given template. The resulting DNA is biotin-labelled and can be quantified by ELISA. A new calibration curve from the provided standard RT solution was established for every assay. Concentrated virus was diluted 1:250 and incubated for 3 h for the RT reaction.

For vectors carrying a reporter gene, both titration methods, RT ELISA and infectious titre, were carried out. Plotting corresponding RT concentrations against infectious titres revealed a correlation of $\sim 1-2 \times 10^4$ infectious particles per ng RT.

2.3. Histological analysis

2.3.1. Cryosections

Tissue fixed in 4% PFA for 1 hour was embedded in O.C.T. medium (R.A. Lamb, UK) and frozen in isopentane, which had been precooled in liquid nitrogen. Specimens were stored at -20°C and 12 to 18 µm thick sections were cut using a Bright cryostat. Slides were stored at -20°C. Sections were air-dried for 10 min and marked with a hydrophobic pen before immunostaining.

2.3.2. Immunocytochemistry and immunohistochemistry

Adherent cells grown on glass coverslips were washed in PBS and fixed in 2% paraformaldehyde (PFA) in PBS, pH 7.4, for 10 min. *Ex vivo* corneal samples were fixed for 15 min in 2% PFA, mouse eyes for up to 90 min in 4% PFA. After washing in PBS, the cell membrane was permeabilized with 0.2% Triton-X for 2 min (cell culture) or up to 8 min (whole human corneas or dissected mouse RPE). 2% normal goat serum (or serum of the species the secondary antibody was raised in), 2% foetal calf serum in PBS was used to block unspecific antibody binding sites (1h at room temperature). Primary antibody was diluted in blocking solution and incubated with the sample for 2 h at room temperature or overnight at 4 °C. A complete list of antibodies and their staining conditions can be found in Table 2. After washing twice in PBS, secondary antibody (usually raised in goat, Alexa Fluor Secondary Antibodies, Invitrogen, UK) in a 1:500 dilution in block solution was added and incubated for 1 h at room temperature. Samples were mounted in fluorescent mounting medium (DAKO, UK) after final repeated washes in PBS.

Specimens were imaged using an upright confocal laser scanning microscope (Leica TCS SPE DM5500 Q, Leica Microsystems, Germany) with the manufacturer's software (Leica LAS AF, Version 2.4.1).

Alternatively, an inverted fluorescence microscope with phase contrast was used (Zeiss Observer.Z1, Zeiss, Germany), which also allowed live cell imaging of cells grown in 6- or 24-well plates.

Table 2. Antibodies and dyes.

Name / Epitope	Company, Catalog-No	Source	Target species	Dilution (Application)	Application notes
β -actin	Sigma A5441	Mouse monoclonal	Human, Mouse, and others	1:5000 (Western blot)	Marked protein size in Western blot: 42 kDa
BrdU	Abcam Ab6326	Rat monoclonal	n/a	1:100 (IHC)	For denatured DNA only (HCl treatment)
BrdU	Invitrogen B35128, Clone MoBU-1	Mouse monoclonal	n/a	1:100 (IHC)	Used in combined EdU labelling
DAPI (4',6-Diamidino-2-phenylindole dihydrochloride)	Sigma D9542	n/a	All DNA	20 mg/mL (stock solution), used 1:5000 (IHC)	Can be used with secondary antibody
E2F2	SANTA CRUZ E2F-2 (L-20): sc-632	Rabbit polyclonal	Human	1:200 (IHC, for PFA-fixed corneal endothelial cells in situ) 1:100 (Western blot)	Marked protein size in Western blot: 55 kDa
Ki67	Abcam Ki67 antibody [PP-67] ab6526	Mouse monoclonal	Human	1:200 (IHC)	
Ki67	Sigma Clone PP-67, P6834	Mouse monoclonal IgM	Human	1:200 (IHC)	

Name / Epitope	Company, Catalog-No	Source	Target species	Dilution (Application)	Application notes
Phalloidin-TRITC (binds to F-Actin, TRITC-conjugated)	Sigma P1951	<i>Amanita phalloides</i>	Human, Mouse, and others	1:1000 or 1:10,000 50 µg/mL (IHC)	Can be used with sec- ondary antibody
PHH3 Anti-phospho Histone H3 (Ser10), Mitosis Marker	Millipore 06-570	Rabbit polyclonal	Human	1:200 (IHC)	Marked protein size in Western blot: ~17 kDa
Rb (all phosphorylation states of Rb)	BD Pharmingen 554136 Clone G3-245	Mouse monoclonal	Human (Reported: Mouse, Rat)	1:250 (Western blot)	
ZO-1	Zymed 40-2200, now Invitrogen	Rabbit polyclonal	Human, Mouse, Rat, Chicken	1:50 – 1:100 (IHC)	
ZONAB	Invitrogen 40-2800	Rabbit polyclonal	Rat, Mouse	1:100 (IHC) 1:100 (Western blot)	Marked protein size in Western blot: ~30 kDa

2.4. *In vitro* experiments

2.4.1. Cell lines

All cell lines were maintained under sterile conditions at 37°C, 5% CO₂ in a humidified atmosphere. Human embryonic kidney 293 cells containing the SV40 Large T-antigen (HEK293T or 293T cells) were used for virus production, testing and titre determination, as well as for transfections to test new plasmids. 293T cells were cultured in Dulbecco's Modified Eagle Medium (DMEM, Invitrogen, Paisley, UK) supplemented with 10% heat inactivated foetal calf serum (FCS, Invitrogen), 100 U/mL penicillin G, 100 µg/mL streptomycin, and 0.25 µg/mL amphotericin B (Antibiotic-Antimycotic solution, Invitrogen). Cells were split regularly three times a week (Monday, Wednesday, 1:3; Friday 1:5 or 1:6).

HeLa human cervix carcinoma cells were used for antibody testing in immunohistochemistry, virus infections and virus titre determination. They were treated the same way as 293T cells.

ARPE19 cells, a spontaneously arising human retinal pigment epithelium cell line with normal karyology (Dunn et al., 1996) were used for virus testing and proliferation assays. For expansion, cells were grown in DMEM/F12 supplemented with 10% heat inactivated foetal calf serum, 100 U/mL penicillin G, 100 µg/mL streptomycin, and 0.25 µg/mL amphotericin B. Cells were split 1:3 once a week. For maintenance and differentiation cultures the same medium was supplemented with only 1% FCS, and changed once a week. Cells in 1% medium hardly ever divide and do not need splitting.

2.4.2. Passaging of cell cultures

Medium was aspirated and cells were washed twice in PBS. 0.05% Trypsin-EDTA solution (Invitrogen) was added to cover the cell layer (4 mL per 15 cm plate) and incubated at 37°C for 5 min or until cells were dissociated. Trypsin was inactivated by adding complete medium with 10% FCS (min. 6 ml). Cells were squirted twice against the tissue culture plate to generate a homogenous cell suspension, which was then split into new plates in the appropriate ratio.

2.4.3. Cell line long-term storage

For long-term storage, cells in their log phase of growth were trypsinised and pelleted by centrifugation ($200 \times g$, 10 min). The pellet was resuspended in Recovery cell culture freezing medium (Invitrogen) containing FCS and 10% DMSO at approximately 5×10^6 cells/ml. Aliquots in cryogenic storage vials were placed in -80°C in a storage container containing isopropanol to ensure a controlled freezing rate. The next day, cells were transferred to liquid N₂.

For recovery, cells were removed from liquid N₂ and thawed rapidly in a 37°C water bath. Cells were added to pre-warmed medium in a plate of appropriate size (10 cm) and left to settle in the tissue culture incubator. After 4 h, medium was replaced. Cells were split when confluent, usually after 24 to 48 h.

2.4.4. Test for *Mycoplasma* contamination

Cells were tested regularly for *Mycoplasma* spp. Due to their small size (0.2–0.3 µm) and lack of a cell membrane, these bacteria can be forced through filters upon filter sterilization (0.22 µm filter). Upon virus production they tend to be purified alongside with the virus. Most

strains are resistant against antibiotics commonly used in cell culture. We used a high sensitivity PCR based detection kit (LookOut, Sigma, UK), cf. Figure 3.

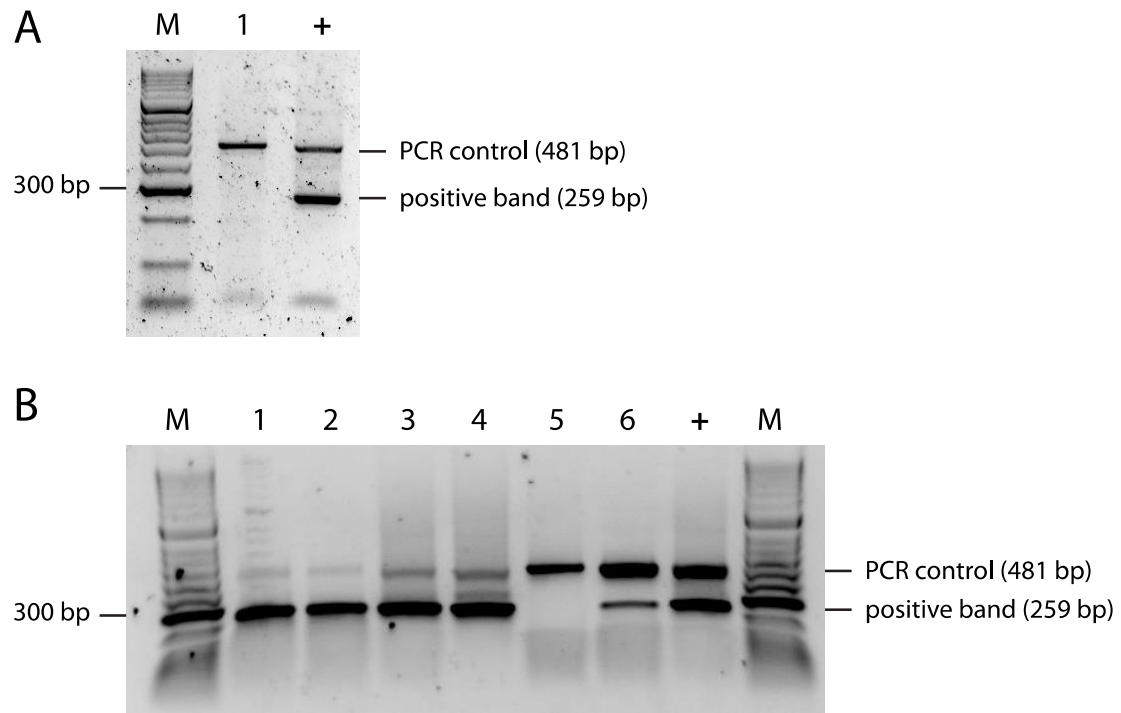


Figure 3. Test for *Mycoplasma* contamination of cell lines by PCR.

A. Example of a negative test. Sample 1 was taken from the supernatant of 293T cells, passage 18, on 10 December 2010. Every test provides an internal control for PCR an efficient reaction revealing a 481 bp band. The 259 bp band only shows up in the positive control (+). M: marker, 100 bp DNA ladder.

B. Example of a positive test. Samples 1-4 were taken from different plates of 293T cells of different passages, maintained by different members of the lab, on 10 June 2011. All show the positive band (259 bp). Sample 5: negative control showing only the internal control band (481 bp), but not the positive band. +: positive control showing both bands. M: marker, 100 bp DNA ladder.

2.5. *Ex vivo* experiments: Human corneal samples

Human corneal samples were obtained from European and United States eye banks or directly from the operating room of Moorfields Eye Hospital.

2.5.1. Ethical requirements

Specimen collection and arrangements for consents were managed in accordance with the Declaration of Helsinki. Approval by the local Research Ethics Committee was obtained to use human corneal samples for research. For the approved application (dated 13 January 2009), protocol (dated 12 December 2008), Participant Consent Form (02 February 2009), Participant Information Sheet (02 February 2009), and letter of approval (9 February 2009), see Appendix 1. Samples were treated according to the Human Tissue Act (2004) and the Human Tissue Authority's codes of practice (2009, see <http://www.hta.gov.uk/policiesandcodesofpractice/codesofpractice.cfml>, accessed 26 July 2011). All samples were disposed of by incineration at the end of each experiment.

Samples from living donors were anonymised through the Human Research Tissue Database of the pathology department of the Institute of Ophthalmology. For corneas of diseased donors, the anonymization process was already done by the eye bank. A consecutive number was allocated to each corneal specimen.

2.5.2. Types of available samples

Three types of corneal tissue were available, each type displaying different advantages and disadvantages.

Fresh corneal specimens. During full thickness corneal transplant surgery, the patient's diseased central cornea is cut out (trephined) at a diameter of 7 to 8.5 mm. This "button" would normally be discarded or, if the diagnosis was not clear, fixed in formalin for further histopathological examination. Before surgery, written informed consent was obtained from the patient after explaining the purpose of this study. None of the patients approached during this study declined this request. Under sterile conditions in the operating room, corneal specimens were immediately transferred into a vial with room temperature medium (DMEM, 2% FCS, or Biochrom Medium I, a medium commercially available and approved by European eye banks for normothermic corneal culture (Biochrom, Berlin, Germany), supplemented with 2% FCS) and then stored in the tissue culture incubator at 37°C.

Cultured donor corneas. Whole corneas with the surrounding scleral rim were obtained from deceased organ donors via Moorfields Eye Bank and other eye banks when corneas were not suitable for transplantation due to reasons unrelated to endothelial function. Common exclusion causes were insufficient donor medical history, missing serology tests, chemotherapy, high dose steroid medication, or brain surgery before 1990 (when tests for prion disease were introduced). Consent for use in research was obtained from relatives at the time of organ collection.

Corneo-scleral donor rims. For corneal transplantation, only the central cornea with a diameter of 7 to 8.75 mm is punched out from the donor cornea. The remaining corneo-scleral rim comprised the peripheral endothelium of ~3 mm width with the adjacent trabecular meshwork.

2.5.3. Culture of donor corneas

Corneas were maintained in Dulbecco's Modified Eagle Medium (DMEM, Invitrogen, Paisley, UK) supplemented with 2% heat inactivated foetal calf serum (FCS, Invitrogen), 100 U/mL penicillin G, 100 µg/mL streptomycin, and 0.25 µg/mL amphotericin B (Antibiotic-Antimycotic

solution, Invitrogen). For experiments longer than 5 days, a ready-made corneal culture medium approved by European eye banks was used (Medium I without dextran, Biochrom, Berlin, Germany – formulation not disclosed by the manufacturer). Samples were kept in 25 mL medium in T25 tissue culture flasks (whole corneas, attached by a suture to float in the middle of the flask), or 8 mL medium in 6-well plates (trephined corneal specimens), and the medium replenished every week.

Epithelial overgrowth was a problem encountered when maintaining samples that were cut in half or quarter. Epithelial cells in corneal culture proliferate almost as rapidly as *in vivo*, with high variability between samples. When the natural barrier between epithelial corneal and conjunctival cells at the limbus is missing, corneal epithelium can migrate over cut edges onto the endothelial monolayer (see Figure 12, page 119), eventually destroying the endothelium. Therefore, epithelium was scraped off the cornea at surgery before trephination. For whole corneas, the epithelial side was dipped into 20% ethanol for 30 seconds to allow easy removal of the epithelium with a blunt blade. Care was taken to not touch the endothelial side. Removal of epithelium reduced the likelihood of epithelial overgrowth after one week in culture.

2.5.4. Transduction of corneal endothelium *ex vivo*

For viral transduction of endothelium, human corneal specimens were incubated in Opti-MEM with concentrated virus preparation for 3 to 4 hours at 37°C. To achieve the highest possible virus concentration, the volume of medium was minimized. Bisected corneal specimens were transduced in 250 µL using 1.5 ml-reaction tubes. Whole corneas were placed endothelium-up on sterile stands (inverted reaction tube lids) in plastic wells and filled with 250 µL virus preparation, thereby confining viral vector to the endothelium and not wasting it on unwanted tissue. After the transduction period, samples were transferred into 6-well plates (bisected trephined specimens) or into T25 tissue culture flasks (whole corneas).

The *multiplicity of infection (MOI)* was calculated as the number of infectious particles per target cell during transduction. MOI was used as an approximation to compare transduction efficacy between virus types and preparations. Because information on endothelial cell density was unavailable for most samples, it was assumed to be on average 2,500 cells per mm², with an expected natural range between 2000 and 3000 cells per mm². The total area of the endothelial layer on the human cornea was calculated using the surface area of an oblate spheroid with the radii 5.8 mm, 5.8 mm, and 2.1 mm, which is ~262 mm² (Weisstein, 2010) , divided by 2. This gives a total number of $\sim 3 \times 10^5$ endothelial cells per whole cornea (range 262.000 to 393.000 cells). Using 50 μ L of a typical lentiviral vector preparation (titre $2\text{--}3 \times 10^8$ infectious particles per ml) for one whole cornea resulted in an MOI of 30 to 46 for an average cornea of 2,500 cells per mm². For a high-density cornea of 3,000 cells per mm², 50 μ L of vector preparation would result in an MOI of 25 to 38, for a low-density cornea of 2000 cells per mm², the same amount of vector would result in an MOI of 38 to 57, and for a very low-density cornea of 1500 cells per mm², in an MOI of 52 to 75. Therefore, due to the variability in endothelial cell density, the expected MOI used here varies between 25 and 76. For both extremes at either end of the range, the calculated MOI still lies within the same order of magnitude. The inaccuracy in MOI calculation due to the unknown variable of endothelial cell density was considered acceptable.

For a trephined corneal “button”, endothelial cell number was estimated at 150,000 cells. Taking into account the cells on the epithelial surface and stromal keratocytes which are also exposed to the virus, a total number of 3×10^5 cells was assumed, resulting in the same range of MOI.

2.5.5. mRNA extraction from corneal endothelium

Under the operating microscope, Descemet’s membrane with attached endothelial cell layer was peeled off the corneal stroma using a toothed forceps and collected directly in lysis buffer.

Total RNA extraction was performed with the RNeasy Mini Kit (Qiagen, UK) according to the manufacturer's instructions. RNA was processed as described in 2.1.9. Typical yields from a trephined corneal specimen were 100 ng, from a whole cornea 300 ng.

2.5.6. Corneal flatmounts

Corneal endothelial cells form a strict monolayer, therefore a flat mount is the only way to image and quantify all endothelial cells of a corneal specimen. Samples were washed in PBS and fixed in 1–4% (depending on the intended antibody staining) PFA in PBS, pH 7.4, for 8 – 12 min. Throughout the procedure, great care was exercised never to touch the endothelium.

After immunostaining (see 2.3.1), four radial cuts were made to flatten corneo-scleral rims or trephined corneal specimens. The sample was attached to a glass microscopic slide endothelium-side up using a small drop of cyanoacrylate glue at the edge. Four spheres of 1 mm diameter were prepared from a pressure-sensitive adhesive (Blu-Tac) and placed on each corner of the slide. A drop of fluorescent mounting medium (DAKO, UK) was added on the endothelium and a glass coverslip placed on the sample, held in place by the Blu-Tac. Human corneas swell during 37°C culture, resulting in Descemet's folds and an irregular endothelial surface. To flatten the cornea, mounted samples were placed under a 5 kg weight for min. 4 hours or overnight. A spacer between weight and base surface limited the compression to the physiological thickness of the cornea.

Imaging of immunostained corneal flatmounts was done using a confocal laser scanning microscope (Leica TCS SPE, Leica Microsystems, Germany). Although corneal samples were flattened, the endothelial surface with Descemet's folds and irregularities is difficult to bring into focus with a confocal microscope, especially when using high magnifications (40× objective). Each micrograph was therefore composed of a z stack of ~12 single images, over a z distance of 15 to 40 µm. Single images were projected on top of each other using the microscope's software.

2.5.7. Corneal endothelial cell density assessment

Corneal endothelial cell density was evaluated in flatmounts stained with 4',6-diamidino-2-phenylindole (DAPI) by counting nuclei in micrographs of defined size. On the confocal laser scanning microscope (Leica TCS SPE DM5500 Q), images were taken with the 40× lens in the blue channel (excitation wavelength 358 nm, emission wavelength 461 nm), giving an image size of 275 × 275 μm (75 625 μm² or ~0.076mm²). The focus plane was chosen so as to only image endothelial nuclei by adjusting aperture and laser power. In some highly irregular endothelial surfaces, a z-stack of ~5 images was overlaid. At least six images were taken per sample, scanning through the flatmount in a standardized method: starting from left to right, then change the y-axis and go back from right to left. A distance of one microscope field of view was left between micrographs counted. An area of 0.5 mm from the cut edges of the cornea was excluded. If the area of interest revealed gross damage of the endothelium (usually a result of manipulation during the experiment or flatmounting), it was also excluded. DAPI-positive nuclei were counted either manually or (if image quality permitted) automatically using NIH ImageJ (<http://rsbweb.nih.gov/ij/>, Version 1.46a) with the MBF Nucleus Counter plugin (http://www.macbiophotonics.ca/imagej/particle_analysis.htm, Version 1.42l, April 2009), after manual thresholding to obtain black and white images. Counts of the six or more images were averaged, comprising a total of min. 1000 to 1400 nuclei, and cell density was expressed as cells/mm².

To obtain standardized and unbiased counts, treatment and control samples were masked at the beginning of the experiment by an independent observer. Equal numbers of micrographs were counted for treatment and control samples. If any cornea had observed massive endothelial damage that prevented standardized imaging and counting, the treatment and control samples were excluded from further analysis.

2.6. *In vivo* experiments

2.6.1. Animals

Wild-type C57BL/6 mice were bred at Harlan Laboratories, UK, and used aged 6-8 weeks or up to 18 months. All animals were cared for in accordance with the Animal Scientific Procedures Act 1986 and procedures were in accordance with the ARVO Statement for the Use of Animals in Ophthalmic and Vision Research.

2.6.2. Anaesthesia

Animals were anaesthetized using a mixture of medetomidine hydrochloride (1 mg/ml, Domitor, Pfizer Pharmaceuticals, UK) and ketamine (100 mg/ml, Fort Dodge Animal Health, UK) and sterile water in the ratio 5:3:42. Adult mice weighing 20g received an intraperitoneal injection of 0.2 ml. After the surgical procedure, anaesthesia was reversed with 0.2 mL of intraperitoneal atipamezole hydrochloride (0.10 mg/ml, Antisedan, Pfizer, UK).

2.6.3. Subretinal injection of vector

Subretinal injections were performed under general anaesthesia under an operating microscope. To enable direct funduscopy, pupils were dilated with 1% topical tropicamide (Chauvin Pharmaceuticals, UK). Corneal refractive power was neutralized by placing a 5 mm coverslip on the cornea covered with a coupling medium solution (Viscotears, Novartis Pharmaceuticals, UK). The eye was held in place by holding a straight extraocular muscle and conjunctiva with a toothed forceps. Solution with vector or control solution was injected with a 34-gauge hypodermic needle mounted on a 5 μ l Hamilton syringe (Hamilton, Switzerland). The tip of the nee-

dle (bevel-up) was directed tangentially through conjunctiva, sclera, choroid, and retinal pigment epithelium where it was visible funduscopically under the retina. 2 μ l of virus suspension or control solution were injected creating a bullous retinal detachment. Retraction of the needle left behind a self-sealing tunnel. This was performed twice, one injection per retinal hemisphere. After treatment, 1% chloramphenicol ointment (FDC International, UK) was carefully applied topically on the cornea.

2.6.4. Labelling of S phase nuclei

Thymidine analogue 5-bromo-2'-deoxyuridine (BrdU) was used to label nuclei entering the S phase *in vivo* by intraperitoneal injection. BrdU (Sigma, B5002, UK) stock solution was prepared in PBS at 10 mg/ml (= 32.6 mM; 200mg BrdU powder + 20ml sterile PBS, left to dissolve for 30 min), filtered through a 0.22 μ m syringe filter, and stored at -20°C in aliquots of 1.5 ml. 30 min before injection, aliquots were thawed and vortex to re-dissolve properly. BrdU injection dose was aimed at 100 μ g/g body weight, which corresponds to approximately 2 mg BrdU per adult mouse (200 μ l peritoneal injection of a 10 mg/ml stock solution).

For immunostaining of RPE, sclera-chorioidea-RPE complex was prepared as described in the next section (2.6.5, RPE flatmounts). To enable antibody access to incorporated BrdU, DNA was denatured by incubation in 2M HCl for 30 min at 37°C . HCl was removed, neutralised with 0.1M Na-Borate for 10 min at room temperature, and the sample washed in PBS (three times for 5 min). After blocking for 1 hour (5% normal goat serum, 1% FCS, 0.2% Triton-X in PBS), the sample was incubated overnight with primary antibody against BrdU 1:100 in blocking solution. After washing, the sample was exposed to secondary antibody 1:500 for 1 hour.

For differential labelling, 5-Ethynyl-2'-deoxyuridine (EdU), also a thymidine analogue, was used as a different S phase marker in combination with BrdU. Resuspending 50 mg EdU (Invitrogen A10044, UK) in 20 ml PBS gave a stock solution of 2.5 μ g/ μ l (\sim 10 mM). EdU injection

dose was aimed at 500 µg (200 µl) per adult mouse. Other protocols suggest between 0.1 (Salic and Mitchison, 2008) and 1 mg per adult mouse (Zeng et al., 2010).

EdU was detected with a fluorescent azide in a click reaction, which was performed subsequent to BrdU staining. For this, Alexa Fluor® 647 Imaging Kit was used according to its instructions (Invitrogen C10340 and A10044, UK).

2.6.5. RPE flatmounts

Flatmounts of the whole RPE were analysed by immunohistochemistry. Mice were sacrificed by spinal dislocation, and the superior position of the eyeball (12 o'clock) was marked at the limbus using a battery cauter. Eyes were enucleated and stored in 4% PFA for 1 hour. Under a dissecting microscope, ocular adnexae and the optic nerve were removed from the sclera, and an incision was made at the cauter mark with a needle. It was extended radially to the optic nerve with small scissors to indicate the 12 o'clock position. A circular limbal cut was made to remove the anterior segment and vitreous. 4 radial cuts toward the optic nerve enabled flattening of the remaining eyecup, and the retina was peeled off the underlying RPE. The sclera-chorioidea-RPE complex was kept in a 1.5 mL reaction tube for immunostaining using a blocking solution of 5% normal goat serum, 1% FCS, 0.2% Triton-X in PBS. Eyecups were then flattened out on a glass slide, RPE facing upwards, with a paintbrush, and covered with a glass coverslip using 40 µL of fluorescent mounting medium (DAKO).

Flatmounts were imaged with a Leica TCS SPE confocal microscope. Pictures shown are multiple confocal images of a z stack projected on top of each other (usually 5 to 10 images within 10-15 µm of z stack height).

2.6.6. RPE cell density counts

Quantification of RPE cell density was done on flatmount confocal micrographs of masked samples by manually counting cells outlined with phalloidin or ZO-1 (using NIH ImageJ software, <http://rsbweb.nih.gov/ij/>, Version 1.46a). Masking was done on two levels: the flatmount slides were masked before imaging by an independent colleague. Image acquisition and image analysis were done by different researchers, and the image labels were again masked. For cell density counts, micrographs showing only the cell borders but not the transgene were used. 6 micrographs per eye acquired in a standard pattern were counted and averaged.

2.7. Statistical calculations

Statistical tests used are indicated for each experiment. For normally distributed data and comparison of two groups, Student's *t*-test was used, for comparison of three or more groups we used analysis of variance (ANOVA). If data were not normally distributed, Mann Whitney U test was used as a non-parametric alternative.

Statistical calculations and plotting of most of the graphs was performed with GraphPad Prism version 5.02 to 6.0g for Mac, GraphPad Software, La Jolla, California, USA, <http://www.graphpad.com>. Levels of significance (*P*) are usually reported with each experiment, if not, an α error ≤ 0.05 was regarded statistically significant. In graphs, the following convention was used:

n.s., not significant	$P > 0.05$
*	$P \leq 0.05$
**	$P \leq 0.01$
***	$P \leq 0.001$
****	$P \leq 0.0001$

For power calculations, we used G*Power, release 3.1.9.2, freely available from <http://www.gpower.hhu.de/> (Faul et al., 2009; Faul et al., 2007).

3. Assessment of viral vectors for human corneal endothelium *ex vivo*

3.1. Introduction

The primary application for cell cycle modulation in the corneal endothelium was improving the donor cornea *ex vivo* before transplantation. Current storage time under 37°C culture conditions in the eye bank is up to 4 weeks, providing enough time to test graft material for sterility, serology and endothelial cell quality, and to plan surgery. A reasonable time frame for *ex vivo* gene transfer would be one to two weeks, allowing the third and fourth week for assessment of gene modulation outcome and quality control. Therefore, requirements for a viral vector are: tropism for the endothelium; fast and efficient gene transfer; early onset, high-level expression; low toxicity to the target cells; and low immunogenicity.

Non-viral gene delivery offers the highest safety profile and lowest immunogenicity. Electroporation achieved high transfection efficacy in cultured human CEC *in vitro* (Engler et al., 2009; Joyce and Harris, 2010) and *in vivo* in animals with regenerative endothelium (Blair-Parks et al., 2002; Oshima et al., 1998). In corneas *ex vivo*, however, electroporation has comparatively low transfection efficacy (mean 7%, (He et al., 2010)) and can cause severe damage to the endothelium, making this method unsuitable for our aims.

Similarly, chemical transfection methods can achieve sufficient transgene expression levels in cultured CEC cells *in vitro* (Kikuchi et al., 2004; Kikuchi et al., 2006) or cultured corneas of species with replicative endothelium (Joyce et al., 2004). For *ex vivo* corneas of species with

amitotic endothelium, the transfection efficacy was below 0.01% in ovine corneas (Klebe et al., 2001b) or 6-10% in human corneas (Hudde et al., 1999).

3.1.1. Aims

Currently, only viral vectors have the prospect to transfer genes to a proportion of endothelium greater than half the cells. While many viral vectors have been thoroughly tested both *in vitro* and *in vivo*, limited knowledge is available on viral transduction in *ex vivo* culture. Especially is there no established protocol for transduction of corneal endothelium *in situ* stored at 31–37°C, as propagated in European eye banks. Our aims were

- (1) To evaluate the available types of human corneal samples for their suitability for *ex vivo* culture and *ex vivo* gene transfer
- (2) To evaluate available vectors to transduce corneal samples *ex vivo*.

We tested three viral vectors for their capability to effectively transduce *ex vivo* human corneal endothelium: Adenovirus, adeno-associated virus, and lentivirus. All vectors delivered the reporter gene *GFP* under a constitutive promoter.

3.2. Adenovirus

Adenovirus delivering GFP under the ubiquitous CMV promoter (Ad-GFP) was kindly provided by Nancy Joyce, Schepens Eye Research Institute, Harvard Medical School, Boston, USA. The serotype 5 adenoviral vector was E1- and E3-depleted and was amplified from a single plaque in transcomplementing 293A cells, a human embryonic kidney cell line stably transfected with adenovirus E1 and E3 region genes. The vector was purified by two cycles of caesium chloride density gradient centrifugation (McAlister et al., 2005). The same batch had been used

in a previous study by members of this group for *ex vivo* human corneal endothelium, where a 60-75% transduction rate is reported (McAlister et al., 2005).

Transduction parameters were based on this publication. *Ex vivo* corneal samples were exposed to Ad-GFP in 3 mL DMEM, 2% FCS, at an MOI of 20 for 3 hours at 37°C. MOI was calculated as described in 2.5.4, Transduction of corneal endothelium *ex vivo*, page 84. The sample was washed in medium and incubated for further 7 days under 37°C culture conditions. This resulted in a transduction efficacy of 80-90% in corneal epithelium, and 40-50% in the trabecular meshwork (Figure 4). Hardly any transduction was observed in the epithelium, none in the stroma or sclera.

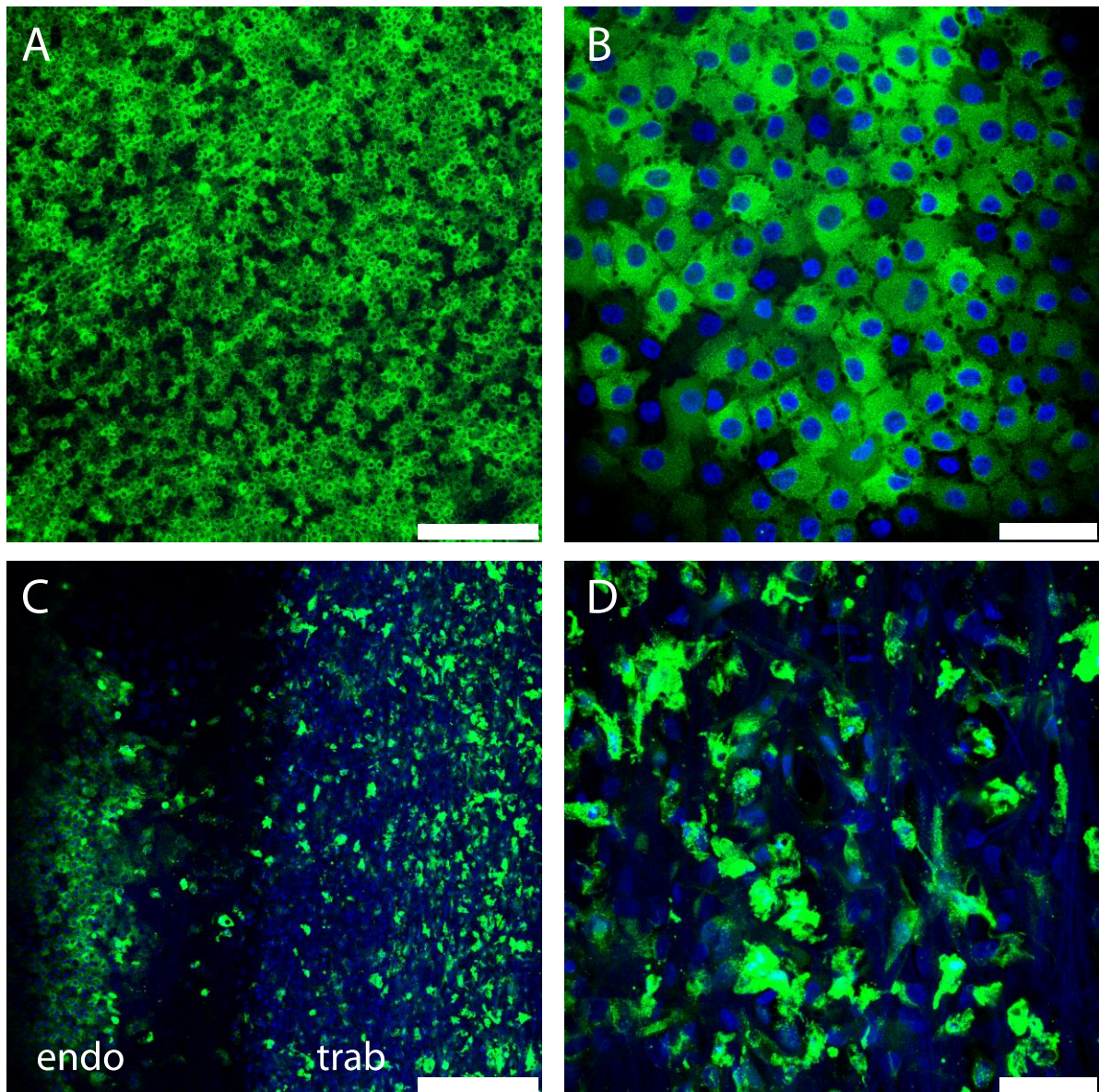


Figure 4. Adenovirus mediated transduction of corneal endothelium *ex vivo*.

Transduction of a whole human donor cornea (age 73, two days post mortem) with adenovirus delivering *GFP* (Ad-*GFP*), for 3 hours at a MOI of 20 infectious particles per cell. The sample was kept in corneal culture conditions for one week. Images show confocal laser scanning micrographs taken from a whole corneal flat mount, the endothelium facing upwards. DAPI (diamidino-2-phenylindole) was used as a nuclear dye (blue).

A. Corneal endothelium, overview. 80-90% transduction efficacy is detectable. Scale bar 250 μm .

B. Corneal endothelium. Scale bar 50 μm .

C. Junction of endothelium ("endo", left) and trabecular meshwork ("trab", right), Schwalbe's line in between. Overview, scale bar 250 μm .

D. Trabecular meshwork. ~50% transduction efficacy is observed. Scale bar 50 μm .

3.3. Adeno-associated virus

Adeno-associated virus (AAV) serotype 2/8 was used to transduce corneas at a high MOI of >50,000 virus particles per cell. AAV was produced by co-worker Dr. Mark Basche by transient transfection of 293T cells using a three plasmid system comprising of

- viral genomic plasmid based on the pd10 backbone
- packaging plasmid containing the AAV2 Rep78 gene and viral capsid gene for capsid 8
- helper plasmid pHGTI-Adeno1 containing three large portions of the Adenovirus 4 genome ligated together to provide all adenovirus genes that AAV requires to package and assemble.

AAV virions were released from cells by freeze/thaw/vortex cycles and then purified by fast protein liquid chromatography (Basche, 2014).

AAV2/8 showed no toxicity to the endothelium one week post infection, as indicated by intact zonula occludens-1 (ZO-1) immunostaining and normal endothelial cell density. However, no GFP was detected in the cornea (Figure 5). As a control, the same virus aliquot was used to infect 293T cells (MOI 8000) alongside, yielding GFP expression in ~75% of cells. A lentiviral vector, in comparison, transduced the same amount of 293T cells more effectively at a 800fold lower MOI (MOI 10). AAV2/8 does not transduce corneal endothelium *ex vivo* within one week after infection.

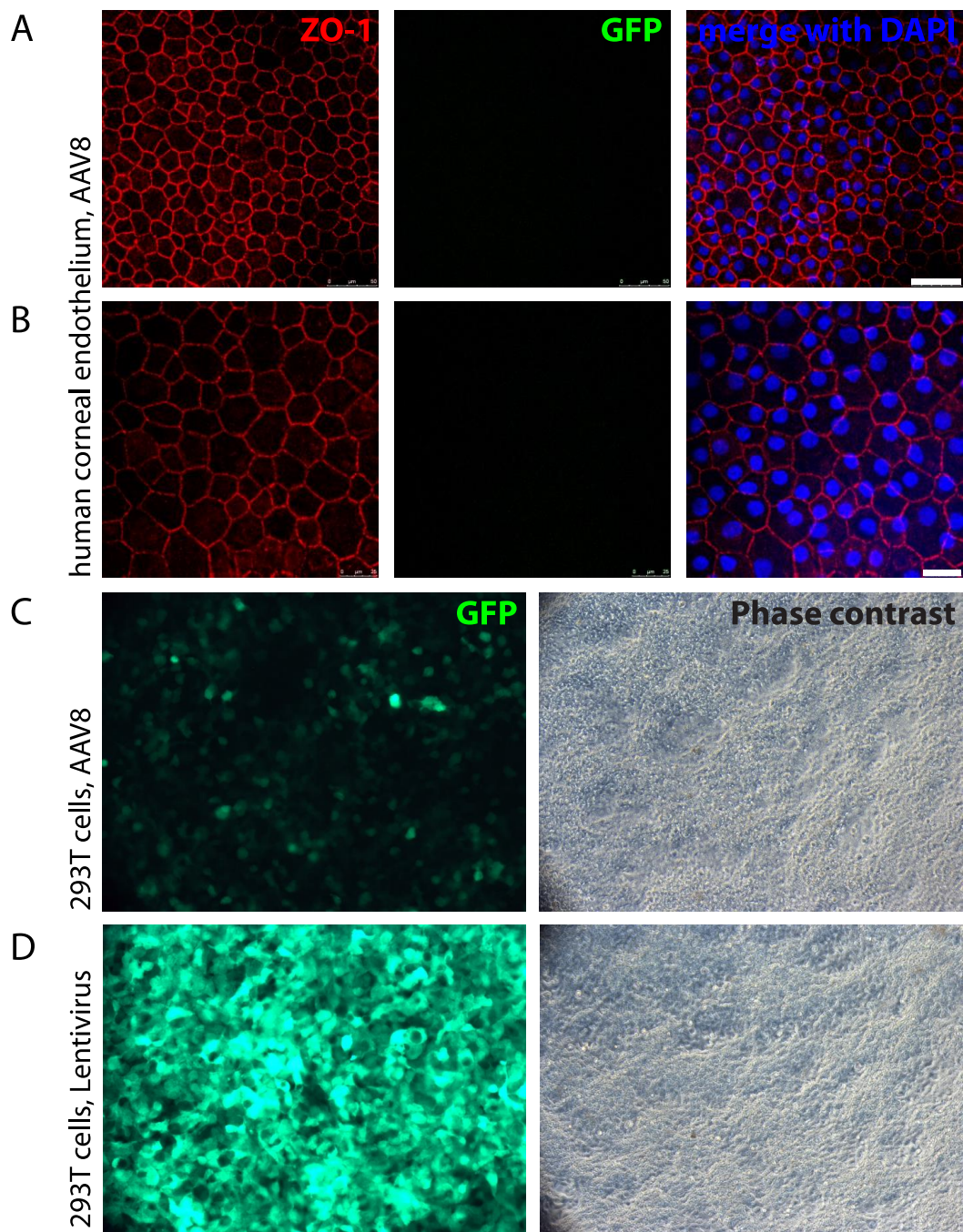


Figure 5. AAV2/8 mediated transduction.

Excised full thickness cornea from a 45-year-old keratoconus patient who underwent penetrating keratoplasty. The sample was incubated in 3 mL DMEM, 2% FCS, with AAV2/8 at an MOI of 50,000 for two hours, then further cultured for one week in 20 mL of medium.

A, B. Confocal laser scanning images of the corneal flat mount, immunostained with ZO-1 (red) to assess integrity of the cell monolayer. No GFP was detectable in the corneal endothelium (A: scale bar 50 μ m; B: scale bar 25 μ m), nor in the epithelium (not shown). DAPI (diamidino-2-phenylindole) was used as a nuclear dye (blue).

C. Positive control: The same AAV2/8 was used to infect 293T cells. At MOI 8000, a transduction efficacy of \sim 20% was observed (live cell imaging with an inverted fluorescent/phase contrast microscope, 10 \times).

D. In comparison, a lentiviral vector at MOI 10 transduced all 293T cells (same exposure as C).

3.4. Lentivirus

Lentiviral vectors transduced corneal endothelium with an efficacy of 10 to 90% (Figure 6). The high variability was dependent on cell viability (freshness of the sample), MOI, purity of the vector, and probably on other factors inherent to the human sample that could not be determined. An MOI of 20 to 50, administered in two rounds of transduction of 3 hours each, proved to be the minimum vector dose to achieve effective transduction of endothelial cells one week later.

Not only the calculated MOI but also the concentration of vector in culture medium was crucial. A high dilution of viral vector in medium resulted in inefficient transduction. Therefore, corneal specimen was submerged in concentrated vector preparation diluted only 1:1 in Opti-MEM.

In the corneal epithelium, around 10% of cells were transduced; keratocytes in the corneal stroma were transduced only when directly exposed at cut edges (trephined corneal specimens or whole corneas cut in halves or quarters). The trabecular meshwork was transduced at ~50%, no GFP was observed in the sclera.

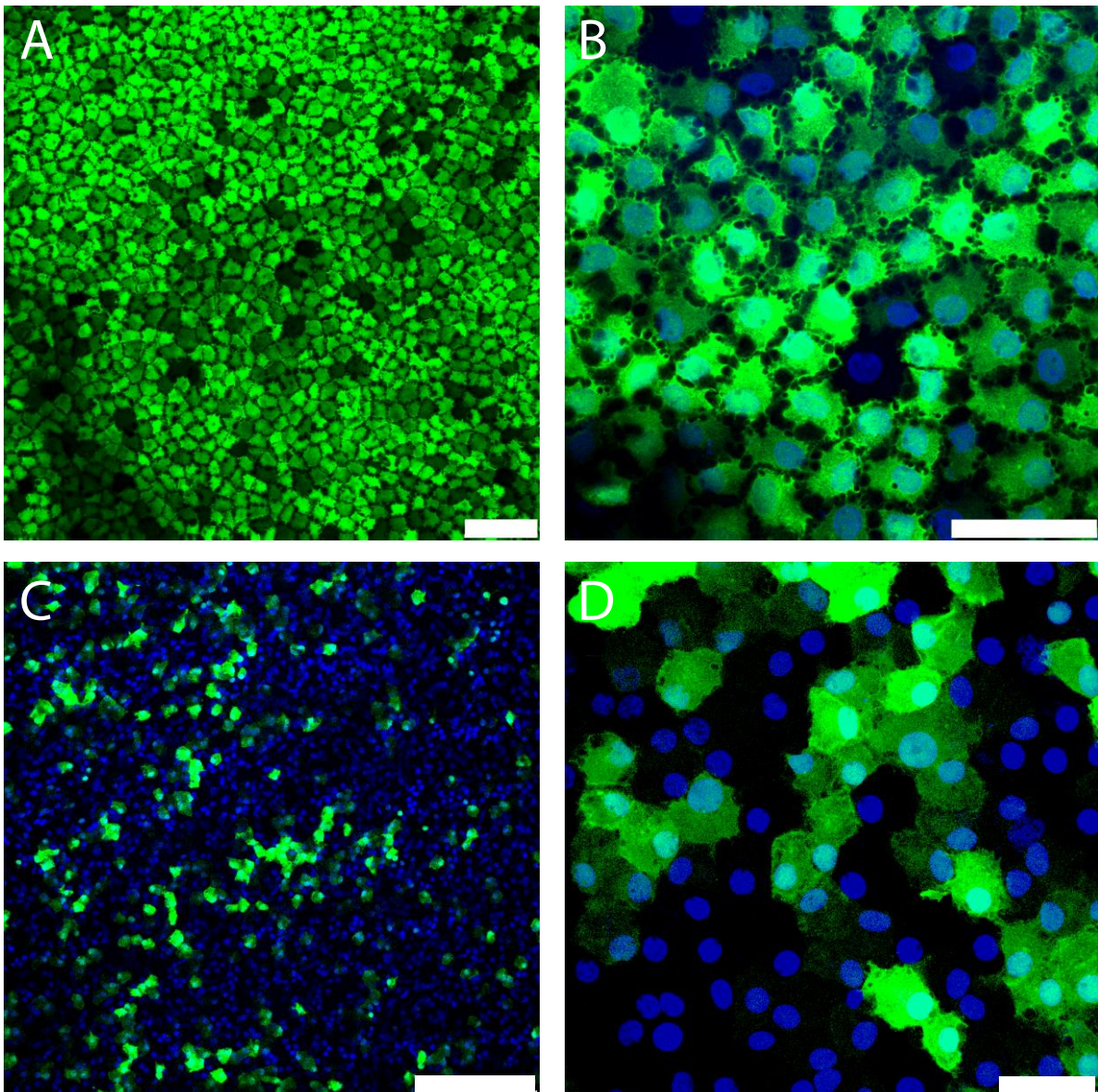


Figure 6. Lentivirus mediated transduction.

A, B. Optimal transduction. Excised full thickness cornea from a 31-year-old keratoconus patient who underwent penetrating keratoplasty was maintained in culture. The sample was incubated in 300 μ L OptiMEM containing $6 \cdot 10^6$ infectious particles of LNT-GFP (MOI of 20) for two hours on day 1 and 3, and cultured 7 days in total in 20 mL of DMEM, 2% FCS. Confocal laser scanning images of the corneal flat mount show GFP expression in 80-90% of corneal endothelial cells.

A: scale bar 100 μ m; B: scale bar 50 μ m, DAPI was used as a nuclear dye (blue).

C, D. Average transduction. Same transduction protocol as in A, B ($2 \times$ MOI 20, different virus preparation) with a corneal specimen from a 21-year-old keratoconus patient. Transduction efficacy was estimated at 20 to 30%.

C: scale bar 250 μ m; D: scale bar 50 μ m.

3.5. Discussion

3.5.1. Choice of human corneal samples for this study

The proliferative capacity of corneal endothelial cells differs among species (Joyce, 2003), showing a high proliferative capacity in small vertebrates enabling regeneration even of large endothelial wounds by mitosis. In primates including human, little to no proliferation is observed after wounding, and age-related cell loss is compensated by migration and cell enlargement (cf. 1.4.4 Proliferative capacity of corneal endothelial cells, page 28).

The aim of this study was to induce proliferation in human corneal endothelial cells. With this fundamental difference in proliferative behaviour between species, it becomes obvious that a translational approach to our aim is only valid when pursued in human material. Especially with regard to current storage methods in eye banks, human *ex vivo* tissue is the sample material closest to future applications to study induced proliferation.

Corneal endothelial cell lines of human origin have been generated by stable transfection with viral oncogenes such as the SV40 large T antigen (Bednarz et al., 2000) and human papilloma viruses E6/E7 gene (Wilson et al., 1993a; Wilson et al., 1995) or with human telomerase reverse transcriptase (TERT) gene (Liu et al., 2012). Although these cells exhibit a morphology and physiology similar to their counterparts *in vivo*, these cells are immortalized and therefore by definition have a nearly unlimited proliferative capacity. The natural inhibitors of proliferation, i.e. contact inhibition, anti-proliferative factors in the aqueous humour and interactions with the extracellular matrix, are not reproduced in current *in vitro* CEC models, and would have little effect in growth-limiting immortalised cell lines. Cell lines therefore would not serve as a basis for translational research in the context of this study.

Similarly, cultured primary human CEC are deprived of many of their natural growth-arresting mechanisms. To maintain primary CEC in culture, they first have to be released from

contact inhibition and then grown in medium containing multiple growth factors (Chen et al., 2001; Engelmann et al., 1988; Zhu and Joyce, 2004).

3.5.2. Variability of human corneal samples under culture conditions

There are three main approaches for corneal tissue storage: 31-37°C culture, hypothermia, and cryopreservation (Armitage, 2011). The latter offers unlimited storage time, but is only suitable for non-viable tissue, i.e. tissue used for emergency tectonic corneal surgery where the only aim is to preserve the eye. Hypothermic storage at 2–8 °C allows preservation of viable tissue including the sensitive endothelium for up to 14 days. This technique is the most widely used owing to its simplicity and effectiveness. However, to prevent corneal swelling a special hyperosmotic medium containing high-molecular dextran is required, which is toxic to the endothelium upon prolonged storage or when storage temperature increases (Lin et al., 1992). The tissue being metabolically inactive, hypothermia does not allow any biological manipulation of the tissue.

In the majority of European eye banks, corneal samples are maintained in culture at 31 – 37°C (Armitage, 2011; <http://www.europeaneyebanks.org>, 2010). Organ culture allows prolonged storage for typically four weeks (Pels and Schuchard, 1983), and minor changes in temperature do not affect endothelial cell viability (Schroeter et al., 2008). This time frame allows planning the surgery, performing highly sensitive but time-consuming serological tests on the donor's blood and the graft itself, and checking the endothelium's quality. Longer storage time also enables better allocation of grafts to the recipient's needs, e.g. to match age or human leukocyte antigen (HLA) system. Although cell biological functions remain active at this temperature, stromal oedema develops after approximately three to five days in culture. This swelling would have to be reversed before transplant surgery by incubation in de-swelling medium

containing 4–8% dextran for 12 hours. Overall, graft outcomes of hypothermia and 37°C culture seem similar (Armitage, 2011).

For these studies, normal biological functions of the cornea are prerequisite. Corneal samples were therefore kept in culture at 37 °C under conditions resembling those applied in the majority of European eye banks. Sources of the samples were Moorfields Eye Bank and other international eye banks, and Moorfields operating theatre for live donors collected during corneal graft surgery.

The variable quality of human samples became obvious when assessing different viral vectors. The same batch of virus would achieve a 90% transduction rate in one sample (Figure 6 A, B), or transduce 30% of endothelial cells in another (Figure 6 C, D). Even transduction of less than 10 cells per whole sample was observed. In this case, the experiment was discontinued. Similar observations were made by other groups using human corneal samples (Jessup et al., 2005a; Parker et al., 2007): a high variability in transduction efficacy most likely reflected variable sample quality. However, transduction efficacy did not correlate with endothelial cell density, donor age, or time in storage before transduction (Jessup et al., 2005a).

Various reasons can be made accountable for the high sample variability. Age ranged from 18 years (fresh corneal specimens from graft surgery for keratoconus) to 90 years (donor corneas from the eye bank). For eye bank samples, eyes were enucleated at various times post mortem, ranging from 2 hours to 20 hours, and were made available for research either directly after enucleation, or after a storage period of up to 4 weeks. During this time, samples were stored either at 4 °C in storage medium containing high molecular dextran, or at 37 °C in corneal culture medium not containing dextran. These variable conditions accounted for the high variability in corneal endothelial cell density, the viability of endothelial cells during the experiment, and their propensity / ability to undergo cell division. Therefore, cut off criteria for use of samples for this research were established, which varied according to sample source and type (Table 3).

Table 3: Overview over human corneal sample types, inclusion and exclusion criteria.

	Fresh corneal specimens	Whole eye bank donor corneas	Corneo-scleral donor rims
Donor	Live donors	Deceased donors	Deceased donors
Source	Moorfields Eye Hospital operating theatre during corneal transplant surgery	Moorfields Eye Bank and other eye banks	Moorfields Eye Bank
Inclusion criteria	Cornea clear enough to visualize endothelium on slit lamp Research consent of the patient prior to surgery	Post-mortem time <12 days Cornea not suitable for transplantation Research consent of relatives prior to enucleation	Post-mortem time <12 days Cornea stored at 4°C Research consent of the relatives prior to enucleation
Exclusion criteria	Previous intraocular surgery Any known or identified endothelial disease Known HIV or Hepatitis B/C infection	Previous intraocular surgery Any known or identified endothelial disease Known HIV or Hepatitis B/C infection Visible corneal abnormalities Normal storage conditions not maintained (e.g. cultured corneas kept in fridge or at room temperature instead of 37°C) Cornea in de-swelling medium at 37°C for >24 hours (Suspected) infection / contamination of medium during storage	Previous intraocular surgery Any known or identified endothelial disease Known HIV or Hepatitis B/C infection Visible corneal abnormalities Normal storage conditions not maintained (e.g. cultured corneas kept in fridge or at room temperature instead of 37°C)

Applying these criteria did not guarantee good sample quality, but with respect to the already low number of samples available, stricter exclusion criteria were not applied. In general, scarcity of human corneal samples did not allow experimental designs with many different conditions (e.g. time courses, dose titrations). In addition to this, the high variability of available

samples would call for high number of replicates, but this demand could not be met. Instead, care was taken to include sufficient controls for each experiment. Eye bank corneas sometimes come as pairs (left and right eye of the same donor), which normally showed high similarity. Cutting one cornea in halves or quarters gave the most consistent controls.

3.5.3. Sample types and their characteristics

Each sample type had their own advantages and disadvantages, making some types unsuitable for specific experimental setups.

Fresh corneal specimens. Collected directly from the live donor during surgery, full-thickness corneal specimens are the freshest tissue available for this study. Disadvantages were the small size: manipulation easily leads to disruption of the endothelial monolayer. Thus one specimen could not be cut in more than two pieces, allowing comparison only between one treatment and one control. The unavoidable monolayer disruption along the cut edges created artefacts, therefore an area around the cut edge had to be excluded from morphological analysis.

Eye bank donor corneas. Advantage of this tissue type was the bigger size resulting in a higher number of available endothelial cells. The attached scleral rim made manipulation easier, guaranteeing an untouched endothelial layer. This allowed their use for time course experiments. A quarter was cut off at each time point. Unfortunately, a post mortem time of over 12 days turned out to give inconsistent results due to a low viability of endothelial cells, resulting in many samples being unsuitable for this study.

Corneo-scleral donor rims. These samples were available on an almost daily basis. However, as with fresh specimens, cut edges created artefacts and had to be excluded, making this type of sample unsuitable for experiments involving cell density counts. Furthermore, before surgery the donor corneas were kept in de-swelling medium containing dextran for up to 3 days, which

can be toxic to endothelial cells. Therefore, only samples from hypothermic storage (which restricts total storage time to 14 days) were used.

3.5.4. Choice of vector for *ex vivo* corneal endothelium transduction

Transgene expression kinetics

In accordance with previous experiments with adenovirus by this group (McAlister et al., 2005), and with respect to future functional experiments using cell cycle modifying transgenes, a one-week period after transduction was chosen for transgene assessment. This time span would allow *ex vivo* modification of the transplant tissue in an eye bank setting, including transduction, transgene transcription and translation, and quality control of the tissue before transplantation. Of the available vectors only adenovirus and lentivirus meet this time constraint.

AAV2/8 vector did not show any GFP expression in *ex vivo* corneas within one week after transduction (Figure 5). Only two publications have used AAV for *ex vivo* corneal endothelium. Hudde et al. estimated transduction efficacy at 2% after 3 and 4 weeks (Hudde et al., 2000). Lui et al. show transduction of endothelial cells with AAV2/1, 2/2, 2/5, and 2/8 after 14 days. However, transgene (GFP) expression was low and only detectable by antibody staining (Liu et al., 2008). In primary corneal endothelial cells *in vitro*, transgene expression started after 9 days post transduction (Fuchsluger et al., 2011c). The slow expression kinetics and low transgene expression levels make AAV unsuitable for our purpose.

Adenovirus has been used previously in *ex vivo* human corneas to deliver viral IL-10 for immunomodulation (Bertelmann et al., 2003), where the transgenic protein was detectable as early as 24 h post transduction. Looking at secreted exogenous protein, Jessup et al. found an expression peak at 15 days post transduction, which then gradually declined, probably reflecting the dying endothelial cells (Bertelmann et al., 2003; Jessup et al., 2005a; McAlister et al.,

2005). Similar expression kinetics were described for lentiviral vectors in corneal endothelium *ex vivo*. Parker et al. detected expression peaks of IL-10 at 6 to 12 days (Parker et al., 2010).

Transgene expression levels

While both LNT and Ad share a similar expression kinetic, the quantity of expressed transgene differs. A direct comparison was made by Parker et al., using analogous LNT and Ad based vectors delivering IL-10 in ovine corneas (Parker et al., 2010). On transcriptional level, expression of IL-10 mRNA induced by LNT was 10³-fold less than when induced by Ad, and the expression of secreted IL-10 protein from LNT was at least three- to four-fold less than from Ad after transduction with the same MOI. Even by increasing the MOI, lentiviral mediated IL-10 protein expression could not match adenovirus mediated IL-10 levels.

We share this observation in human corneas, although inter-sample variability was too high to allow a quantitative comparison. Adenoviral transduction with an MOI of 20 was consistently more efficient (80-90% of cells transduced) than lentiviral transduction with MOI 40 (20-30%). Increasing the MOI tenfold for lentiviral vectors yielded only a marginal increase in transduction rate. This might be due to toxic off-target effects caused by the virus or components in the vector preparation. Because the lentiviral vectors in our study are concentrated by simple ultracentrifugation, cell debris and components of FCS in the culture medium are also concentrated in every vector preparation in uncontrollable amounts. To account for this in future experiments, treatment and control vector (delivering GFP) were produced and concentrated in parallel. Vectors of the same production batch were then used for one experiment.

Vector immunogenicity

Although adenoviral vectors seem more effective, they elicit an inflammatory response of the innate immune system (Hartman et al., 2008). Not only typical immune cells such as dendritic cells, macrophages or peripheral blood mononuclear cells, but also “non-immune cells” such as epithelial, endothelial or mesenchymal cells have been found to initiate a rapid pro-inflammatory response. Human cervical epithelial cells (HeLa), kidney-derived epithelial cells

(REC) as well as mesenchymal cells (MEFs, mouse embryonic fibroblasts) express a variety of inflammatory cytokines as early as 10 minutes after infection with adenoviral vector serotype 5 (Hartman et al., 2007; Liu et al., 2005; Tibbles et al., 2002). This indicates that adenoviral vectors would be unsuitable especially in an allogeneic corneal transplant setting on account of the harmful effect of increased immunogenicity on donor corneal survival. A previous study showed that adenovirus encoding GFP can selectively infect the endothelium of *ex vivo* murine corneas, and transgene expression is high even after re-transplantation in an allogeneic mouse model. However, Ad transduced corneas survived for significantly shorter periods, with a survival time less than half of that of untransduced controls (Qian et al., 2004).

3.5.5. Conclusions

Efficient transgene expression in the human corneal endothelium with a fast onset of expression could be achieved with adenoviral and lentiviral vectors, while no significant expression was detected after AAV2/8 transduction. Out of the vectors currently available, lentivirus seems the best vector for endothelial transduction *ex vivo* for future corneal transplants, compromising between high expression levels and low immunogenicity.

4. Cell cycle modulation via the Rb/E2F pathway

4.1. Introduction

4.1.1. The Rb/E2F pathway

The aim of this study was to assess whether overexpression of E2F can achieve proliferation of normally non-proliferative corneal endothelial cells. The E2F transcription factor and the product of the retinoblastoma tumour suppressor gene (pRB) can be described as opposing molecules that control the G1 to S phase transition (Dyson, 1998). Initially identified as a genetic locus associated with the development of retinoblastoma, an inherited eye tumour, Rb was then recognized not only as a tumour suppressor but as a key regulatory protein to inhibit E2F, a central transcriptional activator (Nevins, 2001). The E2F transcription factor family control a variety of genes involved in DNA replication such as thymidine kinase, thymidylate synthase, dihydrofolate reductase – virtually the entire apparatus of initiation factors that assemble a pre-replication complex at the transition from G1 to S phase (Wu et al., 2001).

In quiescent cells, E2F is inactivated by binding to Rb (Figure 7, from Loughran and La Thangue, 2002, with permission from Elsevier). The ability to bind and inactivate E2F is dependent on the phosphorylation status of Rb: hypophosphorylated Rb binds E2F and thereby prevents its mitogenic activity, hyperphosphorylated Rb releases E2F transcription factors and induces progression in the cell cycle (Dimova and Dyson, 2005; Haberichter et al., 2007). During cell cycle, pRb oscillates between a hypophosphorylated form bound to E2F in early G1-phase and hyperphosphorylated form in late G1, S and G2/M phases liberating E2F. A repressive form

of E2F is observed when forming a complex with hypophosphorylated Rb and chromatin-regulating and remodelling proteins, including histone deacetylase (HDAC) and histone methyltransferase (MTase). Upon growth factor stimulation, cyclin D is synthesized and associates with its cyclin-dependent kinase, CDK4. Formation of the cyclin D/CDK4 complex activates the kinase activity of CDK4. pRb is a specific substrate for this complex. Phosphorylation of pRb by this complex alters the pRb-E2F interaction, promoting release and activation of E2F. Its transcriptional activity through interaction with transcription cofactors such as p300/CBP then leads to mitosis (DeGregori et al., 1995).

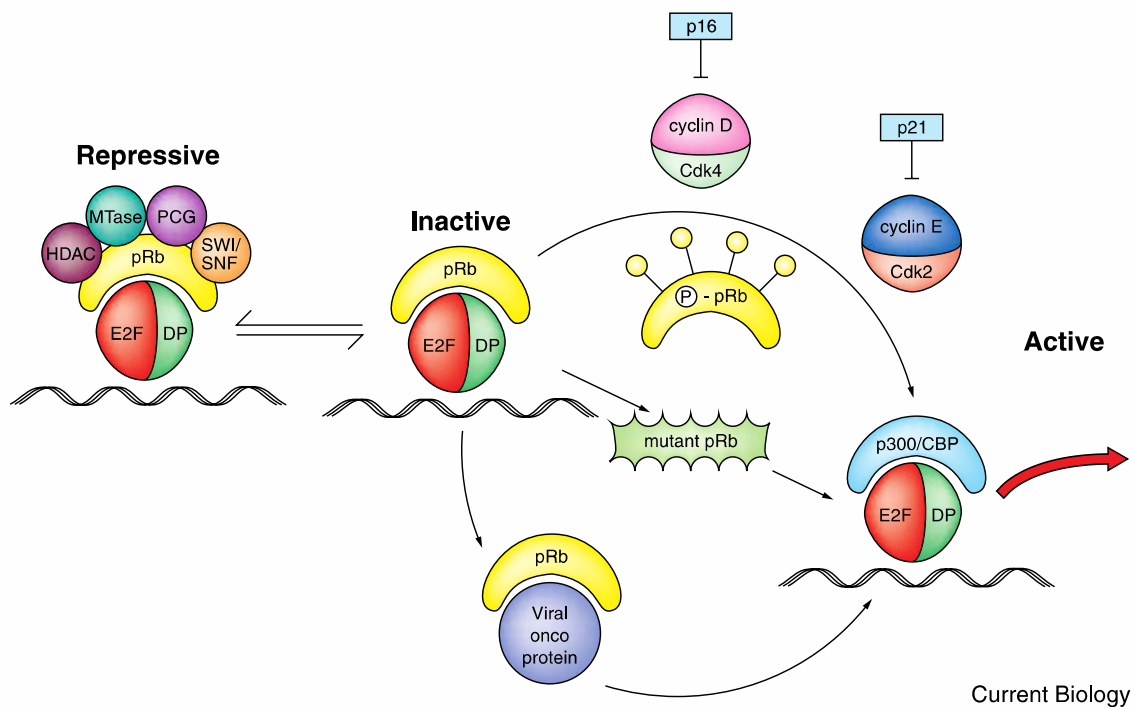


Figure 7. The Rb/E2F pathway.

In non-proliferating cells, the E2F/DP heterodimer binds to pRb, rendering it inactive as a transcription factor. During cell cycle progression, G1 CDK complexes (Cyclin D/CDK4 and Cyclin E/CDK2) sequentially phosphorylate Rb, releasing E2F. E2F becomes transcriptionally active through interaction with transcription cofactors such as p300/CBP.

In tumour cells, mutant pRb fails to bind E2F. Viral oncoproteins can also bind pRb to prevent it from inactivating E2F.

pRb/E2F can also exist in a repressive state when associated with chromatin-regulating and remodeling proteins, including histone deacetylase (HDAC), polycomb group proteins (PCG) and histone methyltransferase (MTase).

Figure from Loughran and La Thangue, 2002, with permission from Elsevier.

Haberichter et al. used a model of synchronised cells (human HCT116 colon carcinoma cells with wildtype Rb and p53, but mutated p16) to establish levels of cell cycle regulating proteins *in vitro* (Haberichter et al., 2007). Applying a mathematical model, they conclude that per single cell, as few as 3 to 4 molecules of E2F are present when the cell enters S phase, increasing to 5 to 6 molecules of E2F per cell during G2/M phase.

Different isoforms of E2F have been identified. E2F1 to -3 activate transcription, while E2F4 and -5 prevent entry of cells from the quiescent, non-replicating state (G0 phase) into the G1 phase. E2F6 negatively regulates the transcription of E2F-responsive genes.

4.1.2. Alterations in the Rb/E2F pathway

Alterations in the Rb/E2F pathway have been investigated extensively in the field of cancerogenesis. Given the important role played by this pathway in controlling cell growth, it is not surprising that oncogenic mutations are frequently seen to disrupt the normal function of this pathway (Nevins, 2001). In tumour cells, mutant pRb fails to bind E2F. With Rb mutations being the most frequent mutations in a wide spectrum of tumours other than retinoblastoma, mutations in the involved cyclin D kinases or CDK inhibitors and deregulated D-type cyclin expression is observed in human tumours. However, strikingly absent from the list of cancerogenic genetic alterations involving the Rb/E2F pathway are the E2F genes themselves (Nevins, 2001). Although one might expect to find deregulations of E2F leading to disruptions of the cell cycle, no such examples have been found in human cancers (Nevins, 2001).

Overexpression of E2F can induce quiescent REF-52 cells (rat embryo fibroblasts) to enter the cell cycle (Johnson et al., 1993), and if overexpression is unregulated, eventually leads to neoplastic transformation (Singh et al., 1994). Overexpression of E2F1 to -3 in human fibroblasts can induce apoptosis (DeGregori et al., 1997).

Different approaches have been described to block the proliferative capacity of the Rb/E2F pathway or to enhance its apoptotic capabilities in order to stop tumour growth, but have not yet found their way into clinical use (Hartwell et al., 1997; Nevins, 2001; Pagliaro et al., 1995).

4.1.3. Aims

The aims of this chapter were

- (1) To assess different possibilities of quantifying proliferation in human endothelium;
- (2) To characterize the effect of adenovirus mediated overexpression of E2F2 on cell density;
- (3) To characterize the effect of lentivirus mediated overexpression of E2F2 on cell density.

The vectors for (2) had already been used by this lab in previous studies (McAlister et al., 2005) and were obtained from Schepens Eye Research Institute, Boston. For (3), new vectors had to be designed, produced, and evaluated *in vitro*.

With respect to future applications, only human corneal specimens were used under conditions closely resembling 37 °C corneal culture in European eye banks. In small animal species including mouse and rat, corneal endothelial proliferation occurs readily *in vivo* and *ex vivo*, limiting their use in proliferation studies.

4.2. Proliferation analysis in *ex vivo* human corneal endothelium

4.2.1. Bromodeoxyuridine labelling

Bromodeoxyuridine (BrdU) is a thymidine analogue and is incorporated into the DNA of cells during S phase. Added to the culture medium during cell proliferation, it can later be visualized by immunohistochemistry. It therefore is used to specifically label all new cells that were generated after addition of BrdU.

To assess the suitability of BrdU labelling for *ex vivo* cultured corneas, samples were incubated under 37°C culture conditions in medium containing 10 µM BrdU for 3 days. Medium was changed daily to maintain a sufficient BrdU concentration. In some samples, scratches were inflicted on the endothelium with a plastic pipette tip to simulate wounds in the monolayer.

Along the scratched area of a corneo-scleral donor ring cut in half, corneal endothelial cells showed the highest BrdU uptake (Figure 8). But also over 0.5 mm away from the scratches, highly BrdU positive cells were distributed evenly throughout the whole sample. As a negative control, the unscratched other half of this corneal sample also showed BrdU positive cells along the cut edges of the trephine.

Similarly, a straight full thickness cut of the sample with a razor blade induced BrdU uptake in the surrounding cells up to 0.5 mm away. Even in a completely untouched corneoscleral ring, BrdU background after 3 days in culture was still high, especially along the cut edges of the trephine.

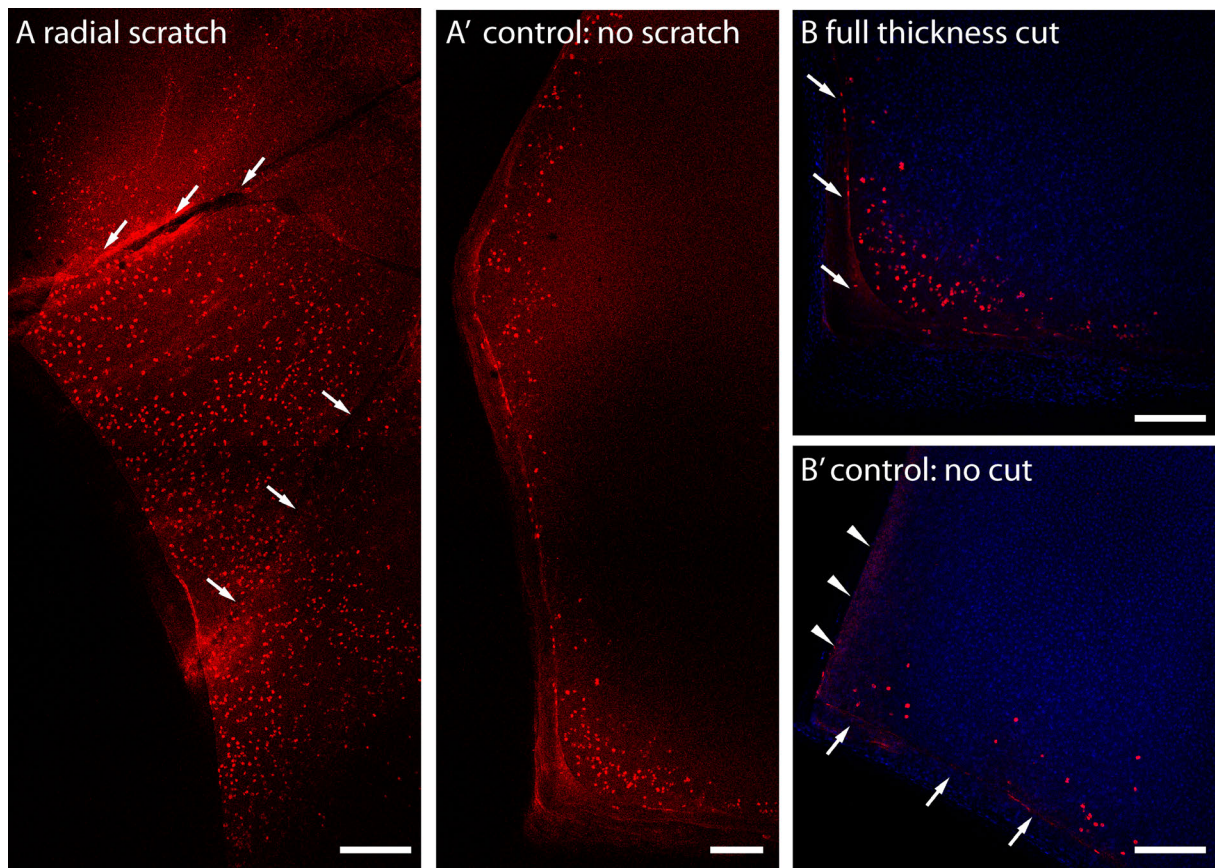


Figure 8. BrdU uptake in endothelium of corneal specimen cultured for 3 days.

Corneas were incubated in DMEM medium, 2% FCS, with BrdU 10mM for 3 days and immunostained for BrdU (red) and nuclei (DAPI in blue, B and C). Scale bar 250 μ m.

A. One half of cornea A received mechanical injury to the endothelium by radial scratches (arrows).

A'. Control: The other half of cornea A received no mechanical injury.

B. Mechanical injury by a full thickness cut with a razor blade (arrows).

B'. Control: No mechanical injury (except the trephination of the donor cornea in the operating theatre, arrows). The other cutting edge resulted from the cut after PFA fixation to enable mounting of the specimen on the glass slide (arrowheads).

4.2.2. Antigen Ki67 immunostaining

Antigen Ki67 is expressed in the nuclei of proliferating cells during any active phase of the cell cycle, G1, S, G2, and mitosis, but not in resting cells (Scholzen and Gerdes, 2000). To test the Ki67 antibody, we used ARPE19 cells, which can be growth-arrested in low serum maintenance medium (DMEM/F12, 1% FCS). Cells were grown to near-confluency in high-serum medium (10% FCS). Medium was then changed to fresh high serum or low serum medium and incubated for 5 days. The high serum population showed Ki67 staining in >80% of cells, while the low serum control showed less than 10% of positive cells (Figure 9).

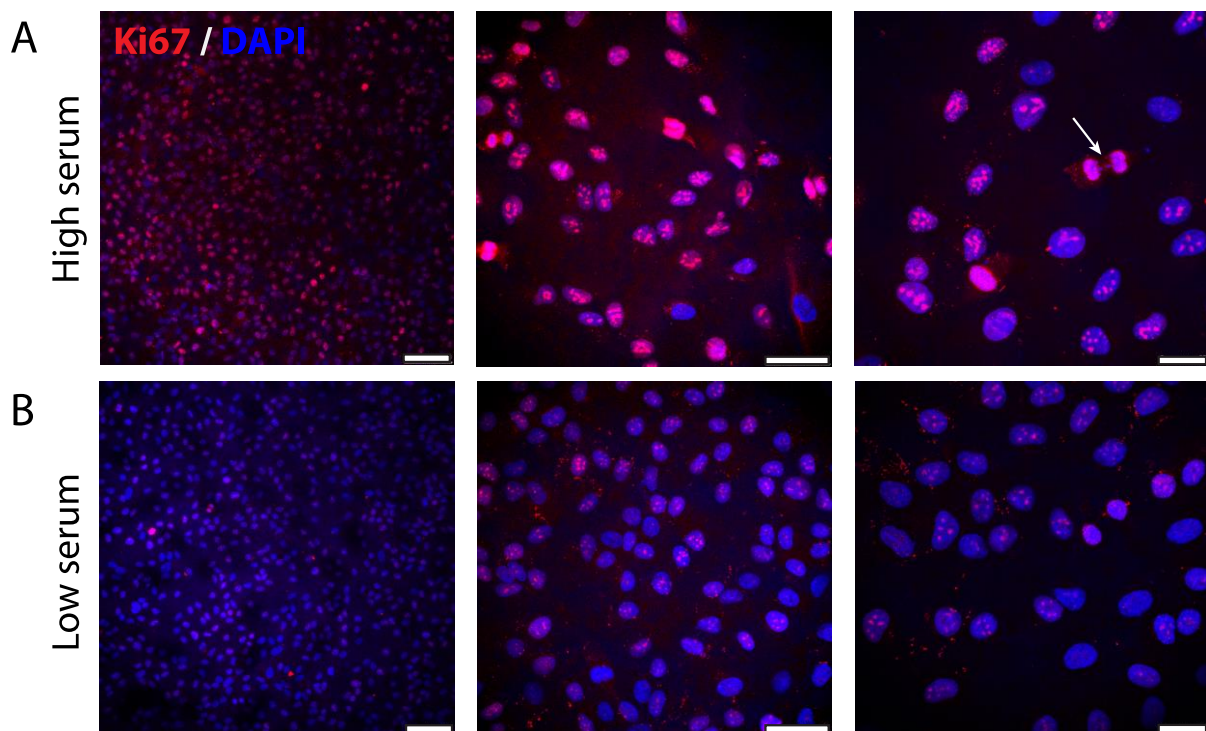


Figure 9. Test of Ki67 antibody *in vitro*.

ARPE19 cells were seeded at 40,000 cells per well on glass coverslips in a 24 well plate in high serum medium (10% FCS) and left to grow for 3 days. Medium was then changed to fresh high serum medium or low serum maintenance medium (1% FCS) and cells were further incubated for 5 days before fixation and immunostaining for Ki67 (red) and DAPI (blue). Panels show confocal laser scanning micrographs in ascending magnifications. Scale bar: Left panel, 100 μm ; middle panel, 50 μm ; right panel, 25 μm .

A. The high serum population shows intensive Ki67 staining in >80% of cells. Arrow: mitotic figure.

B. The low serum population shows growth-arrest with less than 10% of nuclei positive for Ki67.

In vitro, a high correlation between BrdU and Ki67 was found (Figure 10). 293T cells were incubated with BrdU for 24 hours. 80-90% of BrdU positive cells are also positive for Ki67. The remaining BrdU positive, Ki67 negative cells represent the population that had undergone replication but is in a resting stage of the cell cycle at the end of the experiment. Less than 10% of Ki67 positive cells do not show BrdU staining, indicating they are at the transition of G1 to S phase but have not synthesized a significant amount new DNA.

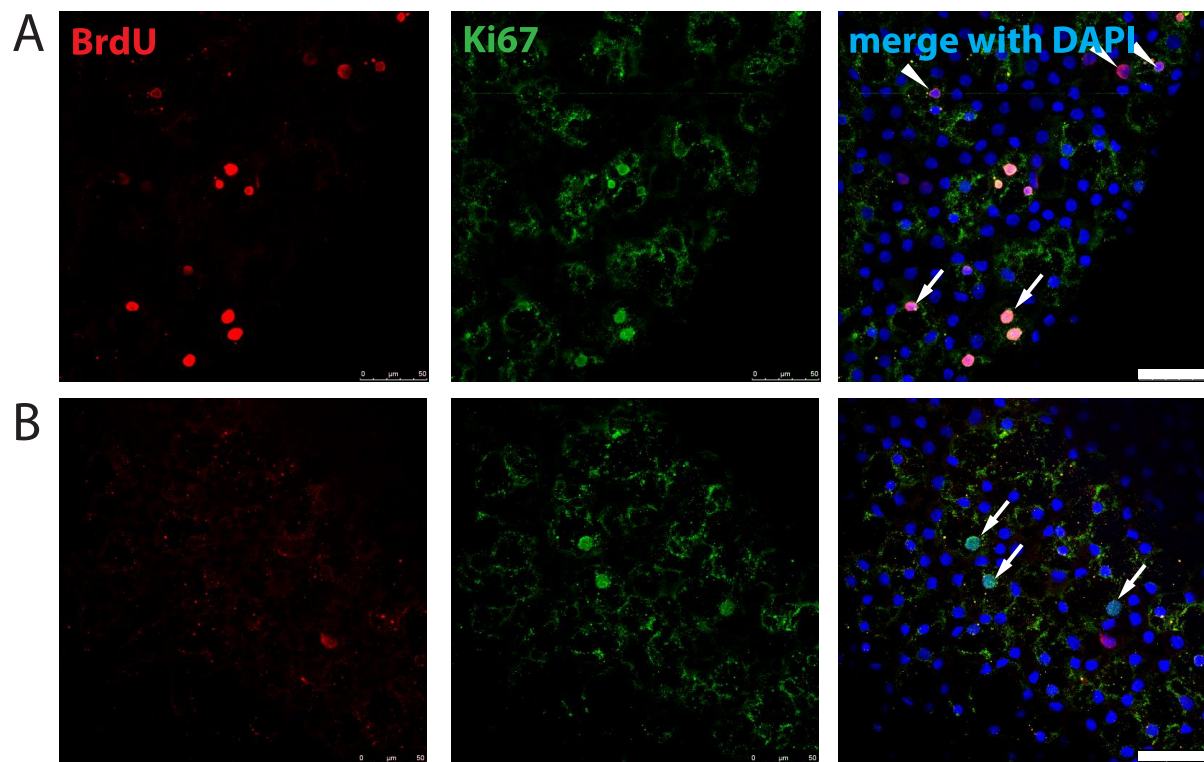


Figure 10. BrdU and Ki67 labelling of proliferating HEK293T cells *in vitro*.

Correlation of BrdU staining (red, left) vs. Ki67 staining (green, middle). Images merged with DAPI nuclear stain (blue, right). Scale bar: 50 μ m.

A. 80-90% of BrdU positive nuclei show co-localized staining against Ki67 (arrows). <10% BrdU positive nuclei do not show Ki67 staining (arrow heads).

B. <10% of Ki67 positive nuclei do not show BrdU staining (arrows).

In corneal endothelium cultured *ex vivo*, Ki67 positive nuclei appear scattered in clusters throughout the whole sample. Especially in areas presumably injured during surgical manipulation and / or experimental procedure, but also along Descemet's folds, or even in areas with completely intact endothelium, Ki67 positive cells can be found (Figure 11).

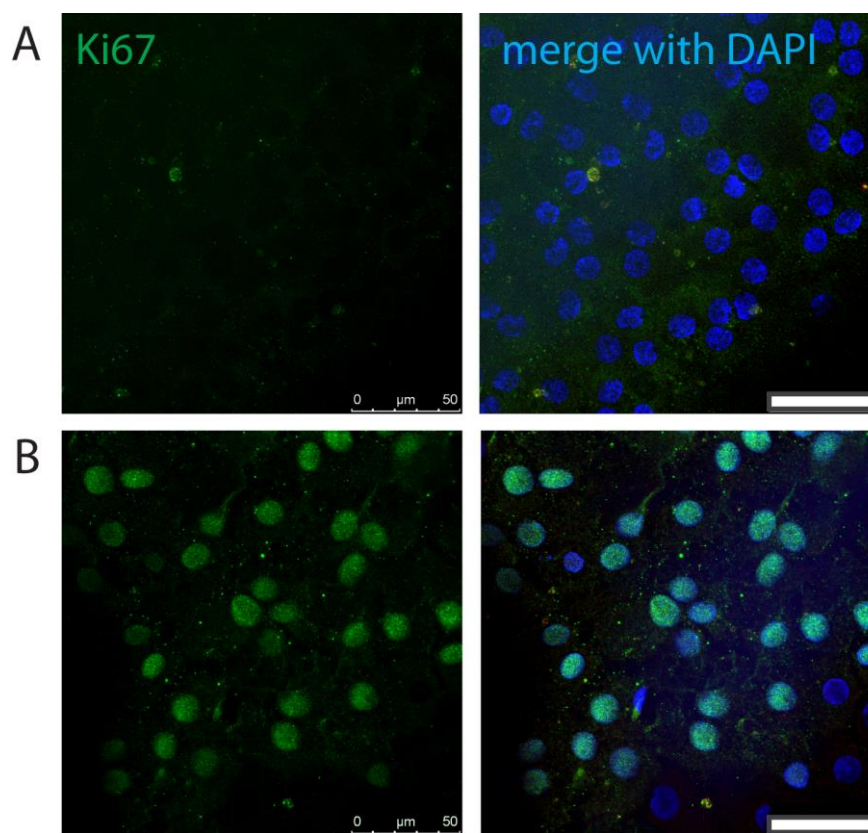
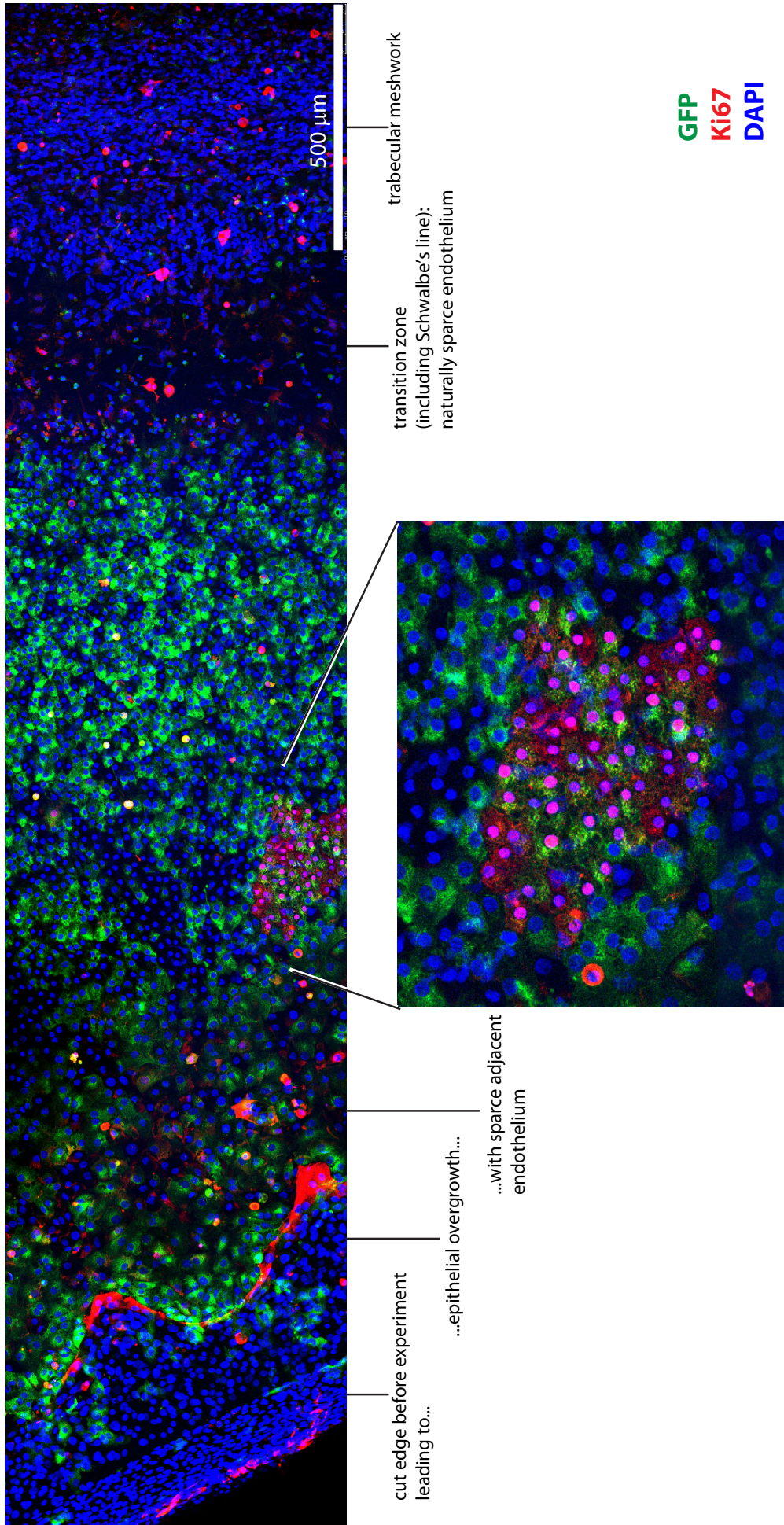


Figure 11. Ki67 staining in *ex vivo*-cultured corneal endothelium.

Different areas within the same corneal sample, maintained for 5 days under corneal culture conditions (excised full thickness cornea of a 29-year-old patient who underwent penetrating keratoplasty for keratoconus). Areas of Ki67 negative cells (A) can be found next to areas of Ki67 positive clusters (B, Ki67 in green). DAPI was used as a nuclear stain (blue). Scale bar 50 μm .

An overview of the endothelium of a corneo-scleral rim illustrates the occurrence of Ki67 positive clusters (Figure 12, insert). The sample was maintained in culture for 3 days after transduction with adenovirus delivering GFP. The montage of seven confocal laser scanning micrographs also illustrates the possibility of epithelial overgrowth at cut edges, which can lead to a density decrease in neighbouring endothelial cells. Towards the periphery, there is an area of naturally high endothelial cell density. Further into the periphery, at the transition to the trabecular meshwork, density is naturally sparse. This sample of a very young eye bank donor (9 years of age) shows a comparatively high transduction rate.



area of normal endothelium away from cut edge

Figure 12. Ki67 distribution in a corneal specimen in culture.

A corneo-scleral rim of a 9 year old donor was maintained for 3 days after transduction adenovirus delivering GFP (green). Ki67 positive endothelial cells (red) cluster in the mid-periphery of the rim (insert), some single cells are spread across the endothelium even when no obvious damage is visible in the monolayer. Nuclear dye (DAPI) in blue. Typical anatomical features of a corneo-scleral rim are marked.

The image is a montage of seven confocal laser scanning micrographs, taken with a 10x objective. For each of the tiled images, 11 z-stack images were taken from a 30-50 µm deep stack and one projection image generated. All images were aligned using Photoshop CS4.

4.3. Adenovirus mediated E2F2 overexpression

4.3.1. Characterization of adenoviral vectors

E1/E3-deleted recombinant adenovirus serotype 5 delivering *E2F2* was kindly provided by Nancy Joyce, Schepens Eye Research Institute, Harvard Medical School, Boston, USA. The same batch had been used in a previous study of this group to transduce *ex vivo* human corneal endothelium (McAlister et al., 2005), see also Chapter 3.2 Adenovirus, page 94. *E2F2* was under the control of a bi-directional CMV promoter: GFP was located upstream of the CMV promoter. Full-length human *E2F2* cDNA was cloned downstream after the human β -globin inverting sequence IVS II and followed by a polyadenylation signal (McAlister et al., 2005, and personal communication with co-author Deshea Harris).

Overexpression and correct cellular localization of the transgene was verified in ARPE19 cells maintained in low serum medium (DMEM/F12, 1% FCS) for at least one week. This ensured a fairly stable cell cycle arrest and down-regulation of endogenous E2F2. In contrast, cell lines with high proliferative capacity like 293T or HeLa cells could not be growth-arrested to show low E2F2 levels. Three days after transduction with Ad-E2F2-GFP, ARPE19 cells show E2F2 protein overexpression as demonstrated by immunohistochemistry (Figure 13).

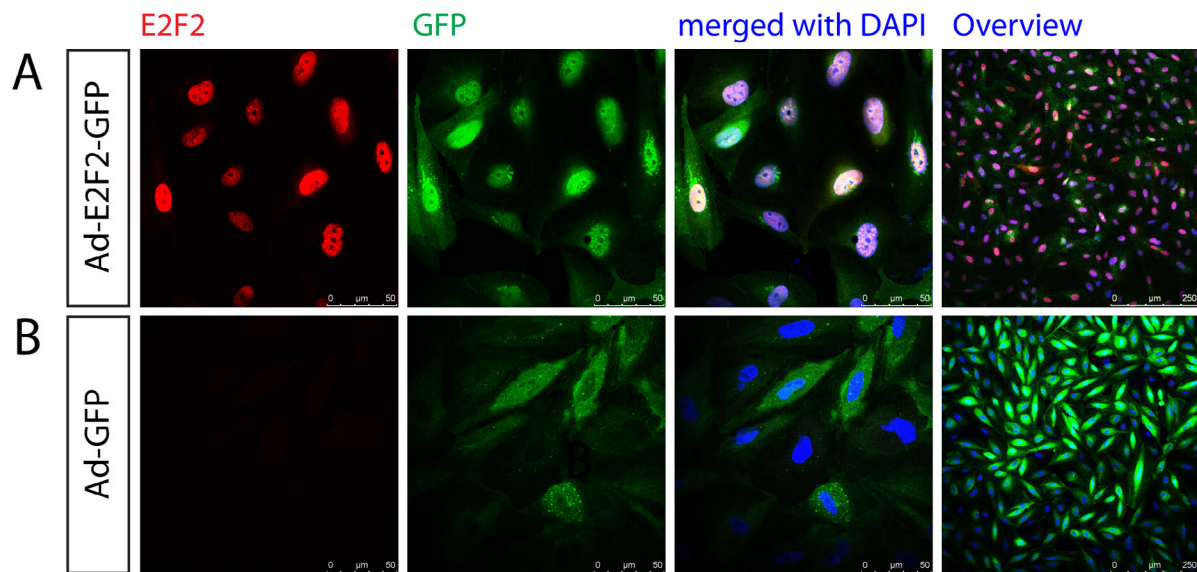


Figure 13. Characterization of adenoviral vector delivering *E2F2*.

Expression of transgenic E2F2 protein after transduction with Ad-E2F2-GFP (MOI 3) was verified in cell culture by immunohistochemistry. ARPE19 cells, grown on coverslips and serum starved for 1 week in DMEM/F12 containing 1% FCS are suitable as they show little endogenous E2F2 expression (in contrast to highly proliferative cell lines like HeLa or 293T cells). Transduced cells show nuclear localization of *E2F2* three days after infection (A). Very little endogenous E2F2 is observed in controls transduced with GFP only (B).

Scale bar 50 μm, for overview 250 μm (right panel).

Different virus concentrations were tested on ARPE19 cells. For Ad-E2F2-GFP, a calculated MOI of 3 infectious particles per cell was sufficient to achieve expression of the reporter gene in all cells. Faint E2F2 overexpression was also detectable by immunohistochemistry, but was markedly increased at an MOI of 30 (Figure 14). Complete cell death was observed when Ad-E2F2-GFP was applied at an MOI of 300 (not shown).

For Ad-GFP, though driven by the same promoter, a higher GFP expression was observed. No E2F2 overexpression was detectable after Ad-GFP infection.

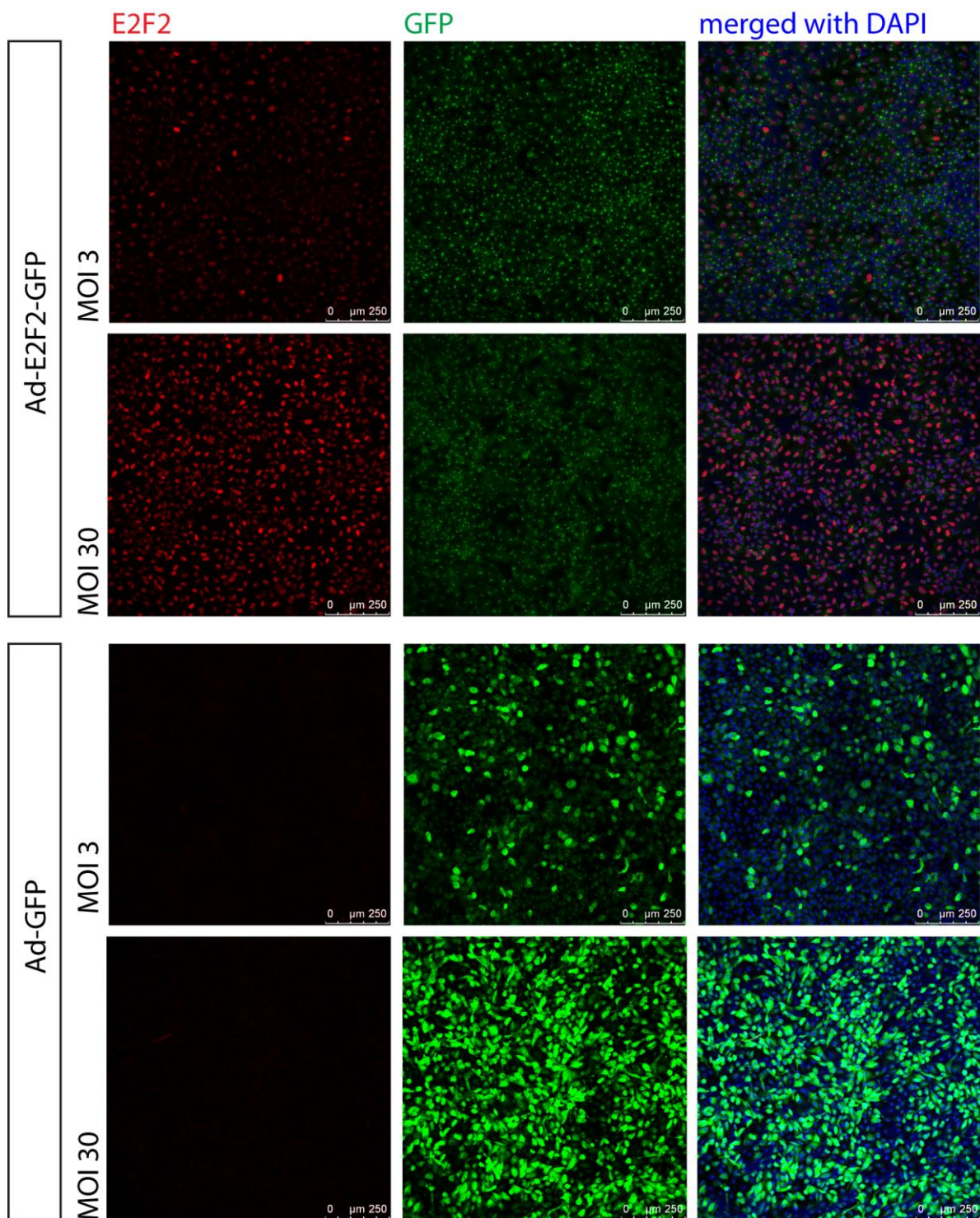


Figure 14. Transgene overexpression at different concentrations of adenoviral vector.

ARPE19 cells grown on coverslips and serum-starved for one week were infected with Ad-E2F2-GFP or Ad-GFP at different concentrations (MOI 3 and 30). At an MOI of 3, all cells expressed the transgene. At an MOI of 30, intensive transgene expression in healthy cells is observed. Though driven by the same promoter, the double construct Ad-E2F2-GFP shows a weaker GFP expression than the single construct.

For all micrographs the same microscope settings were used. E2F2 (red), GFP (green), DAPI (blue). Scale bar 250 μm .

4.3.2. Effect of vector dose on cell viability

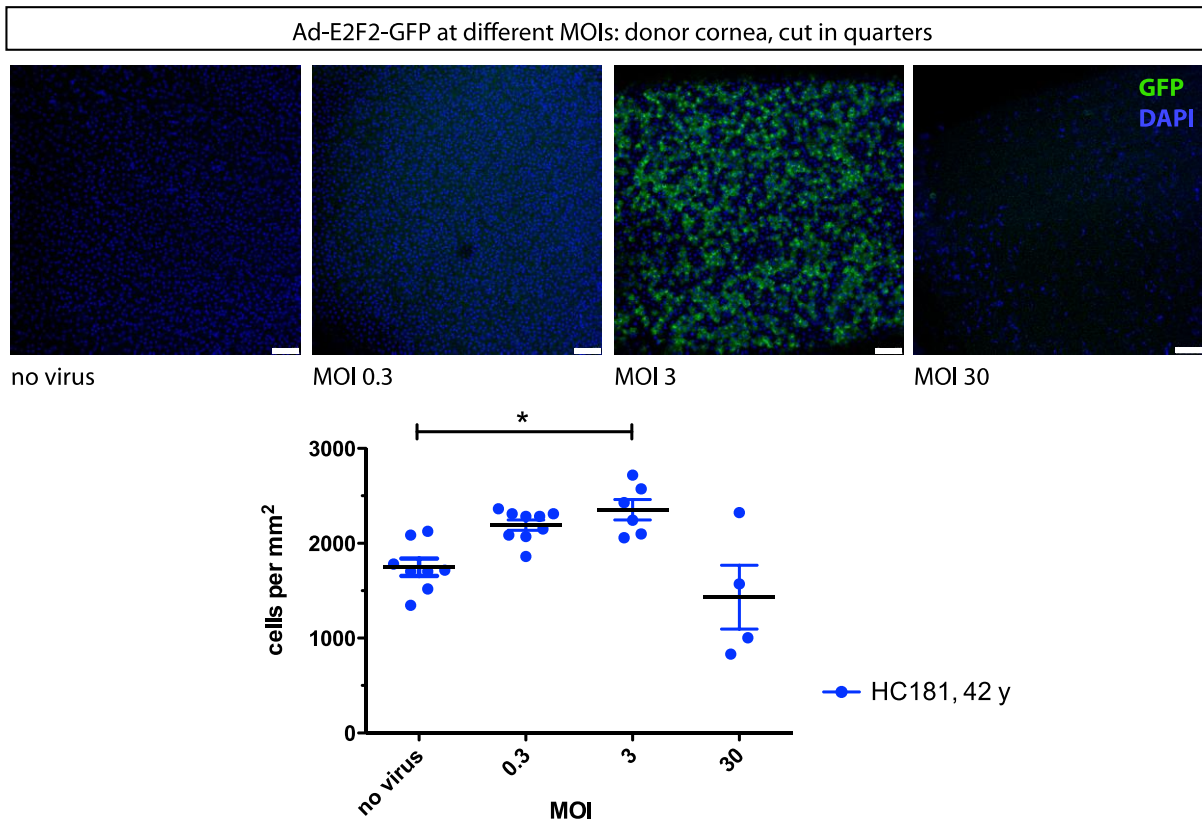
Based the first publication of the Ad-E2F2-GFP vector for use on corneal endothelium *ex vivo* (McAlister et al., 2005), we chose different MOIs to find the maximum effect on endothelial cell proliferation. Corneo-scleral rims were cut in quarters and transduced with Ad-E2F2-GFP in different concentrations, corresponding to an MOI of 0.3, 3, and 30. One quarter was left uninfected as control. After 5 days in culture, cell density in each sample was determined by counting DAPI stained nuclei on corneal flatmounts (counts of normally five micrographs across each sample were averaged). All samples were obtained from Moorfields Eye Bank and were used at similar post mortem times (19–22 days).

An example of a 42-year-old donor cornea is shown in Figure 15 A. Confocal laser scanning micrographs show GFP expression increasing with virus titre. Cell density is plotted in the graph below, while each dot is representing the nuclei counts of one high power micrograph. A significant increase was noted at MOI 3 compared to the uninfected control (35%). Cell density varied widely at MOI 30, with areas of pycnotic nuclei prevailing, an indication of dying cells. Overall, cell density was markedly decreased compared to the uninfected sample.

Figure 15 B gives an overview over four different corneal samples. Only the youngest sample (42 years of age) showed an increase in cell density. In all other samples cell density decreased after infection with Ad-E2F2-GFP. All samples infected with MOI 30 showed wide areas of pycnotic nuclei or bare Descemet's membrane.

Three other corneo-scleral rims were subjected to the same treatment but were excluded from this analysis due to excessive trauma caused by tissue handling. In two samples, cell counts could not be obtained due to massive epithelial overgrowth, one sample showed wide areas of denuded Descemet's membrane in all conditions including the untreated control, presumably due to inadequate handling.

A



B

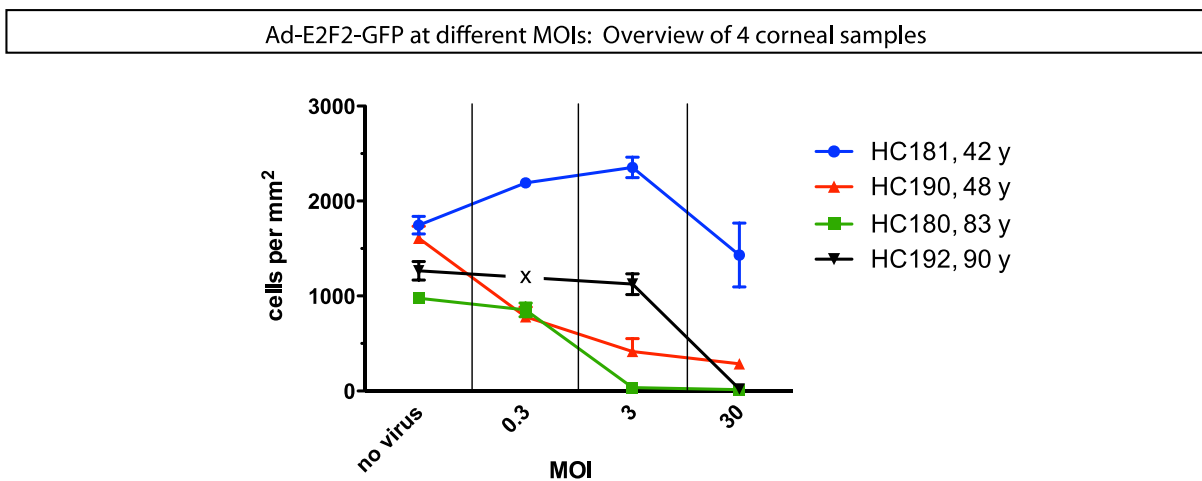


Figure 15. Effect of vector dose on corneal endothelial cell density.

Ad-E2F2-GFP was added in 4 different concentrations to corneo-scleral rims cut in quarters: MOI 0.3, 3, and 30. One quarter was left uninfected. After 2 h of transduction time, samples were cultured for 5 days. Cell density was determined by counting DAPI stained nuclei on flatmounts.

A. Confocal images of a sample from a 42-year-old donor (scale bar 100 μ m). The graph shows cell counts from multiple images, with mean \pm SEM. MOI of 3 led to a 35% increase in cell density compared to the uninfected control (* $P=0.0065$, Kruskal-Wallis test, Dunn's Multiple Comparison test).

B. Overview of 4 different samples, arranged by age. Only the youngest sample shows an increase in cell density after Ad-E2F2-GFP infection. All other samples show an increasing loss of cells with increasing virus titre. Bars show SEM. (x: no counts possible due to epithelial overgrowth, y: donor age in years).

4.3.3. Ad-E2F2 increases corneal endothelial cell density in young corneas

Due to the unpredictable quality of corneo-scleral rims, we focused on freshly excised corneal specimens obtained at full thickness corneal transplantation. We only used explants from patients with clinically normal endothelium: no signs of endothelial decompensation, no guttae, no enlargement of endothelial cells. Indications for corneal grafts therefor were mainly keratoconus or stromal scars.

Due to the small size of corneal specimens (typically 7.5 mm in diameter) and the lack of support from the sclera, samples could only be cut in half (but not in quarters), enabling the direct comparison of treated vs. control in one cornea from one patient. Cutting one sample in 4 or more pieces inevitably damaged the endothelial monolayer, making cell density analysis impossible. Therefore, time scales or virus titration experiments involving more than 2 conditions could not be performed on fresh corneal specimens.

Bisected excised full thickness cornea of 4 patients (aged 16 – 40 years) who underwent penetrating keratoplasty for keratoconus were infected either with adenovirus delivering *E2F2* and the reporter gene *GFP* (Ad-E2F2), or control virus Ad-GFP, delivering *GFP* only. Based on previous experience using different virus concentrations (see 4.3.2, page 123), a calculated MOI of 0.4 was used to minimize the risk of direct cell damage through the virus. After transduction for 2 h at 37°C in 2 mL OptiMEM, corneas were incubated in culture medium (Biocrom Medium I) for 5 days. Endothelial cell density was determined by counting DAPI stained nuclei in at least 5 micrographs per sample. During each experiment, treatment and control samples were masked by another lab member to minimize bias.

Each set of corneal samples showed an increase in cell density after Ad-E2F2 transduction compared control (Ad-GFP), ranging from 1.2fold to 1.8fold (Figure 16A). While Ad-GFP transduced controls showed a mean cell density of 1492 ± 334 cells per mm^2 (mean \pm SEM), Ad-E2F2 transduced samples gave 2198 ± 567 cells per mm^2 (95% CI: 960-2024 vs. 1259-3101), corresponding to an average increase of 1.5fold. Comparing all 4 samples together allowed the appli-

cation of a paired t-test, showing a statistically significant increase after Ad-E2F2 ($P=0.0444$, Figure 16 B).

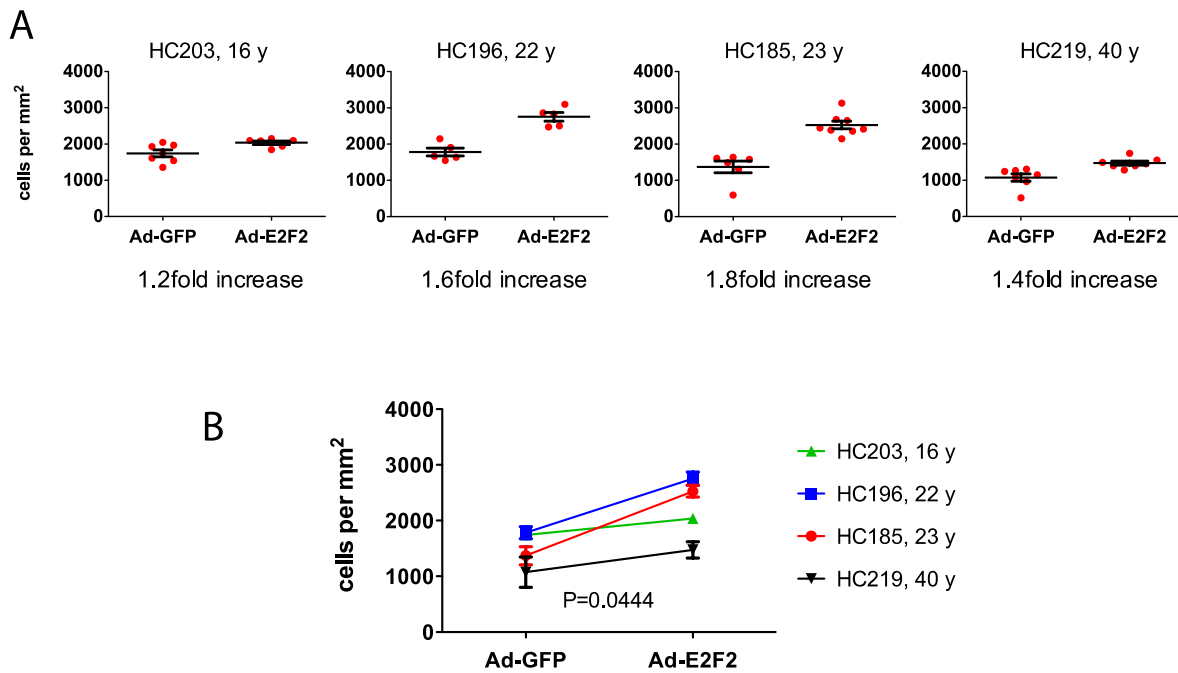


Figure 16. Ad-E2F2 increases endothelial cell density in young corneal samples.

A. Four bisected corneal specimens from young patients with keratoconus who underwent keratoplasty were transduced with either Ad-E2F2 or Ad-GFP (control) at MOI 0.4. After 5 days in culture, endothelial cell density in Ad-E2F2 samples increased 1.2–1.8-fold compared to controls.

y: years of age of donor patient

B. Overview of the four corneal samples, showing a mean 1.5fold increase in cell density after Ad-E2F2 compared to Ad-GFP (1492 ± 334 vs. 2198 ± 567 cells per mm², mean \pm SEM; 95% CI: 960-2024 vs. 1259-3101). Analysis of all data in a paired t-test reveals statistical significance ($P = 0.0444$).

4.4. Lentivirus mediated E2F2 overexpression

Adenoviral vectors, though very effective, have a high immunogenicity. This makes them unsuitable in a corneal transplantation setting where the immune system of the recipient is already alert. We therefore sought to establish *E2F2* transfer by less immunogenic lentiviral vectors.

4.4.1. Construction and characterization of lentiviral plasmids

4.4.1.1. LNT-E2F2

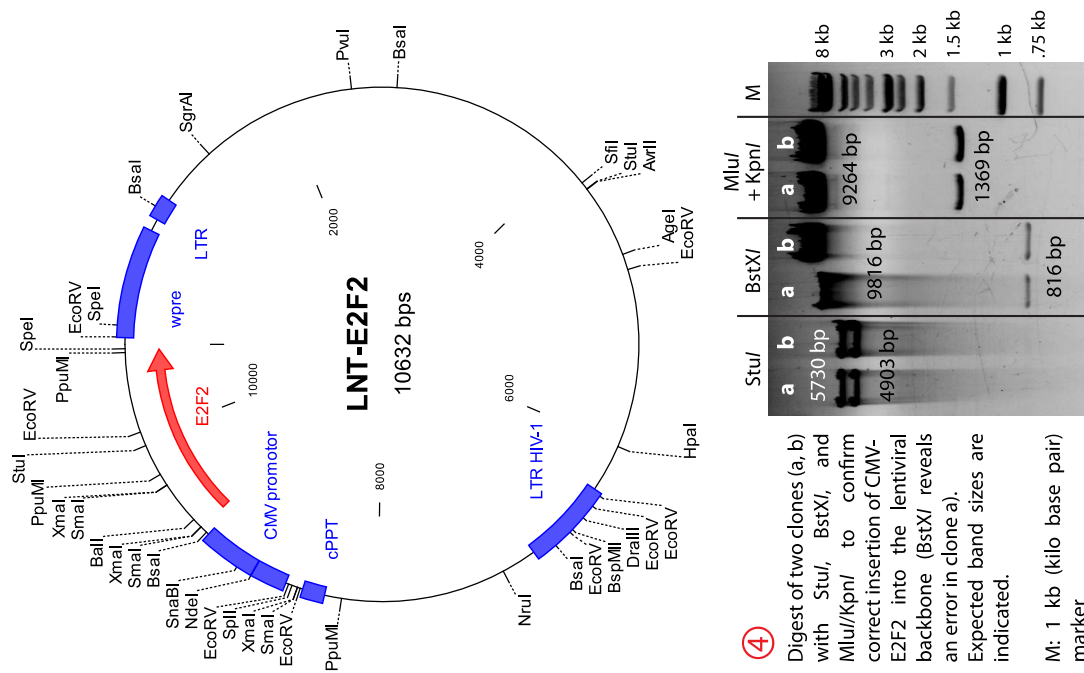
A lentiviral backbone plasmid based on the pHR'SIN vector (see 2.2.1, Lentiviral vector production, p. 70) was constructed to produce vectors delivering *E2F2* cDNA under the ubiquitous cytomegalovirus (CMV) promoter (Figure 17). Human full-length *E2F2* cDNA (1313 bp) was derived from plasmid pCMV-E2F2 (6771 bp), provided by Dr Nancy Joyce, Schepens Eye Research Institute, Harvard Medical School, Boston, USA (Ivey-Hoyle et al., 1993; Joyce et al., 2004). Before further cloning, the *E2F2* region of the plasmid was sequenced confirming 100% identity with the published sequence of *E2F2* (NCBI Reference Sequence: NM_004091.2).

Due to the lack of suitable restriction sites in the lentiviral donor plasmid, a linker was inserted to provide a *MluI* restriction site just after the *E2F2* gene: pCMV-E2F2 was linearized using *EcoRI* and re-ligated in the presence of a 10 bp linker 5'-AATTACGCGT-3' (compatible with the sticky ends created by *EcoRI*). After transformation into *E. coli*, insertion of the linker was confirmed by digestion with *MluI*, now cutting in two sites yielding a 2040 bp and a 4741 bp band (Figure 17, Step 1). The *E2F2* fragment could then be cut out with *MluI* and *NdeI*, resulting in three bands of 256, 4741, and 1784 bp, the latter representing the insert *E2F2* preceded by the CMV promoter (Figure 17, Step 1, left lane, 256 bp band not shown).

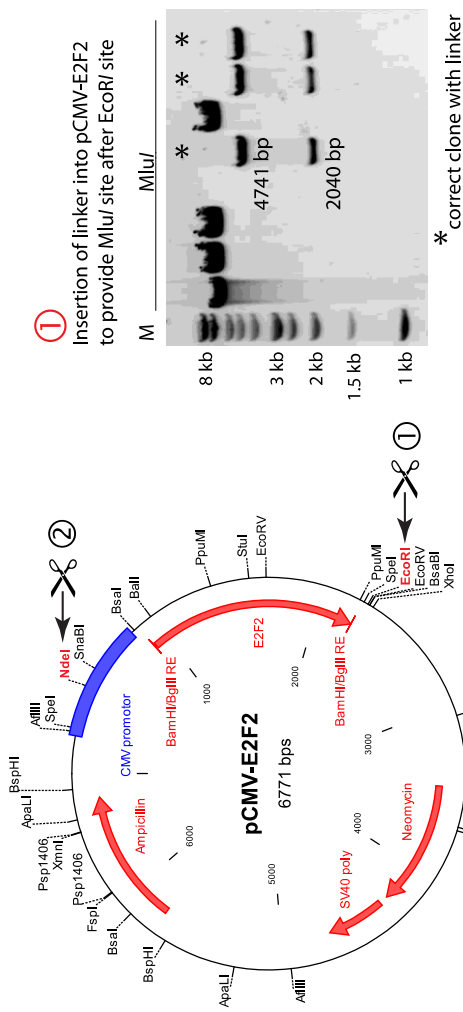
The lentiviral backbone plasmid LNT-CMV-Mertk (12.374 bp, contained the *Mertk* gene from a different study by this group) was also digested with *MluI* and *NdeI*, cutting out *Mertk* with its promoter (3525 bp) and providing the viral backbone (8849 bp) with the same ends as the CMV-*E2F2* insert for a directional ligation (Figure 17, Step 2, middle lane). The resulting plasmid LNT-E2F2 was checked by digestion with *StuI*, *BstXI*, and *KpnI* + *MluI* combined (Figure 17, Step 4). Integrity of the CMV-*E2F2* insert was verified by sequencing.

The LNT-E2F2 plasmid was used to produce non-integrating lentiviral vectors using a second generation production system (2.2.1, page 70), also named LNT-E2F2. A control vector delivering green fluorescent protein gene (LNT-GFP) was produced alongside, which typically resulted in nearly identical titres (determined by reverse transcriptase ELISA).

C New lentiviral transfer vector: LNT-E2F2



A Donor plasmid: pCMV-E2F2



B Lentiviral backbone plasmid: LNT-Merk

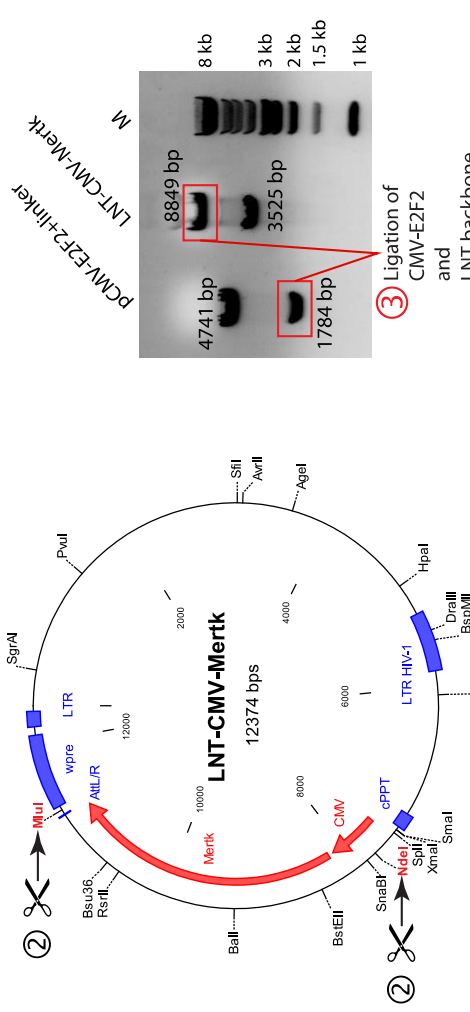


Figure 17.

Outline of the cloning strategy for LNT-E2F2, the lentiviral backbone plasmid based on the pHR'SIN vector, delivering E2F2 under a CMV promoter.

The lentivirus LNT-E2F2 was characterized *in vitro* on mRNA and protein level. E2F2 mRNA was quantified by RT-PCR in 293T cells. Cells were infected with LNT-E2F2 at an MOI of 20 and incubated for 4 days, when total RNA was extracted. E2F2 mRNA was normalized to the housekeeping gene β -actin to then calculate n-fold expression compared to uninfected and LNT-GFP infected controls. LNT-E2F2 infected cells show a 120-fold increase of E2F2 mRNA compared to uninfected controls. LNT-hrGFP infection did not cause E2F2 upregulation.

On protein level, immunohistochemistry of serum starved ARPE19 cells infected with LNT-E2F2 (MOI 20) showed intensive staining of all nuclei, in line with the physiological localization of endogenous E2F2. In LNT-hrGFP infected control cells, no E2F2 was detected. For immunohistochemistry, the antibody against E2F2 was diluted at 1:200, a concentration that did not detect endogenous E2F2.

A titration of different vector concentrations, corresponding to MOIs of 50, 10, 1, and 0, was performed on 293T cells to determine intracellular E2F2 protein by Western blot. Four days after infection, cells were lysed using RIPA buffer with protein inhibitor. 10 μ g of protein were loaded per lane of a 9% polyacrylamide gel. β -actin was used as a loading control. The experiment shows that E2F2 protein expression after LNT-E2F2 infection is dependent on vector dose. Even at a low MOI of 1, E2F2 protein was detectable, while uninfected cells remained negative for E2F2.

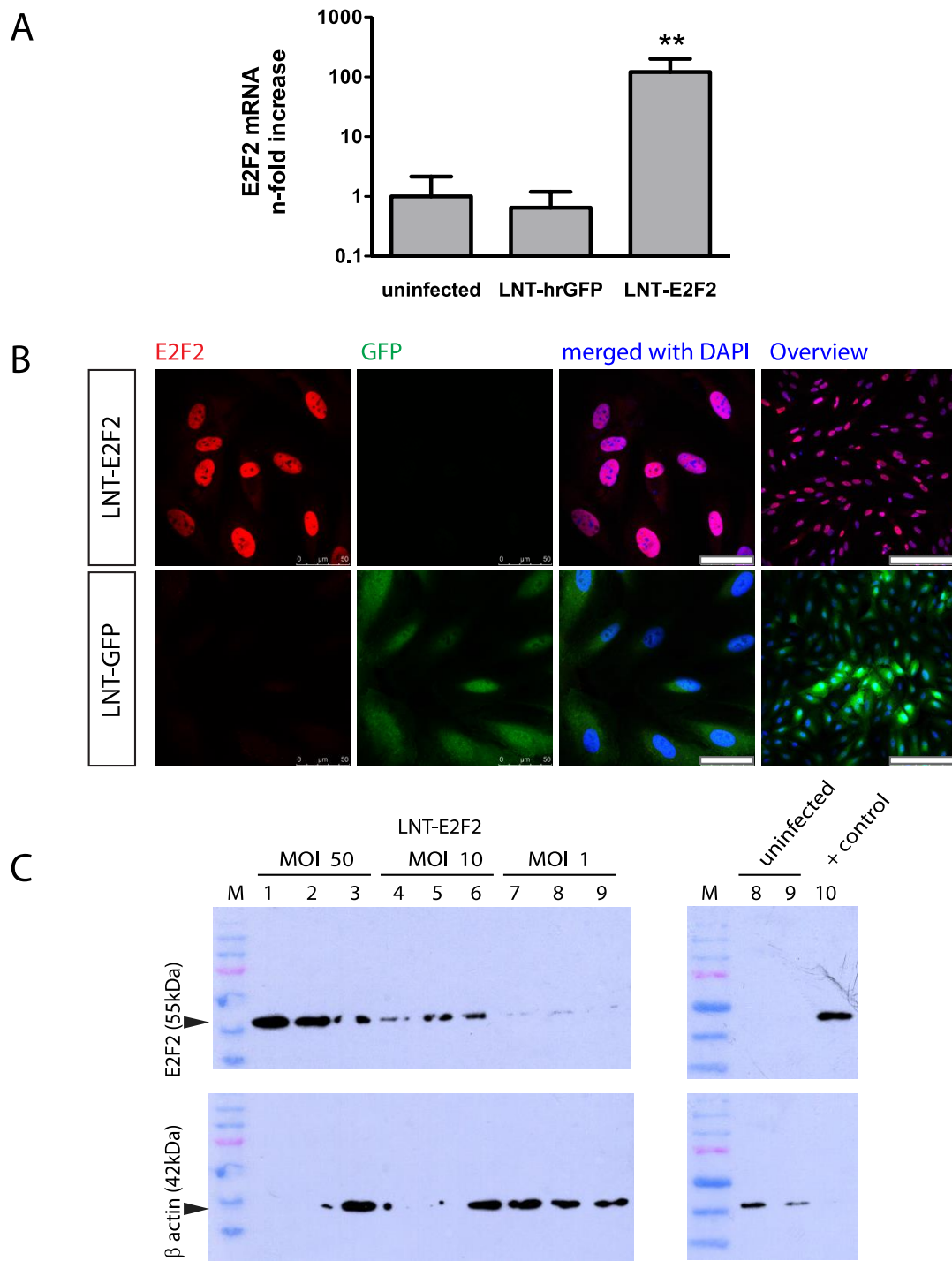


Figure 18. Characterization of lentiviral vector LNT-E2F2.

A. On mRNA level, infection of 293T cells with LNT-E2F2 (MOI 20) induces a 120-fold upregulation of E2F2 mRNA compared to untransduced or LNT-GFP transduced controls, measured by qRT-PCR (**: $P < 0.01$, One-Way-ANOVA, Tukey's Multiple Comparison Test). Error bars are SE of triplicate samples.

B. On protein level, serum starved ARPE19 cells show nuclear localization of transgene E2F2 (red) after LNT-E2F2 transduction, as demonstrated by immunohistochemistry. Cells transduced with LNT-GFP only show GFP expression (green), but no E2F2 staining. Scale bar 50 μm , for overview 250 μm (right panel).

C. Titration of vector (MOI 50, 10, 1, uninfected) shows dose-dependent E2F2 protein expression in 293T cells, as demonstrated by Western blot. +: Positive control (HeLa cell lysate). M: protein marker ladder.

4.4.1.2. LNT-E2F2-IRES-GFP

To discriminate transduced and untransduced cells, a lentiviral packaging plasmid was constructed delivering *E2F2* under an ubiquitous promoter, followed by an internal ribosomal entry site (IRES) and *GFP* reporter gene. This double construct, in theory, should lead to equimolar expression of both E2F2 and GFP. After traditional cloning methods failed, a Gateway cloning strategy (Invitrogen, UK) was used to shuttle *E2F2* into a destination vector harbouring IRES-eGFP in a lentiviral backbone (already used in this group for other studies, cloned and provided by Ulrich Luhmann).

First, *E2F2* was transferred into an Entry clone (pENTR/D-TOPO vector, Invitrogen, UK; 2580 bp). This clone provides the gene of interest flanked by two recombination sites (*attL1* and *attL2* sequence). Using plasmid pCMV-E2F2 (6771 bp, see 4.4.1.1, p. 127), *E2F2* was amplified by PCR using a proofreading polymerase (*Pfu*, Promega, UK) with the following primers: 5'-C ACC GCC ACC **ATG** CTG CAA GGG-3' (forward) and 5'-GCG GCC GCC AGT GTG TGA T -3' (reverse). The forward primer ensured the insertion of a 4 base pair overhang (CACC) before the start codon of *E2F2* (ATG). CACC base pairs with the overhang sequence, GTGG, in the pENTR/D-TOPO vector to enable directional insertion of the gene. After some optimization, the PCR produced a band of the correct size (1.3 kb), which was cut out of the gel and purified. 1 and 5 ng of DNA was used for topoisomerase cloning reactions according to the manufacturer's recommendations. The plasmid was transformed into chemically competent *E. coli* and cultured on ampicillin selective agar plates.

The correct clone (named TOPO-E2F2, 3964 bp) was identified by digesting with *SmaI* and *NheI*, resulting in four bands of 196, 266, 356, and 3153 bp. If insertion occurred in inverse direction, bands of 266, 356, 1177, and 2169 bp were to be expected (Figure 19). Integrity of the *E2F2* insert and adjacent *attL* sites was verified by sequencing.

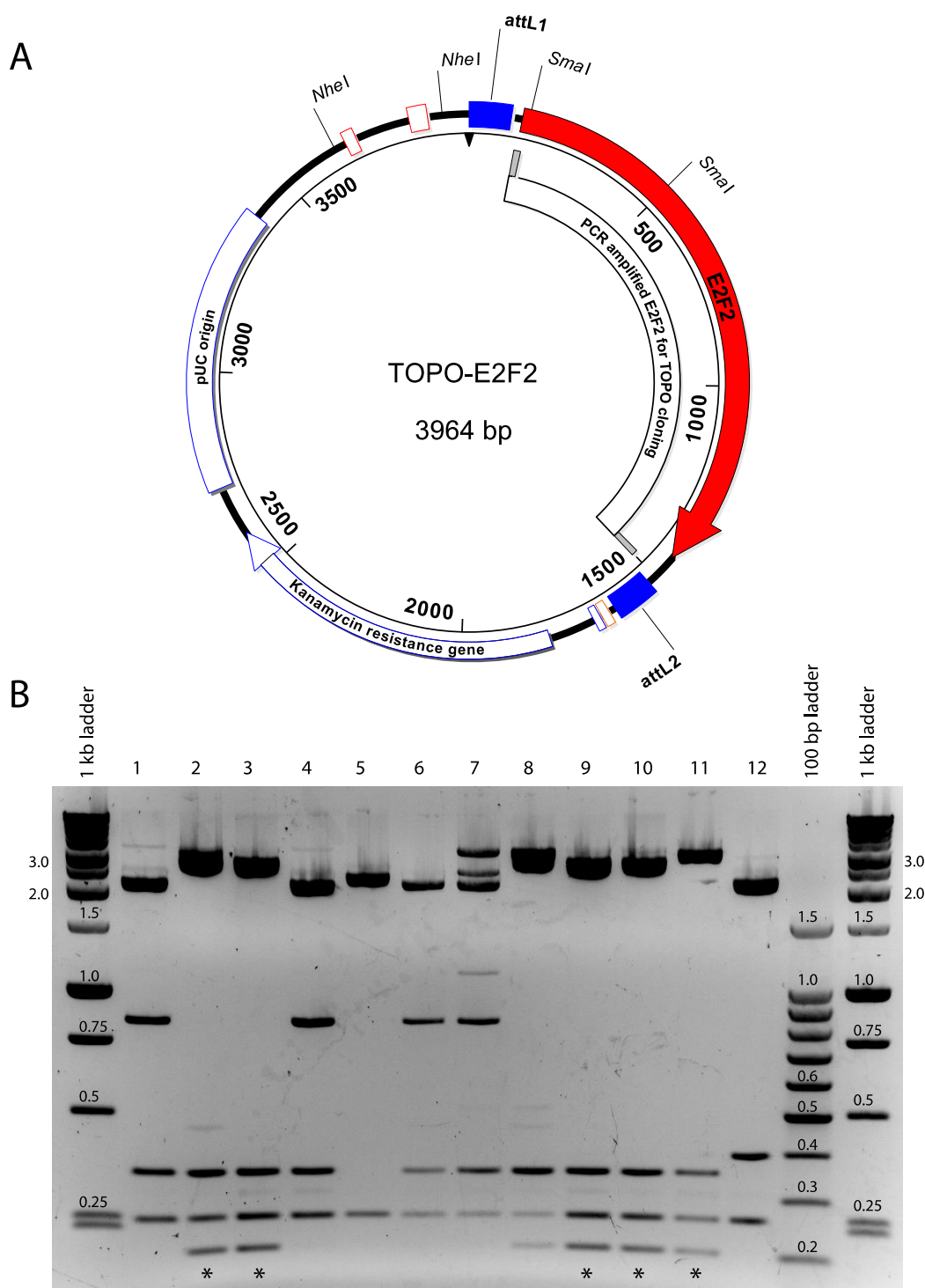


Figure 19. Design of the entry clone TOPO-E2F2.

A. *E2F2* was PCR-amplified using primers to allow directional insertion into the TOPO vector in a topoisomerase cloning reaction.

B. The correct clone of TOPO-E2F2 was identified by restriction enzyme digest with *SmaI* and *NheI*, resulting in four bands of 196, 266, 356, and 3153 bp (*). The clone of lane 11 showed correct sequencing results and was used for further cloning steps.

The destination vector LNT-ccdB-IRES-eGFP contained the corresponding *attR1* and *attR2* sites to allow site-specific recombination with the *attL1* and *attL2* sequence in TOPO-E2F2. Recombination was enabled using a proprietary enzyme mix (Gateway LR Clonase II Plus, Invitrogen, UK) according to the manufacturer's instructions. This resulted in the clone LNT-E2F2-IRES-eGFP (11,731 bp), driving E2F2 expression under the ubiquitous SFFV promoter, while eGFP expression is driven by the IRES. Sequencing results starting from SFFV to E2F2, IRES, eGFP up to WPRE showed 100% identity to the predicted map (Figure 20).

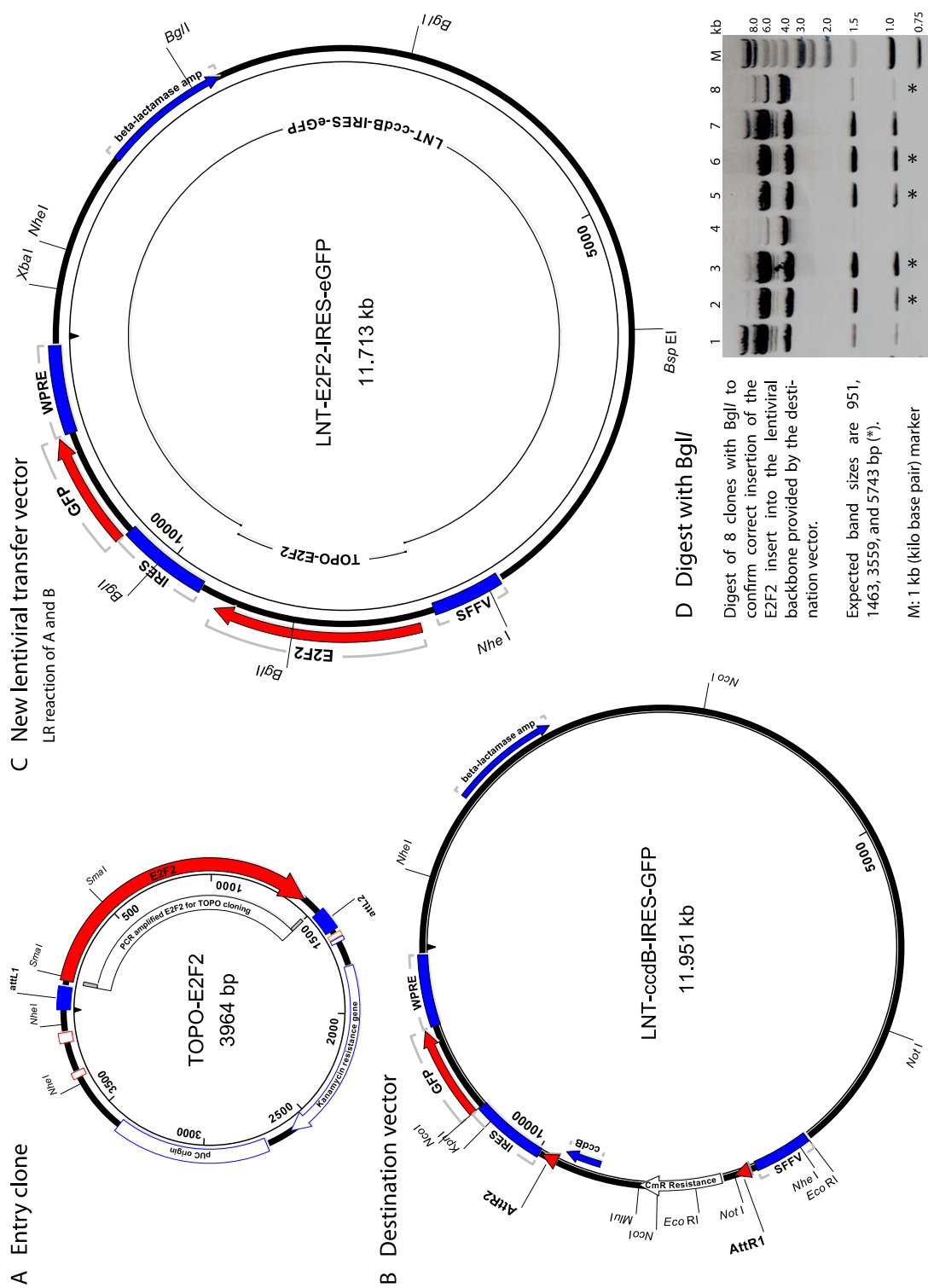


Figure 20. Construction of LNT-E2F2-IRES-eGFP. A lentiviral backbone plasmid based on the pHR'SIN vector was used to clone LNT-E2F2-IRES-eGFP, delivering E2F2 under an SFFV promoter and eGFP driven by IRES. bp: base pairs, kb: kilo base pairs.

LNT-E2F2-IRES-eGFP plasmid was used to produce non-integrating lentiviral vectors using the second-generation production system (2.2.1, page 70), and the vector also named LNT-E2F2-IRES-GFP. Expression of vector-mediated E2F2 was assessed *in vitro* on 293T and ARPE19 cells.

mRNA levels of E2F2 were tested on 293T cells after titre matched transduction with LNT-E2F2-IRES-GFP and LNT-E2F2 (MOI 20), and compared to untransduced or LNT-GFP transduced controls. LNT-E2F2-IRES-GFP yielded an increase in E2F2 mRNA that was not statistically significant. In contrast, LNT-E2F2 induced transgene upregulation was over 30-fold higher compared to the double construct, and over 200-fold higher compared to the untransduced control ($P < 0.01$). LNT-GFP control did not cause any E2F2 upregulation (Figure 21).

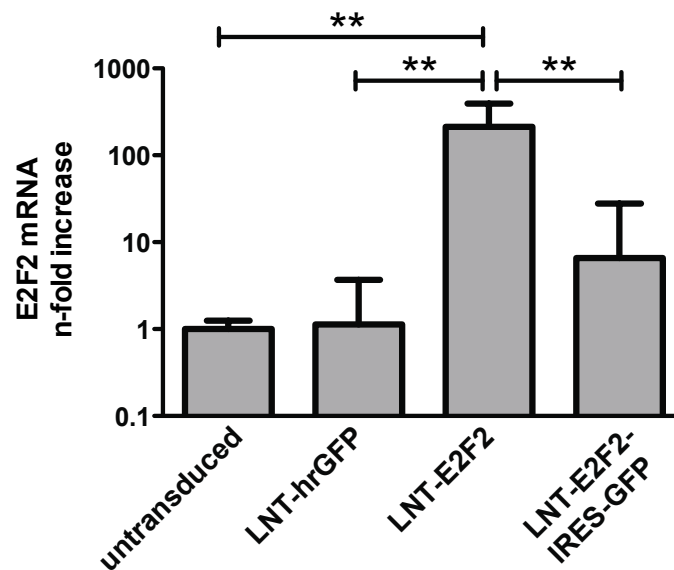


Figure 21. Characterization of lentiviral vector LNT-E2F2-IRES-eGFP on mRNA level.

Infection of 293T cells with LNT-E2F2-IRES-GFP (MOI 20) induced a 7-fold upregulation of *E2F2* mRNA, which was not significant compared to controls (untransduced or LNT-GFP transduced cells). Titre matched LNT-E2F2 induced a significantly higher *E2F2* upregulation both compared to controls and compared to LNT-E2F2-IRES-GFP (** $P < 0.01$, one-way ANOVA, Tukey's multiple comparison post-test; all other differences were not significant). Error bars are SE of triplicate samples.

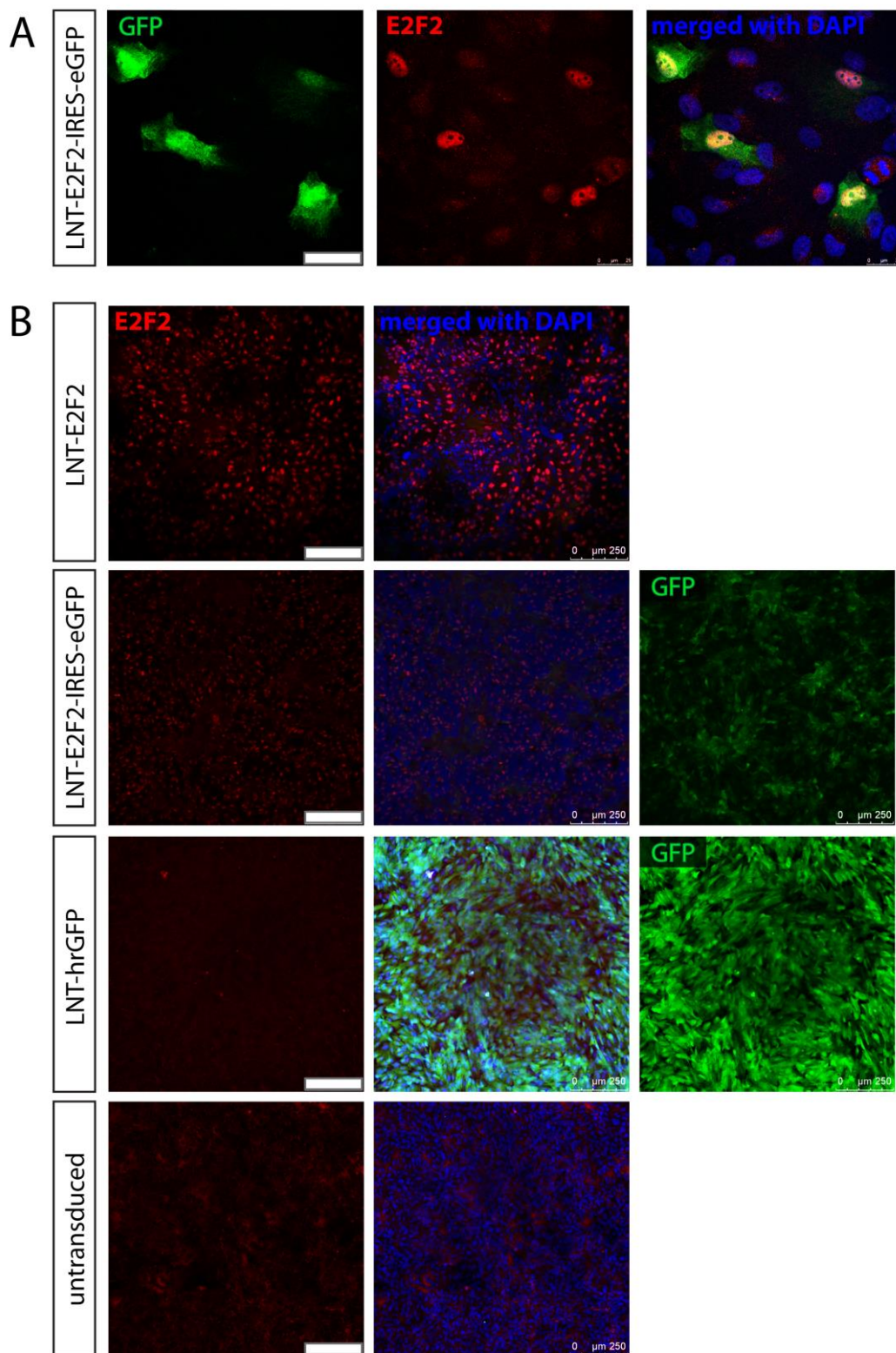


Figure 22. Characterization of lentiviral vector LNT-E2F2-IRES-eGFP on protein level.

A. At low MOI of 0.1, transduction of serum-starved ARPE19 cells with LNT-E2F2-IRES-GFP shows co-localization of transgenic E2F2 (red) and reporter gene (GFP). Scale bar 25 μ m.

B. At MOI of 20, E2F2 staining after LNT-E2F2-IRES-GFP transduction is higher than LNT-GFP or untransduced controls, but not as intensive as after LNT-E2F2. Scale bar 250 μ m.

On protein level, transduction of serum-starved ARPE19 cells with the double construct LNT-E2F2-IRES-GFP showed nuclear staining of exogenous E2F2. At a low MOI of 0.1, co-localisation of E2F2 with reporter gene GFP was observed (Figure 22 A). At an MOI of 20, LNT-E2F2-IRES-GFP induced E2F2 staining clearly above the background level of controls (LNT-GFP or untransduced), but markedly lower than the single-gene vector LNT-E2F2 (Figure 21 B).

4.4.2. *E2F2* overexpression in human corneal endothelium

Human corneal endothelium was transduced *ex vivo* with vectors LNT-E2F2 and LNT-E2F2-IRES-GFP. Using the transduction protocol established with LNT-GFP (see 3.4, p. 99), fresh corneal specimens were exposed to vector on day one and three, and maintained in culture for a total of 4 to 7 days.

E2F2 overexpression was assessed on protein level on whole corneal specimens four days after transduction at an MOI of 20. Western blot analysis showed a 55 kDa band corresponding to E2F2 in the LNT-E2F2 treated sample. This band was barely detectable in the LNT-E2F2-IRES-GFP sample. The untransduced control remained negative (Figure 23).

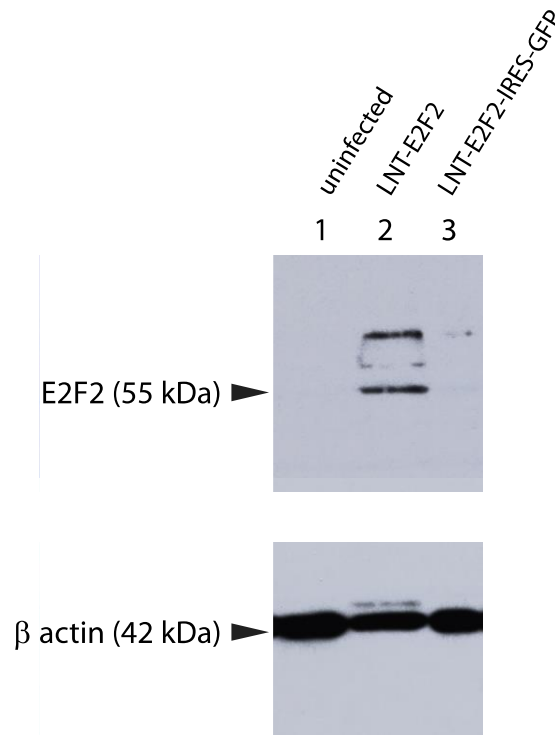


Figure 23. Expression of transgene E2F2 protein after transduction with lentiviral vectors.

Three whole corneal specimens (all keratoconus patients) were either left untransduced (1), or transduced with LNT-E2F2 (2) or LNT-E2F2-IRES-GFP (3) for 3 hours, MOI ~20 in OptiMEM. After four days in culture, Descemet's membrane was peeled off using a dissecting microscope. Sheets of endothelium were transferred into 30 μ L of RIPA buffer with protease inhibitors on ice, vortexed and centrifuged 10 min at maximum speed to pellet cellular debris. 12 μ L of supernatant were directly used for SDS PAGE separation.

4.4.3. Effect of E2F2 overexpression

4.4.3.1. Effect on proliferation marker Ki67

To assess the effect of lentivirus mediated overexpression of E2F2 in human corneal endothelium, we first looked at proliferation marker Ki67. Full thickness corneas excised from keratoconus patients undergoing penetrating keratoplasty were cut in half and transduced with non-integrating LNT-E2F2 or mock-transduced with carrier medium only (OptiMEM serum-free medium). After 7 days in culture, specimens were flatmounted after immunostaining.

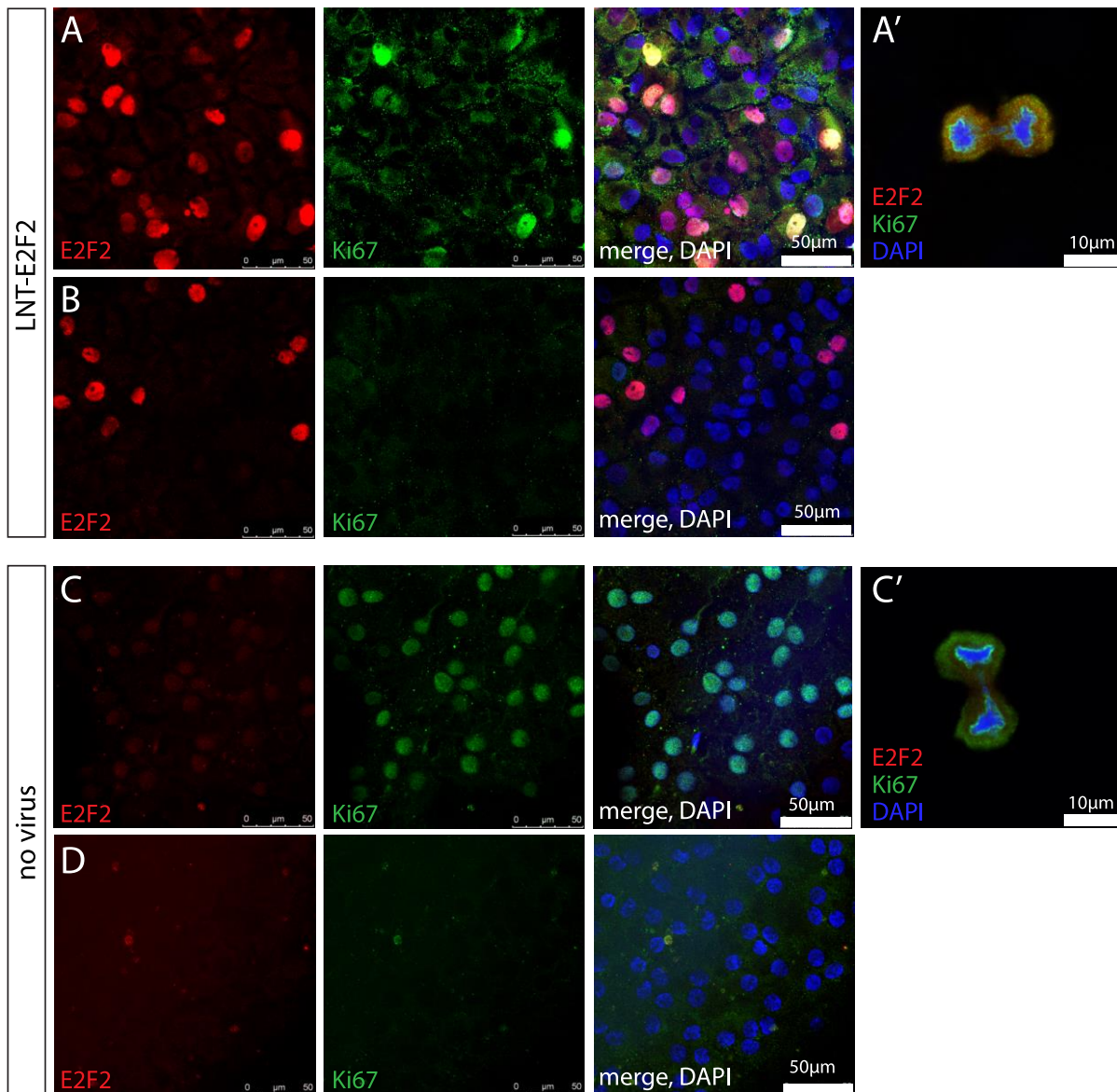


Figure 24. Effect of LNT-E2F2 on Ki67 expression.

A bisected corneal specimen from a 29-year-old keratoconus patient who underwent penetrating keratoplasty was either transduced with non-integrating LNT-E2F2 (A, B) at MOI 20 or mock-infected in carrier medium only (C, D). Representative confocal laser scanning images of the epithelium *en face* show E2F2 (red) and Ki67 (green) expression 7 days after transduction. Areas within 1 mm of the cut edge were excluded.

A. Mid-periphery of the LNT-E2F2 transduced sample shows Ki67 expression in few (<5%) nuclei, co-localizing with E2F2 overexpression. Very few mitotic figures can be found (A').

B. The centre shows E2F2 overexpression, but no Ki67 staining and no mitotic figures.

C. Mid-periphery in the mock-transduced control shows E2F2 background staining, but areas of Ki67 positive nuclei. Very few mitotic figures can be found (C').

D. The centre in the mock-transduced sample shows no Ki67 expression.

Figure 24 shows representative confocal laser scanning micrographs from the mid-peripheral and the central region of the cornea (but avoiding the cut edges). Overexpression of E2F2 was detected in the nuclei in all regions in the LNT-E2F2 transduced sample. The control showed low background E2F2 staining.

Ki67 positive nuclei (less than 5%) were found in both conditions, LNT-E2F2 transduced and mock transduced, only in the mid-periphery but not in the central region of the cornea. These regional differences in Ki67 staining pattern were not caused by a cut edge artefact, because mid-peripheral (panel A, C) and central region of the cornea (panel B, D) of each half were imaged equidistant from any cut edge. Since the excised cornea was bisected precisely through the centre, the geometric centre of the cornea lies within the avoided region of the cut edges and was not imaged.

In the transduced sample, co-localization of Ki67 with E2F2 was evident. In each sample, ~3-4 mitotic figures were found in the mid-periphery. Occasional mitotic figures were also found in subsequent experiments when the cornea was kept in culture, but because of the sporadic nature of their appearance this was not quantified.

4.4.3.2. Effect on endothelial cell density

Because neither the number of Ki67 positive nuclei nor the number of mitotic figures showed a reliable difference between LNT-E2F2 transduced and control samples, we focused on cell density as the main outcome measure. Corneal specimens from patients who underwent penetrating keratoplasty were bisected by the surgeon under the operating microscope. This allowed comparing two samples of the same size from the same cornea, treated with LNT-E2F2 or control vector. The size of the specimen was large enough to exclude the area comprising monolayer damage and therefore staining artefacts at the cut edges. Further cutting into quarters, however, introduced vast disruption of the monolayer and was not pursued.

For each experiment, E2F2 overexpression was verified by immunostaining. Representative immunofluorescence micrographs are shown in Figure 25A. LNT-GFP served as a control vector. ECD was determined by counting DAPI stained nuclei in at least 6 micrographs per specimen, as described in Chapter 2.5.7, Corneal endothelial cell density assessment, p. 87. In none of the corneas could we find a meaningful difference in endothelial cell density after LNT-E2F2 transduction versus LNT-GFP. ECD results of three corneal specimens treated identically were pooled which allowed a paired t-test. No significant difference was detected.

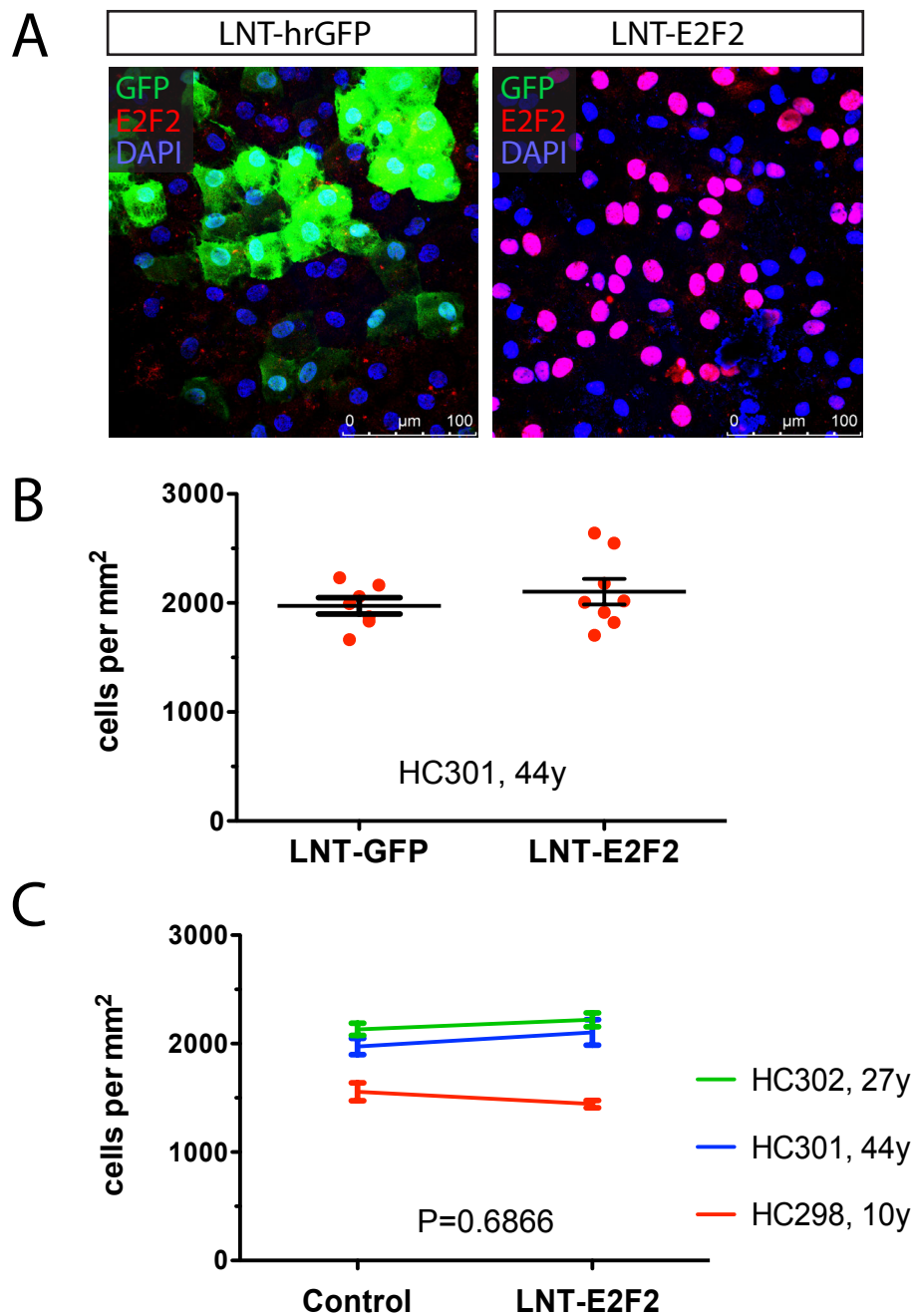


Figure 25. Effect of E2F2 overexpression on cell density.

Bisected fresh corneal specimens of equal size were transduced with either LNT-E2F2 or LNT-GFP (MOI 20, transduction time 4 h) and maintained in culture for 6 – 7 days.

A. Representative immunofluorescence micrographs demonstrating E2F2 overexpression in the LNT-E2F2 transduced specimen only (corneal specimen from a 44-year-old keratoconus patient). Transduction efficacy for both vectors varied between 30 – 60%. Scale bar 100 μ m.

B. Example of endothelial cell density quantification by counting DAPI-positive nuclei in 8 micrographs. Dots represent individual counts per micrograph; bars show mean \pm SEM.

C. Pooling of the ECD results of three corneas treated identically allowed pairwise comparison between treated and control-treated corneal halves in a paired t-test. This showed no statistically significant difference in cell density ($P=0.6126$). Error bars indicate SEM.

4.4.3.3. Effect on cell density over time

It is possible that a proliferative effect of E2F2 overexpression might be masked by the loss of endothelial cells due to suboptimal culture conditions. To assess this question, cell density was assessed before and at different time points after transduction with LNT-E2F2 or LNT-GFP on a pair of whole donor corneas unsuitable for transplantation.

To achieve a high MOI of 50 with a concentrated virus solution, the samples were placed on stands in a moisturized environment. With the endothelium facing upwards, corneal samples formed a bowl that could fit 200 μ L of concentrated virus solution, which was dropped directly onto the endothelium. Samples were incubated for 3 hours. After day 0, 4, 7, and 12, a sector of corneal tissue was cut off for immunohistochemical and cell density analysis in flatmounted samples.

Transgene expression was assessed after day 7. Transgenic E2F2 localized to the nucleus and was present in approximately one third of cells in the LNT-E2F2 transduced sample, while the LNT-GFP control sample showed no E2F2 expression. Transduction efficacy based on GFP expression in the LNT-GFP transduced sample was 30-40%. Integrity of the endothelial monolayer was assessed at the beginning (immediately after transduction) and end of experiment (day 12) by ZO-1 immunohistochemistry. No change in appearance was obvious in either condition.

Cell density was recorded at days 0, 4, 7, and 12 by counting DAPI stained nuclei in six micrographs per sample. At the beginning of the experiment, both samples had similar cell densities at around 2100 cells per mm^2 . For both LNT-E2F2 and LNT-GFP transduced corneas, cell density gradually decreased the following 12 days to around 1900 cells/ mm^2 . The LNT-E2F2 treated sample showed a small increase at day 7. However, none of the changes between time points reached statistical significance. Nor did a comparison between the two conditions, LNT-E2F2- and LNT-GFP-transduced, show significant differences at any given time point.

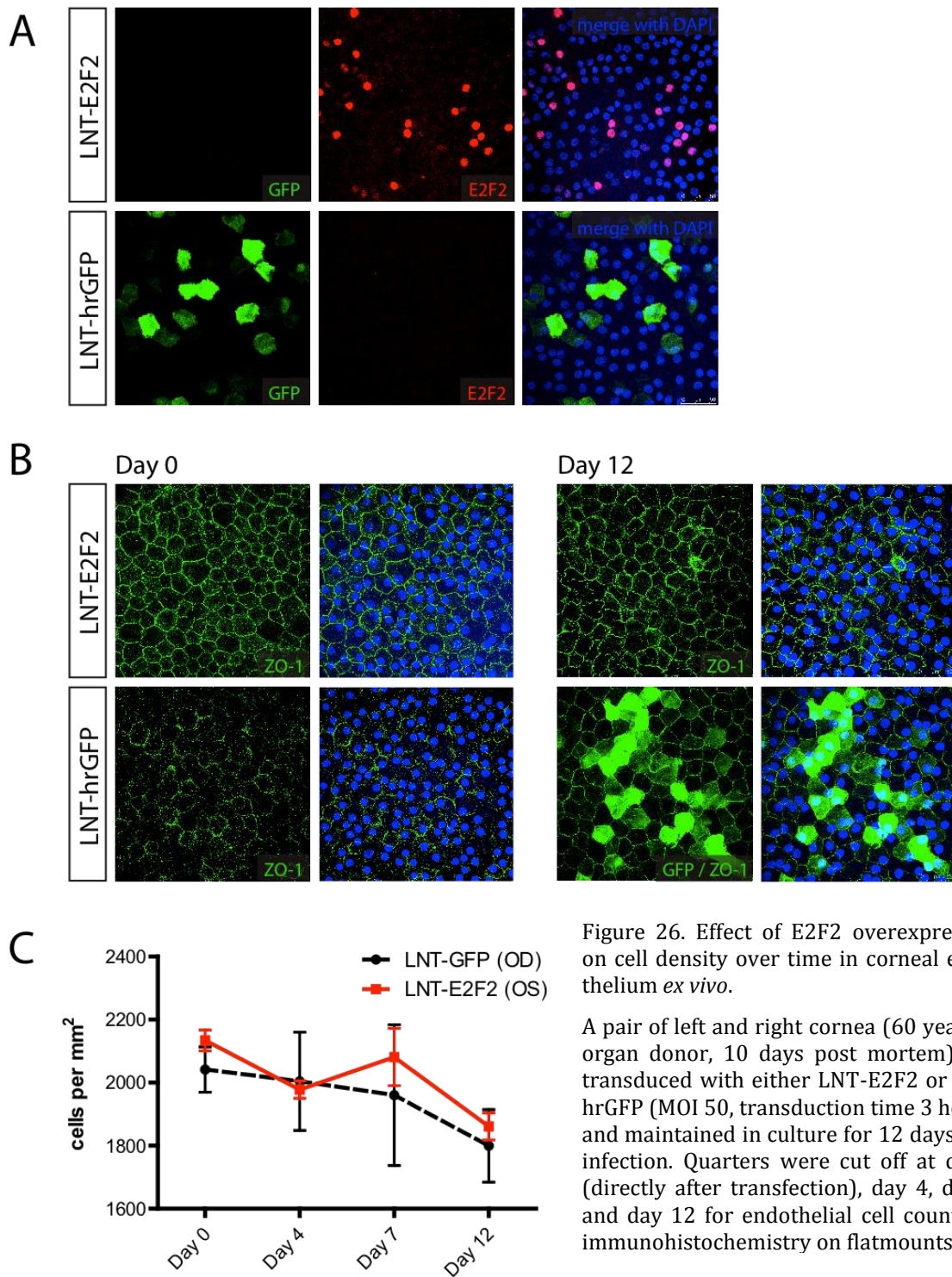


Figure 26. Effect of E2F2 overexpression on cell density over time in corneal endothelium *ex vivo*.

A pair of left and right cornea (60 year old organ donor, 10 days post mortem) was transduced with either LNT-E2F2 or LNT-hrGFP (MOI 50, transduction time 3 hours) and maintained in culture for 12 days post infection. Quarters were cut off at day 0 (directly after transfection), day 4, day 7, and day 12 for endothelial cell count and immunohistochemistry on flatmounts.

A. Transgene expression was verified by immunohistochemistry. E2F2 shows nuclear localization on day 7 post infection only in the LNT-E2F2 infected sample, the control cornea infected with LNT-hrGFP remains negative for E2F2.

B. Integrity of the endothelial cell monolayer was assessed by ZO-1 staining, indicating intact tight junctions in both LNT-E2F2 and LNT-GFP infected corneas throughout the experiment (here shown day 0 and day 12).

C. Endothelial cell density time course. Values are average DAPI counts of 6 micrographs per corneal quarter, calculated as cells per mm². Error bars indicate standard deviation. There was no statistically significant difference between time points or between the two conditions at any given time point.

4.5. Discussion

4.5.1. Proliferation assays and endothelial cell density in cultured donor corneas

Metabolic assays

Classical methods of detecting cell proliferation include monitoring the activity of mitochondrial dehydrogenases as a surrogate for the number of living cells (e.g. MTT assay). However, these assays are designed for cell populations with relatively short doubling times. Human corneal endothelium is considered non-proliferative under normal circumstances and has a very low capacity to proliferate under certain conditions. Therefore, even after mitogenic stimulation under optimal conditions, only a fraction of endothelial cells are expected to be dividing. Also, in a full thickness *ex vivo* corneal sample, the corneal endothelium makes up for only a fraction of total cells. Any increase in endothelial cell density and hence metabolic activity would be masked by other cell types. Especially the epithelium, and at a lower rate, the stromal keratocytes, proliferate in *ex vivo* culture. Hence, any endothelial proliferation would not be detected by classical proliferation assays.

Immunohistochemical assays

Different immunohistochemical methods were evaluated to determine the cell cycle status of the corneal endothelium. Single cell labelling assays with BrdU or Ki67 were tested for their suitability to detect corneal endothelial cell replication *in situ* in culture. BrdU is a thymidine analogue that is incorporated into DNA during the S phase of the cell cycle. Ki67 is a protein necessary for cellular proliferation and is present in cells in any active stage of the cell cycle, G1, S, G2, and mitosis, but not in resting cells in G0 and early G1 (Scholzen and Gerdes, 2000; Zacchetti et al., 2003). BrdU and Ki67 have been widely used for assessing proliferation in the

corneal endothelium (Harris and Joyce, 1999; He et al., 2012; Joyce et al., 1998; McAlister et al., 2005; Patel and Bourne, 2009; Senoo and Joyce, 2000).

Both Ki67 and BrdU labelled an unexpectedly high number of corneal endothelial cells in cultured samples, and showed a high variability between samples. Especially at cut edges of the samples or at areas where the endothelial monolayer was disrupted due to manipulation before or during the culture period, a high number of BrdU or Ki67 positive nuclei was observed. This observation is in accordance with other publications. He et al. observed many Ki67 positive cells in cultured corneas (under eye bank conditions, 2% FCS), but not in fresh, non-stored corneas (He et al., 2012). Patel and Bourne noted Ki67 positive cells along the cut edges, which they excluded in further analysis (Patel and Bourne, 2009). The centre of the endothelium showed ~8% Ki67 positive cells after 4 days in culture medium containing 10% FCS. However, the number of Ki67 positive cells per area inversely correlated with endothelial cell density.

There is dispute about whether BrdU or Ki67 are specific for labelling only proliferating cells. Especially in the field of neurogenesis in the brain, BrdU as a means to monitor cell proliferation is in debate (Bauer and Patterson, 2005; Nowakowski and Hayes, 2000; Taupin, 2007). Through multiple checkpoint mechanisms, the cell cycle is directly linked with apoptosis, the result of an aborted cell cycle (cf. Chapter 1.2, The cell cycle, p. 17). For terminally differentiated neurons, this mechanism has been investigated intensively. When damaged, they can re-enter the cell cycle, activate cell cycle-associated proteins (e.g. Ki67), and initiate DNA synthesis (BrdU uptake). However, breach of cell cycle checkpoints results in abortive DNA synthesis without cell division, and the cells undergo cell death (Chen et al., 2000; Katchanov et al., 2001; Liu and Greene, 2001; Yang et al., 2001). For terminally differentiated corneal endothelial cells, this mechanism might be similar, especially when the conditions *ex vivo* increase cellular stress. In cultured corneas, apoptotic cells can be detected and their number inversely correlates with endothelium quality and cell density (Albon et al., 2000).

BrdU positivity could also result from aneuploid cells that have formed when cells entered the cell cycle and underwent DNA replication, but did not complete M phase, as shown for 'at-risk neurons' in the brain (Busser et al., 1998; Yang et al., 2001). Such polyploid cells can persist for many months before undergoing cell death (Chen et al., 2000; Liu and Greene, 2001). No such studies have yet been undertaken in the corneal endothelium.

BrdU is also incorporated into cells undergoing DNA repair, though only in a very small amount (Selden et al., 1993). This again could increase the number of false-positively labelled cells. Furthermore, BrdU immunohistochemistry is not stoichiometric (in contrast to, for example, tritiated thymidine autoradiography) (Taupin, 2007). The intensity or extent of BrdU labelling is highly dependent on the concentration of BrdU used during the experiment as well as on the methods used for detection, i.e. antibody affinity and penetration, which again is dependent on effective denaturation of DNA (Leuner et al., 2009). BrdU can only be detected on single stranded DNA after hydrolysis of the tissue with hydrochloric acid; this also prevents DNA staining with classical intercalating dyes such as DAPI, Hoechst 33342, or propidium iodine. Hence BrdU positivity does not directly reflect DNA replication (Nowakowski and Hayes, 2000). For neuronal regeneration, many studies have been undertaken to find a saturation dose of BrdU (Cameron and McKay, 2001; Eadie et al., 2005). No study has been published for *ex vivo* human corneas to determine the effect of different BrdU concentrations; often the concentrations used are not even indicated conclusively. Generally, a low concentration of BrdU is desired due to its toxicity to newly generated cells. BrdU reduces DNA stability, increasing the risks of mutations and DNA double strand breaks, which especially for newborn maturing cells could be deleterious (Morris, 1991; Saffhill and Ockey, 1985).

In summary, besides labelling newborn cells, BrdU incorporation can be the result of abortive cell cycle re-entry preceding apoptosis, DNA duplication without mitosis, and DNA repair. Therefore, cell cycle markers such as Ki67 or PCNA (proliferating cell nuclear antigen) are widely used, but they, too, have their limitations. In contrast to thymidine analogues which

accumulate, marker proteins are expressed very temporarily, i.e. only during their phases of the cell cycle. Newly generated cells that exit the cell cycle and begin their maturation process will be missed. As with BrdU, markers do not necessarily indicate true proliferation, as the cell could undergo apoptosis or arrest at any stage of the cell cycle.

The shortcomings of immunohistochemical assays in corneal endothelium in 37°C culture might explain the differences in findings of two similar studies assessing the effect of EDTA on corneal endothelial cell proliferation. Senoo et al. discovered a proliferative effect (as detected by Ki67 immunostaining) of EDTA after incubation in mitogenic medium including 10% FCS and epidermal growth factor and fibroblast growth factor (Senoo et al., 2000). Patel and Bourne did not find any effect of EDTA using the same culture conditions (Patel and Bourne, 2009). Instead, they observed that proliferation (Ki67) did not coincide with increased cell density (DAPI counts) in corresponding regions of the sample, and concluded that it is important to assay corneal endothelial cell density –in contrast to Ki67 only– when evaluating the proliferative response of the endothelium. In culture conditions, endothelial cells are exposed to a variety of factors that may promote cell cycle entry (growth factors in the medium containing FCS), while at the same time the physiologic factors of the aqueous humour inhibiting proliferation (especially TGF- β) are absent.

A new approach for analysing cell proliferation is the FUCCI system (fluorescent ubiquitination-based cell cycle indicator, Sugiyama et al., 2009). FUCCI harnesses two components of the DNA replication control system, Cdt1 and its inhibitor Geminin, which have opposing effects and oscillate during the cell cycle. Cdt1 protein peaks in G1 phase and declines in the S phase. Geminin reaches its highest level during S and G2 phase. FUCCI probes are pairs of different fluorescent proteins fused to either a fragment of Cdt1 or of Geminin. During different phases of the cell cycle, FUCCI probes are degraded and thereby activated, allowing differentiation between G1 or S/G2/M phase (Zielke and Edgar, 2015). This allows precise visualisation of the cell cycle

status even of living cells. FUCCI probes have been integrated in several cell lines and even animals. However, to make use of this technique in corneal endothelium *ex vivo*, viral vectors would be needed to deliver the FUCCI probes (e.g. retrovirus for pRetroX-SG2M-Cyan / pRetroX-G1-Red, Clontech). With difficulties already arising when transducing corneal endothelium with the treatment vector, two additional FUCCI vectors would pose a major challenge.

Cell density assessment

To circumvent the problems associated with BrdU labelling and cell cycle markers such as Ki67, we used endothelial cell density as the main outcome measure. By counting DAPI stained nuclei in at least six microscopic fields of view per sample, with minimum one field in between, a representative area across the whole sample (bisected trephined corneal specimen) was covered while avoiding the cut edges. The counted area per sample comprised 450,000 μm^2 , corresponding to around 1000 nuclei.

For clinical trials, specular *in vivo* microscopy is used to assess endothelial cell density (ECD). The FDA recommends three images to be taken per eye (FDA, 2002), comprising a total area of 240.000 μm^2 (400 × 200 μm image size using a standard specular microscope, cf. Konan Medical USA, 2011). This technique, however, produces high quality images only in the centre of the cornea.

Schimmelfennig noticed a 30% higher ECD in the far periphery near Schwalbe's line (by counting nuclei on flatmounted corneas). Within the central region, comparable to a corneal specimen used in this study, ECD was more consistent, with a *maximum* difference of only 9% (Schimmelfennig, 1984). An *average* difference above 10% over more than three sample pairs can therefore be considered real.

4.5.2. Adenovirus mediated E2F2 overexpression in relation to other studies

Our aim was to study the effect of E2F2 overexpression on corneal endothelial cell density *in situ* on corneas in culture, first using an adenoviral, then a lentiviral vector. The same adenoviral vector had been used in a previous study at Schepens Eye Institute, Boston, in collaboration with this lab (McAlister et al., 2005).

To determine the optimal vector dose, corneas were cut in quarters and subjected to different MOIs. Endothelial cell density was then determined after 5 days. This revealed a high inter-sample variability, suggesting that for some corneas, a certain concentration of Ad-E2F2-GFP is beneficial and promotes endothelial proliferation, while for other corneas the same MOI is detrimental. Corneas from older aged donors showed a trend towards a lower tolerance for Ad-E2F2-GFP. For all samples, an MOI of 30 resulted in massive endothelial cell loss. Because for Ad-GFP, an MOI of 20-30 resulted in a healthy endothelium without any signs of cell loss (cf. Chapter 3.2, Adenovirus, p. 94), the detrimental effect is primarily attributed to E2F2 overexpression and not GFP or the vector itself. An MOI of 1 for Ad-E2F2-GFP appeared safe in younger samples and was used for further experiments. Transgene E2F2 expression was verified for each experiment either directly by immunohistochemistry or indirectly by GFP reporter gene expression.

McAlister et al. used 1.5×10^7 plaque forming units in 1 mL medium per cornea (McAlister et al., 2005), which would correspond to an MOI of 50, an MOI that in our setting caused endothelial cell death in all samples. He used the same vector batch as used for our study. However, he determined the titre by plaque assay, which might give a higher concentration than our infectious titre method on 293T cells.

Because of the high variability of cultured corneas provided by the eye bank, with no control over culture time before clearance for research, we now focused on fresh corneal specimens procured directly from the operating theatre. These were also younger on average and showed

a far lower variability in transduction efficacy. In culture conditions applied in European eye banks, we observed an increase in ECD of ~50% after adenovirus mediated E2F2 overexpression, based on four corneal samples of young donors up to 40 years of age. In corneas from older patients aged 48 to 90 years, we did not observe any increase in cell density.

The ECD increase in young specimens is consistent with McAlister's findings (McAlister et al., 2005), who after E2F2 overexpression calculated a ECD increase of approximately 35%, 20%, and 45% after 1, 2, and 3 weeks in culture, respectively, based on one cornea per time point (percentage estimated from the bar graphs in the publication). No information is given about the age of these specimens, but the authors comment on a possible age dependent effect of E2F2 overexpression.

From a BrdU assay McAlister et al. conclude that even in corneas from older donors proliferation can be induced by E2F2 overexpression. For this BrdU assay, McAlister used a 28- and a 70-year-old cornea. He was able to show increased BrdU uptake in both the young and old specimen transduced with Ad-E2F2-GFP but not in Ad-GFP treated controls. This was observed at 2 days and 7 days post transduction (in the presence of BrdU for 48 h and 5 d, respectively). We could not reproduce these findings. We observed BrdU uptake in both Ad-E2F2-GFP and Ad-GFP treated samples with no significant difference. There were, however, large differences in BrdU uptake between different corneas, cf. Figure 8, p. 114. The same observation was made with Ki67 immunolabelling, though with a generally lower number of positive nuclei. In completely untreated samples, i.e. not kept in culture but instead transferred in fixative directly after extraction in the operating theatre, we observed a low number of Ki67 positive cells comparable to McAlister's findings (0% – 4.5%). As soon as corneas were kept in culture, Ki67 staining was detectable in a range of 5 to 20% (cf. Figure 11 and Figure 12, page 117 et seq.).

The discrepancy might be due to differences in culture conditions, such as lot-to-lot variations in FCS, as Patel and Bourne (Patel and Bourne, 2009) suggest for their discrepancy with findings of Senoo et al. (Senoo et al., 2000) in EDTA treatment effects on endothelial cell density.

Furthermore, McAlister used corneas procured from different eye banks in Europe and USA. In USA only cold storage at 4°C is used, whereas European eye banks use both 37°C and 4°C storage.

Using relative RT-PCR with densitometric analysis, Nancy Joyce et al. in collaboration with this group detected an increase in Ki67 mRNA after E2F2 overexpression in rabbit corneas *ex vivo* (Joyce et al., 2004). They did not use immunohistochemistry due to difficulties in flatmounting the rabbit cornea, which experiences considerable swelling during culture. Transcriptional upregulation of Ki67 and Cyclin B1, a marker for G2 phase, was indicative of cell cycle progression.

4.5.3. Adenoviral versus lentiviral vectors for E2F2 overexpression

A primary goal of this project was to transfer the findings of McAlister who used adenoviral vector to less immunogenic lentiviral vectors. Using fresh corneal specimens from young donors, we could not detect ECD increase after lentivirus mediated E2F2 overexpression, neither in old nor in young samples. This stands in contrast to the effect observed after adenovirus mediated E2F2 overexpression causing an increase in ECD. Several reasons may account for this.

Lower expression levels

Parker et al. undertook a similar transition from adenovirus to lentivirus mediated gene transfer to the endothelium in a corneal transplant model (Parker et al., 2010), published while our study was still in progress. In a previous study from the same lab in 2001, IL-10 overexpression using adenovirus increased median graft survival by 35 days (Klebe et al., 2001a). Lentivirus mediated IL-10 expression achieved a prolongation of merely 7 days. This was attributed to the fact that adenovirus induced a 1000 times higher transgene expression on mRNA level, and a fourfold higher IL-10 protein secretion. Any potential benefits of using the less immunogenic

lentiviral vector were undone by its comparatively low expression. Even by increasing the MOI, lentiviral mediated IL-10 protein expression could not match adenovirus mediated levels.

In our study using lentivirus, a slight increase in ECD was observed in some samples both in the paired comparison of bisected corneas (Chapter 4.4.3.2) as well as in the kinetic at 7 days post transduction with LNT-E2F2 (Chapter 4.4.3.3), but never exceeded 6% and was not statistically significant. Too low transgene expression might explain this lack of proliferative effect of E2F2 overexpression mediated by lentivirus as compared to adenovirus. However, in accordance with Parker et al., increasing the MOI increased transgene expression only marginally. No increase was observed beyond MOI 50. This might be due to off target effects of a high vector concentration.

As with adenovirus mediated E2F2 overexpression, we could not find increased mitosis markers such as Ki67 or BrdU after LNT-E2F2 transduction, which is also due to the high numbers of positive nuclei also in the control group. To discriminate whether the expression of a proliferation marker is induced by transgene E2F2 or by factors inherent to the culture condition, we sought to couple E2F2 transgene expression with a GFP reporter gene. The same strategy was realized in the adenoviral vector Ad-E2F2-eGFP. However, the double lentiviral construct LNT-E2F2-IRES-eGFP achieved only very low transgene expression and was useful only in cell culture but not in *ex vivo* corneal samples. To achieve transgene expression as high as after LNT-E2F2 transduction, LNT-E2F2-IRES-GFP would have to be applied in many fold higher concentrations. Extrapolating from mRNA data, an at least thirty-fold higher transduction efficacy may be needed. While this is possible *in vitro* on a low number of cells, it proved unfeasible for *ex vivo* corneal specimens, where a minimum of MOI 20 is necessary to achieve reasonable transduction with lentivirus. Production of the double construct was already on average one log unit lower than the single construct. Even after concentration, vector production with the present facilities could not be increased to this scale. Multiple transduction periods using larger volumes of vector preparation caused toxic off target effects on endothelial cells.

Simply increasing the volume of vector preparation without increasing the concentration had no beneficial effect regarding overall transduction. The same number of viral particles (e.g. 10^7 infectious particles for an MOI of 20) suspended in 300 μ L of medium would transduce the endothelium sufficiently, while suspended in 3 mL of medium would achieve almost no transduction.

Vector preparation quality

A lower quality of the lentivirus preparation might also contribute to the lack of proliferative effect. Lentivirus was concentrated in-house by ultracentrifugation of cell culture supernatant, a process that also collected particles of similar size, such as cell organelles, cell debris of dead cells and components of FCS. In contrast, the adenovirus preparation was prepared at near clinical grade quality at an external facility (Harvard Gene Therapy Initiative, Boston, USA).

Side effects of proteins endogenous to the vector

Besides expressing the transgene, adenovirus vectors can express low levels of endogenous proteins, which can influence cell proliferation. Early region 1 and 3 (E1 and E3) of the adenoviral genome encode for virus proteins expressed in the early phase after transduction. E1A protein, for example, is known to drive contact-inhibited primary cells into S phase and through the cell cycle by binding to Rb (Barbeau et al., 1992; Berk, 2005; Braithwaite et al., 1983; Zerler et al., 1987). Displacement of Rb from E2F causes E2F activation and can cause oncogenic transformation of the host cell (Peeper and Zantema, 1993).

McAlister used a first generation adenovirus vector devoid of E1 and E3 region, but retaining E2 and E4, regions described to be actively transcribed in the host cell (Gorziglia et al., 1999). The E4 gene product is attributed a role in host cell cycle control, apoptosis, DNA repair, and oncogenic transformation (Tauber and Dobner, 2001). One mechanism interferes directly with the Rb/E2F pathway. While E1A proteins bind to Rb family members to displace them from E2F, the E4 ORF6/7 gene product directly binds free E2F (Marton et al., 1990; Obert et al., 1994). This mediates an increased binding stability of E2F to its cellular E2F1 promoter

(Schaley et al., 2000), causing transcriptional activation (Neill and Nevins, 1991; Reichel et al., 1989). E4 ORF6/7 protein is capable of displacing Rb from E2F even in the absence of E1 gene products (O'Connor and Hearing, 2000).

The interaction of transgene E2F2 and adenoviral E4 and possibly other viral proteins with cellular transcription factors controlling cell cycle or apoptosis pathways may explain the higher proliferative effect reported for adenovirus mediated in comparison to lentivirus mediated E2F2 overexpression. A crude attempt to separate transgene E2F2 effect and viral E4 effect was made by transducing corneal samples either with LNT-E2F2 and Ad-GFP combined or with the single vectors only. We could not detect any difference in Ki67 expression, but no conclusion can be drawn from this experiment. Cell density was not assessed at that time because samples from two different donors were involved. Assessing complex interactions between two or more different proteins cannot be done on *ex vivo* human corneas where the largest variable is the inter-sample difference. In comparison to that, the actual effect to be assessed is expected to be small. This is the domain of cell lines where the number of cells is unrestricted and identical conditions can be replicated.

From the data gathered so far, we conclude that for the induction of cell cycle progression in corneal endothelial cells, a strong E2F2 expression is needed. Lentiviral vectors, although favoured from the immunologic point of view, seem insufficient to induce proliferation. Especially the current lentiviral preparations available at a titre of 10^8 infectious particles per ml confer too little and too inconsistent transgene expression in *ex vivo* endothelium.

A solution might lie in newer adenoviral vectors with a high transgene expression profile but devoid of viral genes causing immunologic response. Fourth generation adenoviral vectors deficient of E1/E2a/E3/E4 (gutless adenovirus vectors) show significantly diminished vector toxicity (Alba et al., 2005; Andrews et al., 2001; Morral et al., 1999).

4.5.4. Conclusions

While we could replicate earlier findings using adenoviral vector to deliver E2F2, we could not transfer this method to a less immunogenic lentiviral vector platform, probably because of lower transgene expression levels. An alternative approach is to find new transgenes that, in the specific context of the corneal endothelium, exert a more potent proliferative effect. If the new transgene were effective even at low concentrations, a lentiviral vector would be sufficient despite its lower transgene expression levels compared to adenovirus.

When culturing primary corneal endothelial cells, an initial disruption of cell-cell contacts is essential to induce proliferation. This observation suggests that interference with contact inhibition may be more potent to induce cell cycle progression in the endothelium.

5. Cell cycle modulation via the ZO-1/ZONAB pathway

5.1. Introduction

5.1.1. Intercellular junctions in the corneal endothelium

The corneal endothelium forms a leaky barrier between stroma and anterior chamber. Leakiness is essential for nourishment of the inner half of the stroma. A constant passive influx of anterior chamber fluid through the endothelial barrier allows nutrients to reach the posterior part of the stroma. Leakiness is counteracted by the endothelial pump, a Na-K-ATPase. To enable *controlled* leakiness, cell-cell contacts consist of gap and adhesion junctions as well as focal tight junctions (reviewed by Joyce, 2003 and Farquhar and Palade, 1963).

Gap junctions are located on the basolateral side anterior to tight junctions, i.e. towards Descemet's membrane in the cornea. They directly connect the cytoplasm of adjacent cells and allow interchange of molecules and ions. Their immunohistochemical marker in the cornea is connexin 43 (Joyce et al., 1998).

Adhesion junctions anchor plasma membranes to the actin filament network of neighbouring cells. Their major structural components are cadherins, predominantly N-(neuronal) cadherin, E-(epithelial) cadherin, and VE-(vascular endothelial) cadherin (Zhu et al., 2008). Cadherins are linked to the cytoskeleton via catenin, in human corneal endothelium catenin subtypes α , β , γ and *p120* (Petroll et al., 1999a; Zhu et al., 2008).

Tight junctions are the most apical cellular junctions and form a tight border between the apical and basolateral environment (Farquhar and Palade, 1963). In the corneal endothelium, their immunohistochemical marker proteins are occludin, whose extracellular component confers cell adhesion and paracellular permeability (Petroll et al., 1999a), and zonula occludens protein 1 (ZO-1), located at the intracellular domain of occludin (Stevenson et al., 1986). ZO-1 links junctional membrane proteins to the cytoskeleton and signalling plaque proteins, and also interacts with transcription factors and cell cycle regulators (Paris et al., 2008).

5.1.2. Contact inhibition in the corneal endothelium

Contact inhibition is considered the most important factor in inhibition of endothelial cell proliferation (Joyce et al., 2002). Joyce et al. investigated the development of corneal endothelium of the rat (Joyce et al., 1998) and observed a correlation between the time at which stable cell-cell contacts were established and proliferation in the endothelium ceased. Gap and tight junctions, visualized by connexin 43 and ZO-1, respectively, matured by postnatal day 21, when S phase marker BrdU disappeared. G1 phase arrest may be mediated by G1 phase inhibitor p27kip1, which starts to be expressed at the same time (Joyce et al., 1998).

But not only during development, also in the mature monolayer contact inhibition plays an important role as it renders corneal endothelium resistant to mitotic stimuli. Senoo et al. demonstrated that strong mitogenic stimuli (FCS and fibroblast growth factor) alone do not promote proliferation in *ex vivo* corneal endothelium (Senoo and Joyce, 2000). However, endothelial cells proliferate after release from contact inhibition by mechanical wounding. Disruption of cell-cell contacts by EDTA also induces proliferation in human corneal endothelium cultured *ex vivo*, as demonstrated by Ki67 expression (Senoo et al., 2000). Patel and Bourne, however, dispute these findings. They could not find a proliferative response to EDTA treatment (Patel and Bourne, 2009).

Second to contact inhibition, the cytokine TGF- β contributes to the endothelium's non-replicative state (Chen et al., 1999). TGF- β has a strong inhibitory effect on proliferation for several cell types (Reddy et al., 1994) and is present in high concentration in the aqueous humour (Picht et al., 2001). However, it does not appear to play a significant inhibitory role neither during endothelial development nor in the mature endothelium (Joyce et al., 2002). TGF- β may rather be of importance in maintaining the endothelium in a non-replicative state should cell-cell contact be lost in the monolayer.

5.1.3. The ZO-1/ZONAB pathway

The ZO-1/ZONAB pathway has been identified as a molecular pathway controlling contact inhibition (Balda et al., 2003; Balda and Matter, 2000). ZO-1, a membrane protein located at the intracellular side of tight junctions, binds the Y-box transcription factor *ZO-1-associated nucleic acid binding protein* (ZONAB). Subcellular localization of ZONAB determines its activity as a transcription factor. In confluent cells expressing many tight junctions, ZONAB is bound to the SH3 domain of ZO-1. If, however, low cell density prevents establishment of tight junctions, ZONAB is released from its binding partner and is free to accumulate in the nucleus. Here it acts as a repressor of the *erb-2* gene, a tyrosine kinase co-receptor regulating epithelial differentiation (Balda and Matter, 2000). Furthermore, free ZONAB associates with cell division kinase 4 (CDK4), a central regulator of the cell cycle. By facilitating nuclear accumulation of CDK4, ZONAB promotes S phase entry (Balda et al., 2003). ZONAB also acts as a transcription factor and directly regulates the expression of proliferating cell nuclear antigen (PCNA), a crucial component of the DNA replication machinery, and cyclin D1, a key regulator of G1/S-phase transition (Sourisseau et al., 2006). These mechanisms eventually lead to increased cell density with formation of tight junctions. By sequestering ZONAB at the tight junctions, ZO-1 reduces cell proliferation in a cell density-dependent manner (Figure 27).

The role of ZONAB and ZO-1 has been investigated *in vitro* in MDCK and MCF-10A cells, mammalian epithelial cells derived from kidney and mammary gland respectively. Overexpression of *ZO-1* reduces proliferation, while overexpression of *ZONAB* increases cell density even in mature monolayers (Balda et al., 2003; Sourisseau et al., 2006). *In vivo* this signalling pathway has been investigated in the retinal pigment epithelium in mice (Georgiadis et al., 2010). Both overexpression of *ZONAB* or knockdown of *ZO-1* promotes RPE proliferation. Modulation of the ZO-1/ZONAB pathway may therefore provide a strategy to overcome contact inhibition and induce cell proliferation also in corneal endothelial cells.

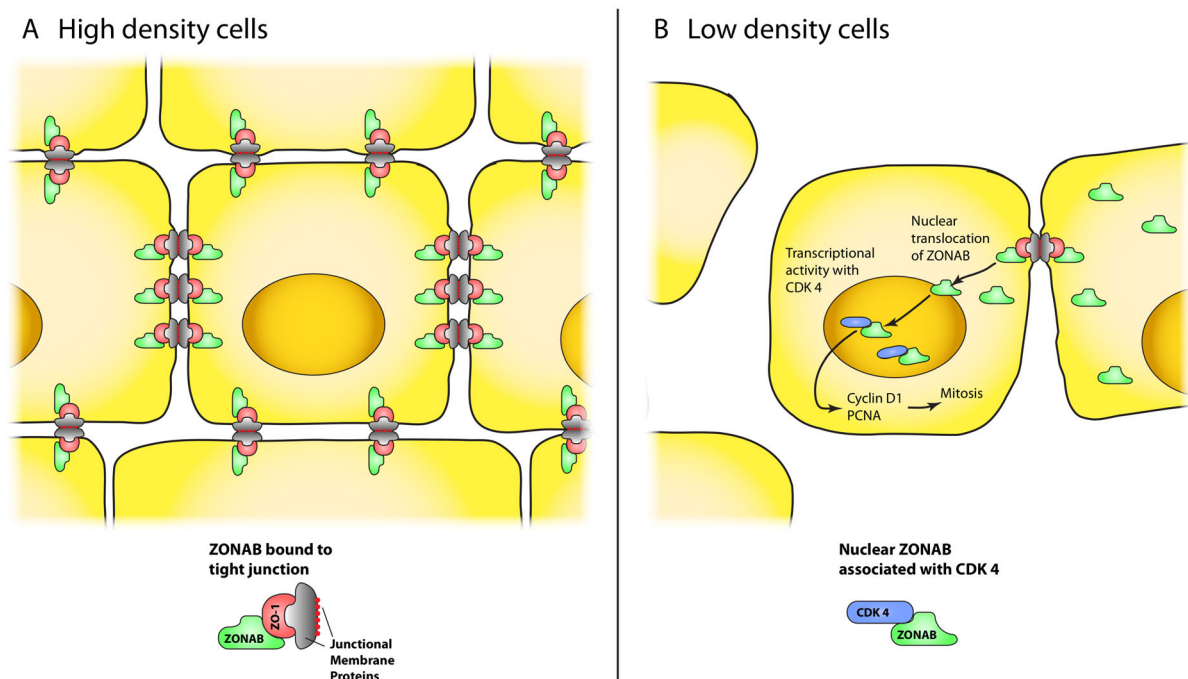


Figure 27. The ZO-1/ZONAB pathway.

A. In confluent monolayers of high cell density, ZONAB is bound to ZO-1 at the intracellular side of tight junctions.

B. In subconfluent monolayers of low cell density, fewer tight junctions are established, leading to fewer ZO-1 molecules available to sequester ZONAB. Free ZONAB is translocated into the nucleus and associates with CDK 4. This enables the cell to enter the cell cycle.

5.1.4. Aims

The working hypothesis for these studies was: Reduced availability of ZO-1 reduces its capacity to sequester ZONAB. Free ZONAB could then act in the nucleus as a transcription factor to promote cell proliferation. Likewise, overexpression of ZONAB exhausts the binding capacity of ZO-1, again making ZONAB available in the nucleus to promote cell proliferation.

The aim was to assess the effects of lentiviral vector-mediated knockdown of *ZO-1* or overexpression of *ZONAB* on corneal endothelial cells in excised human corneas. Outcome measures were endothelial cell density and marker genes of the cell cycle, as measured by RT-PCR.

5.2. Correlation of contact inhibition and proliferation in corneal endothelium

In normal human endothelium, some occasional sign of cell proliferation can be observed in the form of cells that are positive for Ki67 or BrdU staining, or in the form of an occasional mitotic figure. To analyse the correlation between proliferating cells and contact inhibition, we first looked at untreated human corneal endothelium not maintained in *ex vivo* culture.

A full thickness cornea excised at transplantation in a 48-year-old keratoconus patient with healthy endothelium was fixed within one hour of excision and flatmounted. Immunostaining for ZO-1 revealed a largely intact endothelial monolayer (Figure 28). In some regions, however, ZO-1 staining was interrupted, indicating a disruption in tight junctions and cell-cell contact. These regions of loosened contact inhibition corresponded to folds in Descemet's membrane or areas that were mechanically wounded during extraction of the specimen. The majority of nuclei were Ki67 negative. The few (less than 1%) cells that stained positive for Ki67 all showed an impaired ZO-1 expression pattern. Towards the periphery of the corneal specimen at the cut edge, presumably wounded endothelium showed multiple Ki67 positive cells with disrupted

ZO-1 staining, indicating loose cell-cell contacts (Figure 28 D). In central or mid-peripheral areas unlikely to be wounded by manipulation, Ki67 positive nuclei appeared isolated in cells with an interrupted ZO-1 expression pattern, surrounded by a Ki67 negative monolayer with intact ZO-1 localization (Figure 28 B, C). This correlation of Ki67 positivity and ZO-1 disruption in the endothelium was evident in all corneal samples that permitted reliable ZO-1 staining.

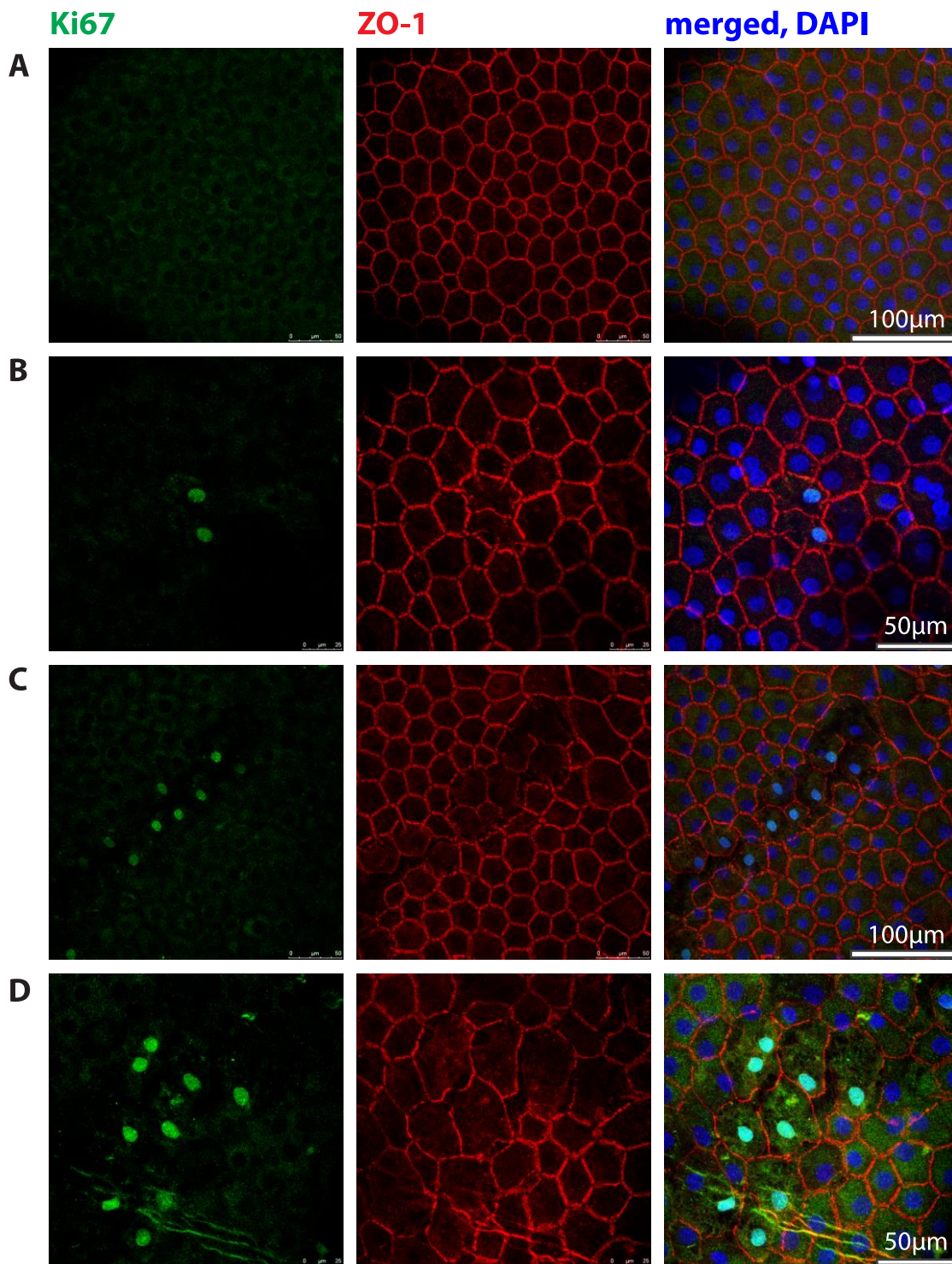


Figure 28. Correlation between tight junctions and proliferation in human corneal endothelium.

Flatmount of a full-thickness corneal explant fixed within one hour of excision for graft surgery. Ki67 positive nuclei can only be found in cells with reduced ZO-1 expression.

A. Mid-peripheral endothelium, intact cell-cell contacts (ZO-1), no Ki67 staining.

B, C. Mid-peripheral endothelium, disrupted cell-cell boundaries along Descemet's membrane fold with Ki67 positive nuclei.

D. Wounded endothelium at the cut edge with loose cell-cell contacts and Ki67 positive nuclei.

5.3. Lentivirus vector mediated down-regulation of ZO-1

To disrupt inter-cellular adhesion on a molecular basis, we first sought to down-regulate ZO-1 mRNA using small hairpin RNA (shRNA). For this, lentiviral vector LNT-shZO-1 was provided by Anastasios Georgiadis of this department (Georgiadis et al., 2010; Sourisseau et al., 2006). The targeting sequence (5'-AAGATAGTTTGGCAGCAAGAG-3') had been cloned into the mU6pro plasmid (Yu et al., 2002) and subsequently into the lentiviral pHR'SIN backbone to produce integrating lentiviral vector LNT-shZO-1. Effective down-regulation of ZO-1 on protein level by LNT-shZO-1 had been confirmed in the human nontransformed mammary epithelial cell line MCF-10A (Sourisseau et al., 2006).

5.3.1. Effect of LNT-shZO-1 on ZO-1 mRNA in corneal endothelial cells

The effect of lentivirus-mediated down-regulation of ZO-1 mRNA was assessed on human corneal endothelium by quantitative RT-PCR. Four corneal samples, whole corneas or fresh full thickness excised specimens, were bisected and transduced with either LNT-shZO-1, or LNT-hrGFP as control, MOI 40 for 4 hours. After incubation under organ culture conditions for 6 days, Descemet's membrane with endothelium was peeled off under the operating microscope and immediately processed for total RNA isolation. Quantitative RT-PCR using 10–70 ng of cDNA was performed for ZO-1 and 18s rRNA as the reference gene. Compared to the LNT-hrGFP transduced control, LNT-shZO-1 achieved a down-regulation of ZO-1 of 53% \pm 32% (mean \pm SD), range 25 to 90%, median 50%. Two-tailed paired *t*-test showed significance at $P=0.04$ (Figure 29 A).

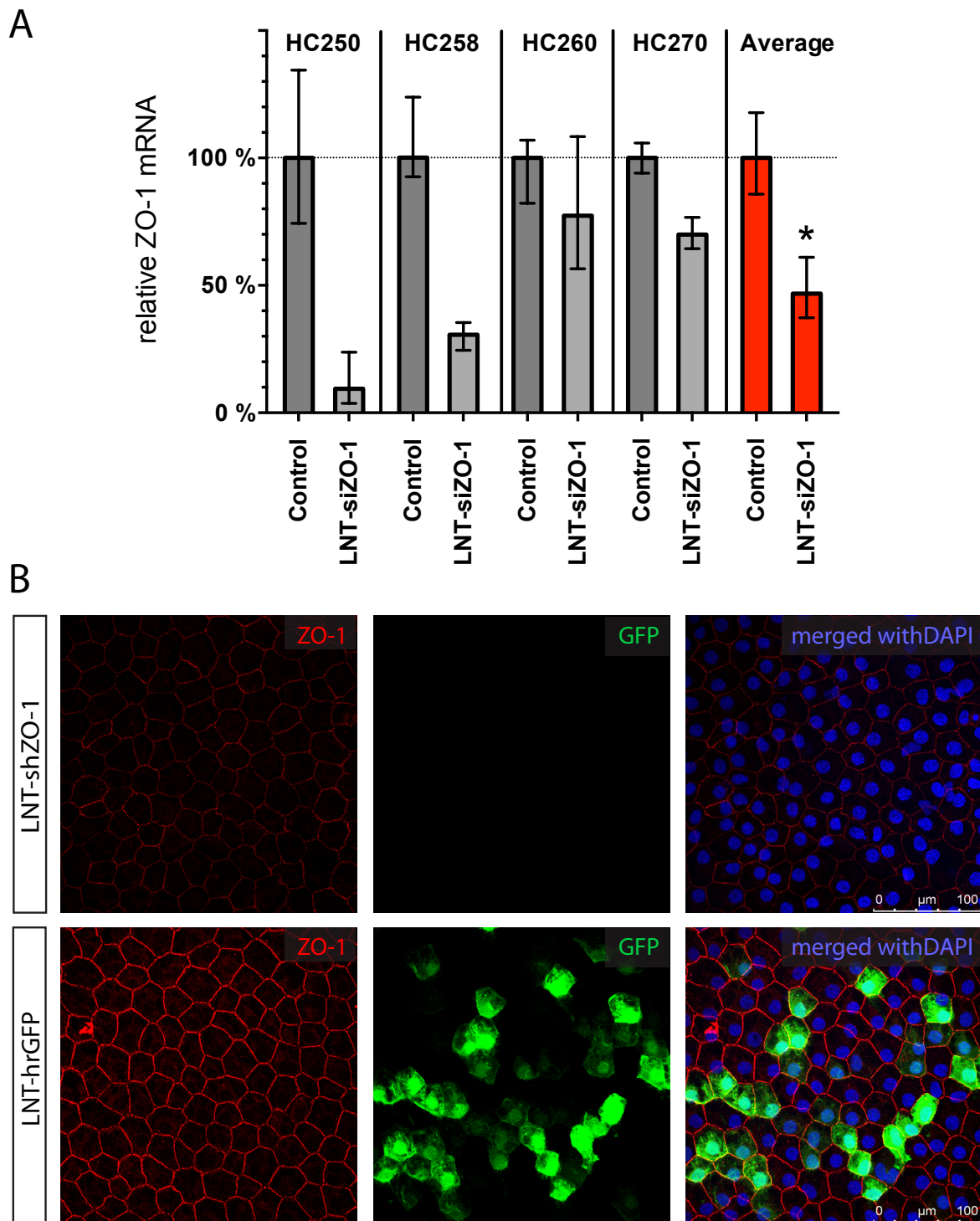


Figure 29. Downregulation of ZO-1 mRNA by LNT-shZO-1.

A. qRT-PCR was performed in four different bisected corneal specimens (donors 26–58 years of age) after endothelial cell isolation 6 days post transduction. LNT-shZO-1 transduced samples show a mean 50% reduction in ZO-1 mRNA compared to LNT-hrGFP transduced hemi-corneas ($P=0.04$, paired t-test).

B. Example of a cornea excised from a keratoconus patient one week after transduction. Reduced ZO-1 immunostaining (red) is seen in the LNT-shZO-1 transduced half while the endothelial layer remains intact. Normal ZO-1 staining is seen in the control half transduced with LNT-hrGFP.

Endothelium transduced with LNT-shZO-1 revealed no obvious changes in the integrity of the monolayer, as visualized by ZO-1 immunohistochemistry on flatmounts. An example of a keratoconus specimen (28 year-old male patient) is shown in Figure 29 B. Five days after transduction, the half infected with LNT-shZO-1 indicated uniformly reduced immunostaining pattern for ZO-1. Regional variation in uniformity of staining occurred was found in some samples.

5.3.2. Effect on cell cycle status determined by gene expression analysis

To assess the effect of ZO-1 downregulation on the cell cycle in endothelial cells, we assessed the expression of a number of cell cycle marker genes. Corneal samples were transduced with either LNT-shZO-1 or LNT-hrGFP as control, or mock-transduced in carrier medium only as a further control. After five to six days in culture, Descemet's membrane with endothelium was peeled off to isolate total RNA. Gene expression levels in the treatment sample were set in relation to those of the control sample using the $\Delta\Delta C_T$ method (cf. 2.1.10 Real-time PCR, p. 66).

6 corneas of donors aged 20 to 54 were used. One corneal half was transduced with LNT-shZO-1, the fellow half with LNT-hrGFP as control; one sample was a pair of corneas from the same donor (Figure 30). Due to the specimens' small size, the amount of mRNA obtained per sample was limiting and not all genes could be analysed in all samples. ZO-1 gene expression levels after LNT-shZO-1 were down-regulated to 54% of the LNT-hrGFP treated control.

Cyclin D1 is the regulatory subunit of cyclin kinases CDK4 and CDK6, whose activity is necessary for G1/S phase transition. At the G1/S transition Cyclin D1 also reaches its expression peak. We found that Cyclin D1 gene was upregulated 2.4-fold in LNT-shZO-1 transduced cornea compared to the control, but this did not reach statistical significance. PCNA (proliferating cell nuclear antigen) is an essential replication factor regulated transcriptionally and is upregulated in most proliferating cells. PCNA mRNA was found to be upregulated 1.5-fold (not statistically

significant). CDC20 activates the anaphase-promoting complex and mediates progression from G2 through mitosis. It is transcribed only during late S phase and mitosis. We could not detect a difference in CDC20 transcription after LNT-shZO-1 transduction compared to the LNT-hrGFP control.

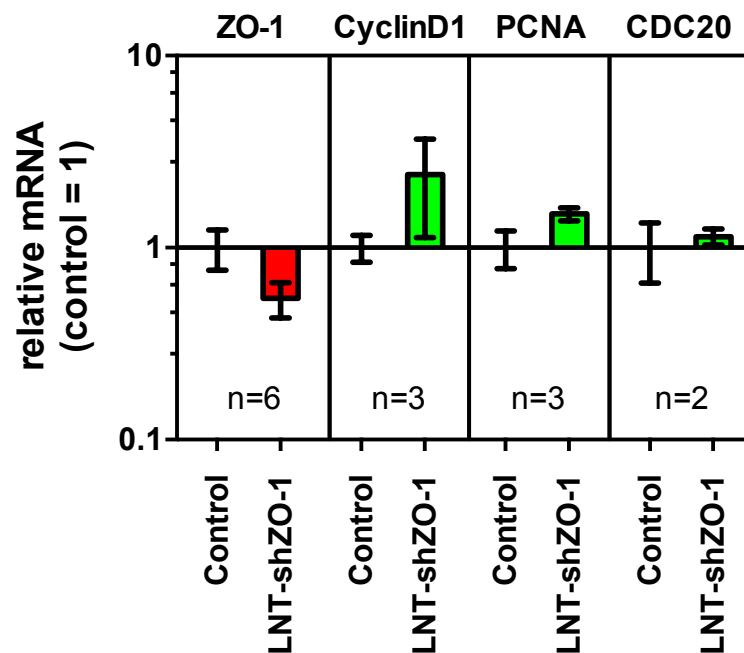


Figure 30. Relative expression of cell cycle related genes after transduction with LNT-shZO-1 in corneal endothelium.

Six bisected corneas from donors aged 20 to 54 were used for transduction with either LNT-shZO-1 or LNT-hrGFP (MOI 50 for 5 h). Total RNA was extracted from the endothelium five days post transduction and analysed by qRT-PCR. Bars show relative expression in the LNT-shZO-1 treated sample compared to the control sample set as 1 (all bars: mean \pm SEM). While ZO-1 was down-regulated to 54% of the control, Cyclin D1 was upregulated 2.4-fold, PCNA upregulated 1.5-fold, and CDC20 unchanged.

5.3.3. Effect on corneal endothelial cell density

CEC density was the principal outcome measure for ZO-1 down-regulation in corneal endothelium *in situ*. Fresh corneal specimens excised at penetrating keratoplasty for keratoconus were bisected with a diamond blade by the surgeon under the operating microscope. Care was taken to minimise injury to the endothelium. Shortly thereafter, they were transduced with

LNT-shZO-1 or control vector LNT-GFP, MOI 50–100 (transduction time 4h). Specimens were maintained in *ex vivo* culture for 7 days and then prepared for immunohistochemistry on flat mounts, the endothelium *en face*.

Visualization of GFP in the LNT-GFP transduced samples allowed assessment of transduction efficacy, which was estimated at 30 to 60%. The monolayer remained intact at the end of the experiment, as verified by ZO-1 or f-actin (phalloidin) staining with DAPI nuclear counterstain. Representative immunofluorescence micrographs are shown in Figure 31A. Endothelial cell density was determined by counting nuclei in seven micrographs, as described in Chapter 2.5.7, Corneal endothelial cell density assessment, p. 87. An example of a corneal specimen from a 20-year-old keratoconus patient is shown in Figure 31B.

Seven bisected corneal specimens from 7 donors up to 60 years of age were processed. An increase in CEC density after LNT-shZO-1 transduction compared to control was found in six of the specimens, one cornea showed a decrease in CEC density after LNT-shZO-1 (Figure 31C). Combining all seven sample pairs, we observed an average increase by 1.21-fold, range 0.94 – 1.69. Two-tailed paired t-test revealed significance at $P=0.0270$.

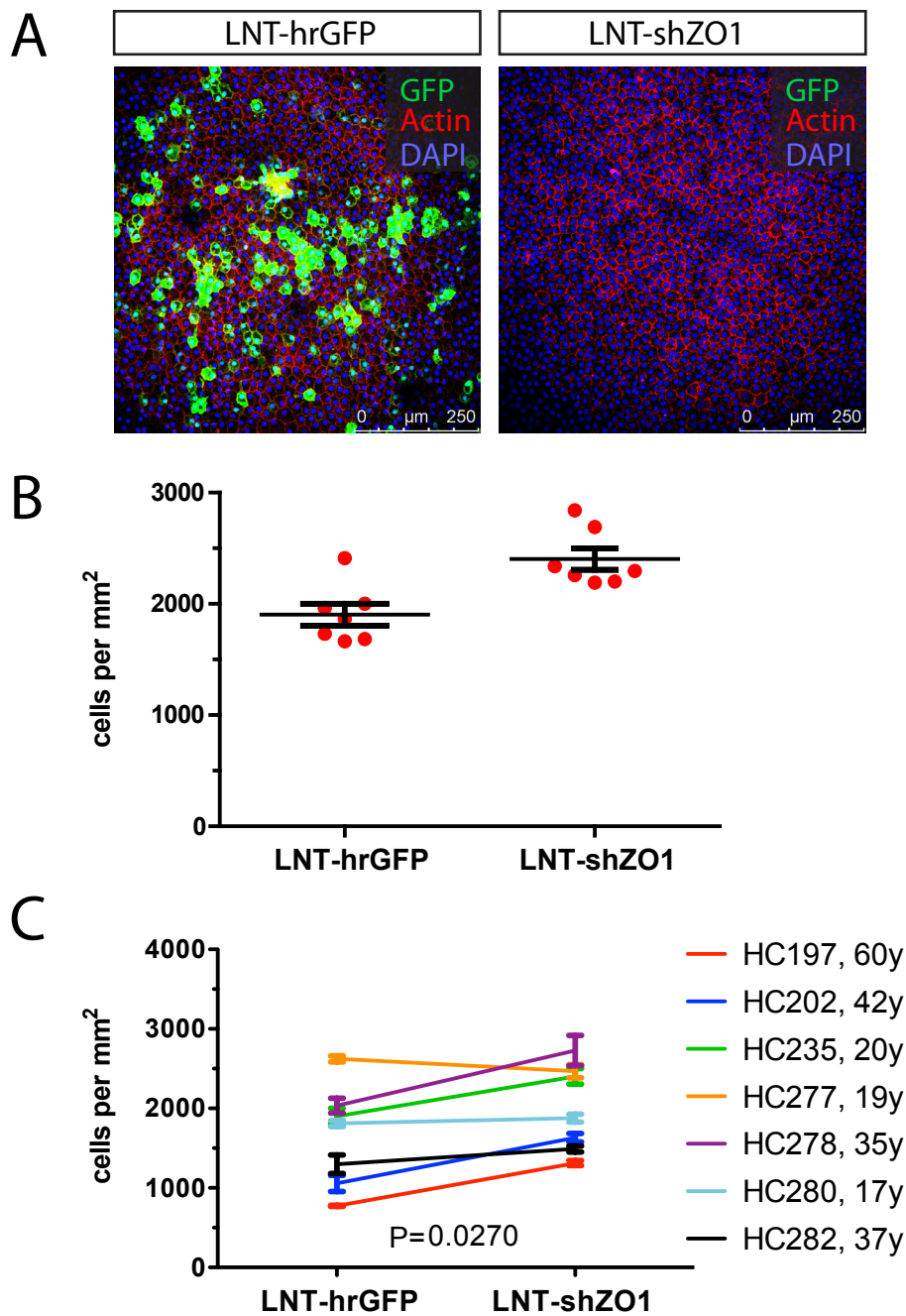


Figure 31. Effect of downregulation of ZO-1 in human corneal endothelium *ex vivo*.

A. Integrity of the endothelial cell monolayer was assessed 7 days post transduction by f-actin and DAPI staining of corneal flat mounts. Transgene expression (GFP) was visible in the control sample. Scale bar 250 μm .

B. Mean endothelial cell density. DAPI counts of seven micrographs per corneal half (40 \times objective), calculated for cells/mm². Results are shown for a cornea of a 20-year-old keratoconus patient, indicating a 1.3-fold increase in density. Error bars indicate standard error.

C. Synopsis of seven corneal samples, donors age range 17 to 60: mean increase in cell density after LNT-shZO-1 compared to LNT-GFP was 1.21fold (range 0.94 to 1.69). A paired t-test of all samples showed statistical significance ($P=0.0270$).

5.3.4. Proliferative effect of LNT-shZO-1 is age-dependent

In a previous study with E2F2-mediated cell cycle modulation, McAlister et al. observed that the proliferative response of the corneal endothelium seemed dependent on the donor age (McAlister et al., 2005). We decided to analyse this systematically and set an arbitrary threshold at 70 years of age for a separate cohort of older donors. Collection of samples for this group was limited by scarcity of excised corneas from older patients with normal endothelium – only three such corneal samples were obtained within the time frame available. Samples were subjected to LNT-shZO-1 or control transduction according to the method described above (Figure 32). Integrity of the endothelial monolayer was verified by ZO-1 and f-actin staining at the end of the experiment. Two samples (donor age 78 and 81 years) showed no difference in endothelial cell density, one sample showed a decrease of 31% (donor age 81 years).

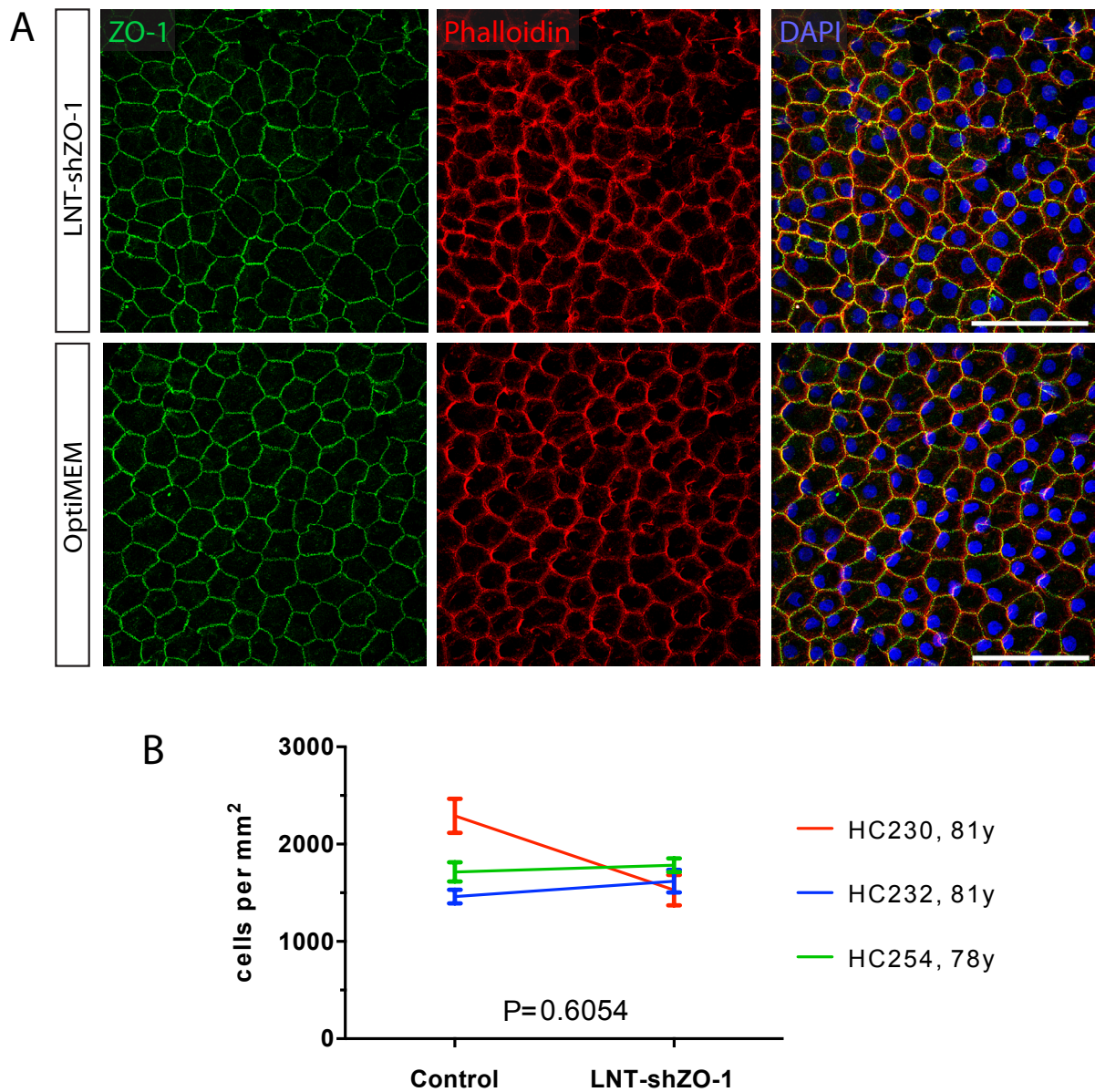


Figure 32. Effect of LNT-shZO-1 on corneal endothelium from older donors.

A. Two halves of a whole cornea (HC232), which had not been maintained in culture, from an 81-year-old donor were transduced with either LNT-shZO-1 (MOI 50) or mock-transduced with serum-free medium (OptiMEM) for 4 hours. Specimens were maintained in 37°C culture for 8 days. Fluorescence immunohistochemistry micrographs of corneal flatmounts, endothelium *en face*, at the end of the experiment show reduced ZO-1 staining in the treatment sample and normal endothelial monolayer configuration.

B. Average cell density in three corneal specimens of older donors transduced with LNT-siZO-1 or control vector. Two specimens show no meaningful increase, for one a decrease was observed. Paired *t*-test of the three samples combined showed no significant difference ($P=0.61$).

5.4. Lentiviral vector-mediated ZONAB overexpression

ZO-1 regulates proliferation by sequestering and thereby inhibiting the activity of ZONAB, a transcription factor. A complementary approach to downregulating ZO-1 would therefore be overexpression of ZONAB. This was realized by integrating lentiviral vector LNT-ZONAB, delivering *ZONAB* mRNA under the ubiquitous spleen-focus forming virus (SFFV) promoter. Vector plasmid was provided by Anastasios Georgiadis of this department (Georgiadis et al., 2010).

5.4.1. LNT-ZONAB vector characterization *in vitro*

LNT-ZONAB was tested *in vitro* on 293T cells. On mRNA level, transduction at a multiplicity of infection of 5 achieved an over 700-fold increase in ZONAB mRNA levels compared to untransduced controls. LNT-hrGFP transduced cells showed no significant difference in ZONAB mRNA to untransduced controls (Figure 33A).

On protein level, tested by Western blot, serum starved 293T cells show a marked increase of ZONAB three days after transduction with LNT-ZONAB at MOI 5. Both controls, LNT-hrGFP transduced and untransduced cells, showed very low levels of ZONAB. Immunohistochemistry revealed ZONAB was located in the nucleus. Retinal pigment epithelium ARPE19 cells were chosen because of their epithelial nature and their ability to firmly adhere on glass coverslips, in contrast to 293T cells whose origin is poorly characterized. The latter may not be related to epithelium but be of neuronal origin (Shaw et al., 2002).

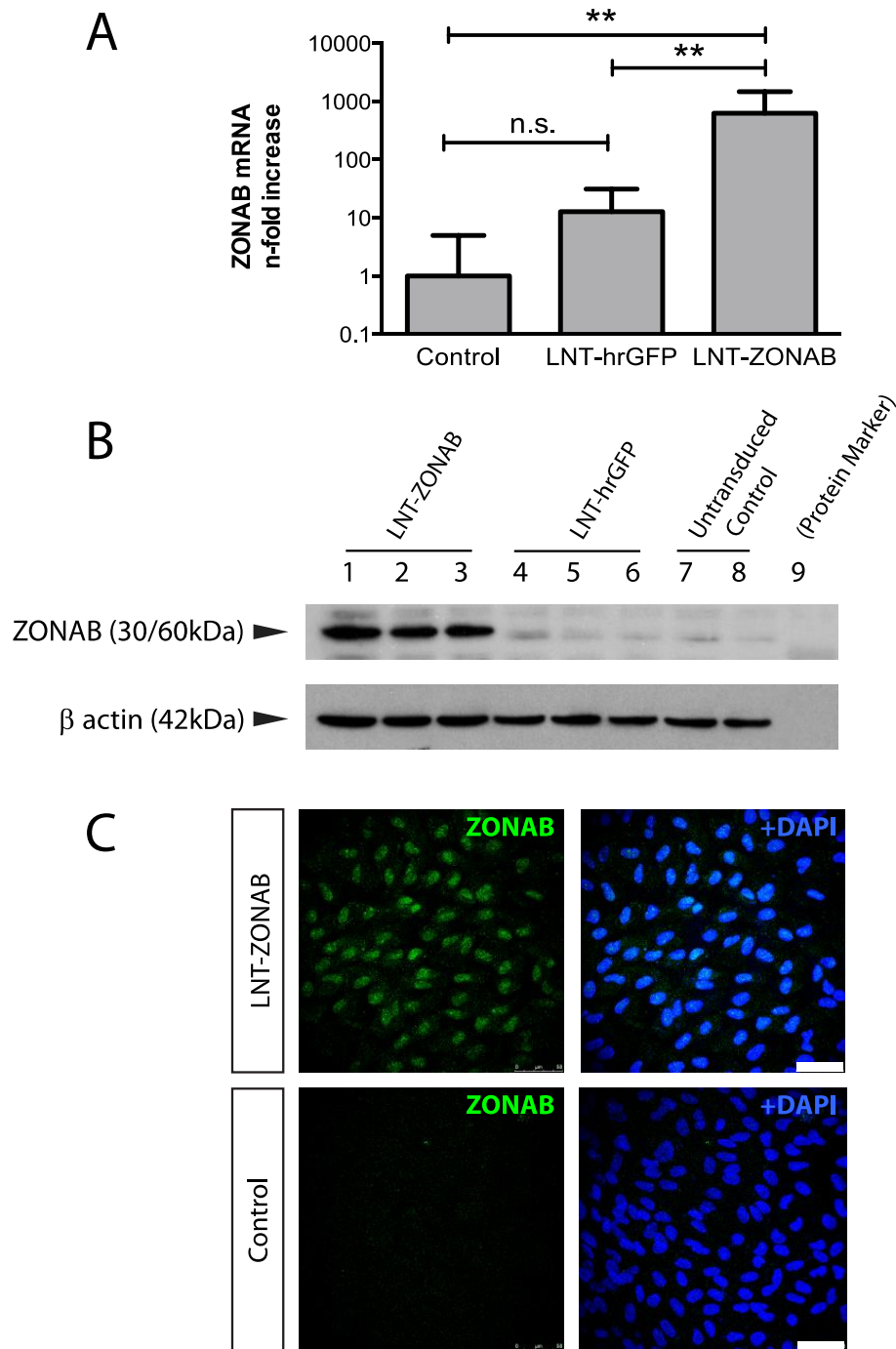


Figure 33. Characterization of lentiviral vector LNT-ZONAB *in vitro*.

A. On mRNA level, infection of 293T cells with LNT-ZONAB (MOI 5) induces a >700-fold upregulation of ZONAB mRNA compared to untransduced controls, measured by qRT-PCR 3 days post infection (increase 726-fold \pm 153 (mean \pm SE), **: $P < 0.01$, One-Way-ANOVA; adjusted $P = 0.0054$ in Tukey's Multiple Comparison Test). Error bars are SE of triplicate samples.

B. Equal amount of protein of different serum starved 293T cell clones were analysed by immunoblotting. LNT-hrGFP transduced and untransduced cells express low amounts of ZONAB undetectable on short exposures, while transduction with LNT-ZONAB at MOI 5 induces ZONAB expression.

C. Immunohistochemistry on ARPE19 cells shows nuclear localization of transgene ZONAB (green) after LNT-ZONAB transduction (MOI 5, 5 days after transduction). Scale bar 50 μ m.

5.4.2. Effect on cell cycle status determined by gene expression

As for ZO-1 downregulation, the effect of ZONAB overexpression on four cell cycle regulatory genes was analysed at the mRNA level (Figure 34). The same marker genes were quantified by qPCR comparing two halves of three corneal samples either transduced with LNT-ZONAB or mock-transduced in serum-free medium. After five days in culture, Descemet's membrane was stripped from the stroma to extract RNA from endothelial cells.

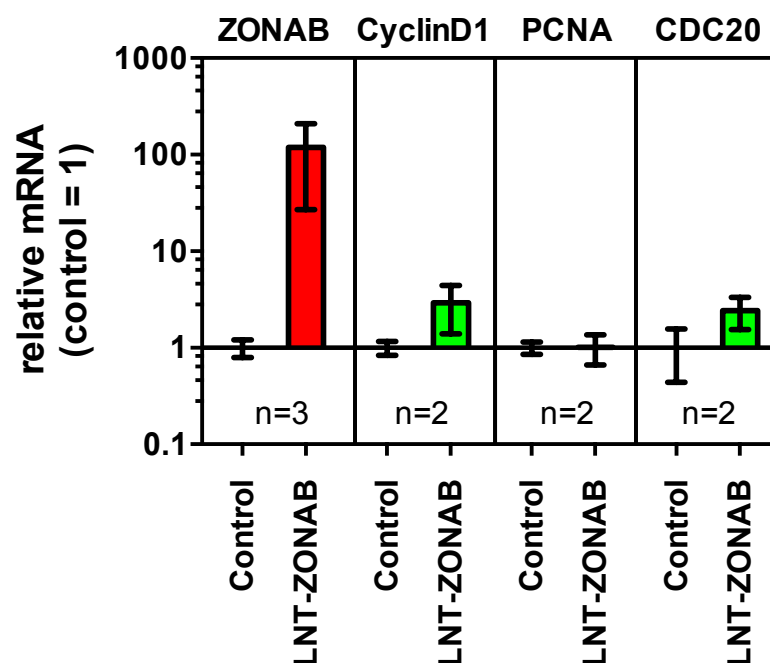


Figure 34. Relative expression of cell cycle related genes after transduction with LNT-ZONAB in corneal endothelium.

Three bisected corneas were transduced with LNT-ZONAB (MOI 50 for 5 h) or mock-transduced in serum-free medium. Total RNA was extracted from the endothelium five days post transduction and analysed by qRT-PCR. Bars show relative expression in the LNT-ZONAB treated sample compared to the control set as 1 (all bars: mean \pm SEM). ZONAB was upregulated over 100-fold, Cyclin D1 upregulated 2.9-fold, PCNA remained unchanged, and CDC20 upregulated 2.4-fold.

Five days after LNT-ZONAB transduction, ZONAB was upregulated 118-fold compared to untransduced endothelium. Cyclin D1 was upregulated 2.9-fold, PCNA remained unchanged, and CDC20 upregulated 2.4-fold compared to control.

5.4.3. Effect on corneal endothelial cell density

To assess the effect on cell density, corneas from five keratoconus patients aged between 21 and 32 years, excised at surgery, were bisected and transduced with LNT-ZONAB or LNT-GFP, MOI 50 to 100, transduction time 3h. Specimens were maintained in culture for 7 days before fixation and flat-mounting. Corneal endothelium was immunostained for ZONAB to verify transgene overexpression, f-actin to assess cell monolayer integrity, and nuclei to facilitate cell counting. For controls, GFP was visualized to assess transduction rate, which was consistent with previous experiments. Representative immunofluorescence micrographs are shown in Figure 35 A.

Cell density was assessed as described previously (Chapter 2.5.7, Corneal endothelial cell density assessment, p. 87). Figure 35 B shows an example of one pair of specimens from a 31-year-old keratoconus patient, revealing a 1.25-fold increase in density.

Cell density was increased in all five samples after LNT-ZONAB transduction compared to controls (Figure 35 C). Mean increase was 1.3-fold (range 1.10–1.32). Paired *t*-test of all samples combined showed a significant increase in cell density at $P=0.0047$.

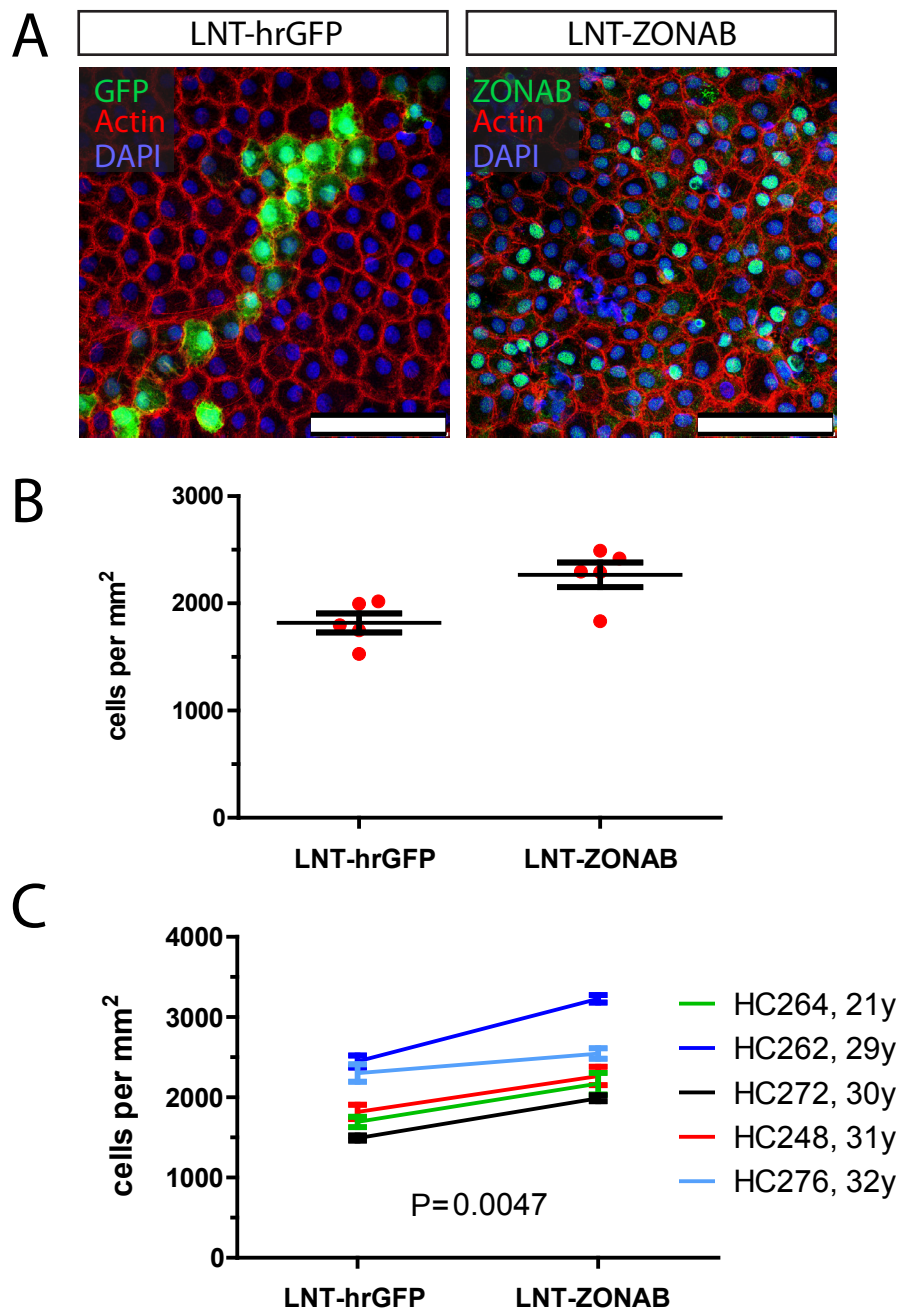


Figure 35. Effect of overexpression of ZONAB in human corneal endothelium *ex vivo*.

A. Integrity of the endothelial cell monolayer was assessed by f-actin and DAPI staining of corneal flat mounts. Transgene expression of ZONAB or GFP was visible after 7 days.

B. Mean endothelial cell density. Values are average DAPI counts of 7 micrographs per hemi-cornea, calculated as cells/mm². Results shown are from cornea excised from a 31-year-old keratoconus patient and show a 1.25-fold increase in density. Error bars indicate standard error.

C. Synopsis of 5 corneal samples, age range 21 to 32 years, show a mean increase in cell density after LNT-ZONAB compared to LNT-GFP of 1.3-fold (range 1.10 to 1.32). Paired *t*-test of all averages was significant ($P=0.0047$).

5.5. Discussion

5.5.1. Breakdown of contact inhibition enables regeneration

Adult human corneal endothelium is subject to strong inhibition of cell proliferation at a molecular level. Contact inhibition, with its molecular equivalent in the ZO-1/ZONAB pathway, is recognised to have the strongest inhibitory effect. Mechanical release from contact inhibition is the basic principle used to generate a primary cell culture of nearly all types of cells, also for endothelial culture, which then proliferate, albeit slowly, *in vitro*. By confocal microscopy of healthy corneal endothelium, we showed that disruption in ZO-1 staining is associated with Ki67 positivity, indicating a close correlation between breakdown of cell-cell contacts and proliferation. The observation that loss of inter-cellular contact also appears in the central, untouched regions of normal cornea suggests that in human corneal endothelium, breakdown of tight junctions can occur naturally to allow cell cycle progression. In endothelium of eyes cultivated in the eye bank, we observed BrdU uptake after endothelial wounding, i.e. mechanically disrupting cell-cell contacts (cf. 4.2 Proliferation analysis in *ex vivo* human corneal endothelium, page 113).

Any proposed inherent tendency of the corneal endothelium to regenerate by mitosis is insufficient to compensate natural age-related endothelial cell loss, yet alone increased loss occurring after corneal transplantation, surgery or in certain disease states. The reason for this might be that contact inhibition continues to be maintained during cell loss. Even in endothelium with very low density, cell-cell contacts remain intact over many years and decades, resulting in enlarged cells (Bourne and McLaren, 2004; Laing et al., 1976; Mishima, 1982). By overcoming contact inhibition on a molecular level, we were able to induce endothelial cell proliferation and increase cell density.

A first attempt to disrupt contact inhibition has been undertaken by Senoo et al. in eye bank corneas. By depleting calcium with EDTA in the presence of mitogens, they could induce Ki67 positive mitotic figures (Senoo et al., 2000). This approach has been considered unlikely to increase overall cell density (Patel and Bourne, 2009). Nakano et al. achieved downregulation of connexin 43, a component of gap junctions and therefore also a structural element of contact inhibition by antisense oligodeoxynucleotide or small interfering RNA, in an *in vivo* rat corneal scrape injury model (Nakano et al., 2008). This induced Ki67 upregulation even in unwounded rat epithelium. Overall cell density was not assessed and human samples were not tested.

Our study is the first to assess not only proliferation markers, but also show cell density increase after molecular breakdown of contact inhibition in human corneal endothelium *in situ, ex vivo*. By using bisected corneal samples from the same donor, we could control for inter-individual CEC starting density. To minimise bias, direct comparison and cell counts of treated and control samples was done in a masked fashion. Both vectors resulted in a similar cell density increase, an average increase of 21% for LNT-shZO-1, and 30% for LNT-ZONAB. This was not unexpected as several studies have established the correlation between either ZO-1 downregulation or ZONAB upregulation and proliferation (Balda et al., 2003; Georgiadis et al., 2010; Sourisseau et al., 2006). Our results confirm the role of the ZO-1/ZONAB pathway as the molecular basis of contact inhibition also in corneal endothelium.

In keeping with the observed cell density increase, (i) LNT-shZO-1 transduction resulted in ~50% reduction in ZO-1 mRNA expression and reduced protein on microscopy and (ii) LNT-ZONAB transduction resulted in >200-fold increase on mRNA expression and increased expression on microscopy.

5.5.2. Marker gene upregulation

We investigated mRNA of several marker genes to assess cell cycle progression, all of which are regulated at least partially at a transcriptional level: Cyclin D1, PCNAS, and CDC20. Cyclin D mediates the G1/S transition (Resnitzky and Reed, 1995) and is upregulated in large T antigen immortalised corneal endothelial cells but not in primary hCEC (Schonthal et al., 1999). PCNA acts as a scaffold to recruit proteins involved in DNA replication and repair and orchestrates replication events (Moldovan et al., 2007). CDC20 is an essential cell-cycle regulator required for the completion of mitosis (Yu, 2007) and the CDC20 gene is transcribed only during late S phase and mitosis (Goh et al., 2000). For all three genes we found a modest upregulation of expression after transduction by LNT-shZO-1 and/or LNT-ZONAB. This upregulation did not reach statistical significance, potentially owing to the low number of available corneal samples. However, the consistent upregulation was in line with cell proliferation being at the basis of the observed increase in cellular density.

Sourisseau et al. have shown in mammary epithelial cell line MCF-10A that transcription of both Cyclin D1 and PCNA are directly regulated by ZONAB on transcriptional level (Sourisseau et al., 2006). Our data in corneal endothelium are in line with both these findings. The relatively small effect on marker genes of proliferation may be due to the fact that only a portion of the transduced cells enter the cell cycle, and that the mitotic phase is comparatively short in relation to the 5 day post transduction period.

5.5.3. Influence of age and cell density on proliferative capacity

Only three samples were available from old donors above 78 years of age, but with normal endothelium. Here we did not find a significant increase in CEC density after LNT-shZO-1 treatment. One sample showed a decrease. While we recognise the limited information from such a small sample number, our findings are not unexpected. The reduced proliferative capacity of

older corneal endothelium has been investigated before in many aspects (reviewed by Joyce, 2003). There is evidence of a senescent phenotype in the endothelial population; endothelial cells' ability to be established in culture is reduced with donor age; and the kinetics of cell cycle entry is different in young and old cells. Age-related decrease in proliferative capacity is not caused by replicative senescence, i.e. the shortening of telomers with age. Telomer length remains constant over the lifetime of the endothelium (Egan et al., 1998; Konomi and Joyce, 2007). Instead nuclear DNA damage from oxidative stress is proposed as the main reason why some older cells are incapable of undergoing a full cell cycle (Joyce et al., 2009). Considering the high variability of oxidative stress over a human lifetime, it is very likely that for some samples the additional stress imposed by viral transduction is more likely to cause cell death rather than proliferation.

To obtain a measure of treatment responsiveness, we calculated the ratio of CEC densities of LNT-shZO-1-treated and control samples. This renders a number above 1 for a density increase after LNT-shZO-1 treatment (above dashed line in Figure 36); non-responder corneas will appear below 1 (below dashed line in Figure 36). We plotted this "treatment responsiveness" as a function of age for all ten samples in the young and old age group (Figure 36 A). Interestingly, this shows that with increasing age, treatment responsiveness seems to peak at about 40 to 60 years of age, but both young (20 years of age) and old corneas (80 years of age) show little treatment effect.

A possible explanation for this becomes evident when plotting treatment responsiveness against CEC density of the corresponding control samples. This reveals a significant inverse correlation between treatment responsiveness and control CEC density (Pearson $r = -0.7627$, $P=0.01$). The tendency to proliferate is dependent on CEC density: a low density permits proliferation; a high density inhibits proliferation (Figure 36 B).

These findings underpin the power of contact inhibition in corneal endothelium: cells will divide only when there is space available. In dense endothelium, contact inhibition will prevent further cell division. However, for older corneas beyond 70 to 80 years of age, there is no proliferation irrespective of the space available.

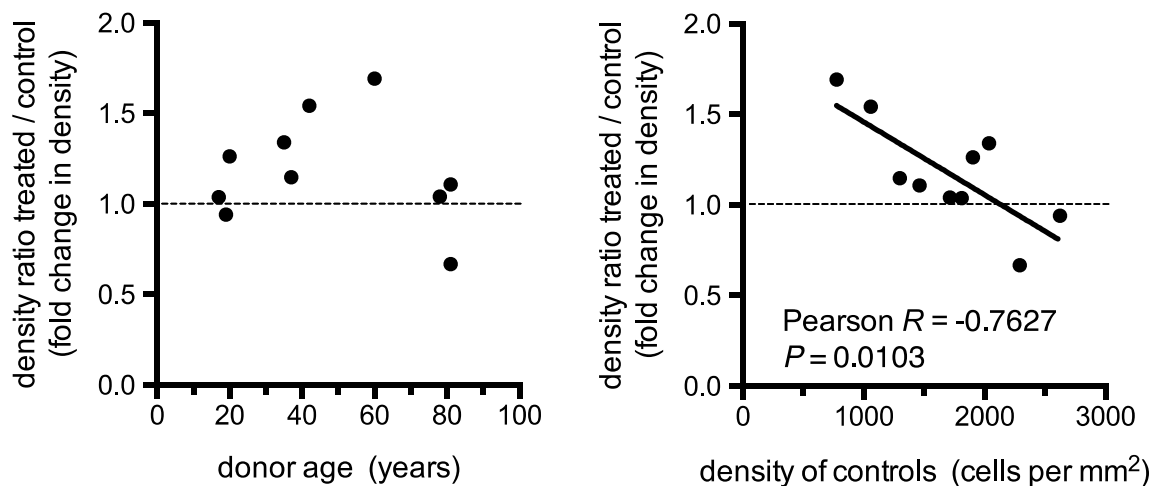


Figure 36. Effect of donor age and initial cell density on responsiveness to LNT-shZO-1 treatment.

The ratio of cell density of LNT-shZO-1- and control-transduced corneal endothelium was used as a measure of treatment responsiveness, plotting dots above the dashed line as treatment responders (ratio >1), and below as treatment failures.

- A. Treatment responsiveness versus donor age. The treatment effect seems to plateau at 40–60 years of age and seems to be lower in young and old donors.
- B. Treatment responsiveness versus CEC density of controls. An inverse correlation between treatment responsiveness and initial cell density is observed.

5.5.4. Role of proposed stem cells and transient amplifying cells

Several studies support the idea of constant yet slow regeneration of the human corneal endothelium. Whikehart et al. were able to induce BrdU uptake by wounding (Whikehart et al., 2005). They showed that BrdU uptake was more pronounced in the periphery towards the limbus, where they also localized positive telomerase activity, a characteristic marker for tran-

sient amplifying cells. From this they conclude that cells in the corneal endothelium may be renewed by stem-like cells located in a niche at the posterior limbus. He et al. observed many Ki67 positive cells in cultured corneas (under eye bank conditions, 2% FCS), but very few in fresh, non-stored corneas, and here only in the periphery (He et al., 2012). Also in the periphery, they located stem cell markers (nestin, telomerase, and breast cancer resistance protein BCRP/ABCG2). They, too, postulate a peripheral renewal zone where progenitors of endothelial cells divide very slowly and migrate towards the centre (He et al., 2012). The concept of centripetal regeneration is corroborated by the fact that endothelial cell density declines from the periphery towards the centre (Amann et al., 2003; Schimmelpfennig, 1984).

It therefore might be that by releasing contact inhibition via ZO-1/ZONAB interference, we are promoting a natural process of regeneration that is too slow to compensate endothelial cell loss in the diseased cornea. For cell density studies we used corneal specimens from transplant surgery, and therefore only the central 7.5 to 8 mm; peripheral cornea populated with the proposed endothelial stem cells was not included. Also the density of possible transient amplifying cells is reported to decline from periphery to centre. Using whole corneas with the attached scleral rim, as cultured in eye banks before transplantation, for treatment with LNT-shZO-1 or LNT-ZONAB might yield a higher increase in cell density. However, fresh post-mortem corneas are rarely available for research in European eye banks.

5.5.5. Limitations of the studies

The small sample size in these experiments is a major limitation. This is due to the limited availability of human corneal samples for research. European eye banks usually clear samples for research only after 4-6 weeks in culture, by which endothelial viability is reduced and unsuitable for further culture in the laboratory. Only if contraindications for transplantation become evident at the early stage of the organ culture process, will a donor cornea be made avail-

able for research. Such contraindications could be previous brain surgery (due to possible use of dura mater and risk of prion disease transmission), corneal scars or other corneal diseases of the epithelium or stroma, with intact endothelium, or gaps in the donor's medical history. If samples became available, sample quality varied hugely, forbidding inter-donor comparisons.

Samples from live donors after transplantation surgery were available directly from the operating room and sample quality was more predictable. However, penetrating keratoplastic surgery providing a full thickness corneal sample including the epithelium becomes more rare as lamellar graft surgery is getting more and more common. Especially samples with normal endothelium as needed for endothelial transduction experiments are scarce because normal endothelium is left in place and only the anterior layers are transplanted (deep anterior lamellar keratoplasty, DALK). To maximise the use of one excised cornea and to have the optimum experimental control, corneas were bisected. Together with masking, these results robustly demonstrate the effect of lentiviral disruption of contact inhibition and thereby proliferation of the corneal endothelium.

5.5.6. Conclusions

Key findings are:

- Knock-down of ZO-1 expression and over-expression of ZONAB is possible in human corneal endothelium *ex vivo*. Harmful effects on the endothelium were not evident in the samples tested.
- The modulation in expression of ZO-1 and ZONAB was associated with approximately 1.3-fold increase in cell density.
- We found limited evidence that this effect does not occur in corneas from donors older than 70 years.

Although the increase seems low one week after treatment, this would be sufficient to rescue a substantial number of donor corneas that would otherwise be discarded due to CEC density below 2000 cells/mm², the standard applied in eye banks. Changes in CEC density might be increased further if cell transduction were more efficient than the 30–50% achieved in these studies, through changes in vector properties or design. Moreover, we have not investigated a dual approach in which both ZO-1 and ZONAB expression are modulated in the same specimens by exposure to both vectors. This might vastly increase the mitotic effect, but toxic side effects may occur.

6. Retinal pigment epithelium regeneration

6.1. Introduction

6.1.1. The concept of *in situ* RPE proliferation

For patients with RPE loss due to AMD or other diseases without primary genetic defect in RPE cells, where photoreceptor cells and choriocapillaris remain relatively intact, transplantation of healthy RPE cells can prevent secondary loss of photoreceptors and potentially keep or restore vision (Binder et al., 2007; da Cruz et al., 2007; Heller and Martin, 2014). However, the complex anatomic and metabolic interactions between RPE and surrounding cells have made this pursuit difficult. Despite of decades of research into RPE transplantation and some promising success, there is no standard procedure clinically available, and basic questions such as cell source (autologous or allogeneic), transplantation technique (cell sheet or suspension), and timing of surgery are still unanswered.

The human RPE has a natural proliferative potential that only unfolds under optimal conditions *in vitro*. *In vivo* under normal conditions, RPE cells are retained in a quiescent state (compare 1.6.4, Proliferative capacity of the RPE, p. 55). If it was possible to either release cell cycle arrest or induce proliferation in the RPE in a controlled manner, this would offer a new therapeutic strategy for diseases with loss of RPE such as macular degeneration. Making use of the natural proliferative potential of the existing RPE has several advantages. Rejection of allogeneic cells would not be an issue. No complex harvesting procedure in the affected eye is necessary, nor any *ex vivo* expansion of RPE cells or their precursors.

Overexpression of free E2F can drive quiescent cells to undergo a full cell cycle (cf. 4.1.1, The Rb/E2F pathway, p. 109). With non-integrating lentiviral vector LNT-E2F2 we are able to overexpress E2F2 in target cells in a relatively controlled manner. The vector can be directed at RPE cells via subretinal injection, a technique that has been used routinely in mouse models as well as in clinical gene therapy trials. Adjacent photoreceptor cells will not be transduced by a VSV-G pseudotyped lentivirus.

Here we investigate whether LNT-E2F2 mediated transduction offers a way to overcome the intrinsic barriers to RPE proliferation and induce RPE regeneration by mitosis *in vivo*, *in situ*. We used wildtype mice for initial studies to assess cell cycle progress and proliferation to then test the concept on an RPE deficient mouse model.

6.1.2. The RPE^{CreER}/DTA mouse

Longbottom and Fruttiger et al. generated a transgenic mouse in which RPE cells could specifically be killed after inducing expression of the diphtheria toxin A (DTA) gene (Longbottom et al., 2009). To genetically target only the RPE, they constructed transgenic mice that express a tamoxifen-inducible form of Cre recombinase under the transcriptional control of the monocarboxylate transporter-3 gene promoter. This gene is specifically expressed in the RPE. They then crossed these mice with transgenic mice harbouring a DTA chain gene rendered transcriptionally silent by a floxed stop sequence. Offspring contained a conditional DTA allele in 100% and the Cre allele in 50%. Double transgenic mice were termed RPE^{CreER}/DTA.

Activation of Cre recombinase by tamoxifen injection in RPE^{CreER}/DTA mice leads to transcription of DTA. This caused a phase of RPE cell death lasting a few days, during which dying RPE cells were extruded from the monolayer towards the photoreceptors where they were phagocytised. After an initial 60–80% loss of RPE cells, cell density remained stable for up to 6 months. Cell loss was compensated with a dramatic increase in size of the surviving cells to

prevent holes in the monolayer. The RPE barrier function seemed intact. Some animals showed changes in the outer retina in the form of retinal folds.

Functional loss was assessed by electroretinography (ERG). Under scotopic conditions (testing primarily rod function), the authors observed a significantly reduced a and b wave amplitude. Under photopic conditions (testing primarily cones), b wave amplitude was reduced. These changes remained stable for over 6 months.

Overall, RPE^{CreER}/DTA mice after induction display RPE cell behaviour similar to what happens in atrophic AMD in humans, and may serve as a useful model for studies aimed at repopulating or replacing RPE following death or dysfunction in disease (Longbottom et al., 2009). This genetic ablation of RPE has distinct advantages over traditional models using chemical RPE ablation or mechanical debridement, especially genetic ablation shows less inflammation and less proliferative vitreoretinopathy.

6.1.3. Aims

We used lentiviral gene transfer of transcription factor *E2F2* to induce proliferation of RPE cells *in situ*, i.e. without harvesting RPE cells for *ex vivo* expansion. Aims were

- (1) To investigate the proliferative effect of *E2F2* overexpression *in vitro* in an RPE cell line
- (2) To investigate the effect of *E2F2* overexpression on RPE cell cycle in wildtype mice
- (3) To investigate the effect of *E2F2* overexpression on RPE cell density in wildtype mice
- (4) To estimate the duration of *E2F2* overexpression in wildtype mice
- (5) To investigate the effect of *E2F2* overexpression in a RPE deficient transgenic mouse model.

6.2. Results

6.2.1. Effect of E2F2 overexpression *in vitro*

Effect of *E2F2* overexpression was assessed *in vitro* on ARPE19 cells. ARPE19 is a spontaneously proliferating human RPE cell line. For proliferation assessment, a quiescent state without mitosis had to be achieved, as is natural for the human RPE. To induce contact inhibition and growth arrest, ARPE19 cells were maintained in starvation medium containing 1% FCS. Over 2–3 weeks, the proportion of Ki67 positive nuclei gradually declined from 96% to 0.4%, while the number of total cells plateaued and ZO-1 expression reached its maximum, indicating contact inhibition (Figure 37.). These were the starting conditions for the following *in vitro* experiments.

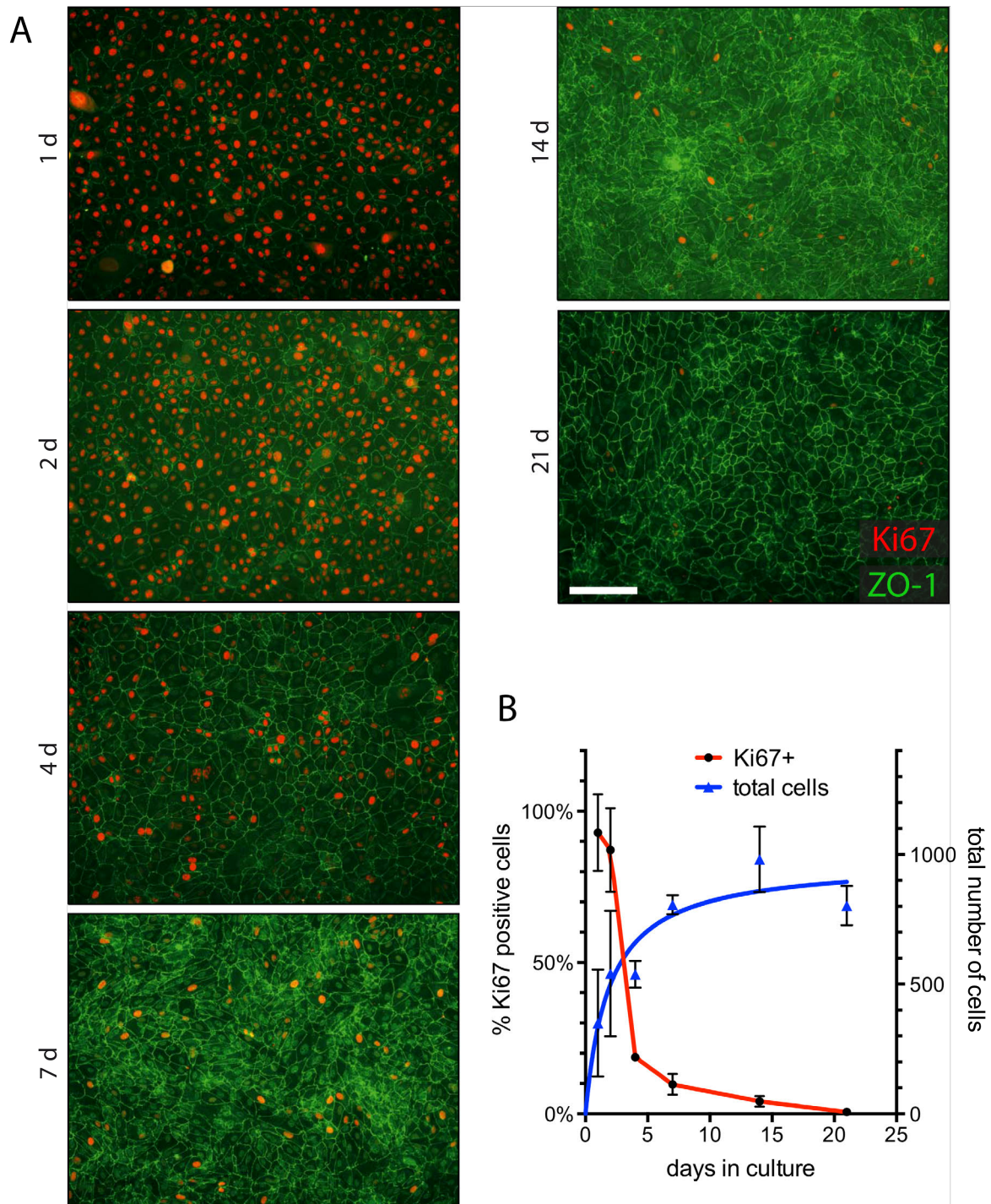


Figure 37. Growth arrest in ARPE19 cells.

A. ARPE19 cells were cultured in starvation medium containing 1 % FCS. Over the course of 2–3 weeks, expression of tight junction marker ZO-1 (green) increased while the proportion of cells positive for proliferation marker Ki67 (red) decreased. Scale bar = 100 μ m.

B. The proportion of Ki67 positive cells showed inverse correlation to the total number of cells, indicating growth arrest.

E2F2 overexpression in ARPE19 cells was achieved by transient transfection using transfection reagent PEI. Plasmids were obtained from Addgene, Cambridge, MA:

- (1) pCMVHA-E2F2 (plasmid #24226, delivering *E2F2* under CMV promoter, Lukas et al., 1996),
- (2) pcDNA3-EGFP (#13031, delivering eGFP under CMV promoter),
- (3) pCMV-Neo-Bam (#16440, empty plasmid).

Transfection of pCMV-E2F2 was achieved at a transfection rate of 10%. *E2F2* mRNA persisted at a >1000-fold increase 21 days post transfection (Figure 38 A), inducing E2F2 protein overproduction by 9-fold after 2 days, and 3-fold after 7 days compared with control plasmid (Figure 38 B, C). *E2F2* overexpression coincided with increased protein levels of proliferation marker Cyclin D1 compared to controls (2- and 3-fold, on day 2 and 7, respectively; Figure 38 B, D).

Two days after transfection of growth-arrested monolayers with pCMVHA-E2F2, or control plasmid pcDNA3-EGFP, there was a substantial increase in Ki67-positive cells – with over 86% of cells Ki67-positive in both groups. On day 7 and 14 post transfection, *E2F2* overexpression resulted in a 2.3-fold and 1.7-fold increase respectively in Ki67-positive nuclei compared with pcDNA3-EGFP controls (40% vs. 18% and 7% vs. 4% of total cells; both $P < 0.05$, *t*-test; Figure 38 E) suggesting that E2F2 stimulates an increase in proliferation *in vitro*. A similar effect was seen with BrdU uptake. After an initial increase in both control and *E2F2*-transfected cells, at 1 and 2 weeks post transfection, BrdU uptake in E2F2-treated cells increased by 3.5- and 5.4-fold, respectively compared with controls (Figure 38 F). Despite the increase in proliferation markers, there was not a significant difference in cell density (not shown). We also observed a similar increase in the levels of Ki67 expression and BrdU uptake following transfection of E2F2 compared with transfection of an empty backbone plasmid (pCMV-Neo-Bam, not shown). Together these results suggest that *E2F2* overexpression can lead to specific induction of cell proliferation in contact-inhibited ARPE19 cells.

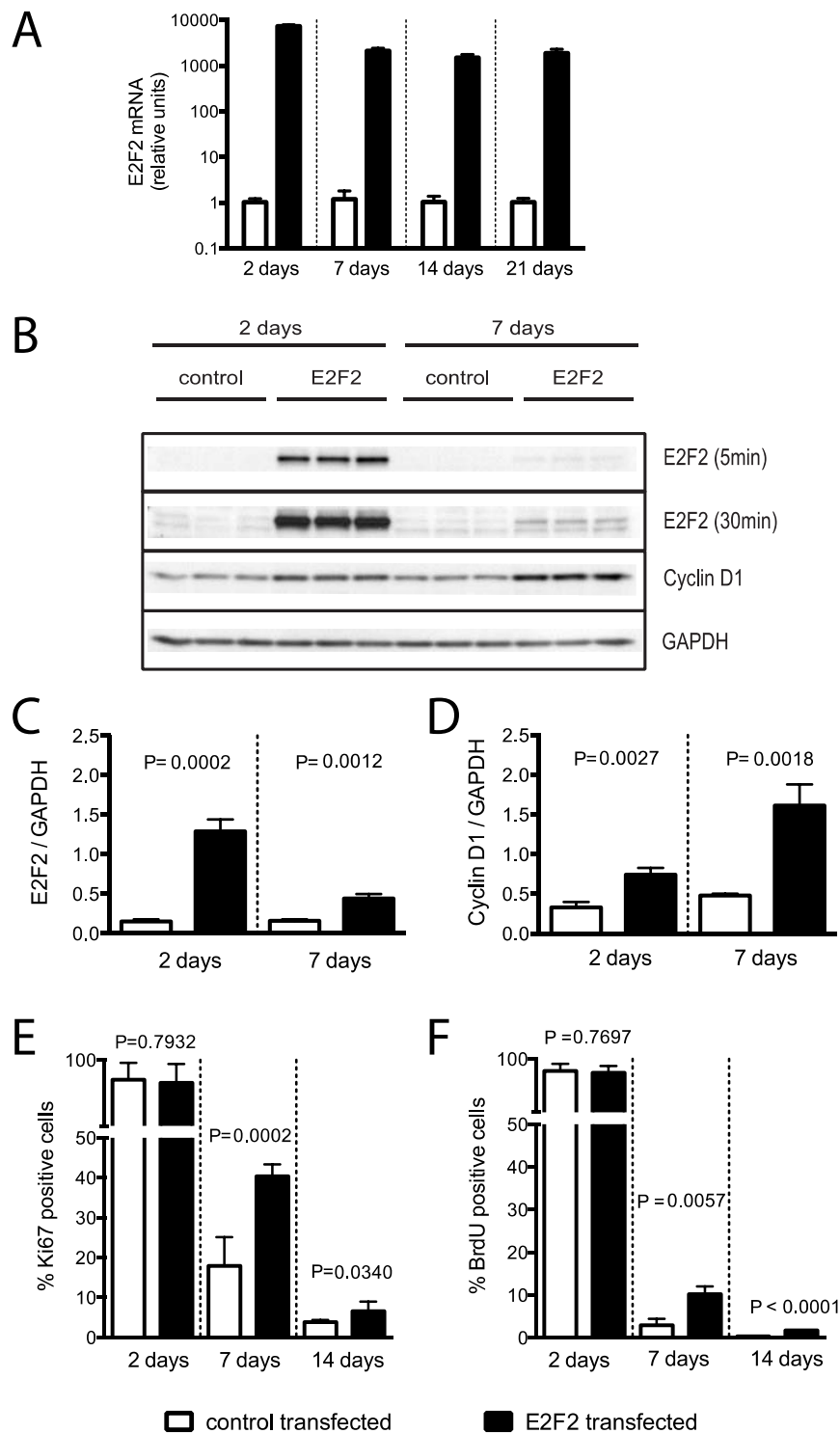


Figure 38. *E2F2* overexpression induces proliferation in a growth arrested, confluent monolayer of ARPE19 cells *in vitro*.

ARPE19 cells, grown to confluence and maintained in low serum for 2 weeks (1% FCS), were used as a model for a contact inhibited monolayer and transfected with pCMVHA-E2F2 or control (pcDNA3-EGFP). Transfection efficacy was ~10%.

A. 21 days after transfection with pCMVHA-E2F2, *E2F2* mRNA is >1000-fold increased compared with controls transfected with pcDNA3-EGFP (mean + SD).

B, C. Increase in protein levels of E2F2 compared with control, assessed by Western blot (9-fold increase after 2 days, 3-fold increase after 7 days; *t*-test; densitometric quantification, 5 min and 30 min indicate different exposure times, mean + SD).

B, D. Levels of proliferation marker Cyclin D1 increased following *E2F2* overexpression (2- and 3-fold, on day 2 and 7, respectively).

E. *E2F2* overexpression induces *Ki67* expression. On day 7 and 14 post transfection, *E2F2* caused a 2.3-fold and 1.7-fold increase in *Ki67* positive nuclei compared with controls (40% vs. 18% and 7% vs. 4% of total cells; *t*-test).

F. *E2F2* overexpression induces BrdU uptake. BrdU positive nuclei were increased by 3.5- and 5.4-fold at 1 and 2 weeks post transfection, respectively (*t*-test).

6.2.2. Effect of E2F2 overexpression on the cell cycle *in vivo*

Non-integrating lentiviral vector LNT-E2F2 described in 4.4.1.1 (p. 127) was used for the following experiments. Non-integrating LNT-GFP served as control vector, and serum-free culture medium OptiMEM as no-vector control, as both vectors were suspended in OptiMEM.

6.2.2.1. LNT-E2F2 induces S phase progression in wildtype mice RPE

Non-integrating LNT-E2F2 was used to transduce RPE of wildtype C57Bl/6 mice aged 9 weeks. We delivered 2×10^5 infectious particles per eye by two subretinal injections of 2 μ l in the superior and inferior hemisphere of the eye. Titre matched LNT-hrGFP and medium (OptiMEM, 2 \times 2 μ l) injected eyes served as controls (n=4 eyes per group from different animals). All mice received daily intraperitoneal injections of BrdU from day 4 onwards until they were sacrificed 10 days post injection. BrdU injection dose was aimed at 100 μ g/g body weight, which corresponds to approximately 2 mg BrdU per adult mouse (200 μ l peritoneal injection of a 10 mg/ml (=32.6 mM) stock solution). In their studies on cytokinetic behaviour in the murine cerebral ventricular zone, Takahashi et al. observed that the duration of saturation labelling of S-phase nuclei after a single dose at 50 μ g/g lies between 2.0 and 3.5 h (Takahashi et al., 1992). Doubling the dose should still not cause apparent cytotoxicity and possibly provide a longer duration of labelling up to 7 h.

Figure 39 shows representative examples of a whole RPE-choroid-sclera complex of the LNT-E2F2-injected and the LNT-GFP-injected group. Transgene expression (E2F2 and GFP) is visible within the injection areas. Intense BrdU staining in the injection areas is apparent only in the E2F2 group, while the GFP group shows very few BrdU positive nuclei.

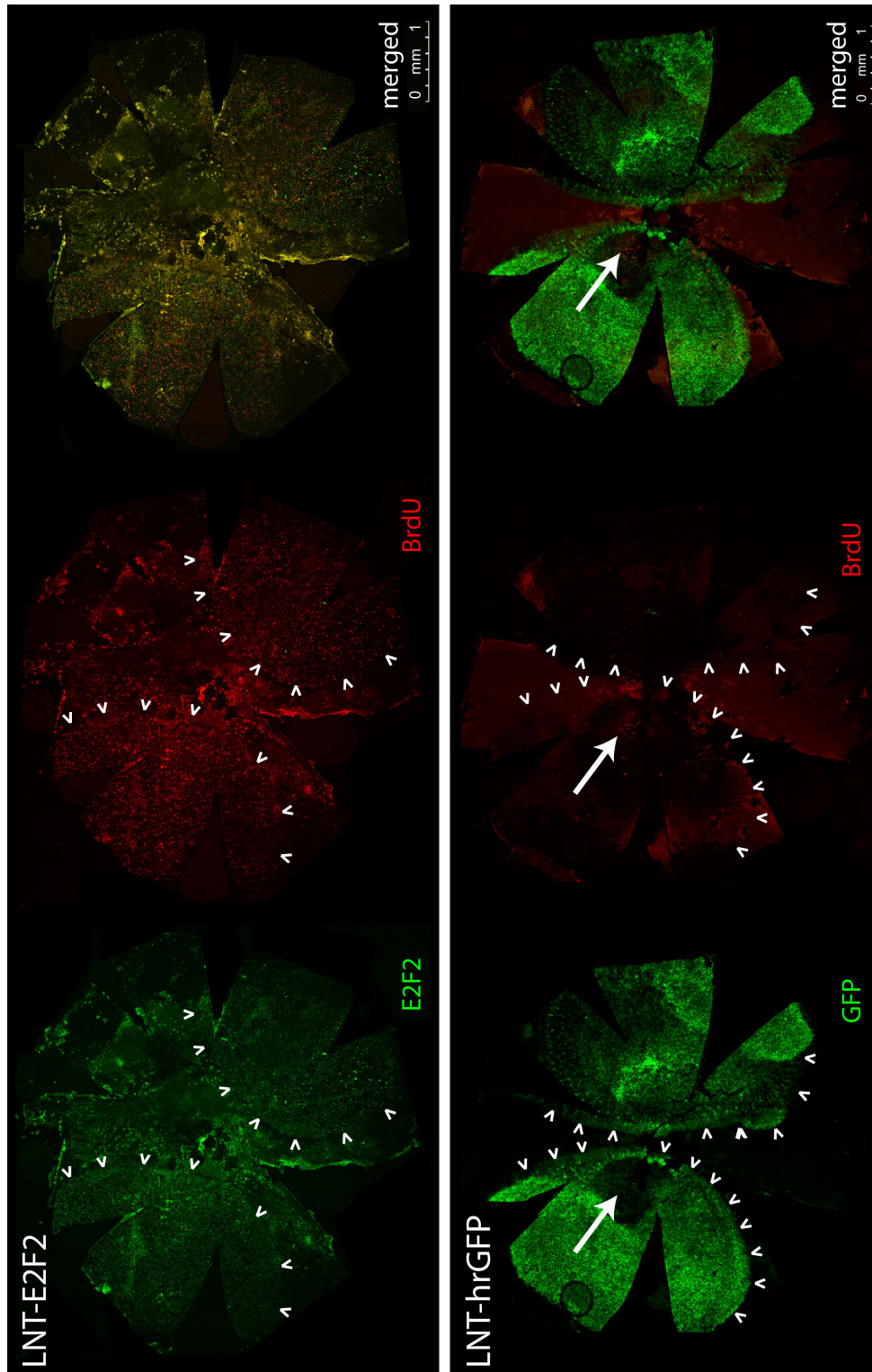


Figure 39. Confocal laser scanning images of whole RPE flatmounts 10 days after subretinal vector injection.

Wildtype mice received subretinal injection of LNT-E2F2 or LNT-GFP as control, alongside with intraperitoneal BrdU injections on day 4–10 post vector injection. Figure shows flatmounts of RPE-choroid-sclera, immunostained for transgene (E2F2 or GFP, green) and BrdU (red). Areas for quantitative analysis included injected areas (outlined by arrowheads), but excluded the injection site with trauma-related artifacts (arrow).

For quantitative analysis, only the areas of the injection blebs were included. The injection site itself displayed trauma related artefacts and was excluded, as were areas with obvious damage due to post mortem manipulation.

In LNT-E2F2 injected eyes, RPE flat mounts show overexpression of E2F2 often co-localizing with BrdU. Both controls (LNT-GFP and medium injection) show hardly any staining for BrdU or E2F2. LNT-GFP injection allowed estimating of transduction efficacy at over 90% (Figure 40A). BrdU uptake in normally quiescent RPE cells is a sign of cell cycle progression into S phase.

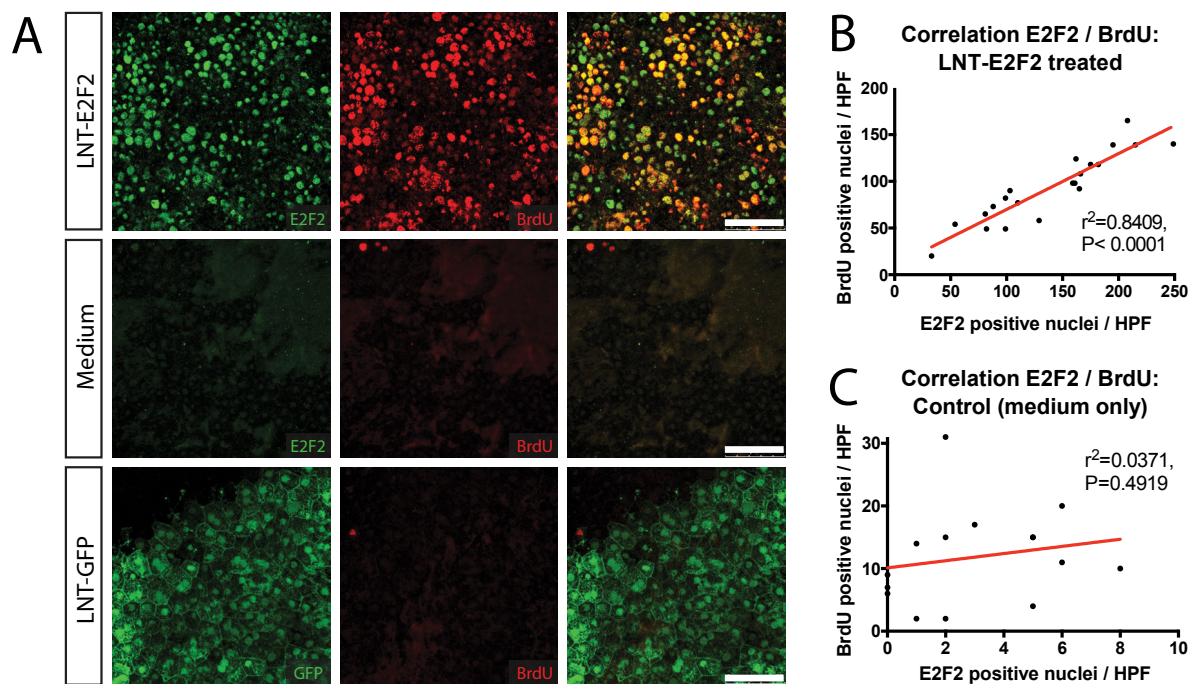


Figure 40. LNT-E2F2 induces BrdU uptake in RPE *in vivo*.

A. Overexpression of E2F2 (green) co-localized with BrdU, as observed in the LNT-E2F2 injected group. Medium and LNT-GFP injected eyes show no BrdU uptake in the RPE.

B, C. Counts of E2F2 per high power microscopic field (HPF) were correlated with counts of BrdU positive nuclei for both the LNT-E2F2 group and the LNT-GFP group (n=20 HPF per group, 5 HPF per eye). In the LNT-E2F2 group (B), a high linear correlation was observed. No correlation was seen in the medium injected control group (C).

E2F2 and BrdU positive nuclei were counted per microscopic high power field (HPF, 40× lens, 5 images per eye, 20 images per group). E2F2 counts were correlated with BrdU counts per HPF to get a surrogate value for their grade of co-localisation. In the LNT-E2F2 group, a high linear correlation was observed (Pearson correlation coefficient 0.9170, 95% confidence interval 0.8033-0.9662, $r^2=0.8409$, $P<0.0001$), indicating a high likelihood of co-localisation of E2F2 and BrdU. No correlation was observed for the medium injected control group (or for the LNT-hrGFP injected control group, data not shown), indicating that E2F2 or BrdU positivity were independent events. We conclude that BrdU uptake is the effect of E2F2 overexpression (Figure 40 B, C).

The LNT-E2F2 injected group showed a significant increase of E2F2 and BrdU staining compared to both control groups ($n=4$ eyes per group from different animals, $P<0.0001$, one-way ANOVA; $P<0.0001$ in Tukey's multiple comparisons test). The two control groups were not significantly different. E2F2 and BrdU positive nuclei were counted in 5 HPF per eye and averaged per eye (Figure 41 A). Compared to the medium control group, E2F2 showed a 48-fold increase (range 30–58) in the LNT-E2F2 group, and BrdU a 10-fold increase (range 3–36). In the control groups a low number of BrdU positive cells was present, while in the treatment group, not all E2F2 overexpressing cells became BrdU positive.

The same experiment was carried out on 18 months old mice (Figure 41 B), which roughly corresponds to a human age of over 50 years. At this age, age-related changes of the macula become apparent. Only 3 old mice were available for pairwise left-right eye comparison, therefore medium injected controls were omitted. This demonstrated a similar increase in BrdU uptake upon E2F2 overexpression ($P=0.0463$, paired *t-test*, two-tailed). A 28-fold (range 19–58) increase in E2F2 positive nuclei was noted, going along with a 12-fold (range 5–22) increase in BrdU positive nuclei.

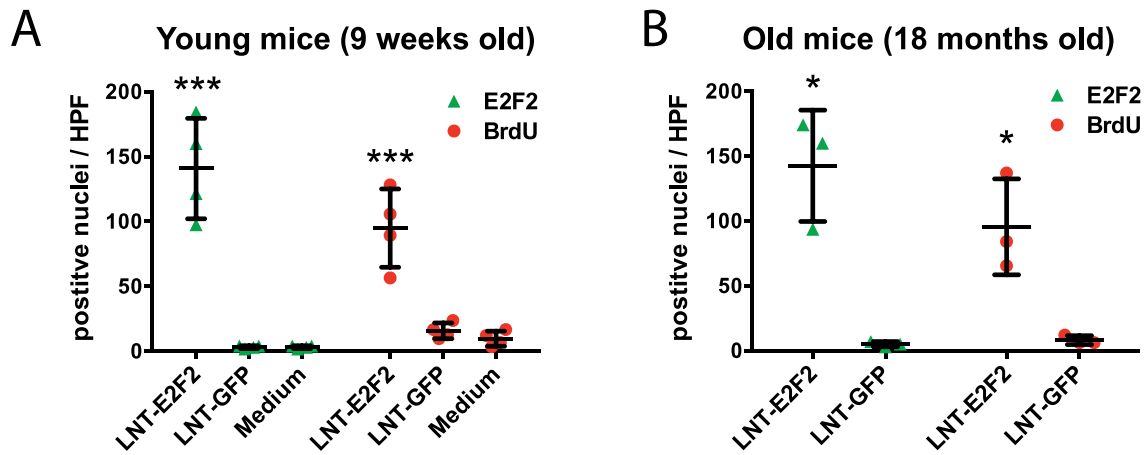


Figure 41. LNT-E2F2 induces BrdU uptake in RPE in both young and old mice.

A. The LNT-E2F2 injected group showed a significant increase of E2F2 and BrdU staining compared to both control groups (mice aged 9 weeks, $n=4$ eyes per group from different animals, *** $P<0.0001$, one-way ANOVA; $P<0.0001$ in Tukey's multiple comparisons test, no significant difference between both control groups; bars represent mean \pm SD). E2F2 and BrdU positive nuclei were counted in 5 HPF per eye and averaged.

B. The same experiment (but omitting the medium injected controls) was carried out on 18 months old mice ($n=3$ mice for pairwise left-right comparison), demonstrating a similar increase in BrdU uptake upon E2F2 overexpression (* $P=0.0463$, paired t -test, two-tailed).

This experiment was repeated twice with different virus batches and both repeat experiments showed comparable results (total $n=20$ eyes from different animals per group). Figure 42 shows results from mice aged 12 weeks, which received subretinal injections of non-integrating LNT-E2F2 vector (2×10^5 infectious particles per eye) in the superior and inferior hemisphere of the eye. Titre matched LNT-hrGFP and medium (OptiMEM) injected eyes served as controls ($n=3$ eyes per group from different animals). All mice received daily intraperitoneal injections of BrdU from day 4 onwards until they were sacrificed 8 days post injection. E2F2 and BrdU positive nuclei were counted on RPE-choroid-sclera flatmounts in 5 HPF per eye and averaged per eye. Here, too, we observed a significant increase in E2F2 (6-fold increase, range 3–11) and an increase in BrdU positive nuclei (13-fold increase, range 5–75) compared to medium injected controls.

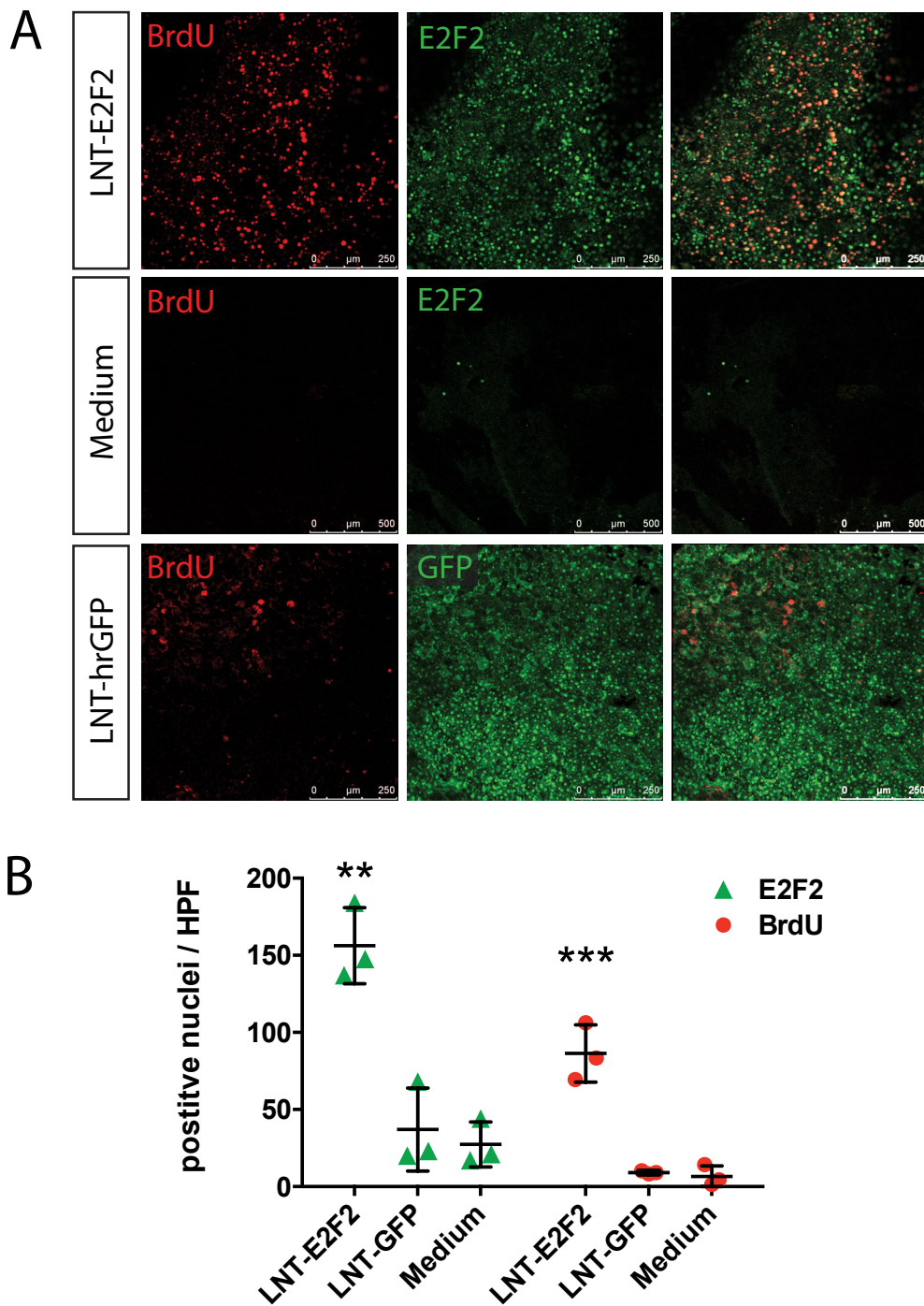


Figure 42. LNT-E2F2 induces BrdU uptake in RPE *in vivo*.

Wildtype mice aged 12 weeks received subretinal injections of non-integrating LNT-E2F2 vector, titre matched LNT-hrGFP and medium (n=3 eyes per group from different animals). All mice received daily intraperitoneal injections of BrdU from day 4 until they were sacrificed 8 days post injection.

A. RPE-choroid-sclera was immunostained for E2F2 and BrdU and flatmounted for imaging on a confocal laser scanning microscope.

B. The LNT-E2F2 injected group showed a significant increase of E2F2 and BrdU staining compared to both control groups (** $P < 0.0005$, one-way ANOVA; $P < 0.0005$ in Tukey's multiple comparisons test, no significant difference between both control groups; bars represent mean \pm SD).

6.2.2.2. LNT-E2F2 mediated S phase progression in relation to vector dose

Decreasing vector titres, i.e. decreasing numbers of total virus particles injected, resulted in a decreasing effect regarding E2F2 overexpression and BrdU uptake. We used three different vector concentrations: undiluted vector suspension and diluted 1:5 and 1:10, resulting in 200.000, 40.000, and 20.000 infectious particles per eye (Figure 43). At these dilutions, a trend to lower numbers of E2F2 and BrdU positive nuclei with decreasing vector particles was observed, but with only three eyes per group, this was not statistically significant. Constraints in time and resources prevented us to repeat this experiment with more eyes and a wider dilution range.

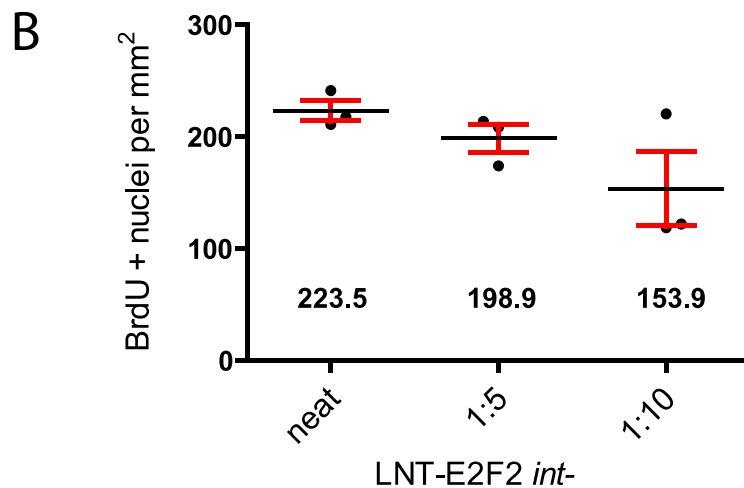
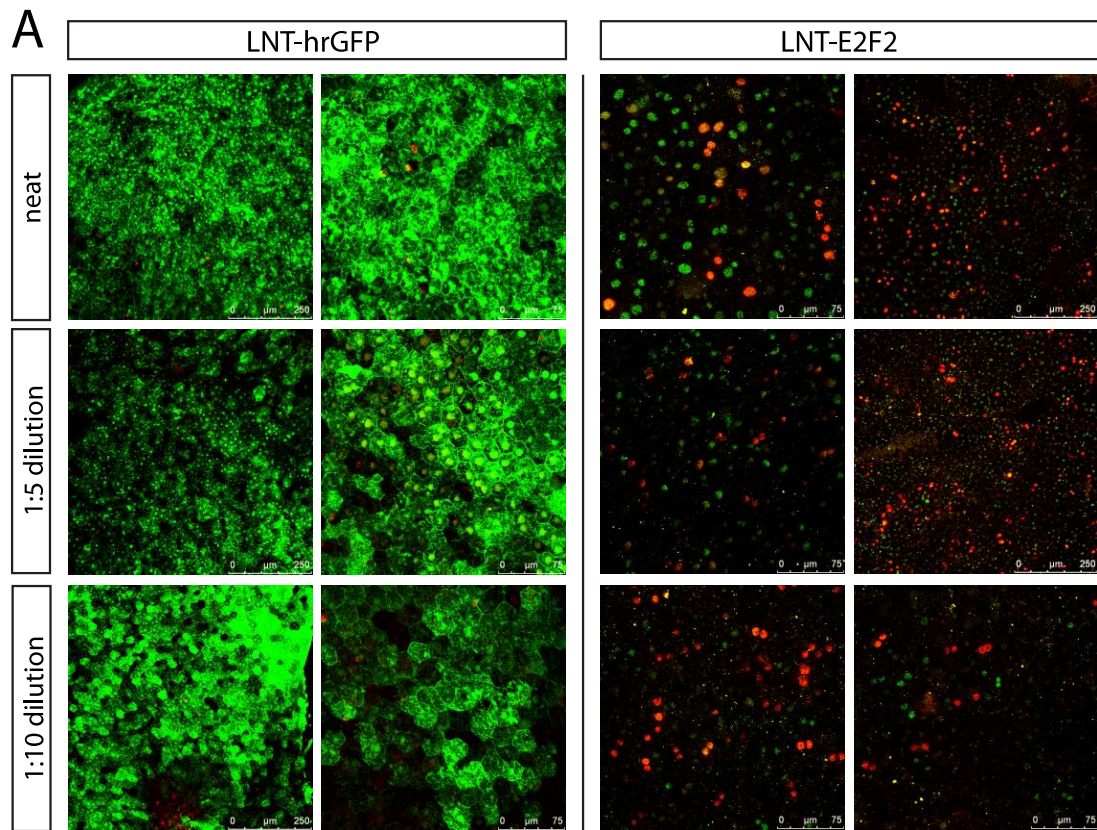


Figure 43. LNT-E2F2 mediated S phase progression in relation to vector dose.

Non-integrating lentiviral vector (LNT-hrGFP or LNT-E2F2) was injected subretinally at different dilutions per eye: undiluted (neat), and diluted 1:5 and 1:10. Mice received daily intraperitoneal injections of BrdU on day 4 till day 8, and were sacrificed on day 10 post injection (3 eyes per group).

A. Confocal laser scanning micrographs of RPE flatmounts. In the LNT-GFP group, decreasing GFP expression (green) is observed. In the LNT-E2F2 group, a similar reduction was observed in both E2F2 (green) and BrdU immunostaining (red).

B. In the LNT-E2F2 group, BrdU uptake showed only a slight (not statistically significant) reduction with decreasing vector titres. BrdU positive nuclei were counted in 5 visual fields (40 \times) per eye, and density per mm² was calculated (mean \pm SEM, $P=0.1411$, one-way ANOVA).

6.2.3. Effect of E2F2 on RPE cell density in wildtype mice

Although BrdU uptake in quiescent cells is regarded as a sign of progression into the S phase of the cell cycle, it does not prove that these cells undergo complete mitosis resulting in two daughter cells. We therefore looked at RPE cell density in female adult C57Bl/6 wildtype mice and compared LNT-E2F2 injected eyes to controls with LNT-GFP or medium injection. RPE cell density was also compared to that of a cohort of age-matched female mice that were left untreated, i.e. did not receive any injection to the eye. No BrdU was injected in this experiment to avoid possible toxic effects on mitotic cells.

Mice aged 8 weeks received subretinal injections of LNT-E2F2, LNT-GFP or medium only in the superior and inferior hemisphere. 10 days after treatment, animals were sacrificed and RPE-choroid-sclera flatmounts immunostained for transgene protein E2F2. Phalloidin stains f-actin and on flatmounts nicely delineates RPE cell borders with their hexagonal formation. This allowed counting individual cells on 40× micrographs. Because in mice as well as in humans the majority of RPE cells have two nuclei, nuclear staining with DAPI or propidium iodine gives inaccurate results. Cell outlines allow accurate counting of cells independent from their nuclei.

Figure 44 shows micrographs of RPE flatmounts representative for each group. As previously, only injection bleb areas were analysed but injection sites with trauma-related artefacts spared. E2F2 overexpression was evident in the LNT-E2F2 injected cohort, but not in the medium injected controls. As previously observed, LNT-GFP achieved to transduce approximately 90% of cells. Variability in cell shape increased in the order: medium/untreated – LNT-GFP – LNT-E2F2. Medium injected eyes showed mostly homogenous cell shapes, LNT-E2F2 injected eyes showed high variability in size and shape, but with no obvious abnormalities in monolayer formation. Here, clusters of smaller cells were often observed.

Quantification of RPE cell density was done on micrographs of masked samples by counting cells outlined with phalloidin. Masking was done on two levels: the slides were masked by an independent colleague. Image acquisition and image analysis was done by different researchers,

and the image labels were again masked. 6 micrographs per eye were counted and averaged. For each condition 15 eyes from different animals were used, for medium controls 8 eyes, resulting in a total of 318 images.

One-way ANOVA revealed highly significant differences among groups ($P=0.0002$). RPE cell density of untreated eyes was 2600 ± 176 cells/mm², of medium-injected eyes 2449 ± 354 cells/mm², and of LNT-GFP injected eyes 2534 ± 318 cells/mm² (medium \pm SD). No statistically significant difference was observed between these controls (all $P>0.6$). In contrast, LNT-E2F2 injected eyes showed a significantly higher RPE cell density at 2961 ± 317 cells/mm². In relative terms, LNT-E2F2 treatment increased cell density by 17% compared to LNT-GFP (adjusted $P=0.0011$), by 21% compared to medium injection (adjusted $P=0.0011$), and by 14% compared to untreated eyes (adjusted $P=0.0071$, Tukey's multiple comparisons test).

Comparing untreated and LNT-E2F2 treated samples, we post hoc calculated the statistical power to be at 0.961 (α error level 0.05, post hoc analysis using G*power 3.1).

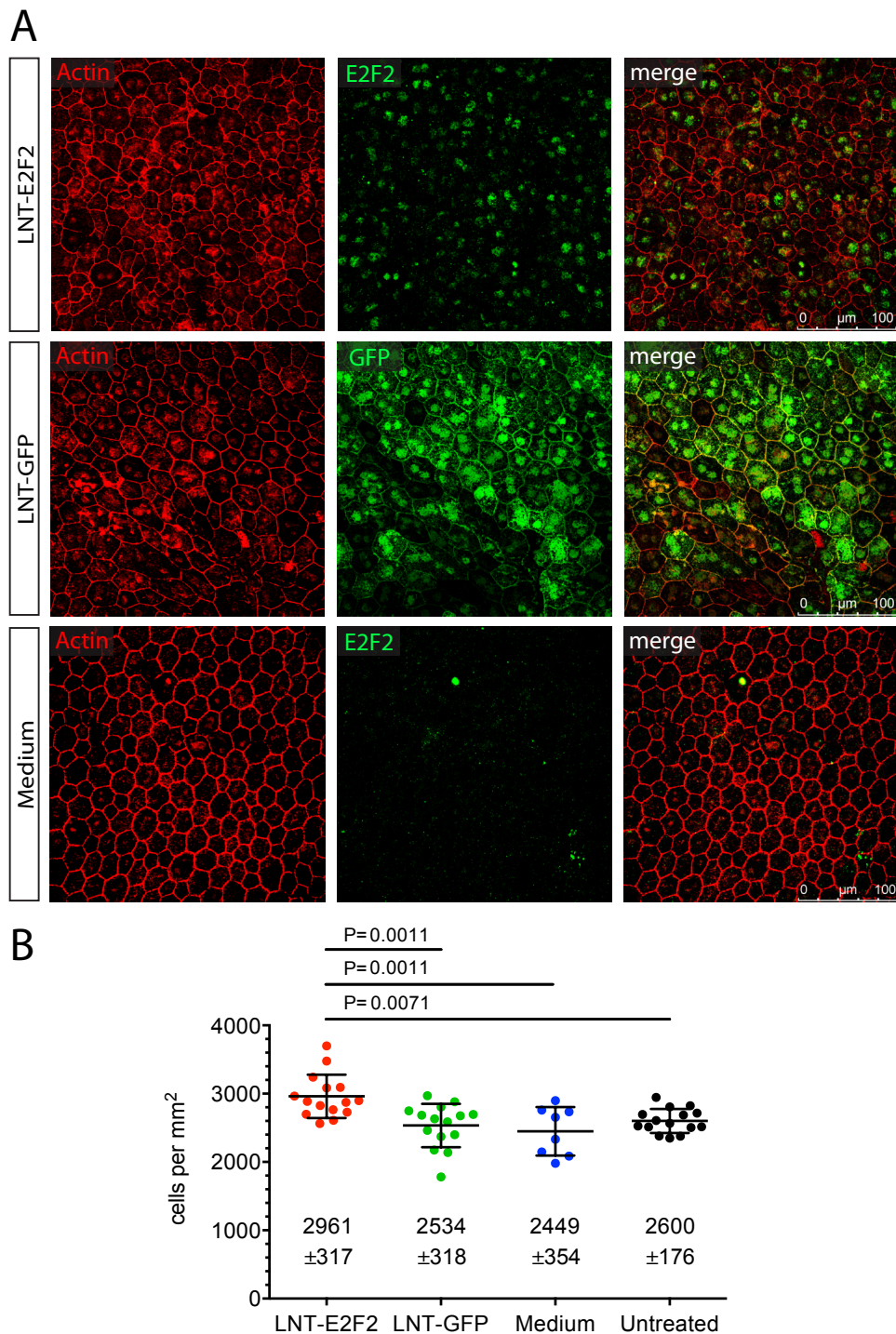


Figure 44. E2F2 overexpression increases RPE cell density *in vivo*.

A. Immunofluorescence staining of f-actin of flatmounted RPE shows cell outlines of the RPE monolayer. E2F2 overexpression in the treatment group was verified by immunostaining. Scale bar 100 μm .

B. Quantification of RPE cell density was done on masked samples by counting cells in the red channel (actin stain). 6 micrographs per eye were counted and averaged, for each condition $n=15$ eyes from different animals, for medium controls $n=8$. Numbers in graph represent mean cell density; error bars represent SD. One-way ANOVA revealed highly significant differences among groups ($P=0.0002$). LNT-E2F2 treatment increased cell density by 17% compared to LNT-GFP, by 21% compared to medium injection, and by 14% compared to untreated eyes (P values from Tukey's multiple comparisons test).

6.2.4. Duration of E2F2 mediated proliferation

To estimate the duration of the LNT-E2F2 induced effect on proliferation, we designed a pulse labelling experiment using two different S phase markers, BrdU and EdU. This allowed differential labelling of proliferating cells at different time points.

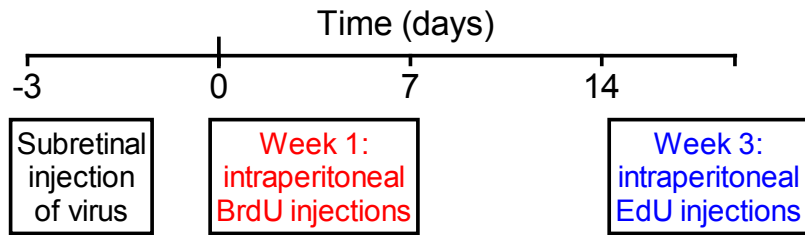
The chronology of the experiment is outlined in Figure 45 A. Wildtype C57Bl/6 mice received subretinal injections of vector LNT-E2F2 or medium. Three days later, proliferating cells were labelled by daily intraperitoneal BrdU injections (2 mg daily per adult mouse) over 5 days. Intraperitoneal EdU was administered to label proliferating cells at the end of the experiment (two intraperitoneal injections of 0.5 mg at the beginning of week 3). The 7-day pause between BrdU and EdU ensured temporal separation of the two markers. Mice were culled at day 19 post injection.

For an internal positive control, we looked at naturally proliferating cells in the cornea. The epithelium on the corneal surface constantly regenerates from stem cells at the limbus. New cells migrate from the basal layers right above the stroma to the surface where they desquamate (compare Figure 45 B, left, showing a schematic cross section through the cornea). In this experiment, en face images of the cornea shows BrdU (red) and EdU positive nuclei (blue) scattered evenly throughout the corneal epithelium. Z sections from epithelial surface through the stroma to the endothelium revealed that BrdU was only found at the epithelial surface representing older cells labelled at the beginning of the experiment. EdU positive cells labelled just before the end of the experiment were found at the basal epithelium where young cells just start their migration. Reconstruction images of a z stack through the full thickness (y/z and x/z) demonstrate that in the corneal epithelium, the temporal separation between BrdU and EdU correlates with a spatial separation of approximately 25 μm .

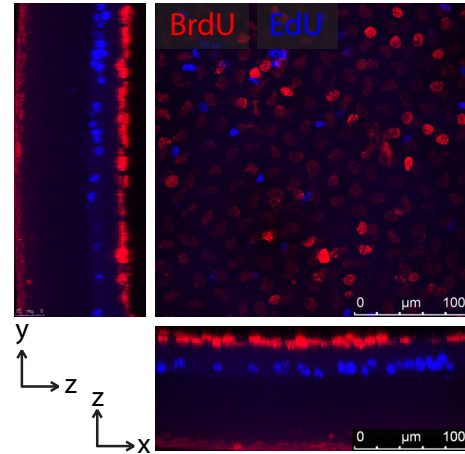
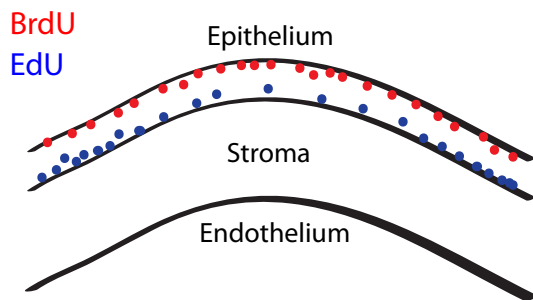
This internal positive control proved EdU staining was reliable. With the concentrations of BrdU and EdU used here and the immunostaining procedure, an equal signal can be detected for both old and young corneal epithelial cells.

Immunohistochemistry of the RPE 19 days after injection showed persisting E2F2 overexpression in the LNT-E2F2 injected cohort. This coincided with an intensive BrdU staining but very few EdU positive cells in the LNT-E2F2 injected cohort (Figure 45 C). In the two control groups, some BrdU positive nuclei could be found in the injection areas, but hardly any EdU staining could be detected. This indicates that the proliferative effect induced by LNT-E2F2 is strong in the first 7 days and is diminishing 19 days after injection.

A. Outline of experiment



B. Corneal flatmount as positive control



C. RPE flatmount 3 weeks after subretinal injection

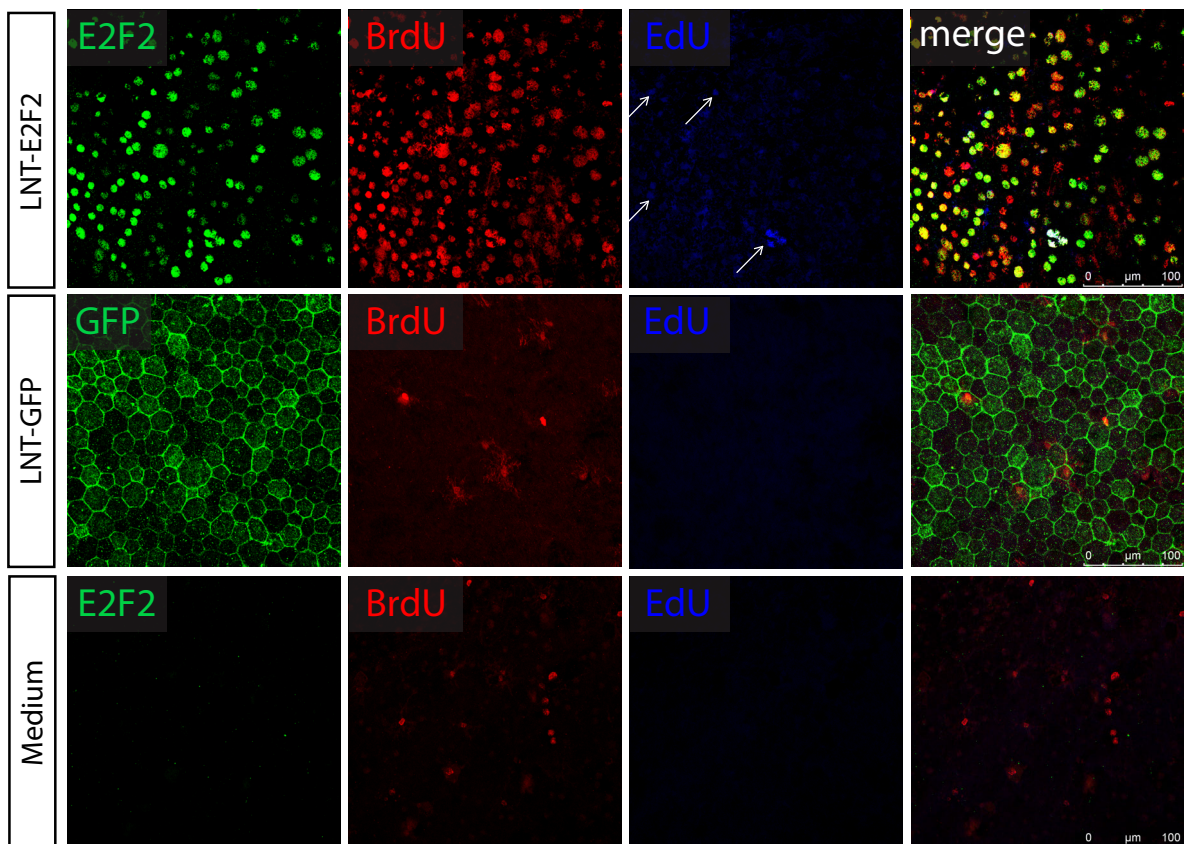


Figure 45. Differential pulse labelling of S phase nuclei to assess duration of proliferative effect.

Figure 45 (cont.)

A. Experimental outline. Wildtype mice received subretinal injections of LNT-E2F2 or medium. BrdU labelling by intraperitoneal injections was performed 3 days later for 5 days, followed by a pause with no labelling. Then intraperitoneal EdU was administered to label proliferating cells at the end of the experiment (week 3).

B. The constantly regenerating corneal epithelium was used as an internal positive control. Older cells labelled at the beginning (BrdU, red) have migrated to the surface, young cells labelled just before the end of the experiment (EdU, blue) are still at the basal layers right above the stroma. En face imaging of the cornea presents a patchwork of old and young cells. Reconstruction images of a z stack through the full thickness (y/z and x/z) demonstrate the temporal separation between BrdU and EdU correlates with a spatial separation of ca. 25 μm .

C. Immunohistochemistry of the RPE 19 days post injection. The LNT-E2F2 cohort showed persistence of E2F2 overexpression coinciding with a strong BrdU staining, but very few EdU positive cells in the LNT-E2F2 injected cohort (arrows). Scale bar 100 μm .

6.2.5. Effect of LNT-E2F2 on RPE in a transgenic RPE-ablated mouse line

To test whether lentiviral-mediated E2F2 overexpression can also increase cell density in diseased RPE, we assessed LNT-E2F2 administration in double-transgenic RPE^{CreER}/DTA mice. RPE^{CreER}/DTA mice were provided by John Greenwood and Stephen E. Moss, Department of Cell Biology, UCL Institute of Ophthalmology. Jennifer A.E. Williams from their group supervised the breeding to cross heterozygous male RPE^{CreER} animals with homozygous female conditional DTA animals. She genotyped the offspring by PCR and induced Cre by tamoxifen intraperitoneal injection. 50 μg were injected per mouse on three subsequent days between postnatal days 12–24. Animals were used for experiments three months later. Because of breeding difficulties with this mouse line, only 4 double-transgenic (RPE^{CreER} +/-/DTA +/-) and 4 wildtype mice (RPE^{CreER} -/-/DTA -/-) of the same background were available for experiments.

Treatment vector LNT-E2F2 or control vector LNT-GFP was injected subretinally in right or left eyes, respectively, of double transgenic mice after RPE ablation by Cre induction. Littermate wildtype controls with normal RPE received the same treatment (n=4 mice per group). Animals received intraperitoneal BrdU injections daily from day 4 to day 10 when they were culled. RPE-chorioid-sklera complexes were immunostained for BrdU and ZO-1 and flatmounted.

6.2.5.1. Reduced RPE cell density in the RPE^{CreER}/DTA mouse

We first looked at untreated animals. At four months of age, RPE showed polymorphous cells with increased cell size compared to wildtype RPE, but the monolayer remained intact without holes (Figure 46 A). This observation was in line with the previous findings (Longbottom et al., 2009). Also consistent with previous observations, RPE degeneration was more pronounced in the centre near the optic nerve where we saw the largest cells. Mean cell density was reduced by $15 \pm 5\%$ (mean \pm SEM, $n=4$ mice, left and right eye averaged, $P=0.0118$, unpaired two-tailed t -test, Figure 46 B). Regional analysis of RPE cell densities revealed a trend to decrease from periphery to centre in all animals. Reduction in cell density in transgenic compared to wildtype mice was most pronounced in the central RPE, where there was a $24 \pm 10\%$ decrease, but this was not statistically significant (mean \pm SEM, $n=4$ mice per group, left and right eye averaged, $P=0.0539$, unpaired t -test, Figure 46 C).

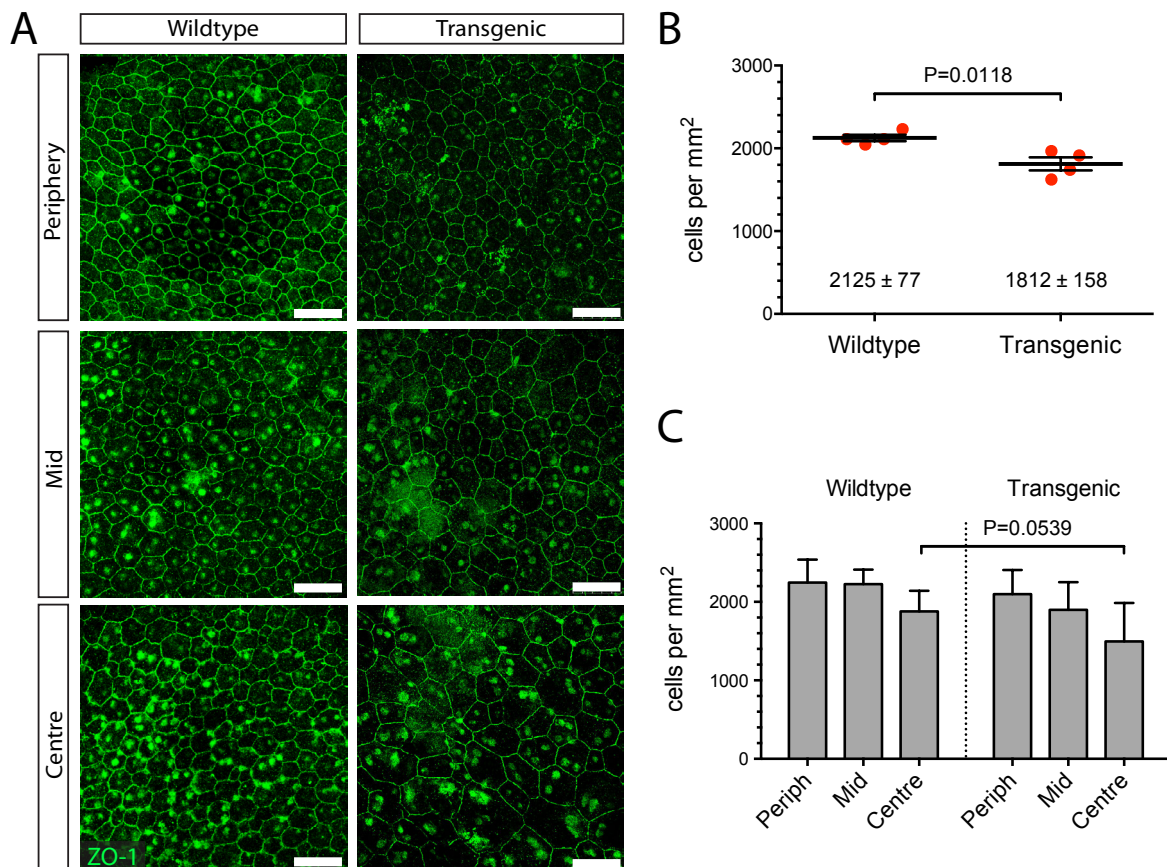


Figure 46. The RPE^{CreER}/DTA mouse line shows reduced RPE cell density most prominently in the centre.

A. ZO-1 staining reveals increased cell size and polymorphism in the RPE ablated group in various locations along the central to peripheral axis. Scale bar = 50 μ m.

B. Overall density was reduced by 15 \pm 5% (mean \pm SEM, range 5 – 25%, values in graph above the x axis are mean \pm SD, n=4 mice per group, left and right eye averaged, $P=0.0118$, unpaired t -test).

C. Reduction was most pronounced in the central RPE, showing a 24 \pm 10% decrease (mean \pm SEM, n=4 mice per group, left and right eye averaged, $P=0.0539$, unpaired t -test).

6.2.5.2. LNT-E2F2 increases BrdU uptake and central RPE cell density

To assess the effect of LNT-E2F2 on diseased RPE, four double transgenic mice were injected subretinally, with treatment vector LNT-E2F2 and control vector LNT-GFP into right and left eyes, respectively, at four months of age. Animals were given intraperitoneal BrdU injections daily from day 4 to day 10 when they were sacrificed. RPE-choroid-sclera complexes were immunostained for BrdU and ZO-1 and flatmounted. We analysed both treated and untreated areas, i.e. areas outside the injection bleb, of the flatmounts throughout all eyes of both groups, as shown schematically in Figure 47 A (injection sites were excluded). Three different areas,

periphery (1 and 4, near Ora serrata), mid-periphery (2 and 5, near equator) and centre (3 and 6, near optic nerve), were imaged. For imaging, all slides were masked. Counting of cells on micrographs was done by a different researcher using ZO-1 staining of RPE cell outlines. To ensure sufficient masking of the images for counting, image files were randomly reshuffled and numbered by an independent researcher.

At day 10 post subretinal delivery of LNT-E2F2 or control LNT-GFP vector, RPE flatmounts were analysed for BrdU uptake within the treated areas of the RPE. In RPE^{CreER} +/- /DTA^{+/-} transgenic LNT-E2F2 treated eyes, we observed BrdU uptake comparable with wildtype C57BL6/J mice after LNT-E2F2 treatment. Also consistent with our experiments described above, LNT-GFP injected control eyes showed almost no BrdU uptake (Figure 47 B, C). LNT-E2F2 treatment of RPE^{CreER}/DTA mice increased BrdU uptake by 9-fold \pm 3.4 (mean \pm SD, $P=0.0173$, paired t -test, $n=4$ eyes from different animals).

Cell density within the treated area was also quantified as described above in 6 different areas of the flatmount. Following LNT-E2F2 treatment, overall cell density was increased compared with control vector injection, in both groups of mice, transgenic and wildtype. Transgenic RPE ablated mice showed a 20 \pm 11% (mean \pm SEM) increase in cell density. However, this did not reach statistical significance ($P=0.2043$ and $P=0.5472$, respectively, unpaired t -test, $n=4$ eyes from different animals).

The centre was the region where Cre-induced degeneration was most prominent (in line with the clinical observation that many forms of RPE degenerations manifest in the macular region). We therefore concentrated on the central RPE near the optic nerve. Regional analysis revealed that the largest increase in cell density was in the centre in RPE ablated mice (Figure 47 D). There we saw a statistically significant increase in cell density of 34 \pm 10% (mean \pm SEM, $P=0.0458$, paired t -test, $n=4$ eyes per group) after *E2F2* overexpression. In the mid-periphery and periphery, a smaller increase in cell density was observed, but this was not statistically significant.

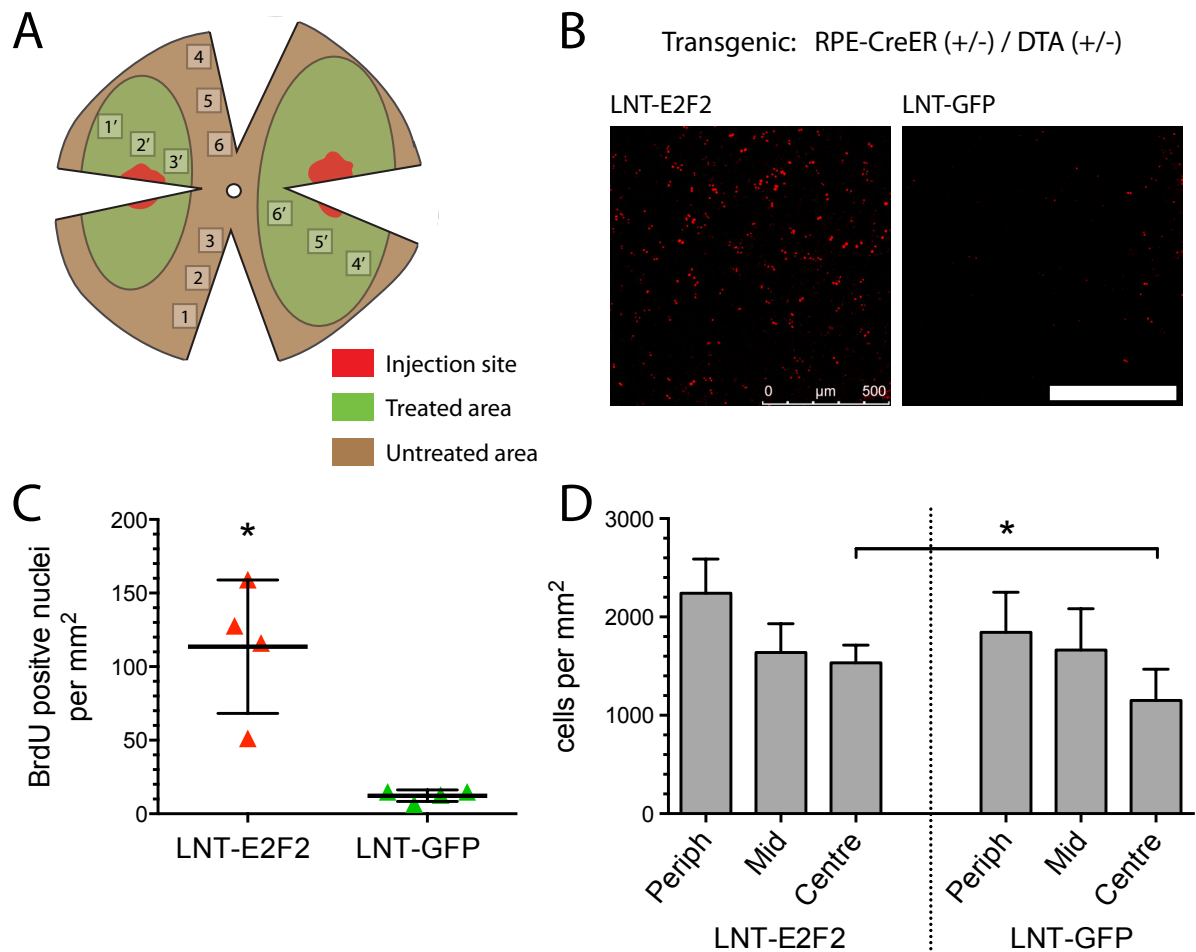


Figure 47. LNT-E2F2 induces increased BrdU uptake in RPE^{CreER}/DTA mice and increases RPE cell density.

A. Schematic representation of the RPE flatmounts to illustrate regional analysis of cell density.

B. Treatment vector LNT-E2F2 and control vector LNT-GFP were injected in right and left eyes, respectively, of RPE^{CreER}/DTA mice (n=4 eyes per group). Mice received daily intraperitoneal BrdU injections on day 3 to 9 post injection. BrdU staining (red) is shown in representative RPE flatmounts. Scale bar = 500 μ m.

C. Quantification of BrdU positive nuclei in 6 micrographs per flatmount revealed a significant increase compared to LNT-GFP treated controls ($P=0.0173$, paired t -test, n=4 eyes per group, bars show mean \pm SEM).

D. Regional analysis shows a statistically significant increase cell density in the centre where RPE degeneration was strongest. Here, an average increase of $34 \pm 10\%$ was observed ($P=0.0458$, paired t -test, n=4 eyes per group, bars show mean \pm SEM).

6.3. Discussion

6.3.1. E2F2 gene transfer to RPE cells induces mitosis *in situ*

Overexpression of transcription factor *E2F2* induces cell cycle progression in the RPE, as shown *in vitro* by upregulation of cell cycle marker genes Cyclin D1 and Ki67, and by increase in BrdU uptake. *In vivo*, after subretinal injection of LNT-E2F2 vector, increase in BrdU uptake in RPE cells coincided with an increase in RPE cell density. This was shown both in young adult as well as very old wildtype mice, and also in in a transgenic mouse model with genetically ablated RPE.

It is long known that RPE cells have an inherent capacity to proliferate under certain conditions. *In vitro*, mammalian RPE cells can be released from cell cycle arrest and can be cultured for up to six months, undergoing several population doublings (Albert et al., 1972). *In vivo*, RPE cells can proliferate as a natural reaction to disruption of the subretinal space during retinal detachment (Anderson et al., 1981; Machemer and Laqua, 1975; Machemer et al., 1978). Necessary precondition for this kind of proliferation is disruption of cell-cell junctions to overcome contact inhibition. By *E2F2* gene transfer, we were able to induce proliferation *in situ* without disruption of the RPE monolayer.

6.3.2. Limitations of the studies

Subretinal injection itself is not free of trauma, but injury was confined to the site of needle entry, which was excluded from analysis. The injection bleb area beyond the injection site itself could be subject to trauma to some degree, which might promote or inhibit proliferation. Controls were therefore subjected to the same injection trauma, but without vector. Injection of

LNT-E2F2 vector caused BrdU uptake in cells evenly distributed throughout the injection area, whereas control injections of medium alone did not induce any significant BrdU uptake.

BrdU uptake is a sign for DNA synthesis and therefore progression in the cell cycle from G1 to S phase, but this does not always lead to completion of mitosis. Terminally differentiated neurons can re-enter the cell cycle, activate cell cycle-associated proteins and initiate DNA synthesis (BrdU uptake), but breach of cell cycle checkpoints results in abortive DNA synthesis without cell division, and the cells undergo apoptosis or death by mitotic catastrophe (Castedo et al., 2004; Chen et al., 2000; Katchanov et al., 2001; Liu and Greene, 2001). For terminally differentiated RPE cells this might be similar, especially when exposed to additional stress by subretinal injection and viral vector gene transfer. Assessing apoptosis in the RPE after *in vivo* subretinal vector injection is challenging, especially in proliferating cells, and can give misleading results. We therefore focused on cell density as the main endpoint, which was highest in the LNT-E2F2 treatment group. To compensate for any effect of the injection trauma, we added untreated eyes that never received any subretinal injection as controls. These eyes showed a slightly higher cell density compared to the other controls (injected with LNT-GFP or medium), possibly indicative of minor injection related cell loss, but this was not statistically significant.

Density assessment in wildtype mice is backed by a reasonable *n* number resulting in a statistical power of 0.961. Transgenic mice, however, were not readily available due to breeding problems with this strain. The results from this experiment therefore have to be viewed with caution. Although in the RPE^{CreER}/DTA line we observed a trend toward lower cell density from periphery to centre, the transgenic mice versus wildtype did not show a statistically significant difference in cell density in the central RPE. When looking at treated versus untreated transgenic mice, we found a significant difference in cell density in the centre where RPE pathology was most striking, indicating a strong effect of the intervention. Further experiments are necessary but were not possible due to time constraints. However, data from the RPE-ablated transgenic mouse model serve as a proof-of-principle for *in situ* RPE regeneration.

6.3.3. Risk of induction of epithelial-mesenchymal transition

When RPE cells proliferate naturally after leaving their natural environment of the sub-retinal space, they transdifferentiate into macrophages and (myo)fibroblast-like cells (Kampik et al., 1981). This process involves epithelial-mesenchymal transition (EMT, reviewed by (Saika et al., 2008)). Here we did not specifically assess EMT markers after transduction, but immunofluorescence staining of f-actin in RPE flatmounts did not show any stress fibres or disruption of the monolayer indicative of EMT (Figure 44, p. 204). Further studies will have to be done to assess EMT after LNT-E2F2 transduction *in vitro* and *in vivo*.

6.3.4. Inherent capacity of regeneration in the RPE

As for 12 week-old adult mice, we observed cell cycle progression also in aged mice older than 18 months, which roughly corresponds to a human age of >50 years, when age-related changes of the macula become apparent. Mice RPE does not show age-related changes comparable to human, and to date there is no commonly acknowledged animal model for AMD. Therefore any extrapolation of our findings to patients with AMD has to be done with great caution. Older human RPE cells in the central macula exposed to life-long oxidative stress may not be capable of undergoing a full cell division. Del Priore et al. found that the proportion of apoptotic cells in human RPE is low, but increases significantly with age (0.56 per 100.000 cells at donors >55 years of age), possibly amounting to a loss of 20% of the macular RPE per decade in older human eyes (Del Priore et al., 2002). Interestingly, apoptosis was confined to the central region. Ach et al. in line with Del Priore confirmed that in the centre, human RPE cell density remains stable over lifetime, providing evidence that RPE undergoes a life-long re-arrangement (Ach et al., 2014). This might be accomplished by migration from the periphery, possibly in combination of mitosis. In human adult RPE mitosis is detected at a very low rate, but only in the periphery (Al Hussaini et al., 2008; Del Priore et al., 2002). Indeed, in several species there is evidence of

continuous regeneration of the RPE arising from stem cells in the marginal zone of the ciliary body (Cicero et al., 2009; Tropepe et al., 2000). By E2F2 transfer, we possibly just accelerated a process of mitotic regeneration that is too slow in the aged / diseased eye.

In the transgenic mouse model, no mitotic regeneration was detected, instead cells expanded to almost 20 times their normal size, similar to what is observed in AMD patients (Longbottom et al., 2009). We observe the greatest proliferative effect of *E2F2* transfer in the centre where cell density was lowest, indicating that the E2F2 triggers mitosis of cells *in situ* rather than recruiting cells from the periphery. Further studies need to address whether regenerated cells are functional by using optical coherence tomography and electrophysiological tests *in vivo*, together with post mortem electron microscopy.

6.3.5. Conclusions

The strategy applied for corneal endothelium was transferred to a different non-replicative tissue equally important to the eye, the retinal pigment epithelium. E2F2 induces proliferation also in RPE cells, as shown *in vitro* in growth-arrested ARPE19 cells, *in vivo* in wildtype mice and, with limitations, *in vivo* in an RPE degeneration mouse model. These findings serve as proof-of-principle for a new strategy of RPE treatment: *in situ* regeneration of cells in their natural environment using gene transfer of cell cycle regulatory factors.

7. Final discussion

7.1. Summary of findings and implications for therapeutic applications

This work investigates methods of *in situ* regeneration for the two amitotic, growth-arrested but not terminally differentiated, tissues essential for vision, the corneal endothelium and retinal pigment epithelium. For both tissues, regeneration was achieved by induction of mitosis of cells *in situ*, without displacing the cells from their monolayer. We exploited the fact that these cells were merely arrested in G1 phase of the cell cycle. Adenoviral and HIV-based lentiviral vectors were used to overexpress or downregulate cell cycle modulating genes, driving cells to continue the cell cycle and undergo mitosis.

Early gene therapy strategies addressed monogenic diseases and hence comprised *gene replacement* for recessive disorders and *gene silencing* for dominant disorders where the mutated allele may exert a toxic effect on the cell. Both strategies have successfully been used for treating animal models. The former is now established in clinical studies for diseases of the hematopoietic and myeloid system, systemic metabolic diseases, treatment of cancer and of retinal degenerative diseases. With *Glybera* (Alipogene tiparvovec), the first gene therapy treatment has been approved by the European Medicines Agency in 2012 (Yla-Herttuala, 2012): an AAV1 vector delivering lipoprotein lipase in the muscle for the treatment of lipoprotein lipase deficiency.

These traditional strategies directly target one single gene defect. To treat multifactorial diseases or diseases of unknown genetic pathomechanism, *modulatory* or *augmentation gene therapy* comprises upregulation of beneficial genes or down-regulation of adverse genes to

ameliorate the course of a disease. In our case, modulation of cell cycle controlling genes induced mitosis and thereby regeneration. Compared to classic gene replacement or gene silencing therapy, modulatory gene therapy imposes different and complex challenges (described below) because the modulatory transgene can exert various side effects on the targeted tissue.

7.1.1. Corneal endothelium

Corneal endothelium maintains the cornea's hydration and thereby its transparency. Being a non-dividing cell layer, cell loss over lifetime or through disease is not compensated by cellular regeneration and can lead to vision loss. We evaluated different methods to induce mitosis in human endothelial cells *in situ*, *ex vivo*, using gene transfer.

Key findings are summarised below:

- Adenoviral vectors effectively transduce human corneal endothelium *ex vivo* (80–90% transduction efficacy). Adenovirus mediated E2F2 overexpression can increase endothelial cell density, but this is limited to young donors not older than ~42 years of age.
- HIV-based lentiviral vectors have a lower transduction efficacy than adenoviral vectors in corneal endothelium *ex vivo*, therefore lentivirus mediated E2F2 overexpression is insufficient to induce endothelial proliferation.
- The ZO-1/ZONAB pathway plays a role in corneal endothelial cell contact inhibition. Lentiviral knock-down of ZO-1 using shRNA, or lentiviral ZONAB overexpression both induces endothelial cell proliferation and increases cell density by ~20–30 % in samples of donors up to ~60 years of age.

Challenges with Adenoviral vectors

Adenoviral vectors offer two major advantages for application in human corneas *ex vivo*: (a) high transduction efficacy in the endothelium with a short onset of transgene expression, which is important for the limited time span of a corneal graft in organ culture, and (b) non-integrating gene transfer, an important safety feature when transferring cell cycle modulating genes. The main disadvantage is immunogenicity, making adenoviral vectors unsuitable for use in allogeneic transplant corneas. The inflammatory response to adenovirus is initiated by the innate immune system and involves not only generic immune cells such as dendritic cells, macrophages or peripheral blood mononuclear cells, but also “non-immune cells” such as epithelial, endothelial or mesenchymal cells (Hartman et al., 2008). Because no pre-sensitization is required in the host, the reaction is fast and occurs already after the very first contact with the vector. In addition, adenovirus infections are a common cause of conjunctivitis in humans. Especially epidemic keratoconjunctivitis (EKC) associated with adenovirus serotypes 4, 8, 19, 37, 53 and 54 is feared for its high contagiousness, potentially substantial morbidity and prolonged visual complications due to corneal infiltrates (Dart et al., 2009; Kaneko et al., 2011). It has not been investigated how an eye pre-sensitized with adenovirus due to conjunctivitis would react to a second exposure caused by an adenoviral vector, but as Qian et al. have shown in a mouse model, *ex vivo* Ad-GFP transduced corneas showed a significantly shorter survival time after re-transplantation than untransduced controls (Qian et al., 2004).

Our studies using adenoviral vector confirm the proliferative effect of E2F2 overexpression in corneal endothelium, as shown previously (Joyce et al., 2004; McAlister et al., 2005). However, this merely serves as proof-of-principle. For clinical application, other vectors have to be considered.

Challenges with Lentiviral vectors

Lentiviral vectors combine lower immunogenicity with high transduction efficacy and fast onset of transgene expression. However, the non-integrating lentivirus mediated *E2F2* overexpression was insufficient to show significant increase in endothelial cell density. Most likely reasons are lower transgene expression levels compared to adenoviral vectors, lower vector preparation quality, and / or the additional effect of adenovirus endogenous proteins expressed in the early phase after transduction.

Changing the transgene to a more potent one was one approach. Interfering with the ZO-1/ZONAB pathway offers a way to directly address contact inhibition, considered the main inhibitor of mitosis in corneal endothelium. This indeed was more effective in increasing corneal endothelial cell density. Although the increase of a mean 30% seems low one week after treatment, this would be sufficient to rescue a substantial number of grafts that would otherwise be discarded due to not passing the CEC density cut-off criterion of usually between 2000 and 2200 cells/mm² in European eye banks.

On the basis of our findings, investigation of longer term stability of the effect on ZO-1 and ZONAB modulation and testing of endothelium function in corneas modified *ex vivo* will be required before proposing clinical application. However, with the right safety measurements in place, transient viral gene transfer of at least ZONAB in *ex vivo* cultured corneal transplants could become a method to improve donor corneal endothelial quality. Safety measures for the use of cell cycle modulating genes in gene therapy are proposed below (Chapter 7.2, Safety measure for gene transfer to induce cell replication, p. 225).

The observation that none of the treated corneas reached an endothelial density above 3000 cells/mm², the density found in humans at birth, might indicate that intrinsic mechanisms of contact inhibition are strong enough to prevent uncontrolled proliferation above that density level. Whether LNT-ZONAB or LNT-shZO-1 treated endothelium maintains this higher density and become self-regenerating, remains speculation.

We investigated this *in situ* regenerative approach in healthy corneas, with application in eye banks pre-transplantation in mind. Whether this might be a therapeutic option also for diseased endothelium remains speculative. The most common endothelial diseases are pseudophakic (and aphakic) bullous keratopathy and Fuchs' endothelial dystrophy. The former is caused by endothelial cell damage during or after cataract surgery, either due to complications during surgery or triggered by the artificial intraocular lenses, especially anterior chamber lenses (Taylor et al., 1983). It might well be that a strong proliferative signal such as ZO-1 down-regulation and / or ZONAB overexpression is enough to induce mitosis in these genetically healthy cells. However, pseudophakic bullous keratopathy normally develops over years after surgery and a constant, chronic state of inflammation in the anterior chamber may be contributing to the cell death (Rosenbaum et al., 1995), leading to permanent loss of mitotic competence.

Fuchs' endothelial dystrophy (FECD) in its most common form, late onset FECD, is an autosomal dominant disorder with incomplete penetrance (Hamill et al., 2013). It is characterized by progressive loss of corneal endothelial and the formation of guttae, excrescences on Descemet's membrane, cells causing vision loss through corneal oedema. The majority of patients show the onset at around 45 years of age. The underlying pathogenetic mechanism is not completely identified, but suggests that environmental factors seem to contribute to disease development. Therefore, it might be that in endothelium with FECD, a proportion of cells despite their genetic disorder are still competent of undergoing mitosis. New-born cells might have enough dehydrating power to keep the cornea clear.

7.1.2. Retinal pigment epithelium

The retinal pigment epithelium (RPE) interacts closely with photoreceptors and is important for maintaining visual function, but does not regenerate. We used gene transfer of *E2F2*, a potent transcriptional regulator of proliferation, to RPE cells to induce cell replication and thereby regeneration.

Key findings are:

- *In vitro*, *E2F2* overexpression induces proliferation.
- *In vivo*, in wildtype mouse RPE (C57BL6/J), *E2F2* delivered by non-integrating lentiviral vector induces cell cycle progression, and this effect seems age-independent. This causes an increase in RPE cell density of 14–17 %.
- In an RPE deficient mouse model (RPE^{CreER +/-}/DTA^{+/-}), *E2F2* overexpression increases cell density primarily in the centre where RPE degeneration was strongest.

From this we conclude that viral vector mediated gene delivery of *E2F2* can induce proliferation in healthy and diseased RPE cells *in vivo* and that this approach can increase cell density of RPE cells preferentially in diseased areas of low density, where contact inhibition may be lowest. This approach may pave the way for an *in situ* regenerative approach to treat RPE cell pathology in disease such as Stargardt's disease and age-related macular degeneration (AMD).

In situ regeneration in relation to cell transplantation

In situ regeneration provides an alternative to current therapeutic options involving RPE cell transplantation. The concept of RPE transplantation has been investigated for decades but has not led to any routinely applied therapy. This might be due to the fact that any such therapy was performed on eyes with low vision and widely degenerated RPE. Consequently, photoreceptors were already degenerated as well and hence even the best RPE regeneration would not yield any significant improvement of vision. The surgical procedure of RPE transplantation itself is comparatively traumatic, involving a vitrectomy, a surgically induced retinal detachment and

– in case of an RPE sheet – also a retinectomy, adding further damage to the photoreceptors. Even newer approaches involving a suspension of stem cells injected under the retina causes vast disruption of photoreceptor arrangement.

A regeneration *in situ* where only a small proportion of RPE cells undergo mitosis over a period of 1–2 weeks would be far more atraumatic, also considering that a vector suspension can be administered through far smaller cannulas than a cell suspension. Subretinal vector injections have been performed in patients in several gene therapy clinical trials.

Route of vector administration

Further reduction of trauma could be realized through an intravitreal vector application. Intravitreal injections of drugs are routinely performed for neovascular age-related macular degeneration, and repeat injections of over 6 injections per year have become commonplace. Continuous vector refinement allows administration of vector even without direct contact with the target cells without compromising transduction efficacy. Especially the small size of AAV (20 nm), together with the right choice of serotype, already allows transduction of the outer retina after intravitreal administration (Dalkara et al., 2013; Igarashi et al., 2013; Park et al., 2009; Schon et al., 2015; Trapani et al., 2014). Overcoming the physical barrier at the vitreoretinal interface by enzymatic digestion enhances transduction efficacy after intravitreal vector administration (Dalkara et al., 2009). Enzymatic vitreolysis by intravitreal injection of a recombinant protease has already found its way into clinical practice for treatment of vitreomacular traction syndrome (Stalmans et al., 2012).

Novel capsid engineering techniques are based on *in vitro* evolution and apply highly diverse capsid libraries with random mutations (Koerber et al., 2009). This enabled the generation of an AAV capsid with specific tropism to Müller glia after via intravitreal administration (Klimczak et al., 2009). Together with well-characterized RPE specific promoters (RPE65,

VMD2), further AAV vector engineering might lead to an easily applicable treatment modality for the RPE minimizing injection-related damage.

Role of Bruch's membrane

It remains the question of whether a diseased Bruch's membrane, as is reported for nearly all degenerative diseases of the RPE, can support newly proliferating cells (Kulkarni and Kuppermann, 2005). For both neovascular and non-exudative AMD, changes in Bruch's membrane correlate with the stage of the disease: degree of calcification of Bruch's membrane; the number of fragmentations in Bruch's membrane; the number of soft, diffuse, and large drusen; and the amount of basal laminar deposit (Spraul et al., 1999). However, changes seem more pronounced in eyes with exudative AMD than in eyes with non-exudative AMD. To date, no animal model is known to accurately reflect the changes of the aging eye, but the combination of light-and and age-induced changes might bring new insight in AMD pathology.

Timing of in situ regeneration

As expected in the course of a gradually progressive disease, the time point of intervention is crucial. As mentioned earlier, current interventions involving RPE regenerations in AMD were done at the end stage of disease. For *in situ* regeneration to be successful, we have to aim at a much earlier stage, when photoreceptor degeneration and Bruch's membrane changes are still in their beginning but awareness of the patient is sufficient to accept invasive therapy. The less invasive the intervention, the lower is the threshold to consent to therapy while visual acuity is still acceptable. Here lies the big advantage of a less invasive *in situ* regeneration compared to highly invasive surgical macular translocation or cell transplantation therapy. Obviously, new safety mechanisms have to be devised.

7.2. Safety measure for gene transfer to induce cell replication

Genetic modulation of cell cycle controlling genes bears high risks. Uncontrolled expression of a potential oncogene would lead to uncontrolled proliferation, i.e. cancer. A variety of safety measures are possible.

7.2.1. Modulation of cDNA integration

Insertional mutagenesis is a risk associated with any transgene delivered by retroviral vectors (Nienhuis et al., 2006). Retroviruses deliver single stranded RNA to the host cell, which is reverse transcribed into cDNA. This transcript then integrates into the host genome at a random position – here the risk of insertional mutagenesis arises: the vector integrates near a protooncogene in the host genome, causing overexpression of a normally silenced gene, leading to clonal expansion of that cell.

HIV based lentiviral vectors, as well as HIV viruses, have to date not been associated with neoplastic transformations caused by DNA insertion into the host genome (Cockrell and Kafri, 2007). Nevertheless, LV still bear the potential for insertional oncogenesis, and when the transgene itself is an oncogene, this fear is even greater. One strategy to avert insertional mutagenesis is to direct lentiviral vector insertion into specific sites within the host genome, genomic safe harbours (GSHs) (Papapetrou and Schambach, 2016). Directing the vector DNA to a specific GSH can be realized by various gene targeting tools introducing site-specific DNA double strand breaks, such as zinc-finger nucleases, mega-nucleases, transcription activator-like effector (TALE) nucleases, or the CRISPR-Cas9 system. Although these tools can provide specific and effective vector direction, little experience has been gained so far for use *in vivo*. In addition, GSH sites need yet to be identified and carefully validated.

To bypass integration risks, non-integrating LV have been developed by mutating the viral *integrase* gene, greatly reducing the risk of insertional mutagenesis (Philpott and Thrasher, 2007; Saenz et al., 2004; Yanez-Munoz et al., 2006). Transgene RNA is transcribed into DNA in the host cell and accumulates in the cell nucleus as double-stranded circles (2-LTR episomal circles) from which transcription occurs. This enables transgene expression until the cell divides, when in the absence of any replication signals, transgene DNA circles dilute or degrade over time.

The LV used with the transgene *E2F2* carry a mutant D64V integrase, which decreases integration of pseudotyped HIV-1 to 1/10,000 of wild type (Leavitt et al., 1996; Yanez-Munoz et al., 2006). For retroviral vectors, the risk of mutagenesis of cellular sequences promoting a malignant clone is about 10^{-7} per insertion (Li et al., 2002; Stocking et al., 1993).

For transduction experiments, we used for the endothelium 6×10^6 infectious particles per cornea and for the RPE 8×10^5 infectious particles per mouse eye. On the basis of these figures, the risk of insertional mutagenesis per cornea is in the dimension of 10^{-5} . However, this figure does not take into account the additional risk imposed when the transgene is itself an oncogene, which might potentiate the risk. No figures are available for such a scenario.

AAV vectors naturally do not integrate their genome, and share the low immunogenicity of lentiviral vectors. Unfortunately their transduction efficacy in corneal endothelium is too low for use during the short period of a cornea *ex vivo* pre transplantation. Recent studies from this group, however, could show that the new serotype AAV2/6(ShH10) is able to mediate a widespread and substantial transduction of the endothelium of both murine and human corneas (Basche, 2014). This new serotype was developed by screening a library of capsid mutations with an artificial selection technique, with the aim to develop vectors to transduce Müller cells in the retina from an intravitreal injection (Klimczak et al., 2009). To apply this novel serotype in a cornea *ex vivo* setting, toxicity of high titre vector to the endothelium has to be evaluated.

7.2.2. Modulation of transgene expression

Continuous expression of a proliferation inducing transgene would also lead to the formation of tumours. Especially the inadvertent transduction of naturally proliferating cells in the vicinity of the target tissue could have catastrophic consequences. For the cornea, stromal keratocytes can be easily transduced by lentiviral vectors, but only when in direct contact with the vector. This would not be the case in the proposed eye bank setting. In addition, their turnover rate is very low: in humans, it would take between 6 to 12 months for the keratocytes to be replaced. No malignancies originating from the stroma are known. Stromal transduction might therefore be a negligible risk.

Corneal epithelial cells, however, are likely to come in contact with the vector and possibly transduce them. In a different project done in cooperation with other members of this group (Satoshi Kawasaki and Mark Basche), we tried to transduce epithelial cells. Superficial cells, which are almost entirely terminally differentiated cells and, to a small degree, post-mitotic wing cells, either were not transduced at all or (hypothetically) detached shortly after transduction. This reflects the natural function of these cells as the first line defence against pathogens. To achieve lasting transgene expression, we tried to transduce limbal epithelial stem cells in mice *in vivo* and in human donor corneas *ex vivo*. Because of the limbal stem cell niche being buried in the basal layers of the epithelium, transduction could only be achieved through vector delivery using a sharp glass capillary.

Overall, the risk of unwanted transgene expression in corneal cells other than the endothelium seems low. It should, however, be further minimized by putting the transgene under the control of a tissue-specific promoter. To date, no such promoter has been specified for the endothelium. Tight junction protein ZO-1 and the Na⁺/K⁺-ATPase are highly expressed in the endothelium, but are not exclusively specific. By high throughput gene expression analysis, Chng et al. identified a panel of genes that are highly expressed in the human corneal endothelium, but not in the stroma (Chng et al., 2013). SLC4A11 is among the top 20 most highly expressed genes

in human corneal endothelium. It encodes a multi-pass membrane protein important for sodium-mediated fluid transport. Promoter analysis should reveal a highly efficient promoter suitable for expression specifically in the corneal endothelium.

Instead of a tissue-specific promoter, an inducible promoter reduces the risk of uncontrolled transgene expression. Parker et al. replaced the constitutive promoter in a lentiviral vector, commonly SFFV, SV40 or CMV, by a synthetic steroid-inducible promoter, to transduce corneas *ex vivo* (Parker et al., 2009b). As transgene, they used IL-10 to act as immunosuppressive after transplantation, when glucocorticosteroid eye drops are routinely administered to minimize inflammation and risk of graft rejection. In the presence of the steroid dexamethasone, IL-10 levels in the supernatant of cell line cultures were 30–40-fold higher and ten times higher in *ex vivo* ovine and human corneas. Withdrawal resulted in restoration of baseline IL-10 levels. Other promoters that respond to antibiotics (tetracyclin) are available. Even though all inducible promoters show some degree of baseline expression in the absence of their specific stimulus, they would still be an additional safety mechanism even in the high-risk context of cell cycle modulating transgenes.

7.2.3. Reverse transcription defective lentiviral vectors

Work by Mark Basche, Ph.D., from this group done in parallel to this thesis aimed at constructing a lentiviral genomic construct that should be unable to undergo reverse transcription (Basche, 2014). Previous reports had demonstrated the feasibility of this so-called “retroviral pseudotransduction” (Galla et al., 2008; Galla et al., 2004). Reverse transcription is the first step in the lentiviral life cycle. If eliminated, all following steps should also be prevented. The vector delivers only its single stranded RNA genome, which serves directly as messenger RNA strand for translation into protein in the cytosol and is then degraded. The basis for the construct was

the same 2nd generation lentiviral backbone as used for experiments in this thesis. Modifications included removal of the primer binding site required to initiate reverse transcription, removal of the central poly purine tract (cPPT) and of the constitutive promoter (SFFV). Expression levels were – as expected – several orders of magnitude below the normal LV vector, genome half-life was around 44 hours. For a transgene potent enough to induce cell division at low levels, this would be a safe method for transferring cell cycle regulating genes.

7.2.4. Lentivirus particle mediated protein transfer

A completely novel transformation of lentiviral vectors would be to generate viral particles carrying a *protein* of interest instead of the encoding RNA, and delivering the protein directly into the cytoplasm. Any gene replication would thereby be eliminated by principle. Current LV vectors already deliver viral proteins to the host cell, such as *integrase* and *reverse transcriptase*. For this we developed a concept to clone a packaging plasmid to package E2F2 as protein into a lentiviral particle. This was done in cooperation with Luis Apolonia, Ph.D. and Professor Adrian Thrasher, UCL Institute of Child Health.

E2F2 cDNA is cloned into a modified LV packaging plasmid (p8.74 P2 ins) featuring a mutation in *p2*, which encodes a structural spacer protein within the lentiviral *gag* gene (the gene product of *p2* is also called SP1, spacer protein 1). This results in duplication of the protease recognition site in the *gag-pol* polyprotein (Figure 48 A). *E2F2* (1313 bp) is inserted to be flanked by the protease recognition site on either side (Figure 48 B), without disrupting the ORF of any following genes produced from *gag* (p8.74 P2 ins-E2F2). This enables the translation and cleavage of E2F2 protein in the producer cells (HEK 293T).

Vector is then produced as normal by transfection of 293T cells with both the *E2F2* containing packaging plasmid and a VSV-G envelope plasmid. VSV-G pseudotyped lentivirus particles are assembled and packaged, containing the exogenous protein E2F2 with the other necessary

structural viral proteins without any RNA. None of the constructs involved in producing these proteins contains the packaging signal Ψ to ensure their transcripts, although translated, cannot subsequently be packaged into the viral particle. Upon host cell infection, E2F2 protein is released into the cytoplasm and transported to the nucleus to act as a transcription factor activating the cell cycle.

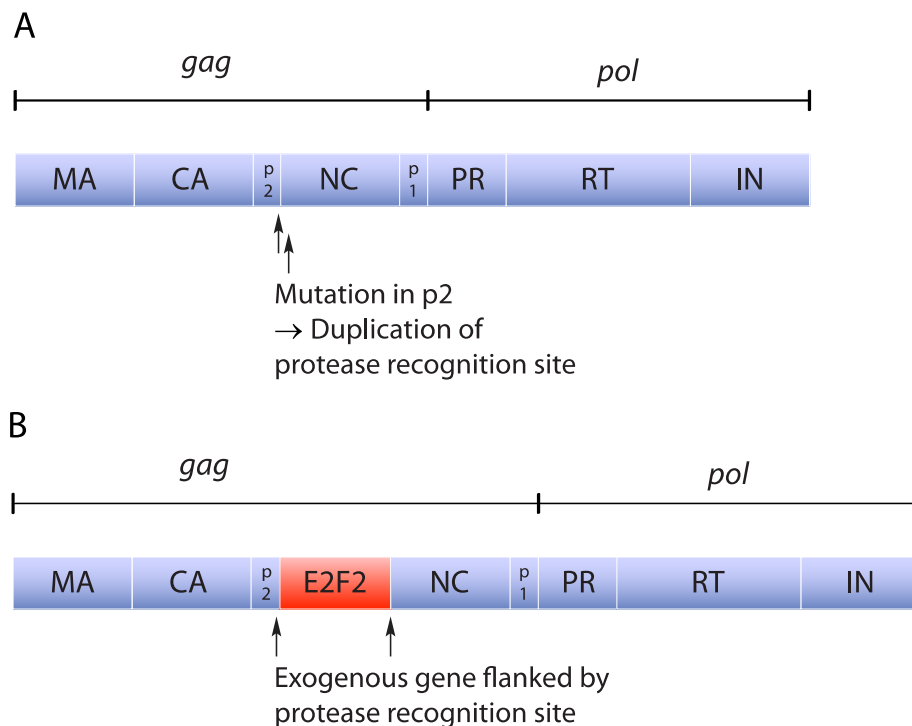


Figure 48. Lentivirus particle mediated protein transfer

A. Modified LV packaging plasmid (p8.74 P2 ins) featuring a mutation in *p2*, causing duplication of the protease recognition site (arrows).

B. Transgene E2F2 inserted between the two protease recognition sites (arrows).

For *in vitro* purposes, the option of adding a reporter protein to the viral genome still remains. A transfer protein containing *GFP* with the packaging signal Ψ would pack the *GFP* gene into the non-integrating viral particle. This enables visual determination of infection efficiency after the *GFP* gene is transcribed and translated in the host cell.

This concept would allow safe delivery of a cell cycle modulating protein, although in very low levels. To be effective, the protein must be very potent. Cloning of the vector has been done, but functional tests (verification of E2F2 presence in the viral particles, infection efficacy) were abandoned, as it emerged that high E2F2 levels were necessary to achieve cell cycle progression. This is in contrast to a study of Haberichter et al., who in a mathematical model showed that E2F2 would trigger cell cycle progression even at very low levels (~5 molecules/cell) (Haberichter et al., 2007). This, however, turned out not to be valid for corneal endothelial or RPE cells. A gene alternative to *E2F2* but more powerful in cell cycle induction would be necessary for those naturally growth-arrested tissues.

7.2.5. Non-viral vectors

A non-viral DNA vector or plasmid mini-circles freed from prokaryotic DNA, delivering only the transgene with its promoter, would be the ideal solution regarding safety, yielding a more transient expression (Lufino et al., 2008; Wong et al., 2015). Combining this with a tissue-specific promoter would limit transgene expression to endothelial cells. However, all current non-viral transfection methods have a comparatively low efficacy and are potentially more toxic to endothelium than viral vectors (cf. Chapter 1.5, Gene transfer to corneal endothelium, p. 31).

For the comparatively high transgene levels required especially in corneal endothelium, currently neither non-viral vectors nor lentivirus particle mediated mRNA or protein transfer would offer high enough transgene expression. Non-integrating LV reduce risk of insertional mutagenesis, however, to completely eliminate the vector from host tissue, a full turnover of the human corneal endothelium with complete elimination of transgene would be necessary and would take years or decades. A persistent low drive to replicate in endothelial cells would be advantageous in many diseases from a clinical point of view. From the standpoint of safety

regulations, this would be a major impediment. A combination of non-integrating vectors with an inducible promoter might be sufficient to enable augmentation gene therapy involving cell cycle modulating genes. For our current studies as proof-of-principle, we intended a high efficacy in gene expression and therefore used lentiviral vectors with a constitutive promoter, non-integrating for LNT-E2F2, integrating for LNT-ZONAB and LNT-shZO-1.

7.3. Which cells regenerate?

For both human corneal endothelium and retinal pigment epithelium, it is likely that in aged human tissue, a proportion of cells have lost its capability to undergo a full mitotic cycle. In both tissues, apoptotic cells have been identified, and their proportion increase with age. This is not surprising, considering the fact that the central cornea as well as the central RPE in the macula are subjected to high metabolic activity and in the same time exposed to oxidative stress induced by light damage. This explains the finding that in corneal endothelium above a certain age, probably over 60 years, we did not see a proliferative response to cell cycle modulating transgenes.

On the other hand, for both tissues, several studies support the idea of a process of natural regeneration. In the human endothelium, endothelial stem cells were located in a niche at the posterior limbus (He et al., 2012; Whikehart et al., 2005). For the RPE, stem cells could be found in the periphery near the ciliary body (Al Hussaini et al., 2008; Del Priore et al., 2002; Salero et al., 2012). Remarkably, these cells could be expanded considerably even from elderly donors up to 99 years of age (Salero et al., 2012). Though the function of these cells *in vivo* has not yet been fully established, it seems likely that they carry the potential to regenerate the tissue *in situ* at least to some extent. By overexpressing cell cycle modulating genes, we might merely be harnessing this natural potential.

7.4. Outlook

For corneal endothelium, the concept of *in situ* regeneration via gene therapy has at least for the medium term lost importance thanks to two exciting new treatment approaches that are currently being developed. Firstly, transplantation of corneal endothelium as a cell suspension generated from donor corneas and expanded *in vitro* has now become feasible. The group of Shigeru Kinoshita, Kyoto Prefectural University of Medicine, constantly refined the method of cultivating and thereby expanding endothelial cells harvested from a donor cornea. Adding Rho-associated protein kinase inhibitor (ROCK-I, Y-27632), a small molecule modulating actin cytoskeletal dynamics increases proliferation and longevity of CEC in culture, and changes their adhesion properties (Okumura et al., 2013; Okumura et al., 2014b; Okumura et al., 2015). The group has validated the concept of CEC injection in a non-human primate model of endothelial dysfunction. 2.0×10^5 cultivated CECs suspended in medium were injected into the anterior chamber and animals kept in face-down position for 3 hours. CECs attached to their physiologic habitat at the posterior surface of the cornea, without forming aggregates or clogging the aqueous outflow tract, and restored corneal transparency (Okumura et al., 2014a; Okumura et al., 2012). Results of a clinical trial started in December 2013 (UMIN-CTR Clinical Trial No. UMIN000012534) are not officially published, but preliminary results reported by the group demonstrated safety and astonishing efficacy in 18 patients (Okumura, Pharmacological stimulation of *in vivo* regeneration, talk held at the annual meeting of the German Ophthalmological Society, 2015).

Secondly, the source for CEC transplantation will most likely change to allogeneic or even autologous induced pluripotent stem (iPS) cells. Hayashi et al. have recently shown that iPS cells, when subjected to a 12-weeks differentiation protocol, grow into a structure that mimics whole-eye development (Hayashi et al., 2016). They extracted cells from the ectoderm zone developing the ocular surface and expanded them *ex vivo* to form a corneal epithelium to recov-

er function in an experimentally induced animal model of corneal blindness. It would require some modifications to this protocol to cultivate corneal endothelial cells, but within the next years this should lead to an infinite source for *in vitro* generated transplantable CECs.

Combination of the cell injection method and iPS cell-generated CECs offers advantages: injecting endothelial cell suspensions is minimally invasive and does not compromise the eye's immune privilege, as compared to transplantation of the whole cornea or even only a Descemet layer with cells. For their pump function, CECs do not need to establish complex interactions with neighbouring cells. *In vitro* generated cells can not only be stocked but also tailored to specific needs of the patient, such as HLA compatibility, to further minimize rejection. This will lead to a revolution in eye banking and corneal transplantation.

For the RPE, induction of regeneration *in situ* by gene transfer has a brighter future. Human ES or iPS cell based differentiation strategies for the RPE are even more advanced than for CEC (Ali and Sowden, 2011; Eiraku et al., 2011), and clinical trials for RPE transplantation are ongoing (Cyranoski, 2013; Kamao et al., 2014; Song et al., 2013). However, while corneal endothelial transplantation, even in form of a suspension of CECs only, restores natural anatomy and function within a day from a completely dysfunctional or absent endothelium, this is not so likely to be achieved when transplanting RPE cells. RPE is not a simple monolayer; it closely interacts with photoreceptors also through its unique anatomy by forming long microvilli and a complex interphotoreceptor matrix. Regeneration of these complex structures from transplanted cells will not occur as easily and quickly as in the endothelium, especially in areas of dysfunctional or absent RPE and photoreceptor cells, as would be the case in advanced AMD.

Even on the verge of photoreceptor or whole retina transplantation, AMD patients most likely would benefit from treatment at an earlier stage of disease when vast damage can still be avoided. Here, stem cell transplantation might seem too invasive. Instead, a far less invasive *in*

situ regenerative approach harnessing the RPE's natural regenerative potential, possibly by gene therapy, would be favoured.

Interestingly, as this manuscript was concluded, the first therapy for *in vivo, in situ* regeneration in the human eye was published. Lin et al. report regeneration of the human lens from endogenous lens epithelial stem/progenitor cells (Lin et al., 2016). This was achieved in infants receiving cataract surgery. A clear lens regrew from residual stem cells within 3 months *in situ*, i.e. inside the capsular bag, in both eyes of all 12 patients. Further understanding of ocular development and identification of near-stem cell like cells might eventually lead to *in situ* regeneration for every tissue of the eye. This demonstrates that *in situ* regeneration of existing cells is a valuable addition to transplantation, and the potential of this approach is just beginning to be explored.

8. References

1. Ach, T., Huisinigh, C., McGwin, G., Jr., Messinger, J.D., Zhang, T., Bentley, M.J., Gutierrez, D.B., Ablonczy, Z., Smith, R.T., Sloan, K.R., Curcio, C.A., 2014. Quantitative autofluorescence and cell density maps of the human retinal pigment epithelium. *Invest Ophthalmol Vis Sci* 55, 4832-4841.
2. Adams, T., Shahabi, G., Hoh-Kam, J., Jeffery, G., 2010. Held under arrest: Many mature albino RPE cells display polyploid features consistent with abnormal cell cycle retention. *Exp Eye Res* 90, 368-372.
3. Agarwal, M.L., Agarwal, A., Taylor, W.R., Chernova, O., Sharma, Y., Stark, G.R., 1998. A p53-dependent S-phase checkpoint helps to protect cells from DNA damage in response to starvation for pyrimidine nucleotides. *Proceedings of the National Academy of Sciences of the United States of America* 95, 14775-14780.
4. Aisenbrey, S., Lafaut, B.A., Szurman, P., Grisanti, S., Luke, C., Krott, R., Thumann, G., Fricke, J., Neugebauer, A., Hilgers, R.D., Esser, P., Walter, P., Bartz-Schmidt, K.U., 2002. Macular translocation with 360 degrees retinotomy for exudative age-related macular degeneration. *Arch Ophthalmol* 120, 451-459.
5. Aisenbrey, S., Lafaut, B.A., Szurman, P., Hilgers, R.D., Esser, P., Walter, P., Bartz-Schmidt, K.U., Thumann, G., 2006. Iris pigment epithelial translocation in the treatment of exudative macular degeneration: a 3-year follow-up. *Arch Ophthalmol* 124, 183-188.
6. Aiuti, A., Cattaneo, F., Galimberti, S., Benninghoff, U., Cassani, B., Callegaro, L., Scaramuzza, S., Andolfi, G., Mirolo, M., Brigida, I., Tabucchi, A., Carlucchi, F., Eibl, M., Aker, M., Slavin, S., Al-Mousa, H., Al, G.A., Ferster, A., Duppenhaler, A., Notarangelo, L., Wintergerst, U., Buckley, R.H., Bregni, M., Markt, S., Valsecchi, M.G., Rossi, P., Ciceri, F., Miniero, R., Bordignon, C., Roncarolo, M.G., 2009. Gene therapy for immunodeficiency due to adenosine deaminase deficiency. *N.Engl.J.Med.* 360, 447-458.
7. Akkina, R.K., Walton, R.M., Chen, M.L., Li, Q.X., Planelles, V., Chen, I.S., 1996. High-efficiency gene transfer into CD34+ cells with a human immunodeficiency virus type 1-based retroviral vector pseudotyped with vesicular stomatitis virus envelope glycoprotein G. *J Virol* 70, 2581-2585.
8. Al Hussaini, H., Kam, J.H., Vugler, A., Semo, M., Jeffery, G., 2008. Mature retinal pigment epithelium cells are retained in the cell cycle and proliferate in vivo. *Mol.Vis.* 14, 1784-1791.
9. Alba, R., Bosch, A., Chillon, M., 2005. Gutless adenovirus: last-generation adenovirus for gene therapy. *Gene therapy* 12 Suppl 1, S18-27.
10. Albert, D.M., Tso, M.O., Rabson, A.S., 1972. In vitro growth of pure cultures of retinal pigment epithelium. *Arch Ophthalmol* 88, 63-69.

11. Albon, J., Tullo, A.B., Aktar, S., Boulton, M.E., 2000. Apoptosis in the endothelium of human corneas for transplantation. *Invest Ophthalmol Vis.Sci.* 41, 2887-2893.
12. Algvare, P.V., Berglin, L., Gouras, P., Sheng, Y., 1994. Transplantation of fetal retinal pigment epithelium in age-related macular degeneration with subfoveal neovascularization. *Graefes Arch Clin Exp Ophthalmol* 232, 707-716.
13. Algvare, P.V., Gouras, P., Dafgard Kopp, E., 1999. Long-term outcome of RPE allografts in non-immunosuppressed patients with AMD. *European journal of ophthalmology* 9, 217-230.
14. Ali, R.R., Sowden, J.C., 2011. Regenerative medicine: DIY eye. *Nature* 472, 42-43.
15. Amann, J., Holley, G.P., Lee, S.B., Edelhauser, H.F., 2003. Increased endothelial cell density in the paracentral and peripheral regions of the human cornea. *American journal of ophthalmology* 135, 584-590.
16. Anderson, D.H., Stern, W.H., Fisher, S.K., Erickson, P.A., Borgula, G.A., 1981. The onset of pigment epithelial proliferation after retinal detachment. *Invest Ophthalmol Vis Sci* 21, 10-16.
17. Andrews, J.L., Kadan, M.J., Gorziglia, M.I., Kaleko, M., Connelly, S., 2001. Generation and characterization of E1/E2a/E3/E4-deficient adenoviral vectors encoding human factor VIII. *Mol Ther* 3, 329-336.
18. Anshu, A., Price, M.O., Price, F.W., Jr., 2012a. Risk of corneal transplant rejection significantly reduced with Descemet's membrane endothelial keratoplasty. *Ophthalmology* 119, 536-540.
19. Anshu, A., Price, M.O., Tan, D.T., Price, F.W., Jr., 2012b. Endothelial keratoplasty: a revolution in evolution. *Survey of ophthalmology* 57, 236-252.
20. AppliedBiosystems, 2008. Guide to Performing Relative Quantitation of Gene Expression Using Real-Time Quantitative PCR. *Applied Biosystems Application Notes* 4371095 Rev B, 56-59.
21. Araki-Sasaki, K., Danjo, S., Kawaguchi, S., Hosohata, J., Tano, Y., 1997. Human hepatocyte growth factor (HGF) in the aqueous humor. *Jpn.J.Ophthalmol* 41, 409-413.
22. Arellano, M., Moreno, S., 1997. Regulation of CDK/cyclin complexes during the cell cycle. *The international journal of biochemistry & cell biology* 29, 559-573.
23. Armitage, W.J., 2011. Preservation of Human Cornea. *Transfus Med Hemother* 38, 143-147.
24. Armitage, W.J., Dick, A.D., Bourne, W.M., 2003. Predicting endothelial cell loss and long-term corneal graft survival. *Invest Ophthalmol Vis Sci* 44, 3326-3331.
25. Armitage, W.J., Easty, D.L., 1997. Factors influencing the suitability of organ-cultured corneas for transplantation. *Invest Ophthalmol Vis.Sci.* 38, 16-24.
26. Arnold, D.R., Moshayedi, P., Schoen, T.J., Jones, B.E., Chader, G.J., Waldbillig, R.J., 1993. Distribution of IGF-I and -II, IGF binding proteins (IGFBPs) and IGFBP mRNA in ocular

- fluids and tissues: potential sites of synthesis of IGFBPs in aqueous and vitreous. *Exp Eye Res.* 56, 555-565.
27. Auricchio, A., 2003. Pseudotyped AAV vectors for constitutive and regulated gene expression in the eye. *Vision Res.* 43, 913-918.
 28. Bainbridge, J.W., Ali, R.R., 2008. Success in sight: The eyes have it! Ocular gene therapy trials for LCA look promising. *Gene Ther.* 15, 1191-1192.
 29. Bainbridge, J.W., Smith, A.J., Barker, S.S., Robbie, S., Henderson, R., Balaggan, K., Viswanathan, A., Holder, G.E., Stockman, A., Tyler, N., Petersen-Jones, S., Bhattacharya, S.S., Thrasher, A.J., Fitzke, F.W., Carter, B.J., Rubin, G.S., Moore, A.T., Ali, R.R., 2008. Effect of gene therapy on visual function in Leber's congenital amaurosis. *N.Engl.J.Med.* 358, 2231-2239.
 30. Bainbridge, J.W., Stephens, C., Parsley, K., Demaison, C., Halfyard, A., Thrasher, A.J., Ali, R.R., 2001. In vivo gene transfer to the mouse eye using an HIV-based lentiviral vector; efficient long-term transduction of corneal endothelium and retinal pigment epithelium. *Gene Ther.* 8, 1665-1668.
 31. Balaggan, K.S., Binley, K., Esapa, M., Iqball, S., Askham, Z., Kan, O., Tschernutter, M., Bainbridge, J.W., Naylor, S., Ali, R.R., 2006. Stable and efficient intraocular gene transfer using pseudotyped EIAV lentiviral vectors. *J.Gene Med.* 8, 275-285.
 32. Balda, M.S., Garrett, M.D., Matter, K., 2003. The ZO-1-associated Y-box factor ZONAB regulates epithelial cell proliferation and cell density. *J.Cell Biol.* 160, 423-432.
 33. Balda, M.S., Matter, K., 2000. The tight junction protein ZO-1 and an interacting transcription factor regulate ErbB-2 expression. *EMBO J.* 19, 2024-2033.
 34. Barbeau, D., Marcellus, R.C., Bacchetti, S., Bayley, S.T., Branton, P.E., 1992. Quantitative analysis of regions of adenovirus E1A products involved in interactions with cellular proteins. *Biochemistry and cell biology = Biochimie et biologie cellulaire* 70, 1123-1134.
 35. Barcia, R.N., Dana, M.R., Kazlauskas, A., 2007. Corneal graft rejection is accompanied by apoptosis of the endothelium and is prevented by gene therapy with bcl-xL. *Am.J.Transplant.* 7, 2082-2089.
 36. Barker, S.E., Broderick, C.A., Robbie, S.J., Duran, Y., Natkunarajah, M., Buch, P., Balaggan, K.S., MacLaren, R.E., Bainbridge, J.W., Smith, A.J., Ali, R.R., 2009. Subretinal delivery of adeno-associated virus serotype 2 results in minimal immune responses that allow repeat vector administration in immunocompetent mice. *J.Gene Med.* 11, 486-497.
 37. Basche, M.D., 2014. Gene Therapy Approaches to Disease of the Cornea and Anterior Chamber, Department of Genetics, Institute of Ophthalmology. University College London, London.
 38. Batten, M.L., Imanishi, Y., Tu, D.C., Doan, T., Zhu, L., Pang, J., Glushakova, L., Moise, A.R., Baehr, W., Van Gelder, R.N., Hauswirth, W.W., Rieke, F., Palczewski, K., 2005. Pharmacological and rAAV gene therapy rescue of visual functions in a blind mouse model of Leber congenital amaurosis. *PLoS medicine* 2, e333.

39. Bauer, S., Patterson, P.H., 2005. The cell cycle-apoptosis connection revisited in the adult brain. *The Journal of cell biology* 171, 641-650.
40. Baum, J.L., Niedra, R., Davis, C., Yue, B.Y., 1979. Mass culture of human corneal endothelial cells. *Arch Ophthalmol* 97, 1136-1140.
41. Bednarz, J., Teifel, M., Friedl, P., Engelmann, K., 2000. Immortalization of human corneal endothelial cells using electroporation protocol optimized for human corneal endothelial and human retinal pigment epithelial cells. *Acta ophthalmologica Scandinavica* 78, 130-136.
42. Bell, K.D., Campbell, R.J., Bourne, W.M., 2000. Pathology of late endothelial failure: late endothelial failure of penetrating keratoplasty: study with light and electron microscopy. *Cornea* 19, 40-46.
43. Bennett, J., 2003. Immune response following intraocular delivery of recombinant viral vectors. *Gene Ther.* 10, 977-982.
44. Bennett, J., Ashtari, M., Wellman, J., Marshall, K.A., Cyckowski, L.L., Chung, D.C., McCague, S., Pierce, E.A., Chen, Y., Bennicelli, J.L., Zhu, X., Ying, G.S., Sun, J., Wright, J.F., Auricchio, A., Simonelli, F., Shindler, K.S., Mingozzi, F., High, K.A., Maguire, A.M., 2012. AAV2 gene therapy readministration in three adults with congenital blindness. *Science translational medicine* 4, 120ra115.
45. Berk, A.J., 2005. Recent lessons in gene expression, cell cycle control, and cell biology from adenovirus. *Oncogene* 24, 7673-7685.
46. Bertelmann, E., Ritter, T., Vogt, K., Reszka, R., Hartmann, C., Pleyer, U., 2003. Efficiency of cytokine gene transfer in corneal endothelial cells and organ-cultured corneas mediated by liposomal vehicles and recombinant adenovirus. *Ophthalmic Res.* 35, 117-124.
47. Beutelspacher, S.C., Ardjomand, N., Tan, P.H., Patton, G.S., Larkin, D.F., George, A.J., McClure, M.O., 2005. Comparison of HIV-1 and EIAV-based lentiviral vectors in corneal transduction. *Exp.Eye Res.* 80, 787-794.
48. Beutelspacher, S.C., Pillai, R., Watson, M.P., Tan, P.H., Tsang, J., McClure, M.O., George, A.J., Larkin, D.F., 2006. Function of indoleamine 2,3-dioxygenase in corneal allograft rejection and prolongation of allograft survival by over-expression. *Eur.J.Immunol.* 36, 690-700.
49. Binder, S., Krebs, I., Hilgers, R.D., Abri, A., Stolba, U., Assadoulina, A., Kellner, L., Stanzel, B.V., Jahn, C., Feichtinger, H., 2004. Outcome of transplantation of autologous retinal pigment epithelium in age-related macular degeneration: a prospective trial. *Invest Ophthalmol Vis Sci* 45, 4151-4160.
50. Binder, S., Stanzel, B.V., Krebs, I., Glittenberg, C., 2007. Transplantation of the RPE in AMD. *Progress in retinal and eye research* 26, 516-554.
51. Biswas, S., Munier, F.L., Yardley, J., Hart-Holden, N., Perveen, R., Cousin, P., Sutphin, J.E., Noble, B., Batterbury, M., Kielty, C., Hackett, A., Bonshek, R., Ridgway, A., McLeod, D., Sheffield, V.C., Stone, E.M., Schorderet, D.F., Black, G.C., 2001. Missense mutations in COL8A2, the gene encoding the alpha2 chain of type VIII collagen, cause two forms of corneal endothelial dystrophy. *Hum.Mol.Genet.* 10, 2415-2423.

52. Blaese, R.M., Culver, K.W., Miller, A.D., Carter, C.S., Fleisher, T., Clerici, M., Shearer, G., Chang, L., Chiang, Y., Tolstoshev, P., Greenblatt, J.J., Rosenberg, S.A., Klein, H., Berger, M., Mullen, C.A., Ramsey, W.J., Muul, L., Morgan, R.A., Anderson, W.F., 1995. T lymphocyte-directed gene therapy for ADA- SCID: initial trial results after 4 years. *Science* 270, 475-480.
53. Blair-Parks, K., Weston, B.C., Dean, D.A., 2002. High-level gene transfer to the cornea using electroporation. *J.Gene Med.* 4, 92-100.
54. Blake, D.A., Yu, H., Young, D.L., Caldwell, D.R., 1997. Matrix stimulates the proliferation of human corneal endothelial cells in culture. *Invest Ophthalmol Vis Sci* 38, 1119-1129.
55. Blake, M.C., Azizkhan, J.C., 1989. Transcription factor E2F is required for efficient expression of the hamster dihydrofolate reductase gene in vitro and in vivo. *Molecular and cellular biology* 9, 4994-5002.
56. Bonilha, V.L., 2013. Retinal pigment epithelium (RPE) cytoskeleton in vivo and in vitro. *Exp Eye Res.*
57. Booij, J.C., Baas, D.C., Beisekeeva, J., Gorgels, T.G., Bergen, A.A., 2010. The dynamic nature of Bruch's membrane. *Progress in retinal and eye research* 29, 1-18.
58. Boonstra, J., 2003. Progression through the G1-phase of the on-going cell cycle. *Journal of cellular biochemistry* 90, 244-252.
59. Boulton, M., Dayhaw-Barker, P., 2001. The role of the retinal pigment epithelium: topographical variation and ageing changes. *Eye (Lond)* 15, 384-389.
60. Bourne, W.M., 1998. Clinical estimation of corneal endothelial pump function. *Trans.Am.Ophthalmol.Soc.* 96, 229-239.
61. Bourne, W.M., 2001. Cellular changes in transplanted human corneas. *Cornea* 20, 560-569.
62. Bourne, W.M., Hodge, D.O., Nelson, L.R., 1994a. Corneal endothelium five years after transplantation. *Am.J.Ophthalmol.* 118, 185-196.
63. Bourne, W.M., McLaren, J.W., 2004. Clinical responses of the corneal endothelium. *Exp.Eye Res.* 78, 561-572.
64. Bourne, W.M., Nelson, L.R., Hodge, D.O., 1994b. Continued endothelial cell loss ten years after lens implantation. *Ophthalmology* 101, 1014-1022.
65. Bourne, W.M., Nelson, L.R., Hodge, D.O., 1997. Central corneal endothelial cell changes over a ten-year period. *Invest Ophthalmol.Vis.Sci.* 38, 779-782.
66. Bourne, W.M., O'Fallon, W.M., 1978. Endothelial cell loss during penetrating keratoplasty. *Am.J.Ophthalmol* 85, 760-766.
67. Braithwaite, A.W., Cheetham, B.F., Li, P., Parish, C.R., Waldron-Stevens, L.K., Bellett, A.J., 1983. Adenovirus-induced alterations of the cell growth cycle: a requirement for expression of E1A but not of E1B. *J Virol* 45, 192-199.

68. Brown, D.M., Michels, M., Kaiser, P.K., Heier, J.S., Sy, J.P., Ianchulev, T., Group, A.S., 2009. Ranibizumab versus verteporfin photodynamic therapy for neovascular age-related macular degeneration: Two-year results of the ANCHOR study. *Ophthalmology* 116, 57-65 e55.
69. Buch, P.K., Bainbridge, J.W., Ali, R.R., 2008. AAV-mediated gene therapy for retinal disorders: from mouse to man. *Gene Ther.* 15, 849-857.
70. Budenz, D.L., Bennett, J., Alonso, L., Maguire, A., 1995. In vivo gene transfer into murine corneal endothelial and trabecular meshwork cells. *Invest Ophthalmol Vis.Sci.* 36, 2211-2215.
71. Builles, N., Kodjikian, L., Burillon, C., Damour, O., 2006. Major endothelial loss from corneas in organ culture: importance of second endothelial count. *Cornea* 25, 815-820.
72. Büning, H., Perabo, L., Coutelle, O., Quadt-Humme, S., Hallek, M., 2008. Recent developments in adeno-associated virus vector technology. *J.Gene Med.* 10, 717-733.
73. Busser, J., Geldmacher, D.S., Herrup, K., 1998. Ectopic cell cycle proteins predict the sites of neuronal cell death in Alzheimer's disease brain. *The Journal of neuroscience : the official journal of the Society for Neuroscience* 18, 2801-2807.
74. Cai, H., Shin, M.C., Tezel, T.H., Kaplan, H.J., Del Priore, L.V., 2006. Use of iris pigment epithelium to replace retinal pigment epithelium in age-related macular degeneration: a gene expression analysis. *Arch Ophthalmol* 124, 1276-1285.
75. Cameron, H.A., McKay, R.D., 2001. Adult neurogenesis produces a large pool of new granule cells in the dentate gyrus. *The Journal of comparative neurology* 435, 406-417.
76. Campisi, J., Morreo, G., Pardee, A.B., 1984. Kinetics of G1 transit following brief starvation for serum factors. *Experimental cell research* 152, 459-466.
77. Campochiaro, P.A., Nguyen, Q.D., Shah, S.M., Klein, M.L., Holz, E., Frank, R.N., Saperstein, D.A., Gupta, A., Stout, J.T., Macko, J., DiBartolomeo, R., Wei, L.L., 2006. Adenoviral vector-delivered pigment epithelium-derived factor for neovascular age-related macular degeneration: results of a phase I clinical trial. *Hum.Gene Ther.* 17, 167-176.
78. Cante-Barrett, K., Mendes, R.D., Smits, W.K., van Helsdingen-van Wijk, Y.M., Pieters, R., Meijerink, J.P., 2016. Lentiviral gene transfer into human and murine hematopoietic stem cells: size matters. *BMC research notes* 9, 312.
79. Cartier, N., Hacein-Bey-Abina, S., Bartholomae, C.C., Veres, G., Schmidt, M., Kutschera, I., Vidaud, M., Abel, U., Dal-Cortivo, L., Caccavelli, L., Mahlaoui, N., Kiermer, V., Mittelstaedt, D., Bellesme, C., Lahlou, N., Lefrere, F., Blanche, S., Audit, M., Payen, E., Leboulch, P., l'Homme, B., Bougneres, P., Von, K.C., Fischer, A., Cavazzana-Calvo, M., Aubourg, P., 2009. Hematopoietic stem cell gene therapy with a lentiviral vector in X-linked adrenoleukodystrophy. *Science* 326, 818-823.
80. Castedo, M., Perfettini, J.L., Roumier, T., Andreau, K., Medema, R., Kroemer, G., 2004. Cell death by mitotic catastrophe: a molecular definition. *Oncogene* 23, 2825-2837.

81. Catt Research Group, Martin, D.F., Maguire, M.G., Ying, G.S., Grunwald, J.E., Fine, S.L., Jaffe, G.J., 2011. Ranibizumab and bevacizumab for neovascular age-related macular degeneration. *The New England journal of medicine* 364, 1897-1908.
82. Cavazzana-Calvo, M., Hacein-Bey, S., de Saint, B.G., Gross, F., Yvon, E., Nusbaum, P., Selz, F., Hue, C., Certain, S., Casanova, J.L., Bouso, P., Deist, F.L., Fischer, A., 2000. Gene therapy of human severe combined immunodeficiency (SCID)-X1 disease. *Science* 288, 669-672.
83. Cavazzana-Calvo, M., Payen, E., Negre, O., Wang, G., Hehir, K., Fusil, F., Down, J., Denaro, M., Brady, T., Westerman, K., Cavallesco, R., Gillet-Legrand, B., Caccavelli, L., Sgarra, R., Maouche-Chretien, L., Bernaudin, F., Girot, R., Dorazio, R., Mulder, G.J., Polack, A., Bank, A., Soulier, J., Larghero, J., Kabbara, N., Dalle, B., Gourmel, B., Socie, G., Chretien, S., Cartier, N., Aubourg, P., Fischer, A., Cornetta, K., Galacteros, F., Beuzard, Y., Gluckman, E., Bushman, F., Hacein-Bey-Abina, S., Leboulch, P., 2010. Transfusion independence and HMGA2 activation after gene therapy of human beta-thalassaemia. *Nature* 467, 318-322.
84. Challa, P., Luna, C., Liton, P.B., Chamblin, B., Wakefield, J., Ramabhadran, R., Epstein, D.L., Gonzalez, P., 2005. Lentiviral mediated gene delivery to the anterior chamber of rodent eyes. *Mol.Vis.* 11, 425-430.
85. Charbel Issa, P., MacLaren, R.E., 2012. Non-viral retinal gene therapy: a review. *Clinical & experimental ophthalmology* 40, 39-47.
86. Chen, F.K., Patel, P.J., Uppal, G.S., Tufail, A., Coffey, P.J., Da Cruz, L., 2010. Long-term outcomes following full macular translocation surgery in neovascular age-related macular degeneration. *The British journal of ophthalmology* 94, 1337-1343.
87. Chen, K.H., Azar, D., Joyce, N.C., 2001. Transplantation of adult human corneal endothelium ex vivo: a morphologic study. *Cornea* 20, 731-737.
88. Chen, K.H., Harris, D.L., Joyce, N.C., 1999. TGF-beta2 in aqueous humor suppresses S-phase entry in cultured corneal endothelial cells. *Invest Ophthalmol.Vis.Sci.* 40, 2513-2519.
89. Chen, Y., McPhie, D.L., Hirschberg, J., Neve, R.L., 2000. The amyloid precursor protein-binding protein APP-BP1 drives the cell cycle through the S-M checkpoint and causes apoptosis in neurons. *The Journal of biological chemistry* 275, 8929-8935.
90. Chen, Z.Y., He, C.Y., Meuse, L., Kay, M.A., 2004. Silencing of episomal transgene expression by plasmid bacterial DNA elements in vivo. *Gene therapy* 11, 856-864.
91. Chevez-Barrios, P., Chintagumpala, M., Mieler, W., Paysse, E., Boniuk, M., Kozinetz, C., Hurwitz, M.Y., Hurwitz, R.L., 2005. Response of retinoblastoma with vitreous tumor seeding to adenovirus-mediated delivery of thymidine kinase followed by ganciclovir. *Journal of clinical oncology : official journal of the American Society of Clinical Oncology* 23, 7927-7935.
92. Chng, Z., Peh, G.S., Herath, W.B., Cheng, T.Y., Ang, H.P., Toh, K.P., Robson, P., Mehta, J.S., Colman, A., 2013. High throughput gene expression analysis identifies reliable expression markers of human corneal endothelial cells. *PloS one* 8, e67546.
93. Cho, K.S., Lee, E.H., Choi, J.S., Joo, C.K., 1999. Reactive oxygen species-induced apoptosis and necrosis in bovine corneal endothelial cells. *Invest Ophthalmol.Vis.Sci.* 40, 911-919.

94. Cicero, S.A., Johnson, D., Reyntjens, S., Frase, S., Connell, S., Chow, L.M., Baker, S.J., Sorrentino, B.P., Dyer, M.A., 2009. Cells previously identified as retinal stem cells are pigmented ciliary epithelial cells. *Proceedings of the National Academy of Sciences of the United States of America* 106, 6685-6690.
95. Cockrell, A.S., Kafri, T., 2003. HIV-1 vectors: fulfillment of expectations, further advancements, and still a way to go. *Current HIV research* 1, 419-439.
96. Cockrell, A.S., Kafri, T., 2007. Gene delivery by lentivirus vectors. *Molecular biotechnology* 36, 184-204.
97. Collins, L., Fabre, J.W., 2004. A synthetic peptide vector system for optimal gene delivery to corneal endothelium. *J.Gene Med.* 6, 185-194.
98. Comer, R.M., King, W.J., Ardjomand, N., Theoharis, S., George, A.J., Larkin, D.F., 2002. Effect of administration of CTLA4-Ig as protein or cDNA on corneal allograft survival. *Invest Ophthalmol.Vis.Sci.* 43, 1095-1103.
99. Counsell, J.R., Asgarian, Z., Meng, J., Ferrer, V., Vink, C.A., Howe, S.J., Waddington, S.N., Thrasher, A.J., Muntoni, F., Morgan, J.E., Danos, O., 2017. Lentiviral vectors can be used for full-length dystrophin gene therapy. *Sci Rep* 7, 44775.
100. Crewe, J.M., Armitage, W.J., 2001. Integrity of epithelium and endothelium in organ-cultured human corneas. *Invest Ophthalmol Vis Sci* 42, 1757-1761.
101. Cyranoski, D., 2013. Stem cells cruise to clinic. *Nature* 494, 413.
102. da Cruz, L., Chen, F.K., Ahmado, A., Greenwood, J., Coffey, P., 2007. RPE transplantation and its role in retinal disease. *Progress in retinal and eye research* 26, 598-635.
103. Dalkara, D., Byrne, L.C., Klimczak, R.R., Visel, M., Yin, L., Merigan, W.H., Flannery, J.G., Schaffer, D.V., 2013. In vivo-directed evolution of a new adeno-associated virus for therapeutic outer retinal gene delivery from the vitreous. *Science translational medicine* 5, 189ra176.
104. Dalkara, D., Kolstad, K.D., Caporale, N., Visel, M., Klimczak, R.R., Schaffer, D.V., Flannery, J.G., 2009. Inner limiting membrane barriers to AAV-mediated retinal transduction from the vitreous. *Mol Ther* 17, 2096-2102.
105. Dart, J.K., El-Amir, A.N., Maddison, T., Desai, P., Verma, S., Hughes, A., MacMahon, E., 2009. Identification and control of nosocomial adenovirus keratoconjunctivitis in an ophthalmic department. *The British journal of ophthalmology* 93, 18-20.
106. Davidson, A.E., Liskova, P., Evans, C.J., Dudakova, L., Noskova, L., Pontikos, N., Hartmannova, H., Hodanova, K., Stranecky, V., Kozmik, Z., Levis, H.J., Idigo, N., Sasai, N., Maher, G.J., Bellingham, J., Veli, N., Ebenezer, N.D., Cheetham, M.E., Daniels, J.T., Thaung, C.M., Jirsova, K., Plagnol, V., Filipec, M., Kmoch, S., Tuft, S.J., Hardcastle, A.J., 2016. Autosomal-Dominant Corneal Endothelial Dystrophies CHED1 and PPCD1 Are Allelic Disorders Caused by Non-coding Mutations in the Promoter of OVOL2. *American journal of human genetics* 98, 75-89.
107. DeGregori, J., Leone, G., Miron, A., Jakoi, L., Nevins, J.R., 1997. Distinct roles for E2F proteins in cell growth control and apoptosis. *Proc.Natl.Acad.Sci.U.S.A* 94, 7245-7250.

108. DeGregori, J., Leone, G., Ohtani, K., Miron, A., Nevins, J.R., 1995. E2F-1 accumulation bypasses a G1 arrest resulting from the inhibition of G1 cyclin-dependent kinase activity. *Genes Dev.* 9, 2873-2887.
109. Del Priore, L.V., Kuo, Y.H., Tezel, T.H., 2002. Age-related changes in human RPE cell density and apoptosis proportion in situ. *Invest Ophthalmol Vis Sci* 43, 3312-3318.
110. Delenda, C., 2004. Lentiviral vectors: optimization of packaging, transduction and gene expression. *The journal of gene medicine* 6 Suppl 1, S125-138.
111. Delori, F.C., Fleckner, M.R., Goger, D.G., Weiter, J.J., Dorey, C.K., 2000. Autofluorescence distribution associated with drusen in age-related macular degeneration. *Invest Ophthalmol Vis Sci* 41, 496-504.
112. Delori, F.C., Goger, D.G., Dorey, C.K., 2001. Age-related accumulation and spatial distribution of lipofuscin in RPE of normal subjects. *Invest Ophthalmol Vis Sci* 42, 1855-1866.
113. Demaison, C., Parsley, K., Brouns, G., Scherr, M., Battmer, K., Kinnon, C., Grez, M., Thrasher, A.J., 2002. High-level transduction and gene expression in hematopoietic repopulating cells using a human immunodeficiency [correction of imunodeficiency] virus type 1-based lentiviral vector containing an internal spleen focus forming virus promoter. *Human gene therapy* 13, 803-813.
114. den Hollander, A.I., Roepman, R., Koenekoop, R.K., Cremers, F.P., 2008. Leber congenital amaurosis: genes, proteins and disease mechanisms. *Progress in retinal and eye research* 27, 391-419.
115. Dikstein, S., Maurice, D.M., 1972. The metabolic basis to the fluid pump in the cornea. *J.Physiol* 221, 29-41.
116. Dimova, D.K., Dyson, N.J., 2005. The E2F transcriptional network: old acquaintances with new faces. *Oncogene* 24, 2810-2826.
117. Dintelmann, T.S., Heimann, K., Kayatz, P., Schraermeyer, U., 1999. Comparative study of ROS degradation by IPE and RPE cells in vitro. *Graefes Arch Clin Exp Ophthalmol* 237, 830-839.
118. Dong, J.Y., Fan, P.D., Frizzell, R.A., 1996. Quantitative analysis of the packaging capacity of recombinant adeno-associated virus. *Human gene therapy* 7, 2101-2112.
119. Dorey, C.K., Wu, G., Ebenstein, D., Garsd, A., Weiter, J.J., 1989. Cell loss in the aging retina. Relationship to lipofuscin accumulation and macular degeneration. *Invest Ophthalmol Vis Sci* 30, 1691-1699.
120. Dull, T., Zufferey, R., Kelly, M., Mandel, R.J., Nguyen, M., Trono, D., Naldini, L., 1998. A third-generation lentivirus vector with a conditional packaging system. *J Virol* 72, 8463-8471.
121. Dunn, K.C., Aotaki-Keen, A.E., Putkey, F.R., Hjelmeland, L.M., 1996. ARPE-19, a human retinal pigment epithelial cell line with differentiated properties. *Exp Eye Res* 62, 155-169.

122. Dyson, N., 1998. The regulation of E2F by pRB-family proteins. *Genes Dev.* 12, 2245-2262.
123. Eadie, B.D., Redila, V.A., Christie, B.R., 2005. Voluntary exercise alters the cytoarchitecture of the adult dentate gyrus by increasing cellular proliferation, dendritic complexity, and spine density. *The Journal of comparative neurology* 486, 39-47.
124. Eandi, C.M., Giansanti, F., Virgili, G., 2008. Macular translocation for neovascular age-related macular degeneration. *The Cochrane database of systematic reviews*, CD006928.
125. Edelhauser, H.F., 2000. The resiliency of the corneal endothelium to refractive and intraocular surgery. *Cornea* 19, 263-273.
126. Egan, C.A., Savre-Train, I., Shay, J.W., Wilson, S.E., Bourne, W.M., 1998. Analysis of telomere lengths in human corneal endothelial cells from donors of different ages. *Invest Ophthalmol Vis.Sci.* 39, 648-653.
127. Eiraku, M., Takata, N., Ishibashi, H., Kawada, M., Sakakura, E., Okuda, S., Sekiguchi, K., Adachi, T., Sasai, Y., 2011. Self-organizing optic-cup morphogenesis in three-dimensional culture. *Nature* 472, 51-56.
128. Engelmann, K., Bohnke, M., Friedl, P., 1988. Isolation and long-term cultivation of human corneal endothelial cells. *Invest Ophthalmol Vis.Sci.* 29, 1656-1662.
129. Engler, C., Kelliher, C., Wahlin, K.J., Speck, C.L., Jun, A.S., 2009. Comparison of non-viral methods to genetically modify and enrich populations of primary human corneal endothelial cells. *Mol.Vis.* 15, 629-637.
130. Evans, T., Rosenthal, E.T., Youngblom, J., Distel, D., Hunt, T., 1983. Cyclin: a protein specified by maternal mRNA in sea urchin eggs that is destroyed at each cleavage division. *Cell* 33, 389-396.
131. Eye Bank Association of America, 2014 Eye Banking Statistical Report. <http://restoresight.org/wp-content/uploads/2015/03/2014-Statistical-Report-FINAL.pdf>. Accessed 2016.
132. Farquhar, M.G., Palade, G.E., 1963. Junctional complexes in various epithelia. *The Journal of cell biology* 17, 375-412.
133. Faul, F., Erdfelder, E., Buchner, A., Lang, A.G., 2009. Statistical power analyses using G*Power 3.1: tests for correlation and regression analyses. *Behavior research methods* 41, 1149-1160.
134. Faul, F., Erdfelder, E., Lang, A.G., Buchner, A., 2007. G*Power 3: a flexible statistical power analysis program for the social, behavioral, and biomedical sciences. *Behavior research methods* 39, 175-191.
135. Phakic Intraocular Lenses - Clinical Topics for Ophthalmic Devices Panel Discussion. http://www.fda.gov/ohrms/dockets/ac/02/briefing/3883b2_clinical_topics_for_guidance_discussion.pdf. Accessed 19.02.2011.
136. Feeney, L., 1973. The phagolysosomal system of the pigment epithelium. A key to retinal disease. *Investigative ophthalmology* 12, 635-638.

137. Fehervari, Z., Rayner, S.A., Oral, H.B., George, A.J., Larkin, D.F., 1997. Gene transfer to ex vivo stored corneas. *Cornea* 16, 459-464.
138. Finnemann, S.C., 2003. Focal adhesion kinase signaling promotes phagocytosis of integrin-bound photoreceptors. *The EMBO journal* 22, 4143-4154.
139. Flood, M.T., Gouras, P., Kjeldbye, H., 1980. Growth characteristics and ultrastructure of human retinal pigment epithelium in vitro. *Invest Ophthalmol Vis Sci* 19, 1309-1320.
140. Flood, M.T., Haley, J.E., Gouras, P., 1984. Cellular aging of human retinal epithelium in vivo and in vitro. *Monographs in developmental biology* 17, 80-93.
141. Follenzi, A., Santambrogio, L., Annoni, A., 2007. Immune responses to lentiviral vectors. *Curr Gene Ther* 7, 306-315.
142. Friedman, D.S., O'Colmain, B.J., Munoz, B., Tomany, S.C., McCarty, C., de Jong, P.T., Nemesure, B., Mitchell, P., Kempen, J., Eye Diseases Prevalence Research, G., 2004. Prevalence of age-related macular degeneration in the United States. *Arch Ophthalmol* 122, 564-572.
143. Fuchs, E., 1910. Dystrophia epithelialis corneae. *Albrecht von Graefes Arch Klin Exp Ophthalmol* 76 478-508.
144. Fuchsluger, T.A., Jurkunas, U., Kazlauskas, A., Dana, R., 2011a. Anti-apoptotic gene therapy prolongs survival of corneal endothelial cells during storage. *Gene Ther*.
145. Fuchsluger, T.A., Jurkunas, U., Kazlauskas, A., Dana, R., 2011b. Corneal endothelial cells are protected from apoptosis by gene therapy. *Hum.Gene Ther.* 22, 549-558.
146. Fuchsluger, T.A., Jurkunas, U., Kazlauskas, A., Dana, R., 2011c. [Viral vectors for gene delivery to corneal endothelial cells]. *Klinische Monatsblätter für Augenheilkunde* 228, 498-503.
147. Gain, P., Jullienne, R., He, Z., Aldossary, M., Acquart, S., Cognasse, F., Thuret, G., 2016. Global Survey of Corneal Transplantation and Eye Banking. *JAMA Ophthalmol* 134, 167-173.
148. Galla, M., Schambach, A., Towers, G.J., Baum, C., 2008. Cellular restriction of retrovirus particle-mediated mRNA transfer. *J.Virol.* 82, 3069-3077.
149. Galla, M., Will, E., Kraunus, J., Chen, L., Baum, C., 2004. Retroviral pseudotransduction for targeted cell manipulation. *Mol.Cell* 16, 309-315.
150. Gaspar, H.B., Bjorkegren, E., Parsley, K., Gilmour, K.C., King, D., Sinclair, J., Zhang, F., Giannakopoulos, A., Adams, S., Fairbanks, L.D., Gaspar, J., Henderson, L., Xu-Bayford, J.H., Davies, E.G., Veys, P.A., Kinnon, C., Thrasher, A.J., 2006. Successful reconstitution of immunity in ADA-SCID by stem cell gene therapy following cessation of PEG-ADA and use of mild preconditioning. *Mol.Ther.* 14, 505-513.
151. Gehrs, K.M., Anderson, D.H., Johnson, L.V., Hageman, G.S., 2006. Age-related macular degeneration--emerging pathogenetic and therapeutic concepts. *Annals of medicine* 38, 450-471.

152. Georgiadis, A., Tschernutter, M., Bainbridge, J.W., Balaggan, K.S., Mowat, F., West, E.L., Munro, P.M., Thrasher, A.J., Matter, K., Balda, M.S., Ali, R.R., 2010. The tight junction associated signalling proteins ZO-1 and ZONAB regulate retinal pigment epithelium homeostasis in mice. *PLoS.One.* 5, e15730.
153. Ghosheh, F.R., Cremona, F., Ayres, B.D., Hammersmith, K.M., Cohen, E.J., Raber, I.M., Laibson, P.R., Rapuano, C.J., 2008a. Indications for penetrating keratoplasty and associated procedures, 2001-2005. *Eye Contact Lens* 34, 211-214.
154. Ghosheh, F.R., Cremona, F.A., Rapuano, C.J., Cohen, E.J., Ayres, B.D., Hammersmith, K.M., Raber, I.M., Laibson, P.R., 2008b. Trends in penetrating keratoplasty in the United States 1980-2005. *Int.Ophthalmol* 28, 147-153.
155. Goh, P.Y., Lim, H.H., Surana, U., 2000. Cdc20 protein contains a destruction-box but, unlike Clb2, its proteolysis is not acutely dependent on the activity of anaphase-promoting complex. *European journal of biochemistry / FEBS* 267, 434-449.
156. Goidin, D., Mamessier, A., Staquet, M.J., Schmitt, D., Berthier-Vergnes, O., 2001. Ribosomal 18S RNA prevails over glyceraldehyde-3-phosphate dehydrogenase and beta-actin genes as internal standard for quantitative comparison of mRNA levels in invasive and noninvasive human melanoma cell subpopulations. *Analytical biochemistry* 295, 17-21.
157. Gong, N., Pleyer, U., Vogt, K., Anegon, I., Flugel, A., Volk, H.D., Ritter, T., 2007. Local overexpression of nerve growth factor in rat corneal transplants improves allograft survival. *Invest Ophthalmol Vis.Sci.* 48, 1043-1052.
158. Gorziglia, M.I., Lapcevich, C., Roy, S., Kang, Q., Kadan, M., Wu, V., Pechan, P., Kaleko, M., 1999. Generation of an adenovirus vector lacking E1, e2a, E3, and all of E4 except open reading frame 3. *J Virol* 73, 6048-6055.
159. Gottsch, J.D., Zhang, C., Sundin, O.H., Bell, W.R., Stark, W.J., Green, W.R., 2005. Fuchs corneal dystrophy: aberrant collagen distribution in an L450W mutant of the COL8A2 gene. *Invest Ophthalmol Vis Sci* 46, 4504-4511.
160. Gouras, P., Flood, M.T., Kjeldbye, H., Bilek, M.K., Eggers, H., 1985. Transplantation of cultured human retinal epithelium to Bruch's membrane of the owl monkey's eye. *Current eye research* 4, 253-265.
161. Gouras, P., Flood, M.T., Kjeldbye, H., 1984. Transplantation of cultured human retinal cells to monkey retina. *Anais da Academia Brasileira de Ciencias* 56, 431-443.
162. Gouras, P., Lopez, R., Kjeldbye, H., Sullivan, B., Brittis, M., 1989. Transplantation of retinal epithelium prevents photoreceptor degeneration in the RCS rat. *Progress in clinical and biological research* 314, 659-671.
163. Granstein, R.D., Staszewski, R., Knisely, T.L., Zeira, E., Nazareno, R., Latina, M., Albert, D.M., 1990. Aqueous humor contains transforming growth factor-beta and a small (less than 3500 daltons) inhibitor of thymocyte proliferation. *J Immunol* 144, 3021-3027.
164. Haberichter, T., Madge, B., Christopher, R.A., Yoshioka, N., Dhiman, A., Miller, R., Gendelman, R., Aksenov, S.V., Khalil, I.G., Dowdy, S.F., 2007. A systems biology dynamical model of mammalian G1 cell cycle progression. *Mol.Syst.Biol.* 3, 84.

165. Hacein-Bey, H., Cavazzana-Calvo, M., Le Deist, F., Dautry-Varsat, A., Hivroz, C., Riviere, I., Danos, O., Heard, J.M., Sugamura, K., Fischer, A., De Saint Basile, G., 1996. gamma-c gene transfer into SCID X1 patients' B-cell lines restores normal high-affinity interleukin-2 receptor expression and function. *Blood* 87, 3108-3116.
166. Hacein-Bey-Abina, S., Von Kalle, C., Schmidt, M., McCormack, M.P., Wulffraat, N., Leboulch, P., Lim, A., Osborne, C.S., Pawliuk, R., Morillon, E., Sorensen, R., Forster, A., Fraser, P., Cohen, J.I., de Saint Basile, G., Alexander, I., Wintergerst, U., Frebourg, T., Aurias, A., Stoppa-Lyonnet, D., Romana, S., Radford-Weiss, I., Gross, F., Valensi, F., Delabesse, E., Macintyre, E., Sigaux, F., Soulier, J., Leiva, L.E., Wissler, M., Prinz, C., Rabbitts, T.H., Le Deist, F., Fischer, A., Cavazzana-Calvo, M., 2003. LMO2-associated clonal T cell proliferation in two patients after gene therapy for SCID-X1. *Science* 302, 415-419.
167. Hageman, G.S., Luthert, P.J., Victor Chong, N.H., Johnson, L.V., Anderson, D.H., Mullins, R.F., 2001. An integrated hypothesis that considers drusen as biomarkers of immune-mediated processes at the RPE-Bruch's membrane interface in aging and age-related macular degeneration. *Progress in retinal and eye research* 20, 705-732.
168. Hamill, C.E., Schmedt, T., Jurkunas, U., 2013. Fuchs endothelial cornea dystrophy: a review of the genetics behind disease development. *Seminars in ophthalmology* 28, 281-286.
169. Hamuro, J., Toda, M., Asada, K., Hiraga, A., Schlotzer-Schrehardt, U., Montoya, M., Sotozono, C., Ueno, M., Kinoshita, S., 2016. Cell Homogeneity Indispensable for Regenerative Medicine by Cultured Human Corneal Endothelial Cells. *Invest Ophthalmol Vis Sci* 57, 4749-4761.
170. Harris, D.L., Joyce, N.C., 1999. Transforming growth factor-beta suppresses proliferation of rabbit corneal endothelial cells in vitro. *J.Interferon Cytokine Res.* 19, 327-334.
171. Hartman, Z.C., Appledorn, D.M., Amalfitano, A., 2008. Adenovirus vector induced innate immune responses: impact upon efficacy and toxicity in gene therapy and vaccine applications. *Virus Res.* 132, 1-14.
172. Hartman, Z.C., Black, E.P., Amalfitano, A., 2007. Adenoviral infection induces a multifaceted innate cellular immune response that is mediated by the toll-like receptor pathway in A549 cells. *Virology* 358, 357-372.
173. Hartwell, L.H., Szankasi, P., Roberts, C.J., Murray, A.W., Friend, S.H., 1997. Integrating genetic approaches into the discovery of anticancer drugs. *Science* 278, 1064-1068.
174. Hartwell, L.H., Weinert, T.A., 1989. Checkpoints: controls that ensure the order of cell cycle events. *Science* 246, 629-634.
175. Haruta, M., Sasai, Y., Kawasaki, H., Amemiya, K., Ooto, S., Kitada, M., Suemori, H., Nakatsuji, N., Ide, C., Honda, Y., Takahashi, M., 2004. In vitro and in vivo characterization of pigment epithelial cells differentiated from primate embryonic stem cells. *Invest Ophthalmol Vis Sci* 45, 1020-1025.
176. Hauswirth, W.W., Aleman, T.S., Kaushal, S., Cideciyan, A.V., Schwartz, S.B., Wang, L., Conlon, T.J., Boye, S.L., Flotte, T.R., Byrne, B.J., Jacobson, S.G., 2008. Treatment of leber congenital amaurosis due to RPE65 mutations by ocular subretinal injection of adeno-

- associated virus gene vector: short-term results of a phase I trial. *Hum.Gene Ther.* 19, 979-990.
177. Hayashi, R., Ishikawa, Y., Sasamoto, Y., Katori, R., Nomura, N., Ichikawa, T., Araki, S., Soma, T., Kawasaki, S., Sekiguchi, K., Quantock, A.J., Tsujikawa, M., Nishida, K., 2016. Co-ordinated ocular development from human iPS cells and recovery of corneal function. *Nature* 531, 376-380.
 178. He, Z., Campolmi, N., Gain, P., Ha Thi, B.M., Dumollard, J.M., Duband, S., Peoc'h, M., Piselli, S., Garraud, O., Thuret, G., 2012. Revisited microanatomy of the corneal endothelial periphery: new evidence for continuous centripetal migration of endothelial cells in humans. *Stem Cells* 30, 2523-2534.
 179. He, Z., Pipparelli, A., Manissolle, C., Acquart, S., Garraud, O., Gain, P., Thuret, G., 2010. Ex vivo gene electrotransfer to the endothelium of organ cultured human corneas. *Ophthalmic Res.* 43, 43-55.
 180. Heller, J.P., Martin, K.R., 2014. Enhancing RPE Cell-Based Therapy Outcomes for AMD: The Role of Bruch's Membrane. *Translational Vision Science & Technology* 3, 4.
 181. Heussen, F.M., Fawzy, N.F., Joeres, S., Lux, A., Maaijwee, K., Meurs, J.C., Kirchhof, B., Jousen, A.M., 2008. Autologous translocation of the choroid and RPE in age-related macular degeneration: 1-year follow-up in 30 patients and recommendations for patient selection. *Eye (Lond)* 22, 799-807.
 182. Hippert, C., Ibanes, S., Serratrice, N., Court, F., Malecaze, F., Kremer, E.J., Kalatzis, V., 2012. Corneal transduction by intra-stromal injection of AAV vectors in vivo in the mouse and ex vivo in human explants. *PloS one* 7, e35318.
 183. Hirsch, M., Faure, J.P., Marquet, O., Payrau, P., 1975. [Regeneration of corneal endothelium in the rabbit: microscopic study and relation with corneal thickness]. *Archives d'ophtalmologie et revue generale d'ophtalmologie* 35, 269-278.
 184. Hirst, L.W., Bancroft, J., Yamauchi, K., Green, W.R., 1995. Immunohistochemical pathology of the corneal endothelium in iridocorneal endothelial syndrome. *Invest Ophthalmol Vis Sci* 36, 820-827.
 185. Hiscott, P., Seitz, B., Schlotzer-Schrehardt, U., Naumann, G.O., 1997. Immunolocalisation of thrombospondin 1 in human, bovine and rabbit cornea. *Cell and tissue research* 289, 307-310.
 186. Hitani, K., Yokoo, S., Honda, N., Usui, T., Yamagami, S., Amano, S., 2008. Transplantation of a sheet of human corneal endothelial cell in a rabbit model. *Mol.Vis.* 14, 1-9.
 187. Hochegger, H., Takeda, S., Hunt, T., 2008. Cyclin-dependent kinases and cell-cycle transitions: does one fit all? *Nature reviews. Molecular cell biology* 9, 910-916.
 188. Hoffman, L.M., Maguire, A.M., Bennett, J., 1997. Cell-mediated immune response and stability of intraocular transgene expression after adenovirus-mediated delivery. *Invest Ophthalmol Vis.Sci.* 38, 2224-2233.

-
189. Hollingsworth, J., Perez-Gomez, I., Mutalib, H.A., Efron, N., 2001. A population study of the normal cornea using an in vivo, slit-scanning confocal microscope. *Optom.Vis.Sci.* 78, 706-711.
 190. Hollyfield, J.G., 1999. Hyaluronan and the functional organization of the interphotoreceptor matrix. *Invest Ophthalmol Vis Sci* 40, 2767-2769.
 191. Hollyfield, J.G., Witkovsky, P., 1974. Pigmented retinal epithelium involvement in photoreceptor development and function. *The Journal of experimental zoology* 189, 357-378.
 192. Honda, H., Ogita, Y., Higuchi, S., Kani, K., 1982. Cell movements in a living mammalian tissue: long-term observation of individual cells in wounded corneal endothelia of cats. *Journal of morphology* 174, 25-39.
 193. Howe, S.J., Mansour, M.R., Schwarzwaelder, K., Bartholomae, C., Hubank, M., Kempinski, H., Brugman, M.H., Pike-Overzet, K., Chatters, S.J., de Ridder, D., Gilmour, K.C., Adams, S., Thornhill, S.I., Parsley, K.L., Staal, F.J., Gale, R.E., Linch, D.C., Bayford, J., Brown, L., Quaye, M., Kinnon, C., Ancliff, P., Webb, D.K., Schmidt, M., von Kalle, C., Gaspar, H.B., Thrasher, A.J., 2008. Insertional mutagenesis combined with acquired somatic mutations causes leukemogenesis following gene therapy of SCID-X1 patients. *The Journal of clinical investigation* 118, 3143-3150.
 194. European Eye Bank Association, Technical guidelines for ocular tissue. <http://www.europeaneyebanks.org/article/Downloads/16>. Accessed 18/09/2011.
 195. Huang, P.T., Nelson, L.R., Bourne, W.M., 1989. The morphology and function of healing cat corneal endothelium. *Invest Ophthalmol.Vis.Sci.* 30, 1794-1801.
 196. Hudde, T., Comer, R.M., Kinsella, M.T., BATTERY, L., Luthert, P.J., Polak, J.M., George, A.J., Larkin, D.F., 2002. Modulation of hydrogen peroxide induced injury to corneal endothelium by virus mediated catalase gene transfer. *Br.J.Ophthalmol.* 86, 1058-1062.
 197. Hudde, T., Rayner, S.A., Comer, R.M., Weber, M., Isaacs, J.D., Waldmann, H., Larkin, D.F., George, A.J., 1999. Activated polyamidoamine dendrimers, a non-viral vector for gene transfer to the corneal endothelium. *Gene Ther.* 6, 939-943.
 198. Hudde, T., Rayner, S.A., De Alwis, M., Thrasher, A.J., Smith, J., Coffin, R.S., George, A.J., Larkin, D.F., 2000. Adeno-associated and herpes simplex viruses as vectors for gene transfer to the corneal endothelium. *Cornea* 19, 369-373.
 199. Igarashi, T., Miyake, K., Asakawa, N., Miyake, N., Shimada, T., Takahashi, H., 2013. Direct comparison of administration routes for AAV8-mediated ocular gene therapy. *Current eye research* 38, 569-577.
 200. Ing, J.J., Ing, H.H., Nelson, L.R., Hodge, D.O., Bourne, W.M., 1998. Ten-year postoperative results of penetrating keratoplasty. *Ophthalmology* 105, 1855-1865.
 201. Ishida, K., Panjwani, N., Cao, Z., Streilein, J.W., 2003. Participation of pigment epithelium in ocular immune privilege. 3. Epithelia cultured from iris, ciliary body, and retina suppress T-cell activation by partially non-overlapping mechanisms. *Ocular immunology and inflammation* 11, 91-105.

202. Ivan Study Investigators, Chakravarthy, U., Harding, S.P., Rogers, C.A., Downes, S.M., Lotery, A.J., Wordsworth, S., Reeves, B.C., 2012. Ranibizumab versus bevacizumab to treat neovascular age-related macular degeneration: one-year findings from the IVAN randomized trial. *Ophthalmology* 119, 1399-1411.
203. Ivey-Hoyle, M., Conroy, R., Huber, H.E., Goodhart, P.J., Oliff, A., Heimbrook, D.C., 1993. Cloning and characterization of E2F-2, a novel protein with the biochemical properties of transcription factor E2F. *Molecular and cellular biology* 13, 7802-7812.
204. Iwakuma, T., Cui, Y., Chang, L.J., 1999. Self-inactivating lentiviral vectors with U3 and U5 modifications. *Virology* 261, 120-132.
205. Jager, R.D., Mieler, W.F., Miller, J.W., 2008. Age-related macular degeneration. *The New England journal of medicine* 358, 2606-2617.
206. Jessup, C.F., Brereton, H.M., Coster, D.J., Williams, K.A., 2005a. In vitro adenovirus mediated gene transfer to the human cornea. *Br.J.Ophthalmol* 89, 658-661.
207. Jessup, C.F., Brereton, H.M., Sykes, P.J., Thiel, M.A., Coster, D.J., Williams, K.A., 2005b. Local gene transfer to modulate rat corneal allograft rejection. *Invest Ophthalmol Vis.Sci.* 46, 1675-1681.
208. Jiao, X., Sultana, A., Garg, P., Ramamurthy, B., Vemuganti, G.K., Gangopadhyay, N., Hejtmancik, J.F., Kannabiran, C., 2007. Autosomal recessive corneal endothelial dystrophy (CHED2) is associated with mutations in SLC4A11. *Journal of medical genetics* 44, 64-68.
209. Johnson, D.G., Schwarz, J.K., Cress, W.D., Nevins, J.R., 1993. Expression of transcription factor E2F1 induces quiescent cells to enter S phase. *Nature* 365, 349-352.
210. Johnson, S., Michaelides, M., Aligianis, I.A., Ainsworth, J.R., Mollon, J.D., Maher, E.R., Moore, A.T., Hunt, D.M., 2004. Achromatopsia caused by novel mutations in both CNGA3 and CNGB3. *Journal of medical genetics* 41, e20.
211. Johnston, M.C., Noden, D.M., Hazelton, R.D., Coulombre, J.L., Coulombre, A.J., 1979. Origins of avian ocular and periocular tissues. *Exp.Eye Res.* 29, 27-43.
212. Joo, C.K., Pepose, J.S., Fleming, T.P., 1994. In vitro propagation of primary and extended life span murine corneal endothelial cells. *Invest Ophthalmol Vis Sci* 35, 3952-3957.
213. Jousseaume, A.M., Joeres, S., Fawzy, N., Heussen, F.M., Llacer, H., van Meurs, J.C., Kirchhof, B., 2007. Autologous translocation of the choroid and retinal pigment epithelium in patients with geographic atrophy. *Ophthalmology* 114, 551-560.
214. Joyce, N.C., 2003. Proliferative capacity of the corneal endothelium. *Prog.Retin.Eye Res.* 22, 359-389.
215. Joyce, N.C., 2005. Cell cycle status in human corneal endothelium. *Exp.Eye Res.* 81, 629-638.
216. Joyce, N.C., 2012. Proliferative capacity of corneal endothelial cells. *Exp Eye Res* 95, 16-23.

-
217. Joyce, N.C., Harris, D.L., 2010. Decreasing expression of the G1-phase inhibitors, p21Cip1 and p16INK4a, promotes division of corneal endothelial cells from older donors. *Mol.Vis.* 16, 897-906.
 218. Joyce, N.C., Harris, D.L., Mc Alister, J.C., Ali, R.R., Larkin, D.F., 2004. Effect of overexpressing the transcription factor E2F2 on cell cycle progression in rabbit corneal endothelial cells. *Invest Ophthalmol.Vis.Sci.* 45, 1340-1348.
 219. Joyce, N.C., Harris, D.L., Mello, D.M., 2002. Mechanisms of mitotic inhibition in corneal endothelium: contact inhibition and TGF-beta2. *Invest Ophthalmol.Vis.Sci.* 43, 2152-2159.
 220. Joyce, N.C., Harris, D.L., Zieske, J.D., 1998. Mitotic inhibition of corneal endothelium in neonatal rats. *Invest Ophthalmol.Vis.Sci.* 39, 2572-2583.
 221. Joyce, N.C., Meklir, B., Joyce, S.J., Zieske, J.D., 1996a. Cell cycle protein expression and proliferative status in human corneal cells. *Invest Ophthalmol.Vis.Sci.* 37, 645-655.
 222. Joyce, N.C., Navon, S.E., Roy, S., Zieske, J.D., 1996b. Expression of cell cycle-associated proteins in human and rabbit corneal endothelium in situ. *Invest Ophthalmol.Vis.Sci.* 37, 1566-1575.
 223. Joyce, N.C., Zhu, C.C., Harris, D.L., 2009. Relationship among oxidative stress, DNA damage, and proliferative capacity in human corneal endothelium. *Invest Ophthalmol.Vis.Sci.* 50, 2116-2122.
 224. Joyce, N.C., Zieske, J.D., 1997. Transforming growth factor-beta receptor expression in human cornea. *Invest Ophthalmol.Vis.Sci.* 38, 1922-1928.
 225. Jun, A.S., Larkin, D.F., 2003. Prospects for gene therapy in corneal disease. *Eye* 17, 906-911.
 226. Kaldarar-Pedotti, S., 1979. [Mitotic activity of the pigment epithelium during embryonic and postembryonic development]. *Advances in ophthalmology = Fortschritte der Augenheilkunde = Progres en ophtalmologie* 39, 37-58.
 227. Kamao, H., Mandai, M., Okamoto, S., Sakai, N., Suga, A., Sugita, S., Kiryu, J., Takahashi, M., 2014. Characterization of human induced pluripotent stem cell-derived retinal pigment epithelium cell sheets aiming for clinical application. *Stem cell reports* 2, 205-218.
 228. Kampik, A., Kenyon, K.R., Michels, R.G., Green, W.R., de la Cruz, Z.C., 1981. Epiretinal and vitreous membranes. Comparative study of 56 cases. *Arch Ophthalmol* 99, 1445-1454.
 229. Kaneko, H., Suzutani, T., Aoki, K., Kitaichi, N., Ishida, S., Ishiko, H., Ohashi, T., Okamoto, S., Nakagawa, H., Hinokuma, R., Asato, Y., Oniki, S., Hashimoto, T., Iida, T., Ohno, S., 2011. Epidemiological and virological features of epidemic keratoconjunctivitis due to new human adenovirus type 54 in Japan. *The British journal of ophthalmology* 95, 32-36.
 230. Katchanov, J., Harms, C., Gertz, K., Hauck, L., Waeber, C., Hirt, L., Priller, J., von Harsdorf, R., Bruck, W., Hortnagl, H., Dirnagl, U., Bhide, P.G., Endres, M., 2001. Mild cerebral ischemia induces loss of cyclin-dependent kinase inhibitors and activation of cell cycle machinery before delayed neuronal cell death. *The Journal of neuroscience : the official journal of the Society for Neuroscience* 21, 5045-5053.

-
231. Kay, E.P., Gu, X., Smith, R.E., 1994. Corneal endothelial modulation: bFGF as direct mediator and corneal endothelium modulation factor as inducer. *Invest Ophthalmol Vis Sci* 35, 2427-2435.
 232. Kay, E.P., Park, S.Y., Ko, M.K., Lee, S.C., 1998. Fibroblast growth factor 2 uses PLC-gamma1 for cell proliferation and PI3-kinase for alteration of cell shape and cell proliferation in corneal endothelial cells. *Mol Vis* 4, 22.
 233. Kenyon, K.R., Antine, B., 1971. The pathogenesis of congenital hereditary endothelial dystrophy of the cornea. *Am.J.Ophthalmol.* 72, 787-795.
 234. Kikuchi, M., Harris, D.L., Obara, Y., Senoo, T., Joyce, N.C., 2004. p27kip1 Antisense-induced proliferative activity of rat corneal endothelial cells. *Invest Ophthalmol.Vis.Sci.* 45, 1763-1770.
 235. Kikuchi, M., Zhu, C., Senoo, T., Obara, Y., Joyce, N.C., 2006. p27kip1 siRNA induces proliferation in corneal endothelial cells from young but not older donors. *Invest Ophthalmol.Vis.Sci.* 47, 4803-4809.
 236. Kim, T.Y., Kim, W.I., Smith, R.E., Kay, E.D., 2001a. Role of p27(Kip1) in cAMP- and TGF-beta2-mediated antiproliferation in rabbit corneal endothelial cells. *Invest Ophthalmol Vis.Sci.* 42, 3142-3149.
 237. Kim, T.Y., Kim, W.I., Smith, R.E., Kay, E.P., 2001b. Differential activity of TGF-beta2 on the expression of p27Kip1 and Cdk4 in actively cycling and contact inhibited rabbit corneal endothelial cells. *Mol.Vis.* 7, 261-270.
 238. Kinnunen, K., Petrovski, G., Moe, M.C., Berta, A., Kaarniranta, K., 2012. Molecular mechanisms of retinal pigment epithelium damage and development of age-related macular degeneration. *Acta Ophthalmol* 90, 299-309.
 239. Klebe, S., Coster, D.J., Sykes, P.J., Swinburne, S., Hallsworth, P., Scheerlinck, J.P., Krishnan, R., Williams, K.A., 2005. Prolongation of sheep corneal allograft survival by transfer of the gene encoding ovine IL-12-p40 but not IL-4 to donor corneal endothelium. *J.Immunol.* 175, 2219-2226.
 240. Klebe, S., Sykes, P., Coster, D., Krishnan, Williams, K., 2001a. Prolongation of sheep corneal allograft survival by ex vivo transfer of the gene encoding interleukin-10. *Transplantation* 2001; 71: 1214. *Transplantation* 71, 1207-1209.
 241. Klebe, S., Sykes, P.J., Coster, D.J., Bloom, D.C., Williams, K.A., 2001b. Gene transfer to ovine corneal endothelium. *Clin.Experiment.Ophthalmol* 29, 316-322.
 242. Klebe, S., Sykes, P.J., Coster, D.J., Krishnan, R., Williams, K.A., 2001c. Prolongation of sheep corneal allograft survival by ex vivo transfer of the gene encoding interleukin-10. *Transplantation* 71, 1214-1220.
 243. Klein, R., Klein, B.E., Jensen, S.C., Meuer, S.M., 1997. The five-year incidence and progression of age-related maculopathy: the Beaver Dam Eye Study. *Ophthalmology* 104, 7-21.
 244. Klein, R., Klein, B.E., Linton, K.L., 1992. Prevalence of age-related maculopathy. The Beaver Dam Eye Study. *Ophthalmology* 99, 933-943.

-
245. Klimczak, R.R., Koerber, J.T., Dalkara, D., Flannery, J.G., Schaffer, D.V., 2009. A novel adeno-associated viral variant for efficient and selective intravitreal transduction of rat Muller cells. *PloS one* 4, e7467.
246. Koerber, J.T., Klimczak, R., Jang, J.H., Dalkara, D., Flannery, J.G., Schaffer, D.V., 2009. Molecular evolution of adeno-associated virus for enhanced glial gene delivery. *Mol Ther* 17, 2088-2095.
247. Kohl, S., Baumann, B., Rosenberg, T., Kellner, U., Lorenz, B., Vadala, M., Jacobson, S.G., Wissinger, B., 2002. Mutations in the cone photoreceptor G-protein alpha-subunit gene GNAT2 in patients with achromatopsia. *American journal of human genetics* 71, 422-425.
248. Kokawa, N., Sotozono, C., Nishida, K., Kinoshita, S., 1996. High total TGF-beta 2 levels in normal human tears. *Current eye research* 15, 341-343.
249. Komuro, A., Hodge, D.O., Gores, G.J., Bourne, W.M., 1999. Cell death during corneal storage at 4 degrees C. *Invest Ophthalmol Vis.Sci.* 40, 2827-2832.
250. Konan Medical USA, Inc., *Specular Microscopy Basics*. <http://www.konan-usa.com/clinical-resources/specular-microscopy-basics>. Accessed 19.02.2011.
251. Konomi, K., Joyce, N.C., 2007. Age and topographical comparison of telomere lengths in human corneal endothelial cells. *Mol.Vis.* 13, 1251-1258.
252. Krafchak, C.M., Pawar, H., Moroi, S.E., Sugar, A., Lichter, P.R., Mackey, D.A., Mian, S., Nairus, T., Elner, V., Schteingart, M.T., Downs, C.A., Kijek, T.G., Johnson, J.M., Trager, E.H., Rozsa, F.W., Mandal, M.N., Epstein, M.P., Vollrath, D., Ayyagari, R., Boehnke, M., Richards, J.E., 2005. Mutations in TCF8 cause posterior polymorphous corneal dystrophy and ectopic expression of COL4A3 by corneal endothelial cells. *American journal of human genetics* 77, 694-708.
253. Kruse, F.E., Schrehardt, U.S., Tourtas, T., 2014. Optimizing outcomes with Descemet's membrane endothelial keratoplasty. *Current opinion in ophthalmology* 25, 325-334.
254. Kulkarni, A.D., Kuppermann, B.D., 2005. Wet age-related macular degeneration. *Advanced drug delivery reviews* 57, 1994-2009.
255. Kumar, M., Keller, B., Makalou, N., Sutton, R.E., 2001. Systematic determination of the packaging limit of lentiviral vectors. *Human gene therapy* 12, 1893-1905.
256. La Thangue, N.B., 2003. The yin and yang of E2F-1: balancing life and death. *Nat.Cell Biol.* 5, 587-589.
257. Lai, C.M., Brankov, M., Zaknich, T., Lai, Y.K., Shen, W.Y., Constable, I.J., Kovesdi, I., Rakoczy, P.E., 2001. Inhibition of angiogenesis by adenovirus-mediated sFlt-1 expression in a rat model of corneal neovascularization. *Hum.Gene Ther.* 12, 1299-1310.
258. Lai, Y.K., Shen, W.Y., Brankov, M., Lai, C.M., Constable, I.J., Rakoczy, P.E., 2002. Potential long-term inhibition of ocular neovascularisation by recombinant adeno-associated virus-mediated secretion gene therapy. *Gene Ther.* 9, 804-813.

-
259. Laing, R.A., Neubauer, L., Leibowitz, H.M., Oak, S.S., 1983. Coalescence of endothelial cells in the traumatized cornea. II. Clinical observations. *Arch.Ophthalmol.* 101, 1712-1715.
 260. Laing, R.A., Sanstrom, M.M., Berrospi, A.R., Leibowitz, H.M., 1976. Changes in the corneal endothelium as a function of age. *Exp Eye Res* 22, 587-594.
 261. Larkin, D.F., Oral, H.B., Ring, C.J., Lemoine, N.R., George, A.J., 1996. Adenovirus-mediated gene delivery to the corneal endothelium. *Transplantation* 61, 363-370.
 262. Larsson, O., Zetterberg, A., Engstrom, W., 1985. Consequences of parental exposure to serum-free medium for progeny cell division. *Journal of cell science* 75, 259-268.
 263. Leavitt, A.D., Robles, G., Alesandro, N., Varmus, H.E., 1996. Human immunodeficiency virus type 1 integrase mutants retain in vitro integrase activity yet fail to integrate viral DNA efficiently during infection. *J Virol* 70, 721-728.
 264. Lebherz, C., Maguire, A., Tang, W., Bennett, J., Wilson, J.M., 2008. Novel AAV serotypes for improved ocular gene transfer. *J.Gene Med.* 10, 375-382.
 265. Leone, G., DeGregori, J., Jakoi, L., Cook, J.G., Nevins, J.R., 1999. Collaborative role of E2F transcriptional activity and G1 cyclindependent kinase activity in the induction of S phase. *Proc.Natl.Acad.Sci.U.S.A* 96, 6626-6631.
 266. Leuner, B., Glasper, E.R., Gould, E., 2009. Thymidine analog methods for studies of adult neurogenesis are not equally sensitive. *The Journal of comparative neurology* 517, 123-133.
 267. Li, Y., Benezra, R., 1996. Identification of a human mitotic checkpoint gene: hsMAD2. *Science* 274, 246-248.
 268. Li, Z., Dullmann, J., Schiedlmeier, B., Schmidt, M., von Kalle, C., Meyer, J., Forster, M., Stocking, C., Wahlers, A., Frank, O., Ostertag, W., Kuhlcke, K., Eckert, H.G., Fehse, B., Baum, C., 2002. Murine leukemia induced by retroviral gene marking. *Science* 296, 497.
 269. Lin, C.P., Bohnke, M., Draeger, J., 1992. Effect of dextran on predamaged corneal endothelium: an organ culture study. *Ophthalmic Res* 24, 125-128.
 270. Lin, H., Ouyang, H., Zhu, J., Huang, S., Liu, Z., Chen, S., Cao, G., Li, G., Signer, R.A., Xu, Y., Chung, C., Zhang, Y., Lin, D., Patel, S., Wu, F., Cai, H., Hou, J., Wen, C., Jafari, M., Liu, X., Luo, L., Zhu, J., Qiu, A., Hou, R., Chen, B., Chen, J., Granet, D., Heichel, C., Shang, F., Li, X., Krawczyk, M., Skowronska-Krawczyk, D., Wang, Y., Shi, W., Chen, D., Zhong, Z., Zhong, S., Zhang, L., Chen, S., Morrison, S.J., Maas, R.L., Zhang, K., Liu, Y., 2016. Lens regeneration using endogenous stem cells with gain of visual function. *Nature* 531, 323-328.
 271. Liu, C., Cheng, Q., Nguyen, T., Bonanno, J.A., 2010. Knockdown of NBCe1 in vivo compromises the corneal endothelial pump. *Invest Ophthalmol Vis Sci* 51, 5190-5197.
 272. Liu, D.X., Greene, L.A., 2001. Neuronal apoptosis at the G1/S cell cycle checkpoint. *Cell and tissue research* 305, 217-228.
 273. Liu, J., Saghizadeh, M., Tuli, S.S., Kramerov, A.A., Lewin, A.S., Bloom, D.C., Hauswirth, W.W., Castro, M.G., Schultz, G.S., Ljubimov, A.V., 2008. Different tropism of adenoviruses

- and adeno-associated viruses to corneal cells: implications for corneal gene therapy. *Mol Vis* 14, 2087-2096.
274. Liu, Q., White, L.R., Clark, S.A., Heffner, D.J., Winston, B.W., Tibbles, L.A., Muruve, D.A., 2005. Akt/protein kinase B activation by adenovirus vectors contributes to NFkappaB-dependent CXCL10 expression. *J Virol* 79, 14507-14515.
 275. Liu, Z., Zhuang, J., Li, C., Wan, P., Li, N., Zhou, Q., Zhou, C., Huang, Z., Wang, Z., 2012. Long-term cultivation of human corneal endothelial cells by telomerase expression. *Exp Eye Res* 100, 40-51.
 276. Longbottom, R., Fruttiger, M., Douglas, R.H., Martinez-Barbera, J.P., Greenwood, J., Moss, S.E., 2009. Genetic ablation of retinal pigment epithelial cells reveals the adaptive response of the epithelium and impact on photoreceptors. *Proceedings of the National Academy of Sciences of the United States of America* 106, 18728-18733.
 277. Loughran, O., La Thangue, N.B., 2002. E2F proteins. *Curr.Biol.* 12, R377.
 278. Lu, J., Lu, Z., Reinach, P., Zhang, J., Dai, W., Lu, L., Xu, M., 2006. TGF-beta2 inhibits AKT activation and FGF-2-induced corneal endothelial cell proliferation. *Experimental cell research* 312, 3631-3640.
 279. Lufino, M.M., Edser, P.A., Wade-Martins, R., 2008. Advances in high-capacity extrachromosomal vector technology: episomal maintenance, vector delivery, and transgene expression. *Mol Ther* 16, 1525-1538.
 280. Lukas, J., Petersen, B.O., Holm, K., Bartek, J., Helin, K., 1996. Deregulated expression of E2F family members induces S-phase entry and overcomes p16INK4A-mediated growth suppression. *Molecular and cellular biology* 16, 1047-1057.
 281. Lund, R.D., Wang, S., Klimanskaya, I., Holmes, T., Ramos-Kelsey, R., Lu, B., Girman, S., Bischoff, N., Sauve, Y., Lanza, R., 2006. Human embryonic stem cell-derived cells rescue visual function in dystrophic RCS rats. *Cloning and stem cells* 8, 189-199.
 282. Machemer, R., Laqua, H., 1975. Pigment epithelium proliferation in retinal detachment (massive periretinal proliferation). *American journal of ophthalmology* 80, 1-23.
 283. Machemer, R., Steinhorst, U.H., 1993. Retinal separation, retinotomy, and macular relocation: II. A surgical approach for age-related macular degeneration? *Graefes Arch Clin Exp Ophthalmol* 231, 635-641.
 284. Machemer, R., van Horn, D., Aaberg, T.M., 1978. Pigment epithelial proliferation in human retinal detachment with massive periretinal proliferation. *American journal of ophthalmology* 85, 181-191.
 285. MacLaren, R.E., Bird, A.C., Sathia, P.J., Aylward, G.W., 2005. Long-term results of submacular surgery combined with macular translocation of the retinal pigment epithelium in neovascular age-related macular degeneration. *Ophthalmology* 112, 2081-2087.
 286. MacLaren, R.E., Uppal, G.S., Balaggan, K.S., Tufail, A., Munro, P.M., Milliken, A.B., Ali, R.R., Rubin, G.S., Aylward, G.W., da Cruz, L., 2007. Autologous transplantation of the retinal

- pigment epithelium and choroid in the treatment of neovascular age-related macular degeneration. *Ophthalmology* 114, 561-570.
287. Maguire, A.M., Simonelli, F., Pierce, E.A., Pugh, E.N., Jr., Mingozzi, F., Bennicelli, J., Banfi, S., Marshall, K.A., Testa, F., Surace, E.M., Rossi, S., Lyubarsky, A., Arruda, V.R., Konkle, B., Stone, E., Sun, J., Jacobs, J., Dell'Osso, L., Hertle, R., Ma, J.X., Redmond, T.M., Zhu, X., Hauck, B., Zeleniaia, O., Shindler, K.S., Maguire, M.G., Wright, J.F., Volpe, N.J., McDonnell, J.W., Auricchio, A., High, K.A., Bennett, J., 2008. Safety and efficacy of gene transfer for Leber's congenital amaurosis. *N.Engl.J.Med.* 358, 2240-2248.
 288. Marmorstein, A.D., 2001. The polarity of the retinal pigment epithelium. *Traffic* 2, 867-872.
 289. Marshall, J., 1987. The ageing retina: physiology or pathology. *Eye (Lond)* 1 (Pt 2), 282-295.
 290. Marshall, J., Grindle, C.F., 1978. Fine structure of the cornea and its development. *Trans.Ophthalmol.Soc.U.K.* 98, 320-328.
 291. Marton, M.J., Baim, S.B., Ornelles, D.A., Shenk, T., 1990. The adenovirus E4 17-kilodalton protein complexes with the cellular transcription factor E2F, altering its DNA-binding properties and stimulating E1A-independent accumulation of E2 mRNA. *J Virol* 64, 2345-2359.
 292. Massague, J., 2004. G1 cell-cycle control and cancer. *Nature* 432, 298-306.
 293. Matsubara, M., Tanishima, T., 1983. Wound-healing of corneal endothelium in monkey: an autoradiographic study. *Japanese journal of ophthalmology* 27, 444-450.
 294. Matsuda, M., Manabe, R., 1988. The corneal endothelium following autokeratoplasty. A case report. *Acta Ophthalmol (Copenh)* 66, 54-57.
 295. McAlister, J.C., Joyce, N.C., Harris, D.L., Ali, R.R., Larkin, D.F., 2005. Induction of replication in human corneal endothelial cells by E2F2 transcription factor cDNA transfer. *Invest Ophthalmol.Vis.Sci.* 46, 3597-3603.
 296. Melles, G.R., Ong, T.S., Ververs, B., van der Wees, J., 2006. Descemet membrane endothelial keratoplasty (DMEK). *Cornea* 25, 987-990.
 297. Miceli, M.V., Liles, M.R., Newsome, D.A., 1994. Evaluation of oxidative processes in human pigment epithelial cells associated with retinal outer segment phagocytosis. *Experimental cell research* 214, 242-249.
 298. Michaelides, M., Hardcastle, A.J., Hunt, D.M., Moore, A.T., 2006. Progressive cone and cone-rod dystrophies: phenotypes and underlying molecular genetic basis. *Survey of ophthalmology* 51, 232-258.
 299. Minkowski, J.S., Bartels, S.P., Delori, F.C., Lee, S.R., Kenyon, K.R., Neufeld, A.H., 1984. Corneal endothelial function and structure following cryo-injury in the rabbit. *Invest Ophthalmol Vis Sci* 25, 1416-1425.
 300. Mishima, S., 1982. Clinical investigations on the corneal endothelium-XXXVIII Edward Jackson Memorial Lecture. *American journal of ophthalmology* 93, 1-29.

-
301. Moldovan, G.L., Pfander, B., Jentsch, S., 2007. PCNA, the maestro of the replication fork. *Cell* 129, 665-679.
 302. Morral, N., O'Neal, W., Rice, K., Leland, M., Kaplan, J., Piedra, P.A., Zhou, H., Parks, R.J., Velji, R., Aguilar-Cordova, E., Wadsworth, S., Graham, F.L., Kochanek, S., Carey, K.D., Beaudet, A.L., 1999. Administration of helper-dependent adenoviral vectors and sequential delivery of different vector serotype for long-term liver-directed gene transfer in baboons. *Proceedings of the National Academy of Sciences of the United States of America* 96, 12816-12821.
 303. Morris, S.M., 1991. The genetic toxicology of 5-bromodeoxyuridine in mammalian cells. *Mutation research* 258, 161-188.
 304. Mruthyunjaya, P., Stinnett, S.S., Toth, C.A., 2004. Change in visual function after macular translocation with 360 degrees retinectomy for neovascular age-related macular degeneration. *Ophthalmology* 111, 1715-1724.
 305. Murphy, C., Alvarado, J., Juster, R., Maglio, M., 1984. Prenatal and postnatal cellularity of the human corneal endothelium. A quantitative histologic study. *Invest Ophthalmol.Vis.Sci.* 25, 312-322.
 306. Nakano, Y., Oyamada, M., Dai, P., Nakagami, T., Kinoshita, S., Takamatsu, T., 2008. Connexin43 knockdown accelerates wound healing but inhibits mesenchymal transition after corneal endothelial injury in vivo. *Invest Ophthalmol Vis Sci* 49, 93-104.
 307. Naldini, L., Blomer, U., Gage, F.H., Trono, D., Verma, I.M., 1996a. Efficient transfer, integration, and sustained long-term expression of the transgene in adult rat brains injected with a lentiviral vector. *Proceedings of the National Academy of Sciences of the United States of America* 93, 11382-11388.
 308. Naldini, L., Blomer, U., Gally, P., Ory, D., Mulligan, R., Gage, F.H., Verma, I.M., Trono, D., 1996b. In vivo gene delivery and stable transduction of nondividing cells by a lentiviral vector. *Science* 272, 263-267.
 309. Nanavaty, M.A., Wang, X., Shortt, A.J., 2014. Endothelial keratoplasty versus penetrating keratoplasty for Fuchs endothelial dystrophy. *The Cochrane database of systematic reviews* 2, CD008420.
 310. Nathwani, A.C., Tuddenham, E.G., Rangarajan, S., Rosales, C., McIntosh, J., Linch, D.C., Chowdhary, P., Riddell, A., Pie, A.J., Harrington, C., O'Beirne, J., Smith, K., Pasi, J., Glader, B., Rustagi, P., Ng, C.Y., Kay, M.A., Zhou, J., Spence, Y., Morton, C.L., Allay, J., Coleman, J., Sleep, S., Cunningham, J.M., Srivastava, D., Basner-Tschakarjan, E., Mingozzi, F., High, K.A., Gray, J.T., Reiss, U.M., Nienhuis, A.W., Davidoff, A.M., 2011. Adenovirus-associated virus vector-mediated gene transfer in hemophilia B. *The New England journal of medicine* 365, 2357-2365.
 311. Neill, S.D., Nevins, J.R., 1991. Genetic analysis of the adenovirus E4 6/7 trans activator: interaction with E2F and induction of a stable DNA-protein complex are critical for activity. *J.Virol.* 65, 5364-5373.
 312. Nevins, J.R., 2001. The Rb/E2F pathway and cancer. *Hum.Mol.Genet.* 10, 699-703.

-
313. Newsome, D.A., Dobard, E.P., Liles, M.R., Oliver, P.D., 1990. Human retinal pigment epithelium contains two distinct species of superoxide dismutase. *Invest Ophthalmol Vis Sci* 31, 2508-2513.
 314. UK NHS Blood and Transplant website. <https://www.organdonation.nhs.uk/supporting-my-decision/statistics-about-organ-donation/>. Accessed 05 March 2017.
 315. Nienhuis, A.W., Dunbar, C.E., Sorrentino, B.P., 2006. Genotoxicity of retroviral integration in hematopoietic cells. *Mol Ther* 13, 1031-1049.
 316. Nojima, H., 2004. G1 and S-phase checkpoints, chromosome instability, and cancer. *Methods Mol Biol* 280, 3-49.
 317. Nowakowski, R.S., Hayes, N.L., 2000. New neurons: extraordinary evidence or extraordinary conclusion? *Science* 288, 771.
 318. Nucci, P., Brancato, R., Mets, M.B., Shevell, S.K., 1990. Normal endothelial cell density range in childhood. *Arch.Ophthalmol.* 108, 247-248.
 319. O'Connor, R.J., Hearing, P., 2000. The E4-6/7 protein functionally compensates for the loss of E1A expression in adenovirus infection. *J Virol* 74, 5819-5824.
 320. Obert, S., O'Connor, R.J., Schmid, S., Hearing, P., 1994. The adenovirus E4-6/7 protein transactivates the E2 promoter by inducing dimerization of a heteromeric E2F complex. *Molecular and cellular biology* 14, 1333-1346.
 321. Okumura, N., Kinoshita, S., Koizumi, N., 2014a. Cell-based approach for treatment of corneal endothelial dysfunction. *Cornea* 33 Suppl 11, S37-41.
 322. Okumura, N., Koizumi, N., Kay, E.P., Ueno, M., Sakamoto, Y., Nakamura, S., Hamuro, J., Kinoshita, S., 2013. The ROCK inhibitor eye drop accelerates corneal endothelium wound healing. *Invest Ophthalmol Vis Sci* 54, 2493-2502.
 323. Okumura, N., Koizumi, N., Ueno, M., Sakamoto, Y., Takahashi, H., Tsuchiya, H., Hamuro, J., Kinoshita, S., 2012. ROCK inhibitor converts corneal endothelial cells into a phenotype capable of regenerating in vivo endothelial tissue. *The American journal of pathology* 181, 268-277.
 324. Okumura, N., Nakano, S., Kay, E.P., Numata, R., Ota, A., Sowa, Y., Sakai, T., Ueno, M., Kinoshita, S., Koizumi, N., 2014b. Involvement of cyclin D and p27 in cell proliferation mediated by ROCK inhibitors Y-27632 and Y-39983 during corneal endothelium wound healing. *Invest Ophthalmol Vis Sci* 55, 318-329.
 325. Okumura, N., Okazaki, Y., Inoue, R., Nakano, S., Fullwood, N.J., Kinoshita, S., Koizumi, N., 2015. Rho-Associated Kinase Inhibitor Eye Drop (Ripasudil) Transiently Alters the Morphology of Corneal Endothelial Cells. *Invest Ophthalmol Vis Sci* 56, 7560-7567.
 326. Organisciak, D.T., Vaughan, D.K., 2010. Retinal light damage: mechanisms and protection. *Progress in retinal and eye research* 29, 113-134.
 327. Oshima, Y., Sakamoto, T., Yamanaka, I., Nishi, T., Ishibashi, T., Inomata, H., 1998. Targeted gene transfer to corneal endothelium in vivo by electric pulse. *Gene Ther.* 5, 1347-1354.

-
328. Pagliaro, L.C., Antelman, D., Johnson, D.E., Macheimer, T., McCulloch, E.A., Freireich, E.J., Stass, S.A., Shepard, H.M., Maneval, D., Gutterman, J.U., 1995. Recombinant human retinoblastoma protein inhibits cancer cell growth. *Cell Growth Differ.* 6, 673-680.
 329. Papapetrou, E.P., Schambach, A., 2016. Gene Insertion Into Genomic Safe Harbors for Human Gene Therapy. *Mol Ther.*
 330. Pardee, A.B., 1989. G1 events and regulation of cell proliferation. *Science* 246, 603-608.
 331. Paris, L., Tonutti, L., Vannini, C., Bazzoni, G., 2008. Structural organization of the tight junctions. *Biochimica et biophysica acta* 1778, 646-659.
 332. Park, T.K., Wu, Z., Kjellstrom, S., Zeng, Y., Bush, R.A., Sieving, P.A., Colosi, P., 2009. Intravitreal delivery of AAV8 retinoschisin results in cell type-specific gene expression and retinal rescue in the Rs1-KO mouse. *Gene therapy* 16, 916-926.
 333. Parker, D.G., Brereton, H.M., Coster, D.J., Williams, K.A., 2009a. The potential of viral vector-mediated gene transfer to prolong corneal allograft survival. *Curr.Gene Ther.* 9, 33-44.
 334. Parker, D.G., Brereton, H.M., Klebe, S., Coster, D.J., Williams, K.A., 2009b. A steroid-inducible promoter for the cornea. *Br.J.Ophthalmol* 93, 1255-1259.
 335. Parker, D.G., Coster, D.J., Brereton, H.M., Hart, P.H., Koldej, R., Anson, D.S., Williams, K.A., 2010. Lentivirus-mediated gene transfer of interleukin 10 to the ovine and human cornea. *Clin.Experiment.Ophthalmol* 38, 405-413.
 336. Parker, D.G., Kaufmann, C., Brereton, H.M., Anson, D.S., Francis-Staite, L., Jessup, C.F., Marshall, K., Tan, C., Koldej, R., Coster, D.J., Williams, K.A., 2007. Lentivirus-mediated gene transfer to the rat, ovine and human cornea. *Gene Ther.* 14, 760-767.
 337. Parks, R.J., Graham, F.L., 1997. A helper-dependent system for adenovirus vector production helps define a lower limit for efficient DNA packaging. *J Virol* 71, 3293-3298.
 338. Passmore, L.A., McCormack, E.A., Au, S.W., Paul, A., Willison, K.R., Harper, J.W., Barford, D., 2003. Doc1 mediates the activity of the anaphase-promoting complex by contributing to substrate recognition. *The EMBO journal* 22, 786-796.
 339. Patel, S.P., Bourne, W.M., 2009. Corneal endothelial cell proliferation: a function of cell density. *Invest Ophthalmol Vis Sci* 50, 2742-2746.
 340. Pearson, B.E., Nasheuer, H.P., Wang, T.S., 1991. Human DNA polymerase alpha gene: sequences controlling expression in cycling and serum-stimulated cells. *Molecular and cellular biology* 11, 2081-2095.
 341. Peeper, D.S., Zantema, A., 1993. Adenovirus-E1A proteins transform cells by sequestering regulatory proteins. *Molecular biology reports* 17, 197-207.
 342. Pels, E., Schuchard, Y., 1983. Organ-culture preservation of human corneas. *Doc Ophthalmol* 56, 147-153.

-
343. Pertile, G., Claes, C., 2002. Macular translocation with 360 degree retinotomy for management of age-related macular degeneration with subfoveal choroidal neovascularization. *American journal of ophthalmology* 134, 560-565.
 344. Petroll, W.M., Hsu, J.K., Bean, J., Cavanagh, H.D., Jester, J.V., 1999a. The spatial organization of apical junctional complex-associated proteins in feline and human corneal endothelium. *Current eye research* 18, 10-19.
 345. Petroll, W.M., Jester, J.V., Bean, J., Cavanagh, H.D., 1999b. Labeling of cycling corneal endothelial cells during healing with a monoclonal antibody to the Ki67 antigen (MIB-1). *Cornea* 18, 98-108.
 346. Petrukhin, K., Koisti, M.J., Bakall, B., Li, W., Xie, G., Marknell, T., Sandgren, O., Forsman, K., Holmgren, G., Andreasson, S., Vujic, M., Bergen, A.A., McGarty-Dugan, V., Figueroa, D., Austin, C.P., Metzker, M.L., Caskey, C.T., Wadelius, C., 1998. Identification of the gene responsible for Best macular dystrophy. *Nature genetics* 19, 241-247.
 347. Peyman, G.A., Blinder, K.J., Paris, C.L., Alturki, W., Nelson, N.C., Jr., Desai, U., 1991. A technique for retinal pigment epithelium transplantation for age-related macular degeneration secondary to extensive subfoveal scarring. *Ophthalmic surgery* 22, 102-108.
 348. Pfaffl, M.W., 2001. A new mathematical model for relative quantification in real-time RT-PCR. *Nucleic acids research* 29, e45.
 349. Pfaffl, M.W., Horgan, G.W., Dempfle, L., 2002. Relative expression software tool (REST) for group-wise comparison and statistical analysis of relative expression results in real-time PCR. *Nucleic acids research* 30, e36.
 350. Philpott, N.J., Thrasher, A.J., 2007. Use of nonintegrating lentiviral vectors for gene therapy. *Human gene therapy* 18, 483-489.
 351. Picht, G., Welge-Luessen, U., Grehn, F., Lutjen-Drecoll, E., 2001. Transforming growth factor beta 2 levels in the aqueous humor in different types of glaucoma and the relation to filtering bleb development. *Graefes Arch Clin Exp Ophthalmol* 239, 199-207.
 352. Pleyer, U., Bertelmann, E., Rieck, P., Hartmann, C., Volk, H.D., Ritter, T., 2000. Survival of corneal allografts following adenovirus-mediated gene transfer of interleukin-4. *Graefes Arch Clin.Exp Ophthalmol* 238, 531-536.
 353. Pleyer, U., Groth, D., Hinz, B., Keil, O., Bertelmann, E., Rieck, P., Reszka, R., 2001. Efficiency and toxicity of liposome-mediated gene transfer to corneal endothelial cells. *Exp Eye Res.* 73, 1-7.
 354. Preising, M.N., Lorenz, B., 2009. [Genetic diseases of the retinal pigment epithelium]. *Ophthalmologie* 106, 311-319.
 355. Price, M.O., Price, F.W., Jr., 2008. Endothelial cell loss after descemet stripping with endothelial keratoplasty influencing factors and 2-year trend. *Ophthalmology* 115, 857-865.

-
356. Price, M.O., Price, F.W., Jr., 2013. Descemet's membrane endothelial keratoplasty surgery: update on the evidence and hurdles to acceptance. *Current opinion in ophthalmology* 24, 329-335.
 357. Proulx, S., Audet, C., d'Arc, U.J., Deschambeault, A., Carrier, P., Giasson, C.J., Brunette, I., Germain, L., 2009. Tissue Engineering of Feline Corneal Endothelium Using a Devitalized Human Cornea as Carrier. *Tissue Eng Part A*.
 358. Qian, Y., Leong, F.L., Kazlauskas, A., Dana, M.R., 2004. Ex vivo adenovirus-mediated gene transfer to corneal graft endothelial cells in mice. *Invest Ophthalmol Vis.Sci.* 45, 2187-2193.
 359. Rahman, I., Carley, F., Hillarby, C., Brahma, A., Tullo, A.B., 2008. Penetrating keratoplasty: indications, outcomes, and complications. *Eye*.
 360. Rakoczy, E.P., Lai, C.M., Magno, A.L., Wikstrom, M.E., French, M.A., Pierce, C.M., Schwartz, S.D., Blumenkranz, M.S., Chalberg, T.W., Degli-Esposti, M.A., Constable, I.J., 2015. Gene therapy with recombinant adeno-associated vectors for neovascular age-related macular degeneration: 1 year follow-up of a phase 1 randomised clinical trial. *Lancet* 386, 2395-2403.
 361. Ramrattan, R.S., van der Schaft, T.L., Mooy, C.M., de Bruijn, W.C., Mulder, P.G., de Jong, P.T., 1994. Morphometric analysis of Bruch's membrane, the choriocapillaris, and the choroid in aging. *Invest Ophthalmol Vis Sci* 35, 2857-2864.
 362. Raymond, G.M., Jumblatt, M.M., Bartels, S.P., Neufeld, A.H., 1986. Rabbit corneal endothelial cells in vitro: effects of EGF. *Invest Ophthalmol Vis Sci* 27, 474-479.
 363. Rayner, S.A., Larkin, D.F., George, A.J., 2001. TNF receptor secretion after ex vivo adenoviral gene transfer to cornea and effect on in vivo graft survival. *Invest Ophthalmol.Vis.Sci.* 42, 1568-1573.
 364. Reddy, K.B., Hocevar, B.A., Howe, P.H., 1994. Inhibition of G1 phase cyclin dependent kinases by transforming growth factor beta 1. *Journal of cellular biochemistry* 56, 418-425.
 365. Redmond, R.M., Armitage, W.J., Whittle, J., Moss, S.J., Easty, D.L., 1992. Long-term survival of endothelium following transplantation of corneas stored by organ culture. *Br.J.Ophthalmol* 76, 479-481.
 366. Reichel, R., Neill, S.D., Kovesdi, I., Simon, M.C., Raychaudhuri, P., Nevins, J.R., 1989. The adenovirus E4 gene, in addition to the E1A gene, is important for trans-activation of E2 transcription and for E2F activation. *J.Virol.* 63, 3643-3650.
 367. Resnitzky, D., Reed, S.I., 1995. Different roles for cyclins D1 and E in regulation of the G1-to-S transition. *Molecular and cellular biology* 15, 3463-3469.
 368. Ritter, T., Yang, J., Dannowski, H., Vogt, K., Volk, H.D., Pleyer, U., 2007. Effects of interleukin-12p40 gene transfer on rat corneal allograft survival. *Transpl.Immunol.* 18, 101-107.
 369. Romano, G., Marino, I.R., Pentimalli, F., Adamo, V., Giordano, A., 2009. Insertional mutagenesis and development of malignancies induced by integrating gene delivery

- systems: implications for the design of safer gene-based interventions in patients. *Drug news & perspectives* 22, 185-196.
370. Rosenbaum, J.T., Planck, S.T., Huang, X.N., Rich, L., Ansel, J.C., 1995. Detection of mRNA for the cytokines, interleukin-1 alpha and interleukin-8, in corneas from patients with pseudophakic bullous keratopathy. *Invest Ophthalmol Vis Sci* 36, 2151-2155.
 371. Rosenfeld, P.J., Brown, D.M., Heier, J.S., Boyer, D.S., Kaiser, P.K., Chung, C.Y., Kim, R.Y., Group, M.S., 2006. Ranibizumab for neovascular age-related macular degeneration. *The New England journal of medicine* 355, 1419-1431.
 372. Saenz, D.T., Loewen, N., Peretz, M., Whitwam, T., Barraza, R., Howell, K.G., Holmes, J.M., Good, M., Poeschla, E.M., 2004. Unintegrated lentivirus DNA persistence and accessibility to expression in nondividing cells: analysis with class I integrase mutants. *J Virol* 78, 2906-2920.
 373. Saffhill, R., Ockey, C.H., 1985. Strand breaks arising from the repair of the 5-bromodeoxyuridine-substituted template and methyl methanesulphonate-induced lesions can explain the formation of sister chromatid exchanges. *Chromosoma* 92, 218-224.
 374. Saika, S., Yamanaka, O., Sumioka, T., Miyamoto, T., Miyazaki, K., Okada, Y., Kitano, A., Shirai, K., Tanaka, S., Ikeda, K., 2008. Fibrotic disorders in the eye: targets of gene therapy. *Prog.Retin.Eye Res.* 27, 177-196.
 375. Salero, E., Blenkinsop, T.A., Corneo, B., Harris, A., Rabin, D., Stern, J.H., Temple, S., 2012. Adult human RPE can be activated into a multipotent stem cell that produces mesenchymal derivatives. *Cell stem cell* 10, 88-95.
 376. Salic, A., Mitchison, T.J., 2008. A chemical method for fast and sensitive detection of DNA synthesis in vivo. *Proceedings of the National Academy of Sciences of the United States of America* 105, 2415-2420.
 377. Sarks, S.H., 1976. Ageing and degeneration in the macular region: a clinico-pathological study. *The British journal of ophthalmology* 60, 324-341.
 378. Savion, N., Isaacs, J.D., Shuman, M.A., Gospodarowicz, D., 1982. Proliferation and differentiation of bovine corneal endothelial cells in culture. *Metabolic, pediatric, and systemic ophthalmology* 6, 305-320.
 379. Schaley, J., O'Connor, R.J., Taylor, L.J., Bar-Sagi, D., Hearing, P., 2000. Induction of the cellular E2F-1 promoter by the adenovirus E4-6/7 protein. *J Virol* 74, 2084-2093.
 380. Scheef, E.A., Huang, Q., Wang, S., Sorenson, C.M., Sheibani, N., 2007. Isolation and characterization of corneal endothelial cells from wild type and thrombospondin-1 deficient mice. *Mol Vis* 13, 1483-1495.
 381. Schimmelpfennig, B.H., 1984. Direct and indirect determination of nonuniform cell density distribution in human corneal endothelium. *Invest Ophthalmol Vis Sci* 25, 223-229.

-
382. Schmid, E., Lisch, W., Philipp, W., Lechner, S., Gottinger, W., Schlotzer-Schrehardt, U., Muller, T., Utermann, G., Janecke, A.R., 2006. A new, X-linked endothelial corneal dystrophy. *American journal of ophthalmology* 141, 478-487.
 383. Scholzen, T., Gerdes, J., 2000. The Ki-67 protein: from the known and the unknown. *Journal of cellular physiology* 182, 311-322.
 384. Schon, C., Biel, M., Michalakis, S., 2015. Retinal gene delivery by adeno-associated virus (AAV) vectors: Strategies and applications. *European journal of pharmaceuticals and biopharmaceutics : official journal of Arbeitsgemeinschaft fur Pharmazeutische Verfahrenstechnik e.V* 95, 343-352.
 385. Schonthal, A.H., Hwang, J.J., Stevenson, D., Trousdale, M.D., 1999. Expression and activity of cell cycle-regulatory proteins in normal and transformed corneal endothelial cells. *Exp Eye Res* 68, 531-539.
 386. Schroeter, J., Meltendorf, C., Ohrloff, C., Rieck, P., 2008. Influence of temporary hypothermia on corneal endothelial cell density during organ culture preservation. *Graefes Arch Clin Exp Ophthalmol* 246, 369-372.
 387. Schultz-Cherry, S., Lawler, J., Murphy-Ullrich, J.E., 1994. The type 1 repeats of thrombospondin 1 activate latent transforming growth factor-beta. *The Journal of biological chemistry* 269, 26783-26788.
 388. Schulz, M.W., Chamberlain, C.G., de Iongh, R.U., McAvoy, J.W., 1993. Acidic and basic FGF in ocular media and lens: implications for lens polarity and growth patterns. *Development* 118, 117-126.
 389. Schwartz, S.D., Hubschman, J.P., Heilwell, G., Franco-Cardenas, V., Pan, C.K., Ostrick, R.M., Mickunas, E., Gay, R., Klimanskaya, I., Lanza, R., 2012. Embryonic stem cell trials for macular degeneration: a preliminary report. *Lancet* 379, 713-720.
 390. Schwartz, S.D., Regillo, C.D., Lam, B.L., Elliott, D., Rosenfeld, P.J., Gregori, N.Z., Hubschman, J.P., Davis, J.L., Heilwell, G., Sporn, M., Maguire, J., Gay, R., Bateman, J., Ostrick, R.M., Morris, D., Vincent, M., Anglade, E., Del Priore, L.V., Lanza, R., 2015. Human embryonic stem cell-derived retinal pigment epithelium in patients with age-related macular degeneration and Stargardt's macular dystrophy: follow-up of two open-label phase 1/2 studies. *Lancet* 385, 509-516.
 391. Schwartzkopff, J., Bredow, L., Mahlenbrey, S., Boehringer, D., Reinhard, T., 2010. Regeneration of corneal endothelium following complete endothelial cell loss in rat keratoplasty. *Mol Vis* 16, 2368-2375.
 392. Selden, J.R., Dolbeare, F., Clair, J.H., Nichols, W.W., Miller, J.E., Kleemeyer, K.M., Hyland, R.J., DeLuca, J.G., 1993. Statistical confirmation that immunofluorescent detection of DNA repair in human fibroblasts by measurement of bromodeoxyuridine incorporation is stoichiometric and sensitive. *Cytometry* 14, 154-167.
 393. Selvey, S., Thompson, E.W., Matthaei, K., Lea, R.A., Irving, M.G., Griffiths, L.R., 2001. Beta-actin--an unsuitable internal control for RT-PCR. *Molecular and cellular probes* 15, 307-311.

-
394. Senoo, T., Joyce, N.C., 2000. Cell cycle kinetics in corneal endothelium from old and young donors. *Invest Ophthalmol.Vis.Sci.* 41, 660-667.
 395. Senoo, T., Obara, Y., Joyce, N.C., 2000. EDTA: a promoter of proliferation in human corneal endothelium. *Invest Ophthalmol.Vis.Sci.* 41, 2930-2935.
 396. Sha, W., Moore, J., Chen, K., Lassaletta, A.D., Yi, C.S., Tyson, J.J., Sible, J.C., 2003. Hysteresis drives cell-cycle transitions in *Xenopus laevis* egg extracts. *Proceedings of the National Academy of Sciences of the United States of America* 100, 975-980.
 397. Shaw, G., Morse, S., Ararat, M., Graham, F.L., 2002. Preferential transformation of human neuronal cells by human adenoviruses and the origin of HEK 293 cells. *FASEB journal : official publication of the Federation of American Societies for Experimental Biology* 16, 869-871.
 398. Shimizu, S., Krafchak, C., Fuse, N., Epstein, M.P., Schteingart, M.T., Sugar, A., Eibschitz-Tsimhoni, M., Downs, C.A., Rozsa, F., Trager, E.H., Reed, D.M., Boehnke, M., Moroi, S.E., Richards, J.E., 2004. A locus for posterior polymorphous corneal dystrophy (PPCD3) maps to chromosome 10. *American journal of medical genetics. Part A* 130A, 372-377.
 399. Simonelli, F., Maguire, A.M., Testa, F., Pierce, E.A., Mingozzi, F., Bennicelli, J.L., Rossi, S., Marshall, K., Banfi, S., Surace, E.M., Sun, J., Redmond, T.M., Zhu, X., Shindler, K.S., Ying, G.S., Ziviello, C., Acerra, C., Wright, J.F., McDonnell, J.W., High, K.A., Bennett, J., Auricchio, A., 2010. Gene therapy for Leber's congenital amaurosis is safe and effective through 1.5 years after vector administration. *Mol Ther* 18, 643-650.
 400. Singh, P., Wong, S.H., Hong, W., 1994. Overexpression of E2F-1 in rat embryo fibroblasts leads to neoplastic transformation. *EMBO J.* 13, 3329-3338.
 401. Slansky, J.E., Li, Y., Kaelin, W.G., Farnham, P.J., 1993. A protein synthesis-dependent increase in E2F1 mRNA correlates with growth regulation of the dihydrofolate reductase promoter. *Mol.Cell Biol.* 13, 1610-1618.
 402. Smith, A.J., Bainbridge, J.W., Ali, R.R., 2009. Prospects for retinal gene replacement therapy. *Trends Genet.* 25, 156-165.
 403. Smith, A.J., Schlichtenbrede, F.C., Tschernutter, M., Bainbridge, J.W., Thrasher, A.J., Ali, R.R., 2003. AAV-Mediated gene transfer slows photoreceptor loss in the RCS rat model of retinitis pigmentosa. *Mol.Ther.* 8, 188-195.
 404. Somia, N., Verma, I.M., 2000. Gene therapy: trials and tribulations. *Nat.Rev.Genet.* 1, 91-99.
 405. Song, P., Inagaki, Y., Sugawara, Y., Kokudo, N., 2013. Perspectives on human clinical trials of therapies using iPS cells in Japan: reaching the forefront of stem-cell therapies. *Bioscience trends* 7, 157-158.
 406. Sourisseau, T., Georgiadis, A., Tsapara, A., Ali, R.R., Pestell, R., Matter, K., Balda, M.S., 2006. Regulation of PCNA and cyclin D1 expression and epithelial morphogenesis by the ZO-1-regulated transcription factor ZONAB/DbpA. *Mol.Cell Biol.* 26, 2387-2398.
 407. Sparrow, J.R., Hicks, D., Hamel, C.P., 2010. The retinal pigment epithelium in health and disease. *Current molecular medicine* 10, 802-823.

-
408. Spitznas, M., Hogan, M.J., 1970. Outer segments of photoreceptors and the retinal pigment epithelium. Interrelationship in the human eye. *Arch Ophthalmol* 84, 810-819.
 409. Spraul, C.W., Lang, G.E., Grossniklaus, H.E., Lang, G.K., 1999. Histologic and morphometric analysis of the choroid, Bruch's membrane, and retinal pigment epithelium in postmortem eyes with age-related macular degeneration and histologic examination of surgically excised choroidal neovascular membranes. *Survey of ophthalmology* 44 Suppl 1, S10-32.
 410. Stalmans, P., Benz, M.S., Gandorfer, A., Kampik, A., Girach, A., Pakola, S., Haller, J.A., Group, M.-T.S., 2012. Enzymatic vitreolysis with ocriplasmin for vitreomacular traction and macular holes. *The New England journal of medicine* 367, 606-615.
 411. Steinberg, R.H., 1985. Interactions between the retinal pigment epithelium and the neural retina. *Doc Ophthalmol* 60, 327-346.
 412. Stevenson, B.R., Siliciano, J.D., Mooseker, M.S., Goodenough, D.A., 1986. Identification of ZO-1: a high molecular weight polypeptide associated with the tight junction (zonula occludens) in a variety of epithelia. *The Journal of cell biology* 103, 755-766.
 413. Stocking, C., Bergholz, U., Friel, J., Klingler, K., Wagener, T., Starke, C., Kitamura, T., Miyajima, A., Ostertag, W., 1993. Distinct classes of factor-independent mutants can be isolated after retroviral mutagenesis of a human myeloid stem cell line. *Growth Factors* 8, 197-209.
 414. Strauss, O., 1995. The Retinal Pigment Epithelium, in: Kolb, H., Fernandez, E., Nelson, R. (Eds.), *Webvision: The Organization of the Retina and Visual System*, Salt Lake City (UT).
 415. Strauss, O., 2005. The retinal pigment epithelium in visual function. *Physiological reviews* 85, 845-881.
 416. Streeten, B.W., 1969. Development of the human retinal pigment epithelium and the posterior segment. *Arch Ophthalmol* 81, 383-394.
 417. Streilein, J.W., Ma, N., Wenkel, H., Ng, T.F., Zamiri, P., 2002. Immunobiology and privilege of neuronal retina and pigment epithelium transplants. *Vision research* 42, 487-495.
 418. Sugiyama, M., Sakaue-Sawano, A., Iimura, T., Fukami, K., Kitaguchi, T., Kawakami, K., Okamoto, H., Higashijima, S., Miyawaki, A., 2009. Illuminating cell-cycle progression in the developing zebrafish embryo. *Proceedings of the National Academy of Sciences of the United States of America* 106, 20812-20817.
 419. Suh, L.H., Zhang, C., Chuck, R.S., Stark, W.J., Naylor, S., Binley, K., Chakravarti, S., Jun, A.S., 2007. Cryopreservation and lentiviral-mediated genetic modification of human primary cultured corneal endothelial cells. *Invest Ophthalmol Vis.Sci.* 48, 3056-3061.
 420. Sun, L., Li, J., Xiao, X., 2000. Overcoming adeno-associated virus vector size limitation through viral DNA heterodimerization. *Nature medicine* 6, 599-602.
 421. Sundaram, V., Moore, A.T., Ali, R.R., Bainbridge, J.W., 2012. Retinal dystrophies and gene therapy. *European journal of pediatrics* 171, 757-765.

-
422. Takahashi, K., Yamanaka, S., 2006. Induction of pluripotent stem cells from mouse embryonic and adult fibroblast cultures by defined factors. *Cell* 126, 663-676.
423. Takahashi, T., Nowakowski, R.S., Caviness, V.S., Jr., 1992. BUdR as an S-phase marker for quantitative studies of cytokinetic behaviour in the murine cerebral ventricular zone. *Journal of neurocytology* 21, 185-197.
424. Takeuchi, K., Kachi, S., Iwata, E., Ishikawa, K., Terasaki, H., 2012. Visual function 5 years or more after macular translocation surgery for myopic choroidal neovascularisation and age-related macular degeneration. *Eye (Lond)* 26, 51-60.
425. Tan, P.H., Manunta, M., Ardjomand, N., Xue, S.A., Larkin, D.F., Haskard, D.O., Taylor, K.M., George, A.J., 2003. Antibody targeted gene transfer to endothelium. *J.Gene Med.* 5, 311-323.
426. Tauber, B., Dobner, T., 2001. Adenovirus early E4 genes in viral oncogenesis. *Oncogene* 20, 7847-7854.
427. Taupin, P., 2007. BrdU immunohistochemistry for studying adult neurogenesis: paradigms, pitfalls, limitations, and validation. *Brain research reviews* 53, 198-214.
428. Taylor, D.M., Atlas, B.F., Romanchuk, K.G., Stern, A.L., 1983. Pseudophakic bullous keratopathy. *Ophthalmology* 90, 19-24.
429. Thalmeier, K., Synovzik, H., Mertz, R., Winnacker, E.L., Lipp, M., 1989. Nuclear factor E2F mediates basic transcription and trans-activation by E1a of the human MYC promoter. *Genes & development* 3, 527-536.
430. The Journal of Gene Medicine, John Wiley & Sons, Gene Therapy Clinical Trials Worldwide. <http://www.abedia.com/wiley/phases.php>. Accessed 15/03/2016.
431. Thiadens, A.A., den Hollander, A.I., Roosing, S., Nabuurs, S.B., Zekveld-Vroon, R.C., Collin, R.W., De Baere, E., Koenekoop, R.K., van Schooneveld, M.J., Strom, T.M., van Lith-Verhoeven, J.J., Lotery, A.J., van Moll-Ramirez, N., Leroy, B.P., van den Born, L.I., Hoyng, C.B., Cremers, F.P., Klaver, C.C., 2009. Homozygosity mapping reveals PDE6C mutations in patients with early-onset cone photoreceptor disorders. *American journal of human genetics* 85, 240-247.
432. Thiel, M.A., Saydam, C., Pavlovic, J., Hemmi, S., 2005. Effect of ex vivo gene transfer with an adenoviral vector on human eye bank corneas. *Ophthalmic Res.* 37, 67-71.
433. Thompson, D.A., Li, Y., McHenry, C.L., Carlson, T.J., Ding, X., Sieving, P.A., Apfelstedt-Sylla, E., Gal, A., 2001. Mutations in the gene encoding lecithin retinol acyltransferase are associated with early-onset severe retinal dystrophy. *Nature genetics* 28, 123-124.
434. Thumann, G., Aisenbrey, S., Schraermeyer, U., Lafaut, B., Esser, P., Walter, P., Bartz-Schmidt, K.U., 2000. Transplantation of autologous iris pigment epithelium after removal of choroidal neovascular membranes. *Arch Ophthalmol* 118, 1350-1355.
435. Thumann, G., Schraermeyer, U., Bartz-Schmidt, K.U., Heimann, K., 1997. Descemet's membrane as membranous support in RPE/IPE transplantation. *Current eye research* 16, 1236-1238.

-
436. Tibbles, L.A., Spurrell, J.C., Bowen, G.P., Liu, Q., Lam, M., Zaiss, A.K., Robbins, S.M., Hollenberg, M.D., Wickham, T.J., Muruve, D.A., 2002. Activation of p38 and ERK signaling during adenovirus vector cell entry lead to expression of the C-X-C chemokine IP-10. *J Virol* 76, 1559-1568.
437. Toda, M., Ueno, M., Hiraga, A., Asada, K., Montoya, M., Sotozono, C., Kinoshita, S., Hamuro, J., 2017. Production of Homogeneous Cultured Human Corneal Endothelial Cells Indispensable for Innovative Cell Therapy. *Invest Ophthalmol Vis Sci* 58, 2011-2020.
438. Toma, N.M., Ebenezer, N.D., Inglehearn, C.F., Plant, C., Ficker, L.A., Bhattacharya, S.S., 1995. Linkage of congenital hereditary endothelial dystrophy to chromosome 20. *Hum.Mol.Genet.* 4, 2395-2398.
439. Toth, C.A., Lapolice, D.J., Banks, A.D., Stinnett, S.S., 2004. Improvement in near visual function after macular translocation surgery with 360-degree peripheral retinectomy. *Graefes Arch Clin Exp Ophthalmol* 42, 541-548.
440. Trapani, I., Puppo, A., Auricchio, A., 2014. Vector platforms for gene therapy of inherited retinopathies. *Progress in retinal and eye research* 43, 108-128.
441. Trimarchi, J.M., Lees, J.A., 2002. Sibling rivalry in the E2F family. *Nature reviews. Molecular cell biology* 3, 11-20.
442. Tropepe, V., Coles, B.L., Chiasson, B.J., Horsford, D.J., Elia, A.J., McInnes, R.R., van der Kooy, D., 2000. Retinal stem cells in the adult mammalian eye. *Science* 287, 2032-2036.
443. Tsai, M.L., Chen, S.L., Chou, P.I., Wen, L.Y., Tsai, R.J., Tsao, Y.P., 2002. Inducible adeno-associated virus vector-delivered transgene expression in corneal endothelium. *Invest Ophthalmol Vis.Sci.* 43, 751-757.
444. Tuft, S.J., Coster, D.J., 1990. The corneal endothelium. *Eye* 4 (Pt 3), 389-424.
445. Tuft, S.J., Williams, K.A., Coster, D.J., 1986. Endothelial repair in the rat cornea. *Invest Ophthalmol Vis Sci* 27, 1199-1204.
446. Uchida, E., Mizuguchi, H., Ishii-Watabe, A., Hayakawa, T., 2002. Comparison of the efficiency and safety of non-viral vector-mediated gene transfer into a wide range of human cells. *Biol.Pharm.Bull.* 25, 891-897.
447. van den Hurk, J.A., Schwartz, M., van Bokhoven, H., van de Pol, T.J., Bogerd, L., Pinckers, A.J., Bleeker-Wagemakers, E.M., Pawlowitzki, I.H., Ruther, K., Ropers, H.H., Cremers, F.P., 1997. Molecular basis of choroideremia (CHM): mutations involving the Rab escort protein-1 (REP-1) gene. *Human mutation* 9, 110-117.
448. Van Horn, D.L., Sendele, D.D., Seideman, S., Bucu, P.J., 1977. Regenerative capacity of the corneal endothelium in rabbit and cat. *Invest Ophthalmol Vis Sci* 16, 597-613.
449. van Meurs, J.C., ter Averst, E., Hofland, L.J., van Hagen, P.M., Mooy, C.M., Baarsma, G.S., Kuijpers, R.W., Boks, T., Stalmans, P., 2004. Autologous peripheral retinal pigment epithelium translocation in patients with subfoveal neovascular membranes. *The British journal of ophthalmology* 88, 110-113.

-
450. van Meurs, J.C., Van Den Biesen, P.R., 2003. Autologous retinal pigment epithelium and choroid translocation in patients with exudative age-related macular degeneration: short-term follow-up. *American journal of ophthalmology* 136, 688-695.
451. Vermeulen, K., Van Bockstaele, D.R., Berneman, Z.N., 2003. The cell cycle: a review of regulation, deregulation and therapeutic targets in cancer. *Cell proliferation* 36, 131-149.
452. Vithana, E.N., Morgan, P., Sundaresan, P., Ebenezer, N.D., Tan, D.T., Mohamed, M.D., Anand, S., Khine, K.O., Venkataraman, D., Yong, V.H., Salto-Tellez, M., Venkatraman, A., Guo, K., Hemadevi, B., Srinivasan, M., Prajna, V., Khine, M., Casey, J.R., Inglehearn, C.F., Aung, T., 2006. Mutations in sodium-borate cotransporter SLC4A11 cause recessive congenital hereditary endothelial dystrophy (CHED2). *Nat.Genet.* 38, 755-757.
453. Vlodavsky, I., Folkman, J., Sullivan, R., Fridman, R., Ishai-Michaeli, R., Sasse, J., Klagsbrun, M., 1987. Endothelial cell-derived basic fibroblast growth factor: synthesis and deposition into subendothelial extracellular matrix. *Proceedings of the National Academy of Sciences of the United States of America* 84, 2292-2296.
454. Vogt, A., 1921. Weitere Ergebnisse der Spaltlampenmikroskopie des vordern Bulbusabschnittes; I. Abschnitt: Hornhaut. *Graefes Archive for Clinical and Experimental Ophthalmology* 106 63-103.
455. Walia, S., Fishman, G.A., 2009. Natural history of phenotypic changes in Stargardt macular dystrophy. *Ophthalmic genetics* 30, 63-68.
456. Walker, D.H., Maller, J.L., 1991. Role for cyclin A in the dependence of mitosis on completion of DNA replication. *Nature* 354, 314-317.
457. Wang, Q., Chen, Q., Zhao, K., Wang, L., Wang, L., Traboulsi, E.I., 2001. Update on the molecular genetics of retinitis pigmentosa. *Ophthalmic genetics* 22, 133-154.
458. Wang, X., Appukuttan, B., Ott, S., Patel, R., Irvine, J., Song, J., Park, J.H., Smith, R., Stout, J.T., 2000. Efficient and sustained transgene expression in human corneal cells mediated by a lentiviral vector. *Gene Ther.* 7, 196-200.
459. Waring, G.O., III, Bourne, W.M., Edelhauser, H.F., Kenyon, K.R., 1982. The corneal endothelium. Normal and pathologic structure and function. *Ophthalmology* 89, 531-590.
460. Waring, G.O., III, Rodrigues, M.M., Laibson, P.R., 1978. Corneal dystrophies. II. Endothelial dystrophies. *Surv.Ophthalmol* 23, 147-168.
461. Weber, W., Fussenegger, M., 2006. Pharmacologic transgene control systems for gene therapy. *The journal of gene medicine* 8, 535-556.
462. Weiss, J.S., Moller, H.U., Lisch, W., Kinoshita, S., Aldave, A.J., Belin, M.W., Kivela, T., Busin, M., Munier, F.L., Seitz, B., Sutphin, J., Bredrup, C., Mannis, M.J., Rapuano, C.J., Van Rij, G., Kim, E.K., Klintworth, G.K., 2008. The IC3D classification of the corneal dystrophies. *Cornea* 27 Suppl 2, S1-83.
463. Wolfram Research, Inc., Oblate Spheroid. <http://mathworld.wolfram.com/OblateSpheroid.html> Accessed 21.02.2012.

-
464. Whikehart, D.R., Parikh, C.H., Vaughn, A.V., Mishler, K., Edelhauser, H.F., 2005. Evidence suggesting the existence of stem cells for the human corneal endothelium. *Mol Vis* 11, 816-824.
 465. Wilson, S.E., Lloyd, S.A., 1991. Epidermal growth factor and its receptor, basic fibroblast growth factor, transforming growth factor beta-1, and interleukin-1 alpha messenger RNA production in human corneal endothelial cells. *Invest Ophthalmol Vis.Sci.* 32, 2747-2756.
 466. Wilson, S.E., Lloyd, S.A., He, Y.G., McCash, C.S., 1993a. Extended life of human corneal endothelial cells transfected with the SV40 large T antigen. *Invest Ophthalmol Vis.Sci.* 34, 2112-2123.
 467. Wilson, S.E., Lloyd, S.A., Kennedy, R.H., 1991. Epidermal growth factor messenger RNA production in human lacrimal gland. *Cornea* 10, 519-524.
 468. Wilson, S.E., Walker, J.W., Chwang, E.L., He, Y.G., 1993b. Hepatocyte growth factor, keratinocyte growth factor, their receptors, fibroblast growth factor receptor-2, and the cells of the cornea. *Invest Ophthalmol.Vis.Sci.* 34, 2544-2561.
 469. Wilson, S.E., Weng, J., Blair, S., He, Y.G., Lloyd, S., 1995. Expression of E6/E7 or SV40 large T antigen-coding oncogenes in human corneal endothelial cells indicates regulated high-proliferative capacity. *Invest Ophthalmol Vis.Sci.* 36, 32-40.
 470. Wiznerowicz, M., Trono, D., 2005. Harnessing HIV for therapy, basic research and biotechnology. *Trends in biotechnology* 23, 42-47.
 471. Wong, S.P., Argyros, O., Harbottle, R.P., 2015. Sustained expression from DNA vectors. *Advances in genetics* 89, 113-152.
 472. Wu, L., Timmers, C., Maiti, B., Saavedra, H.I., Sang, L., Chong, G.T., Nuckolls, F., Giangrande, P., Wright, F.A., Field, S.J., Greenberg, M.E., Orkin, S., Nevins, J.R., Robinson, M.L., Leone, G., 2001. The E2F1-3 transcription factors are essential for cellular proliferation. *Nature* 414, 457-462.
 473. Yamada, Y., Miyamura, N., Suzuma, K., Kitaoka, T., 2010. Long-term follow-up of full macular translocation for choroidal neovascularization. *American journal of ophthalmology* 149, 453-457 e451.
 474. Yamagami, S., Mimura, T., Yokoo, S., Takato, T., Amano, S., 2006. Isolation of human corneal endothelial cell precursors and construction of cell sheets by precursors. *Cornea* 25, S90-S92.
 475. Yanez-Munoz, R.J., Balaggan, K.S., MacNeil, A., Howe, S.J., Schmidt, M., Smith, A.J., Buch, P., MacLaren, R.E., Anderson, P.N., Barker, S.E., Duran, Y., Bartholomae, C., von Kalle, C., Heckenlively, J.R., Kinnon, C., Ali, R.R., Thrasher, A.J., 2006. Effective gene therapy with nonintegrating lentiviral vectors. *Nature medicine* 12, 348-353.
 476. Yang, Y., Geldmacher, D.S., Herrup, K., 2001. DNA replication precedes neuronal cell death in Alzheimer's disease. *The Journal of neuroscience : the official journal of the Society for Neuroscience* 21, 2661-2668.

-
477. Yellore, V.S., Rayner, S.A., Nguyen, C.K., Gangalum, R.K., Jing, Z., Bhat, S.P., Aldave, A.J., 2012. Analysis of the role of ZEB1 in the pathogenesis of posterior polymorphous corneal dystrophy. *Invest Ophthalmol Vis Sci* 53, 273-278.
 478. Yla-Herttuala, S., 2012. Endgame: glybera finally recommended for approval as the first gene therapy drug in the European union. *Mol Ther* 20, 1831-1832.
 479. Young, R.W., 1971. The renewal of rod and cone outer segments in the rhesus monkey. *The Journal of cell biology* 49, 303-318.
 480. Yu, H., 2007. Cdc20: a WD40 activator for a cell cycle degradation machine. *Molecular cell* 27, 3-16.
 481. Yu, J.Y., DeRuiter, S.L., Turner, D.L., 2002. RNA interference by expression of short-interfering RNAs and hairpin RNAs in mammalian cells. *Proceedings of the National Academy of Sciences of the United States of America* 99, 6047-6052.
 482. Zacchetti, A., van Garderen, E., Teske, E., Nederbragt, H., Dierendonck, J.H., Rutteman, G.R., 2003. Validation of the use of proliferation markers in canine neoplastic and non-neoplastic tissues: comparison of KI-67 and proliferating cell nuclear antigen (PCNA) expression versus in vivo bromodeoxyuridine labelling by immunohistochemistry. *APMIS : acta pathologica, microbiologica, et immunologica Scandinavica* 111, 430-438.
 483. Zarbin, M.A., 2004. Current concepts in the pathogenesis of age-related macular degeneration. *Arch Ophthalmol* 122, 598-614.
 484. Zeng, C., Pan, F., Jones, L.A., Lim, M.M., Griffin, E.A., Sheline, Y.I., Mintun, M.A., Holtzman, D.M., Mach, R.H., 2010. Evaluation of 5-ethynyl-2'-deoxyuridine staining as a sensitive and reliable method for studying cell proliferation in the adult nervous system. *Brain research* 1319, 21-32.
 485. Zerler, B., Roberts, R.J., Mathews, M.B., Moran, E., 1987. Different functional domains of the adenovirus E1A gene are involved in regulation of host cell cycle products. *Molecular and cellular biology* 7, 821-829.
 486. Zhu, C., Joyce, N.C., 2004. Proliferative response of corneal endothelial cells from young and older donors. *Invest Ophthalmol.Vis.Sci.* 45, 1743-1751.
 487. Zhu, Y.T., Hayashida, Y., Kheirkhah, A., He, H., Chen, S.Y., Tseng, S.C., 2008. Characterization and comparison of intercellular adherent junctions expressed by human corneal endothelial cells in vivo and in vitro. *Invest Ophthalmol Vis Sci* 49, 3879-3886.
 488. Zielke, N., Edgar, B.A., 2015. FUCCI sensors: powerful new tools for analysis of cell proliferation. *Wiley Interdiscip Rev Dev Biol* 4, 469-487.
 489. Zufferey, R., Donello, J.E., Trono, D., Hope, T.J., 1999. Woodchuck hepatitis virus posttranscriptional regulatory element enhances expression of transgenes delivered by retroviral vectors. *J Virol* 73, 2886-2892.
 490. Zufferey, R., Dull, T., Mandel, R.J., Bukovsky, A., Quiroz, D., Naldini, L., Trono, D., 1998. Self-inactivating lentivirus vector for safe and efficient in vivo gene delivery. *J Virol* 72, 9873-9880.

491. Zufferey, R., Nagy, D., Mandel, R.J., Naldini, L., Trono, D., 1997. Multiply attenuated lentiviral vector achieves efficient gene delivery in vivo. *Nat Biotechnol* 15, 871-875.

9. Appendix

9.1. Abbreviations

aa	amino acid
AAV	adeno-associated virus
ABCR	ATP-binding cassette transporter
Ad	adenovirus / adenoviral vector
ADA	adenosine deaminase
ADP	adenosine-5'-diphosphate
AJ	adherens junction
AMD	age related macular degeneration
arRP	autosomal recessive retinitis pigmentosa
ATP	adenosine-5'-triphosphate
BDNF	brain-derived neurotrophic factor
bFGF	basic fibroblast growth factor
BHK	baby hamster kidney cells
BIV	bovine immunodeficiency virus
Bmp	bone morphogenetic protein
BNB	blood-neural barrier
bp	base pairs
BRB	brain-retina barrier
BrdU	5-bromo-2-deoxyuridine
CAEV	caprine arthritis-encephalitis virus
cAMP	cyclic AMP
Cdc20	cell-division cycle protein 20
CDK	Cyclin D kinase
cDNA	complementary DNA
CEC	corneal endothelial cells
CFH	complement factor H

CGD	chronic granulomatous disease
cGMP	cyclic GMP
CMV	cytomegalovirus
CMZ	ciliary margin zone
CNS	central nervous system
CNTF	ciliary neurotrophic factor
CNV	choroidal neovascularisation
CORD	cone-rod dystrophy
cPPT	central poly purine tract
CRALBP	cellular retinaldehyde binding protein
CRBP	cellular retinol-binding protein
CRX	cone-rod otx-like homeobox
Cx	connexin
DMEM	Dulbecco's Modified Eagle Medium
DMSO	dimethylsulfoxide
DNA	deoxyribonucleic acid
ds	double stranded
DTA	diphtheria toxin A
EAM	encapsidated adenoviral mini-chromosome
EAU	experimental autoimmune uveoretinitis
ECD	endothelial cell density
EdU	5-Ethynyl-2'-deoxyuridine
eGFP	enhanced green fluorescent protein
EIAV	equine infectious anaemia virus
ERG	electroretinogram
ES cell	embryonic stem cell
Exp	exportin
eYFP	enhanced yellow fluorescent protein
FACS	fluorescence-activated cell sorter
FBS	fetal bovine serum
Fgf	fibroblast growth factor
FITC	fluorescein isothiocyanate
FIV	feline immunodeficiency virus
FIV	feline immunodeficiency virus
g	gram; unit of gravity

G	gauge
GC	ganglion cell
GCAP	guanylate cyclase activator protein
GDNF	glial-cell line derived neurotrophic factor
GDP	guanosine- 5'-diphosphate
GJ	gap junction
GMP	guanosine 5'-monophosphate
GTP	guanosine-5'-triphosphate
h	hour
HEK	human embryonic kidney cells
HIV	human immunodeficiency virus
HLA	human leukocyte antigen
hrGFP	humaized recombinant green fluorescent protein
HRP	horseradish peroxidase
HSV	herpes simplex virus
IL	interleukin
IP	infectious particles
iPS cell	induced pluripotent stem cell
ITR	inverted terminal repeats
JAM	junction adhesion molecule
kb	kilobase
kDa	kilodalton
L	litre
LNT	lentivirus / lentiviral vector
LTR	long tandem repeats
m	meter
m-	micro-
m-	milli
MDCK	Madin-Darby canine kidney cells
MerTK	mer-receptor tyrosine kinase
min	minute
miRNA	micro RNA
MOI	multiplicity of infection (infectious vector particles / cell)
mRNA	messenger RNA
MST	Median survival time

MTT	3-(4,5-Dimethylthiazol-2-yl)-2,5-diphenyltetrazolium bromide
n-	nano-
NACos	nucleus and adhesion complexes
ncRNA	non-coding RNA
NF	nerve fibre layer
NRL	neural retina leucine zipper transcription factor
nt	nucleotide
OD	oculus dexter, right eye
OIR	oxygen-induced retinopathy
OLM	outer limiting membrane
ONL	outer nuclear layer
OPL	outer plexiform layer
OS	oculus sinister, left eye
P	postnatal day
PAGE	polyacrylamide gel electrophoresis
PCNA	proliferating cell nuclea antigen
PCR	polymerase chain reaction
PDE	phosphodiesterase
PEDF	pigment epithelium derived factor
PEG	Polyethylene glycol
Ph	phagosome
pi	post injection
piRNA	Piwi-interacting RNA
PTGS	post transcriptional gene silencing
PVDF	polyvinylidene difluoride
qRT-PCR	quantitative reverse transcription polymerase chain reaction
rAAV	recombinant AAV
rasiR	NA repeat-associated siRNA
RCS	royal college of surgeons
rcf	relative centrifugation force
rd	retinal degeneration
RFP	red fluorescent protein
RGC	retinal ganglion cells
Rho	rhodopsin
RISC	RNA induced silencing complex

RK	rhodopsin kinase
RNA	ribonucleic acid
RNAi	RNA interference
ROCK	Rho-associated protein kinase
RP	retinitis pigmentosa
RPE	retinal pigment epithelium
RPM	revolutions per minute
rRNA	ribosomal RNA
RT	reverse transcriptase
RT-PCR	reverse transcription polymerase chain reaction
RVE	retinal vascular endothelium
scAAV	self-complementary AAV
SCID	severe combined immunodeficiency
SDS	sodium dodecyl sulfate
SFFV	spleen focus-forming virus
sFLT	soluble fms-like tyrosine kinase 1
shRNA	short hairpin RNA
SIN	self inactivating
siRNA	short interfering RNA
ss	single strand
SV40	simian virus type-40
TEM	transmission electron microscopy
TERT	telomerase reverse transcriptase
TG	transgenic
TGF- β	transforming growth factor beta
TIMP3	tissue inhibitor of metalloproteinase 3
TJ	tight junction
TNF-a	tumour necrosis factor alpha
Tris	tris(hydroxymethyl)aminomethane
tRNA	transfer RNA
TU	transducing units
UTR	untranslated regions
VEGF	vascular endothelial growth factor
vp	viral particles
VSV	vesicular-stomatitis virus

VSV-G	vesicular-stomatitis virus G-protein
w/v	weight per volume
w/w	weight per weight
WPRE	Woodchuck hepatitis virus post-transcriptional element
WT	wildtype
xl	X-linked
YFP	yellow fluorescent protein
ZO-1	zonula occludens-1
ZONAB	ZO-1 associated nucleic-acid binding

9.2. Ethical approval for use of human tissue

To apply for the permissions and approval for this research study, we used the Integrated Research Application System (IRAS). After review, ethical approval of the use of human tissue for this study was granted by the Moorfields & Whittington Research Ethics Committee. Relevant documents concerning ethical approval are amended:

- Study Protocol
- Participant Information Sheet
- Participant Consent Form
- Letter of Approval of the Moorfields & Whittington Research Ethics Committee

9.2.1. Study Protocol (12 December 2008)

Protocol Version 1, 12/12/2008

Study Title

PROMOTER - RESTRICTED INDUCTION OF CORNEAL ENDOTHELIAL CELL REPLICATION: EX VIVO ANALYSIS

Researchers

Mr Frank Larkin, Consultant Ophthalmic Surgeon, Moorfields Eye Hospital / UCL Institute of Ophthalmology

Professor Robin Ali, Professor of Genetics, UCL Institute of Ophthalmology

Mr Daniel Kampik, Clinical Research Fellow, Moorfields Eye Hospital / UCL Institute of Ophthalmology

1. Objectives

To develop efficient lentiviral vector-mediated gene transfer into the corneal endothelium and to examine efficacy and safety of gene therapy for the induction of corneal endothelial cell replication.

2. Background and rationale

- A monolayer of endothelial cells, which are non-replicative in humans, constitutes the internal surface of the cornea. As this monolayer is critical for the maintenance of corneal transparency, disorders of the endothelium lead to loss of corneal transparency and thus blindness. The endothelial cells in corneas stored and transplanted as a treatment of corneal blindness are themselves vulnerable to injury and death. Falling endothelial cell density due to post-mortem cell death is the reason for discard of 33% of donor corneas in eye banks in the UK [1]. Evaluation of gene therapy methods to improve the capability of transplanted donor corneas to function better and longer in the recipient eye is the subject of this proposed research.
- Proof of principle studies using the first direct molecular approach to induction of human corneal endothelial cell replication have been undertaken by the applicants in collaboration with Dr Nancy Joyce (Schepens Eye Research Institute, Boston). In this work, a recombinant adenoviral vector was used to transfer cDNA encoding the transcription factor E2F2 ex vivo to whole thickness rabbit [2] and human [3] corneas. While human corneal endothelial cells are generally regarded as non-replicative later than infancy, E2F2 gene transfer resulted in cell cycle progression and increase in endothelial cell density in human corneas.
- Adenoviral vectors of the type described above have in other studies been found to cause substantial inflammatory reactions when delivered intraocularly. Lentiviral vectors are considerably less immunogenic than adenoviral vectors, and for this reason reduce the risk of loss of endothelial cells due to immune reactions to either the viral proteins or the transgene product. Non-integrating lentiviral vectors, previously developed in Professor Ali's laboratory, rapidly give rise to high levels of transgene expression in a variety of tissues including corneal endothelium [4]. In contrast to normal lentiviral vectors, this recombinant viral genome does not integrate into the host genome and as a result the transgene is lost after cell division. As long-term expression of E2F2 could possibly lead to transformation of transduced cells, the use of non-integrating vector diminishes the risk of iatrogenic transformation events. For these reasons, we will examine non-integrating lentivirus vectors for gene transfer to the corneal endothelium.

Protocol Version 1, 12/12/2008

3. Plan of investigation

Further studies are required to advance this research to the stage that proof of principle trials of post-transplantation function of genetically modified donor corneas can be assessed in patients.

- (a) In this project, lentiviral constructs will be created which contain either the murine or the human E2F2 gene under control of a ubiquitous promoter. After transduction of various cell types in vitro, the expression of E2F2 and its effect on cellular replication will be assessed through immunocytochemistry, cell counting and BrdU incorporation assays. Integrating and non-integrating lentiviral vectors containing a fluorescent marker gene in addition to the functional E2F2 sequence will be used to test the efficacy of transduction of the target cells. Once the efficacy of the transgene construct has been established, the lentiviral constructs will be used to transduce the endothelium of excised human corneas ex vivo. These will be keratoconus specimen corneas removed at transplantation. Based on findings in our earlier work with adenovirus vectors, the subsequent expression of the E2F2 gene is likely to result in the induction of cellular replication and increased corneal endothelial cell density. After one or more rounds of replication, it is anticipated that transgene expression will be lost and that cell cycle progression and division will stop. We will assess the efficacy of cell cycle progression as well as the efficacy of subsequent re-entry to the quiescent phase by microscopy and by BrdU incorporation studies at various time points after transduction. Transverse sections of cornea will be examined by light and electron microscopy to ascertain whether a monolayer is maintained or whether multilayering of cells supervenes. Density of endothelial cells will be quantified by analysis of en face images of corneas in standard methodology [3]. Existing expertise in vector development, exogenous promoter cloning and vector production in the laboratory will be essential in developing this aspect of the project.
- (b) It is envisaged that gene transfer to corneal endothelium will be performed ex vivo before transplantation of the cornea into the recipient. This is likely to limit the presence of free vector in the eye. Nevertheless, dissemination of the vector to other tissues in the anterior chamber or even outside the eye remains a concern, as ectopic expression of the E2F2 gene could result in the transformation of the transduced cells. One level of safety is afforded by the use of non-integrating lentiviral vectors. Because these vectors are lost after the cells undergo cell division, any ectopic cell replication will result in the loss of the vector and cessation of cell division. Another method to guard against transformation is the use of tissue-specific promoters, as these will prevent the expression of the transgene should the vector transduce cells other than the target cells. No corneal endothelium specific promoters have been described in the literature, but several studies describe genes that are specifically expressed in the corneal endothelium [5,6]. Using in silico and in vitro techniques we will identify the promoter sequences of various endothelium specific genes and use these to drive expression of fluorescent marker genes from integrating and non-integrating lentiviral vectors. We will confirm that this promoter(s) results in efficient cell-specific gene expression in human donor corneas ex vivo. Finally, specificity and efficacy of expression will be assessed by the injection of these vectors into the anterior chambers of mice [please note that these in vivo studies will be funded and undertaken with the support of funding from an existing research grant.]

Protocol Version 1, 12/12/2008

- (c) We will then produce non-integrating lentiviral vectors carrying the corneal endothelium specific promoter, developed in (b), to drive the expression of the human E2F2 gene. We will test the ability of this vector to induce endothelial cell proliferation in human cornea ex vivo as described in (a) above.

4. Timetable

To month 12:	Assessment of transduction efficiency of corneal endothelium comparing integrating and non-integrating lentiviral vectors ex vivo in mouse and human cornea using marker genes Production of murine and human E2F2-containing vector constructs and production of viral vector Production of vector constructs containing corneal endothelium specific promoter driving fluorescent marker and production of viral vector
To month 24:	In vitro assessment of induction of cell replication through expression of E2F2 in human and murine cells Assessment of efficacy in human corneas ex vivo
To month 30:	Production of vector constructs containing a corneal endothelium specific promoter driving the human E2F2 gene and production of viral vectors Assessment of induction of cell division in human corneas ex vivo
To month 36:	Writing up papers and PhD thesis

5. Reasons for support requested

This application seeks support for running costs for 3 years for Dr Daniel Kampik. He has been appointed as a research training fellow within the Ocular surface & Cornea theme of the BMRC and commences in December 2008. Accordingly no salary support is requested in this proposal.

6. References

- 1 Armitage WJ, Easty DL. Factors influencing the suitability of organ-cultured corneas for transplantation. *Invest Ophthalmol Vis Sci* 1997;38:16-24
- 2 [Joyce NC, Harris DL, Mc Alister JC, Ali RR, Larkin DF](#). Effect of overexpressing the transcription factor E2F2 on cell cycle progression in rabbit corneal endothelial cells. *Invest Ophthalmol Vis Sci* 2004;45:1340-1348
- 3 McAlister JC, Joyce NC, Harris DL, Ali RR, Larkin DF. Induction of replication in human corneal endothelial cells by E2F2 transcription factor cDNA transfer. *Invest Ophthalmol Vis Sci* 2005;46:3597-3603
- 4 [Yáñez-Muñoz RJ, Balaggan KS, MacNeil A, Howe SJ, Schmidt M, Smith AJ, Buch P, MacLaren RE, Anderson PN, Barker SE, Duran Y, Bartholomae C, von Kalle C, Heckenlively JR, Kinnon C, Ali RR, Thrasher AJ](#). Effective gene therapy with nonintegrating lentiviral vectors. *Nat. Med.* 2006;12:348-353
- 5 [Sakai R, Kinouchi T, Kawamoto S, Dana MR, Hamamoto T, Tsuru T, Okubo K, Yamagami S](#). Construction of human corneal endothelial cDNA library and

Protocol Version 1, 12/12/2008

identification of novel active genes. Invest Ophthalmol Vis Sci 2002;43:1749-1756

6 Jung SE, Seo KY, Kim H, Kim HL, Chung IH, Kim EK. Expression of MUC1 on corneal endothelium of human. Cornea 2002;21:691-695

9.2.2. Participant Information Sheet (02 February 2009)



Moorfields Eye Hospital **NHS**

NHS Foundation Trust

City Road
London
EC1V 2PD

Tel: 020 7253 3411
www.moorfields.nhs.uk

PATIENT INFORMATION SHEET (For Patients Receiving Corneal Transplantation)

TITLE OF PROJECT: Induction of corneal endothelial cell replication

Researchers: Frank Larkin, Daniel Kampik

You are being invited to take part in a research study. Before you decide it is important for you to understand why the research is being done and what it will involve. Please take time to read the following information and discuss it with friends, relatives and your GP if you wish. Ask us if there is anything that is not clear or if you would like more information.

Thank you for reading this.

1. What is the purpose of the study?

We are trying to improve the outcome of corneal transplantation which is much dependant on the function of the endothelial cells at the inner surface of the cornea. Endothelial cells normally do not replicate and might be harmed over time, especially after corneal transplantation. This causes the cornea to lose its transparency. We are looking for ways to make these cells replicate, thereby keeping the transplant clear for a longer time.

2. Why have I been chosen?

You have been chosen because you are having corneal transplantation surgery. In the course of your surgery, diseased corneal tissue will be removed and replaced by the corneal graft. We would like to take a sample of your diseased cornea to study in the laboratory.

3. Do I have to take part?

Not at all. Involvement is entirely voluntary.

4. What will happen to me if I take part?

Patron: Her Majesty The Queen
Chairman: Rudy Markham
Chief Executive: John Pelly

You would be listed for corneal transplantation as per the normal management for your condition. Instead of discarding all the corneal tissue that will be replaced during the course of your surgery, we will keep a sample. This sample will be labelled with a study number and sent to a laboratory in the UCL Institute of Ophthalmology, where various experiments will be done that attempt to find what causes endothelial cells to divide and regain normal function. No personal details will be attached to your sample.

5. What do I have to do?

Nothing, we just need your consent so that we can collect a sample of your cornea and send it to the laboratory.

6. What will happen to my tissue sample once the research study is completed?

Your sample will be stored in an anonymised form in the UCL Institute of Ophthalmology and will be destroyed at the end of the study

7. What are the side effects of taking part?

None. Your treatment will not be affected in any way.

8. What are the possible disadvantages or risks of taking part?

None. There are no additional risks involved for the surgery above the normal surgical procedure.

9. What are the possible benefits of taking part?

Although there will be no benefit to you personally, you will be allowing us to get a better understanding of corneal tissue which we hope will translate in better results for patients.

10. What if something goes wrong?

We do not anticipate that anything will go wrong, as all we wish to do is collect a small piece of tissue from your cornea that would be discarded anyway, and study it in the laboratory.

In the unlikely event that taking part in this research project harms you, there are no special compensation arrangements. If you are harmed due to someone's negligence, then you may have grounds for a legal action but you may have to pay for it. Regardless of this, if you wish to complain about any aspect of the way you have been approached or treated during the course of this study, the normal National Health Service complaints mechanisms may be available to you.

11. Will my taking part in this study be kept confidential?

Yes. The tissue sample that you donate for our research will be labelled with a study number only. All information that is collected during the course of the research will be kept strictly confidential. Any information about you which leaves the hospital will have your name and address removed so that you cannot be recognised from it.

12. What will happen to the results of the research study?

We hope that these would be published in a medical journal, allowing professionals from around the world to benefit from our results.

13. Who is sponsoring and funding the research?

Moorfields Eye Hospital is sponsoring this study, which is being funded by the NHS Biomedical Research Centre (BMRC).

14. Who has reviewed the study?

The study has been reviewed by the Moorfields & Whittington Research Ethics Committee.

15. Contact for Further Information

Mr Frank Larkin MD FRCPI FRCOphth
Consultant Ophthalmic Surgeon
& Director, Cornea / External Diseases Service,
Moorfields Eye Hospital
City Road
London EC1V 2PD
Tel: 020 7566 2045

Mr Daniel Kampik MD
Clinical Research Fellow

Moorfields Eye Hospital
City Road
London EC1V 2PD
Tel: 020 7608 6981

Thank you for reading this and considering taking part in our study.

9.2.3. Participant Consent Form (02 February 2009)



Moorfields Eye Hospital **NHS**

NHS Foundation Trust

City Road
London
EC1V 2PD

Study Number:
Patient Identification Number for this trial:

Tel: 020 7253 3411
www.moorfields.nhs.uk

CONSENT FORM

Title of Project: Induction of corneal endothelial cell replication

— Name of Researchers: Mr Frank Larkin, Mr Daniel Kampik

Please initial box

1. I confirm that I have read and understand the information sheet dated.....
(version) for the above study and have had the opportunity to ask questions.
2. I understand that my participation is voluntary and that I am free to withdraw at any time,
without giving any reason, without my medical care or legal rights being affected.
3. I understand that sections of any of my medical notes may be looked at by responsible
individuals from regulatory authorities where it is relevant to my taking part in research.
I give permission for these individuals to have access to my records.
4. I understand that the tissue sample that I donate will be sent to a laboratory in the
UCL Institute of Ophthalmology, where various tests relating to this condition will be
studied, and I agree to this.
5. I agree to take part in the above study.

Name of Patient

Date

Signature

Researcher

Date

Signature

Patron: Her Majesty The Queen
Chairman: Rudy Markham
Chief Executive: John Pelly

9.2.4. Letter of Approval (9 February 2009)

Moorfields & Whittington Research Ethics Committee

Royal Free Hospital
Pond Street
London
NW3 2QG

Telephone: 020 7794 0552

Mr Frank Larkin
Consultant Ophthalmic Surgeon & Director, Cornea / External Diseases Service
Moorfields Eye Hospital
162 City Road
London, EC1V 2PD

09 February 2009

Dear Mr Larkin

Full title of study:	Promoter-restricted induction of corneal endothelial cell replication: Ex-vivo analysis
REC reference number:	09/H0721/6

Thank you for your letter of 03 February 2009, responding to the Committee's request for further information on the above research and submitting revised documentation.

The further information has been considered on behalf of the Committee by the Chair.

Confirmation of ethical opinion

On behalf of the Committee, I am pleased to confirm a favourable ethical opinion for the above research on the basis described in the application form, protocol and supporting documentation as revised, subject to the conditions specified below.

Ethical review of research sites

The Committee has designated this study as exempt from site-specific assessment (SSA). The favourable opinion for the study applies to all sites involved in the research. There is no requirement for other Local Research Ethics Committees to be informed or SSA to be carried out at each site.

Conditions of the favourable opinion

The favourable opinion is subject to the following conditions being met prior to the start of the study.

Management permission or approval must be obtained from each host organisation prior to the start of the study at the site concerned.

Management permission at NHS sites ("R&D approval") should be obtained from the relevant care organisation(s) in accordance with NHS research governance arrangements. Guidance on applying for NHS permission is available in the Integrated Research Application System or at <http://www.rdforum.nhs.uk>.

Approved documents

The final list of documents reviewed and approved by the Committee is as follows:

Document	Version	Date
Letter from Sponsor		17 December 2008
Covering Letter		13 January 2009
Protocol	1	12 December 2008
Investigator CV		13 January 2009
Application		13 January 2009
Response to Request for Further Information		03 February 2009
Participant Consent Form	1.1	02 February 2009
Participant Information Sheet	1.1	02 February 2009

Statement of compliance

The Committee is constituted in accordance with the Governance Arrangements for Research Ethics Committees (July 2001) and complies fully with the Standard Operating Procedures for Research Ethics Committees in the UK.

After ethical review

Now that you have completed the application process please visit the National Research Ethics Website > After Review. You are invited to give your view of the service that you have received from the National Research Ethics Service and the application procedure. If you wish to make your views known please use the feedback form available on the website.

The attached document "After ethical review –guidance for researchers" gives detailed guidance on reporting requirements for studies with a favourable opinion, including:

- Notifying substantial amendments
- Progress and safety reports
- Notifying the end of the study

The NRES website also provides guidance on these topics, which is updated in the light of changes in reporting requirements or procedures.

We would also like to inform you that we consult regularly with stakeholders to improve our service. If you would like to join our Reference Group please email referencegroup@nres.npsa.nhs.uk

09/H0721/6	Please quote this number on all correspondence
-------------------	---

With the Committee's best wishes for the success of this project

Yours sincerely

John Farrell
Chair

Email: katherine.clark@royalfree.nhs.uk

Enclosures:	"After ethical review – guidance for researchers"
Copy to:	Mrs Sue Lydeard, R&D office